DESIGN, SYNTHESIS, AND STRUCTURAL STUDY OF PORPHYRIN-BASED ORGANIC MATERIALS

by

SHILI CHEN

(Under the direction of Thomas E. Johnson)

ABSTRACT

The unique properties of porphyrins, such as intense light absorption and emission, electron and oxygen transporting ability, make porphyrins desirable targets to incorporate into conjugated polymers for potential applications as semiconductors, or optic-electronic devices. However, low solubility and the lack of efficient polymerization methods have hampered the exploitation of monomeric porphyrins. The focus of this research is design and synthesis of highly soluble porphyrin monomers, and investigation of polymerization methods for constructing highly conjugated, high quality porphyrin materials. The accomplishments in this work include (1) study of solubility-structure relationships in porphyrins; (2) structure design to increase porphyrin solubility in organic solvents; (3) synthesis of a group of novel porphyrin molecules with specific structure design; (4) structure analysis of soluble porphyrin molecules by X-ray crystallography; (5) synthesis of monomers for porphyrin polymerization; (6) development and comparison of polymerization methods, including palladium mediated oxidative coupling, acyclic diyne metathesis (ADIMET) and acyclic diene metathesis (ADMET). Porphyrin solubility has been increased by tens to thousands of times when compared to other alkylporphyrins in this work. Alkene and alkyne metatheses reactions, which are applied for the first time to porphyrin polymerizations, show promising results for the preparation of defect-free conjugated porphyrin polymers.

INDEX WORDS: Porphyrin, Solubility, Conjugated Polymer, Facial encumbrance, Palladium mediated coupling reaction, Acyclic diyne metathesis reaction, Acyclic diene metathesis reaction

DESIGN, SYNTHESIS, AND STRUCTURAL STUDY OF PORPHYRIN-BASED ORGANIC MATERIALS

by

SHILI CHEN

B.S., Wuhan University of Hydraulic & Electric Engineering, P.R.China, 1982

M.E., Wuhan University of Hydraulic & Electric Engineering, P.R.China, 1986

A Dissertation Submitted to the Graduate Faculty of The University of Georgia in Partial Fulfillment of the Requirements for the Degree

DOCTOR OF PHILOSOPHY

ATHENS, GEORGIA

2002

DESIGN, SYNTHESIS, AND STRUCTURAL STUDY OF PORPHYRIN BASED ORGANIC MATERIALS

by

SHILI CHEN

Major Professor:	Robert S. Phillips
Committee:	Thomas E. Johnson Charles Kutal I. Jonathan Amster Gregory H. Robinson

Electronic Version Approved:

Gordhan L. Patel
Dean of the Graduate School
The University of Georgia
August 2002

DEDICATION

To my husband Wei Ding, my daughter Chen (Jennifer) Ding, my parents Jianqiu Chen and Jinlan Pu, who have always supported my endeavors.

ACKNOWLEDGEMENTS

I would like to thank Dr. Johnson, my dissertation advisor, for his encouragement, support and advice. Without his extensive knowledge, experience, creative ideas and imagination, the achievements of this project would not have been possible. I also would like to express my sincere thanks to my committee members, Dr. Phillips, Dr. Kutal, Dr. Amster, and Dr. Robinson for their precious advice and inspiration. I am the beneficiary of their knowledge and dedication to the chemistry. I also thank Dr. Majetich for his advice in synthetic organic chemistry, and his generosity when we needed to borrow chemicals and journals. Thank you, Dr. Hardcastle (Emory University) and Jason Vohs, for your successful collaboration to our porphyrin crystal structure analysis.

I would also like to thank my co-workers, members of the Johnson group: Walter Michael, Andrew Pearson, Brad Wright, Tony Warren, Angil Butler and Pallavi Apte for providing a comfortable and fun workplace, and helping each other in chemistry and in other aspects of life as well. I extend special thanks to Walter for helping me in organic synthesis; to Andrew for his selfless technical support in computers, instruments and other facilities; and to Brad and Tony for their help in my language and cultural studies.

I am grateful to my family for their unconditional sacrifices and support through hard times. I would like to share my happiness for the fulfillment of this dissertation with my husband Wei Ding, my lovely daughter Jennifer, my parents, sisters, brothers, and my friends.

TABLE OF CONTENTS

Page

ACKNOWLEDGEMENTS v

CHAPTER

I INTRODUCTION 1

1.1 Organic polymer materials and π−conjugated polymers 1

1.2 Porphyrin-based organic materials 11

1.3 Objectives of this project 35

References 37

II SOLUBILITY-STRUCTURE STUDIES OF PORPHYRINS 49

2.1 Monomeric porphyrin solubility in organic solvents 49

2.2 Strategies to reduce strong interaction between porphyrins 54

2.3 Syntheses of designed porphyrin molecules 61

2.4 Solubility-structure relationships in designed porphyrins 92

2.5 Conclusions 114

References 115

III INVESTIGATION ON PORPHYRIN POLYMERIZATION METHODS 118

3.1 Palladium-mediated polymerization 118

3.2 Acyclic diyne metathesis (ADIMET) polymerization 131

3.3 Acyclic diene metathesis (ADMET) polymerization 148

3.4 Conclusions to the polymerization methods investigation.................157
References..159
IV CONCLUSIONS..166
4.1 Achievements in this project...166
4.2 Directions of this project in the future................................167
APPENDICES FOR CHAPTER II..169

CHAPTER I

INTRODUCTION

1.1 Organic polymer materials and π–conjugated polymers

Organic polymer materials have been studied, prepared and applied in countless technological fields since the commercial development of nylon in 1940. These materials are commonly classified as adhesives, fibers, paints, plastics and rubbers according to their applications in past years.[1] Due to the tremendous and ever growing demands for unprecedented or improved properties, advanced organic materials are continuously desired, invented and incorporated to our daily lives, as well as to many industries such as aerospace, automobile and electronics. After the discovery of metallic conductivity in iodine-doped polyacetylene, organic materials, with applications in electronic and optical devices, have become one of the most exciting and innovative branches of materials science. For instance, the new TFT (Thin Film Transistor) LCD (Liquid Crystal Display) monitors display pictures with better quality and higher resolution than conventional displays but in super thin panels. Novel ultra-thin batteries in cell phones and laptops, and much smaller and lighter computers doing more complex work in spacecraft are also some good examples of semiconductors made from organic polymers or polymer blends. These applications are all especially demanding with respect to density and complexity increases in semiconductor chip circuits and other functional units. Such demands have already promoted rapid development of new revolutionary semiconductor technologies.[2] Conventional inorganic materials can no longer meet all of these demands since further modifications of size, diversity and related properties have met some unavoidable limitations. Consequently, the exploitation of a totally different class of materials has become the new trend in electronics, photonics and other related fields.

Organic polymers have become one of the most promising classes of materials that can meet the above trends for enhancing density and complexity in various electronic and optical devices as “plastic” conductors and semiconductors at the molecular level. In organic materials used in the electronics industry (termed molecular electronics), the electronic and optical properties are locked into the molecular structure by molecular engineering, instead of being produced by processing techniques, as in the fabrication of inorganic electronics. This unique molecular engineering provides the possibility of establishing predictive structure–function relationships between chemical structures and materials properties, and ensures suitable and flexible control on the electronic and optical properties of a resulting device by altering or modifying the organic molecular structure before fabricating the actual device. Therefore, organic polymer materials can offer viable alternatives to the traditional inorganic materials in many applications because of their extremely small size, abundance, diversity, ease of production and fabrication, tunable properties, potential high performance and low cost. Sophisticated semiconducting, insulating, and conducting polymers enable many of the electrical functionalities of conventional silicon materials without the vacuum deposition and photolithography steps required by silicon electronics manufacturing processes.

The most important organic polymeric materials used in molecular electronics are π-conjugated organic polymers, the polymers with spatially extended π-bonding systems. The intensive exploration of π-conjugated organic polymers as advanced electronic materials began in the late 1970s with the discovery of metallic conductivity in iodine-doped polyacetylene.[3,4] Since then, a vast array of conjugated polymers with many desirable properties have been synthesized and found applications in many industrial fields. For example, the transparent coatings in thin layers with color and color change in chemical or electrolytic environments, or materials with high specific conductivity that shield against electromagnetic interference (EMI) are entirely prepared from π-conjugated organic polymers. Examples of conjugated organic polymers that have been intensively studied include polydiacetylenes (PDAs) **1**,[5] polyacetylene **2**,[4] poly(*p*-phenylene vinylene)s **3**,[6-9] aromatic poly(azomethine)s **4**,[10,11] polythiophenes (polypyrroles and polyfurans) **5**,[12-21] polyaniline **6**,[22,23] or copolymers with alternating π−structured building blocks **7-9**[24-28] (Fig. 1-1 and 1-2).

Most of the aforementioned conjugated polymers are semiconducting in their neutral (undoped) form with band gaps of HOMO-LUMO energy levels roughly between 1-3 eV. They can be used as semiconductors in polymer light-emitting diodes(LEDs),[6,29-33] polymer lasers,[34-36] photovoltaic cells,[37] field-effect transistors,[38] solid-state rechargeable batteries[39,40] and supercapacitors,[41,42] etc. After redox or acid-base doping, the doped conjugated polymers (**10-11**, Fig. 1-3) exhibit great changes of their structural, spectroscopic and electronic properties. Most importantly, the band gap of these materials decreases and they can become conductive polymer materials or organic "metals".[4,19,43,44] However, when a conjugated polymer is doped with oxidants like I_2, $FeCl_3$, or with

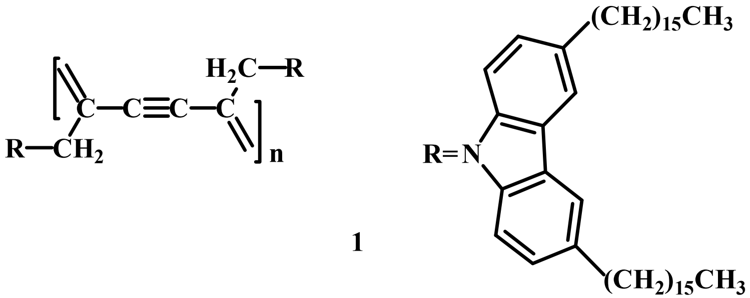

1

Polydiacetylenes (PDAs)

Cis-polyacetylene **Trans-polyacetylene**

2

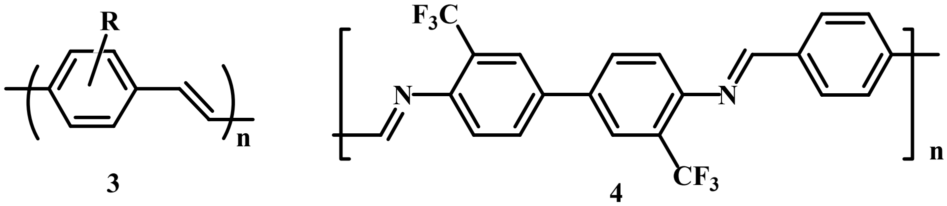

3 **4**

Poly(*p*-phenylene vinylene) **Aromatic poly(azomethine)**

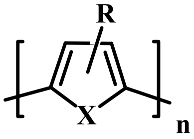

5

X = NH **Poly(pyrrole)**
S **Poly(thiophene)**
O **Poly(furan)**

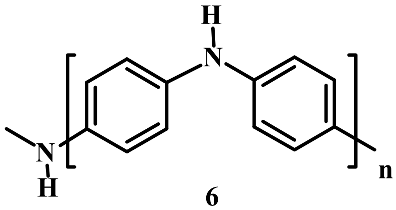

6

Poly(aniline)

Figure 1-1. Conjugated Organic Polymers

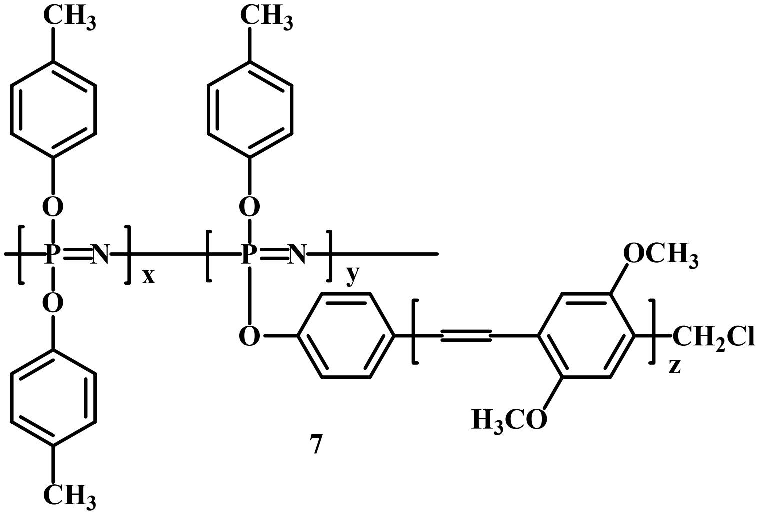

7

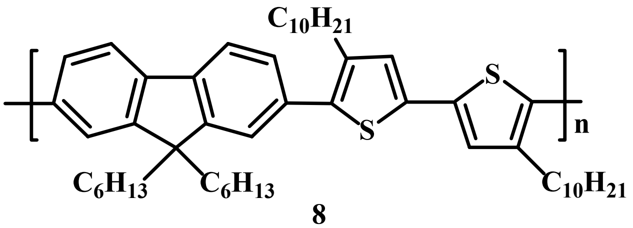

8

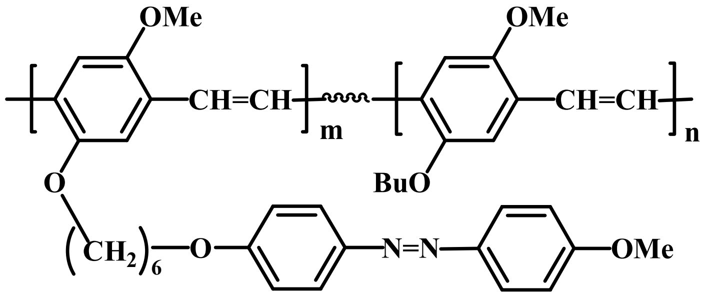

9

Figure 1-2. Conjugated Organic Copolymers

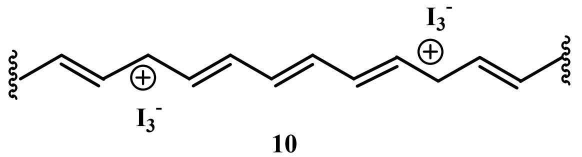

10

doped trans-polyacetylene

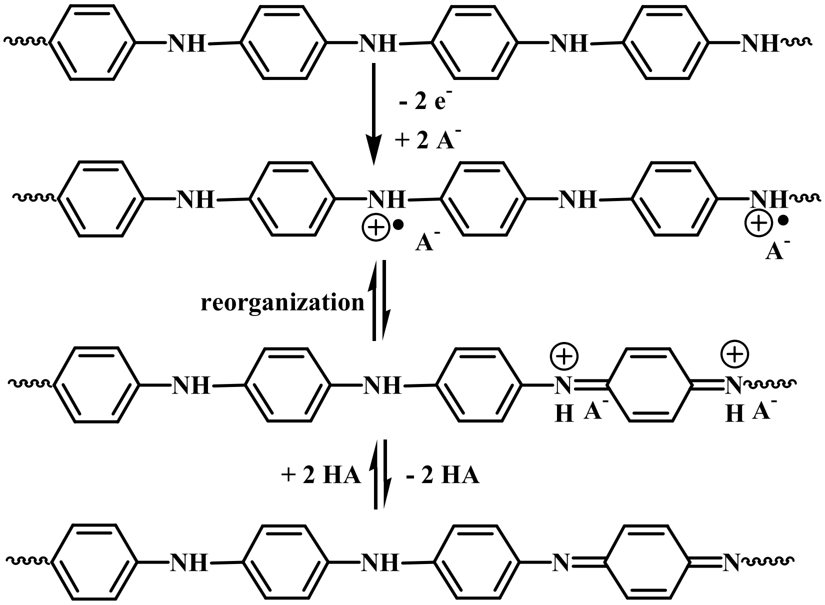

11

doped polyaniline

Figure 1-3. Doped Conjugated Polymers

acid (HA) or base (B), the introduction of charge carriers into polymers is inevitably accompanied by the introduction of counter-ions (Ox $^-$, A$^-$ or B$^+$). In Figure 1-3, I_2 grabs electrons from π–conjugated polyacetylene during I_2 redox doping and leaves the polymer main chain carrying positive charges with I_3^- as the counter-ion (**10**). Similarly, the loss of electrons resulted in the polyaniline chain carrying positive charges with A$^-$ as the counter-ion (the upper part of **11**). For acid doping of oxidized polyaniline, protons in the acid are captured by the electron pair of nitrogen, thus making the polymer chain carry positive charges with A^- (the conjugate base of the acid HA, the lower part of **11**) as the counter-ion. These charged species go through a reorganization of π–electrons in the benzenoid rings attached to the two neighboring nitrogen atoms to form unpaired electrons, which then delocalize along the chain to yield semiquinoid units. While the charge carriers can be delocalized along the conjugated main chain, the counter-ions are not delocalized.[45] This lack of mobility can influence the electronic properties of polymers and may even destabilize the conjugated polymers.

To overcome these limitations, current research efforts are largely directed toward the synthesis of intrinsically conductive organic polymers, materials that do not require redox or acid-base doping. Intrinsic conductivity is very critical and desirable for many specific applications. For example, intrinsically conductive organic materials show considerable promise for the simple fabrication of the conductive films for electromagnetic shielding or antistatic protection.

π–Conjugated organic polymers are one of the organic materials that can be further developed to become conductive organic materials. Since organic polymers allow virtually endless control on their structures, π–conjugated organic polymers can be designed to increase their electron transport ability within the π–system by manipulation of their π–orbitals. By comparing to or imitating real metals, scientists have determined that the π–orbitals in a polymer must fully overlap to form energy bands. This can be achieved by increasing π–conjugation length over the polymer chain. With the π–system in conjugated polymers getting bigger or the polymer chain becoming longer, more π orbitals are produced in the HOMO and LUMO region and the energy difference between adjacent levels decreases. After a point, the discrete energy levels eventually form conduction and valence bands as shown in Fig.1-4.

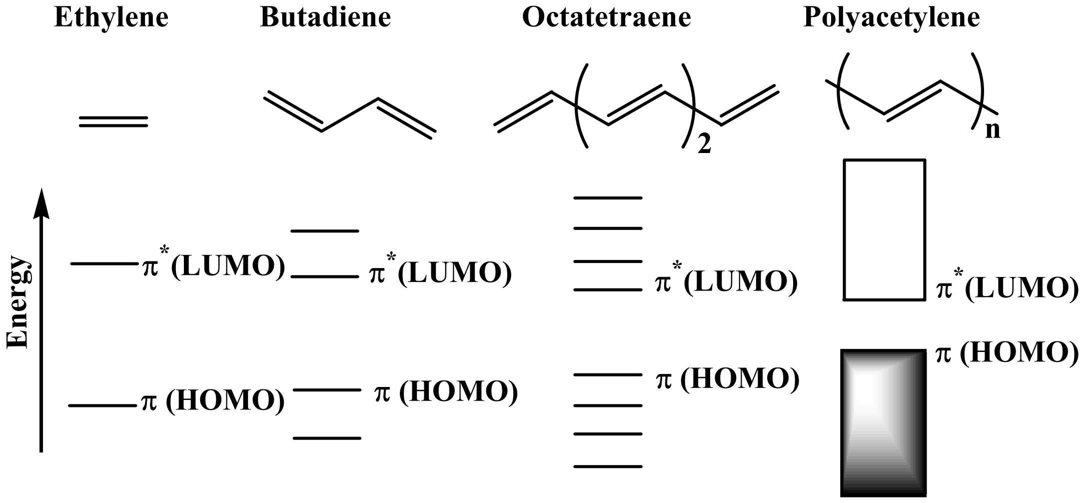

Figure 1-4. Molecular Orbital (MO) Diagram for Polyacetylene

Another important design requirement for intrinsically conducting organic polymers as analogs of metals is to minimize the band gap between the conduction band and the valence band, which in π−conjugated polymers still approach those of semiconductors, while the band gap in metals is zero or close to zero. Only after the band gap between the HOMO and LUMO bands in an organic polymer approaches zero to form one partially filled valence band, can the conjugated polymer become a true organic metal with intrinsic conductivity (Fig. 1-5). Structure manipulation and high conjugation in polymer chains can be two of the key factors to reduce the band gap.

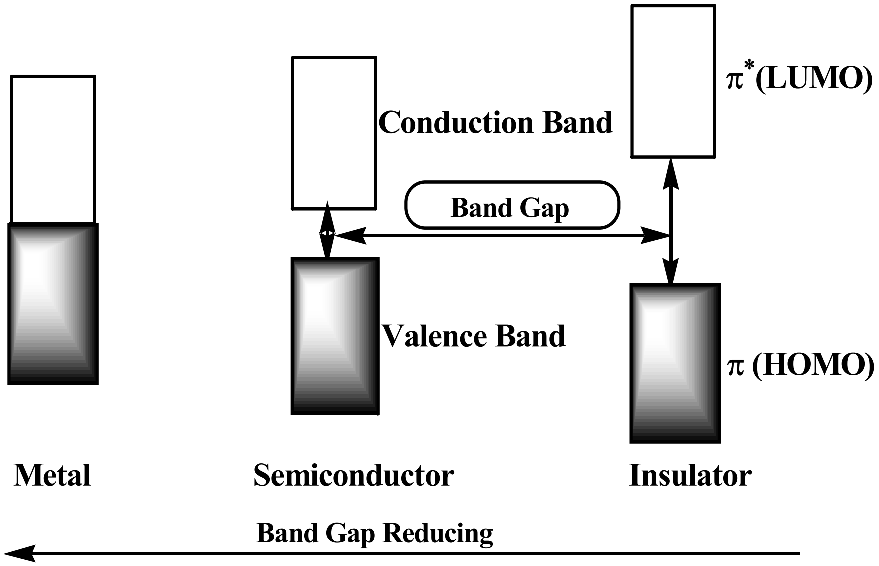

Figure 1-5. Conductivity Changes with Band Gap

While some conjugated polymers with high molecular weight have been obtained, as we see in Fig. 1-1 and 1-2, both experimental and theoretical efforts have focused on band gap reduction engineering. Well-known approaches are mainly aimed at making π−orbitals further delocalized, obtaining equal bond lengths along the polymer chain, or increasing the double bond character between aromatic chromophores to form quinoid structures. In this way, the band gap between a "bonding" ground state and "anti-bonding" excited state will be zero or close to zero due to the equivalence of both structures.[45] For instance, the band gap of polyisothianaphthenes (PITNs, Fig. 1-6) is greatly reduced by making the quinonoid structure energetically more favorable through fused six-membered rings gaining aromaticity. Ladder polymers (Fig. 1-7) were designed

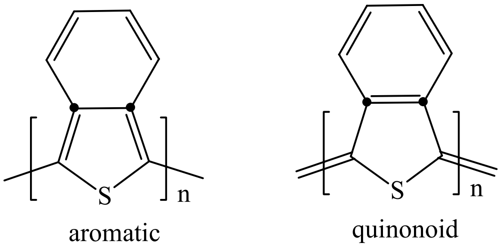

Figure 1-6. Poly (isothianaphthene)

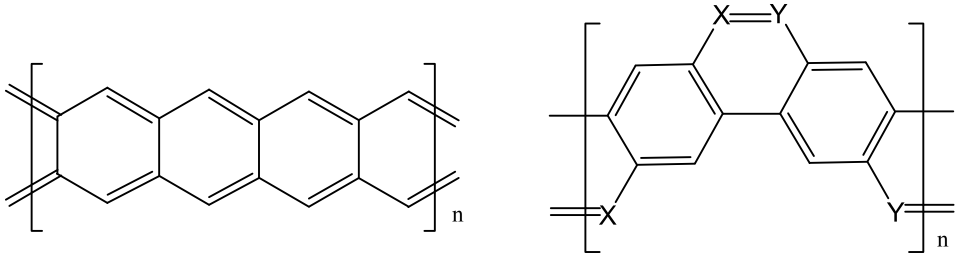

Figure 1-7. Ladder Polymers

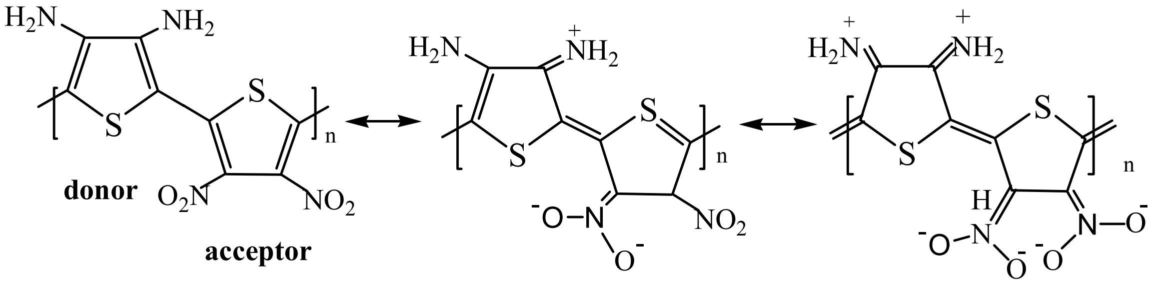

Figure 1-8. Alternation of Electron-Donors and Acceptors

to have a small band gap by reducing the structural deformations to avoid localization of alternating double-single bonds. And donor-acceptor polymers were also synthesized to reduce the band gap by alternating electron-donors and acceptors in the main chain to give rise to increased double bond character between these donor-acceptor units and reduce the difference of alternating double-single bond length (Fig. 1-8). Although the first narrow band gap polyisothianaphthene (Fig. 1-6) with Eg = 1.1 eV and dozens of its derivatives have been prepared, a conjugated polymer with a vanishing band gap has not yet been synthesized.[34] According to the "Peierls effect",[45] bond length alternation is a result of structure deformation that keeps a rigid linear polymer chain stable. This electronic energy gain overcompensates the loss of 'elastic' energy and determines the finite band gap existing in linear conjugated polymers. Therefore, we believe that it will be very difficult to achieve zero band gaps in linear conjugated polymer system through only minimization of bond length alternation. More effort on elaborate molecular designs and structure modifications for conjugated polymers are required to make the band gap smaller or close to zero. Consequently, the search for other strategies such as applying novel building blocks with unique electronic and photonic properties or having different electron transfer mechanisms into the conjugated polymer may be necessary to further reduce the band gap.

1.2 Porphyrin-based organic materials

1.2.1 Monomeric porphyrin

Porphyrins are one of the most attractive building blocks for the construction of conjugated and conductive organic polymers due to their unique chemical and physical properties.[46-56] It has been recognized for almost one century that porphyrins play an extremely important role in life. The energy processes, photosynthesis and cellular metabolism, that make life on Earth possible, are mainly driven by the high efficiency of electron and energy transfer processes in porphyrin systems.[57] Since nature has selected and utilized porphyrins for their outstanding electronic and optical properties, it is reasonable to consider porphyrins as excellent building blocks in the search for new organic materials.

Great effort has been devoted to elucidate the basis for the chemical, physical, and spectroscopic properties that porphyrins display. It has been demonstrated that the monomeric porphyrin, an aromatic macrocycle composed of 20 carbon atoms and 4 nitrogen atoms (Fig. 1-9), exhibits many interesting properties that may be useful in organic materials, including (1) chemical and thermal stability; (2) rigid planar geometry (Fig. 1-9); (3) intense UV-Visible absorption, fluorescence and phosphorescence emission (Fig. 1-10); (4) the ability to coordinate metals (Fig. 1-11); (5) rich substitution chemistry; (6) heteroatom-containing aromatic system; (7) through-space electron transfer between porphyrin molecules; and (8) small HOMO-LUMO energy band gap of monomeric porphyrin molecules.

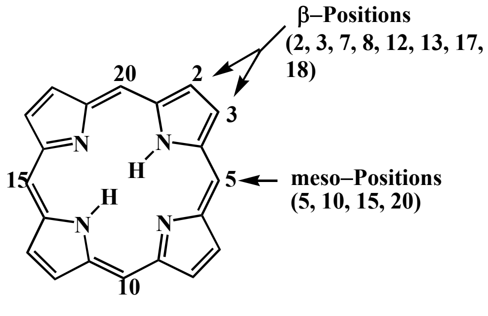

Figure 1-9. The Core Structure of Porphyrins

Chemical and thermal stability are the basic requirements for organic materials to maintain functions under various work conditions. Rigid planar geometry (Fig. 1-9) can contribute to good mechanical properties, and may help to extend the conjugation of the polymeric materials. Intense UV-Visible absorption, fluorescence and phosphorescence emission (Fig. 1-10) are the properties most widely utilized in electronic and optical devices. The ability to coordinate over 50 metals can produce flexibly tunable electronic, optical and redox properties in porphyrin materials upon appropriate metalation (Fig. 1-11). Furthermore, it is well known that metals in the centers of porphyrins can perform metal-to-metal or metal-to-ligand electron transfer.[58] When metalloporphyrins are incorporated into polymer chains, the electron or charge transporting ability in each chromophore can help to increase conductivity along the porphyrin polymer chains. The insertion of different metals can be used to tune the conductivity or band gaps of these materials.

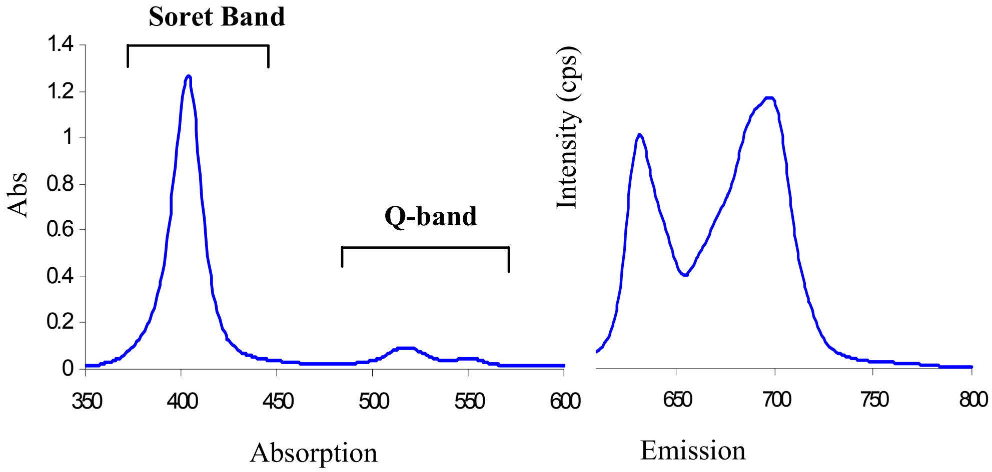

Figure 1-10. **Absorption and Emission Spectra of 5,15-bis(2,4,6-triisopropylphenyl)-10*H*, 20*H*-porphyrin**

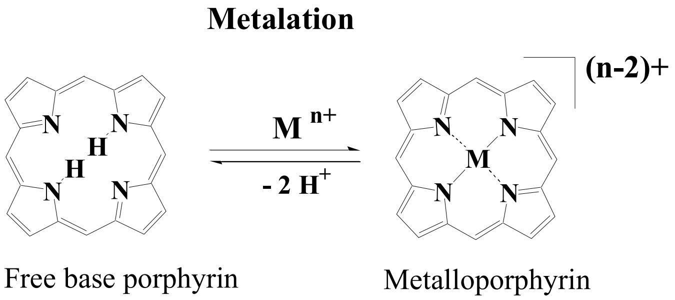

Li												B			
Na	Mg*											Al	Si		
K	Ca	Sc	Ti	V*	Cr	Mn*	Fe*	Co*	Ni*	Cu*	Zn*	Ga	Ge	As	
Rb	Sr	Y	Zr	Nb	Mo	Tc	Ru	Rh	Pd	Ag	Cd	In	Sn	Sb	
Cs	Ba	La	Hf	Ta	W	Re	Os	Ir	Pt	Au	Hg	Tl	Pb	Bi	
				Ce	Pr				Eu	Gd					Yb
				Th		U									

* found in nature

Figure 1-11. Metals Suitable in the Metalation of Porphyrins

The rich substitution chemistry, with twelve sites (8 *β*-positions, and 4 *meso*-positions, Fig. 1-9) on the porphyrin periphery, allows a variety of structural designs that may be used to optimize the performance of porphyrin materials. For example, the possible substitution of porphyrin monomers furnishes more approaches to overcome the solubility problems commonly encountered in π–conjugated polymers, owing to strong π–π interaction. There are more positions or different ways to attach solubilizing groups to interrupt π–π. interactions between molecules or polymer chains. We can construct straps above and below the porphyrin plane to prevent the porphyrin from interacting with each other (Fig. 1-12). In addition, with many substitutable sites of substitution on the periphery, porphyrin molecules can offer more possibilities and easier access to add electron donating and accepting groups to increase intramolecular charge transfer (ICT) to make small band gap polymers. ICT can result in consecutive zwitterion-like interactions with high double bond character between the repeat units for stabilizing the quinoid forms (Fig. 1-13),[59] which will further delocalize π–conjugation in polymers and result in a smaller band gap.

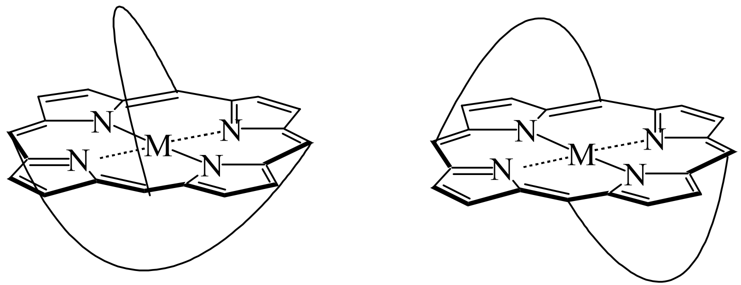

trans-strapped porphyrin cis-strapped porphyrin

Figure 1-12. Strapped Porphyrins for Increasing Solubility

D: Electron-donating monomer
A: Electron-accepting monomer
ICT: Intramolecular Charge Transfer

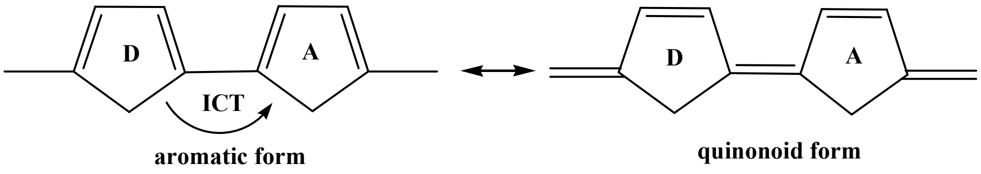

Figure 1-13. Donor-Acceptor Structure for Small Band Gap Polymers

Porphyrins are also heteroatom-containing compounds (Fig. 1-9). Having heteroatoms in the conjugated polymer chain can help to further minimize the band gap. Though the π–system of hydrocarbon polymers is formed by the overlapping of carbon p_z orbitals, the orbitals of nitrogen atoms can also contribute to the conjugation in porphyrin polymers. Despite the fact that the effects of these contributions on band gap minimization are not well understood, polarizable heteroatoms support the formation of radicals and cations, and in some cases contribute p_z and d electrons to conjugation. Each of these contributions can be used to tune the band gap of corresponding materials. Through-space electron transfer between porphyrin molecules, which does not often occur in other organic materials, introduces a different conducting mechanism and provides another path to further increase the conductivity of porphyrin materials. This is one of the unique features that make porphyrins very useful in photosynthesis and other energy conversion activities. Since the proper orientation of porphyrin molecules in the system is necessary for through-space electron transport, this through-space electron transfer ability can be controlled for different application purposes by linking porphyrin molecules in the desired orientation along the polymer chain. Finally, given that the average HOMO-LUMO energy band gap (Eg) of the porphyrins is about 2.2 eV,[50] the monomeric porphyrin already approaches the band gap of some conjugated polymers, such as polythiophene (Eg is around 2.1 eV).[34] The intense color and the ability of porphyrins for photosynthesis and electrical transportation originate from their easy $\pi-\pi^*$ and $n-\pi^*$ electron transitions due to the small energy band gap. Considering the general trend that the energy band gap is always reduced in conjugated oligomers and polymers compared to monomers, this already small band gap of porphyrin monomers should result in conjugated polymers with much smaller band gaps than most of other conjugated polymer systems. These chemical, physical and spectroscopic properties in free base porphyrins and metalloporphyrins demonstrate that they are not only one of the most interesting building blocks for organic materials, they also provide great potential for the synthesis of intrinsically conductive polymers.

The extraordinary richness of synthetic porphyrin chemistry can offer hundreds of porphyrin molecules and many sophisticated methodologies to synthesize novel porphyrin molecules as building blocks for the construction of organic materials. During the past years, the study of porphyrin complexes and arrays has been a rapidly expanding research field. It has not only helped in our understanding of photosynthetic processes and other related properties in various porphyrin systems, such as enzyme catalysts, optical switches, molecular photonic or electronic wires, and light-harvest arrays, but also laid the foundation for the future development of advanced porphyrin materials including conjugated and conductive porphyrin polymeric materials. The unique properties and electronic and photonic communication in porphyrin oligomers and polymers can be deduced from the properties and behavior exhibited in porphyrin complexes and arrays.

Some porphyrin complexes, such as diad **13**, triad **14** or tetrad **15** (Fig. 1-14), have been prepared to mimic natural reaction center complexes where basically one porphyrin and one quinone molecule are embedded in a protein for the conversion of light to chemical energy, as in biological systems. In these photosynthetic complexes, one or two porphyrins are electron donors and one or two quinones are electron acceptors. The photo-induced electron transfer (PET) takes place within about 3 ps after singlet excitation of porphyrins and the initial energy conversion proceeds with a quantum yield of nearly unity owing to the strong photon absorbing and energy transporting ability of porphyrins. These porphyrins-quinone model systems are of fundamental importance for the study of electron transfer (ET) in many organic materials applications, such as photovoltaics,[60] solar energy conversion,[61] and ET processes in DNA.[62] Porphyrin array

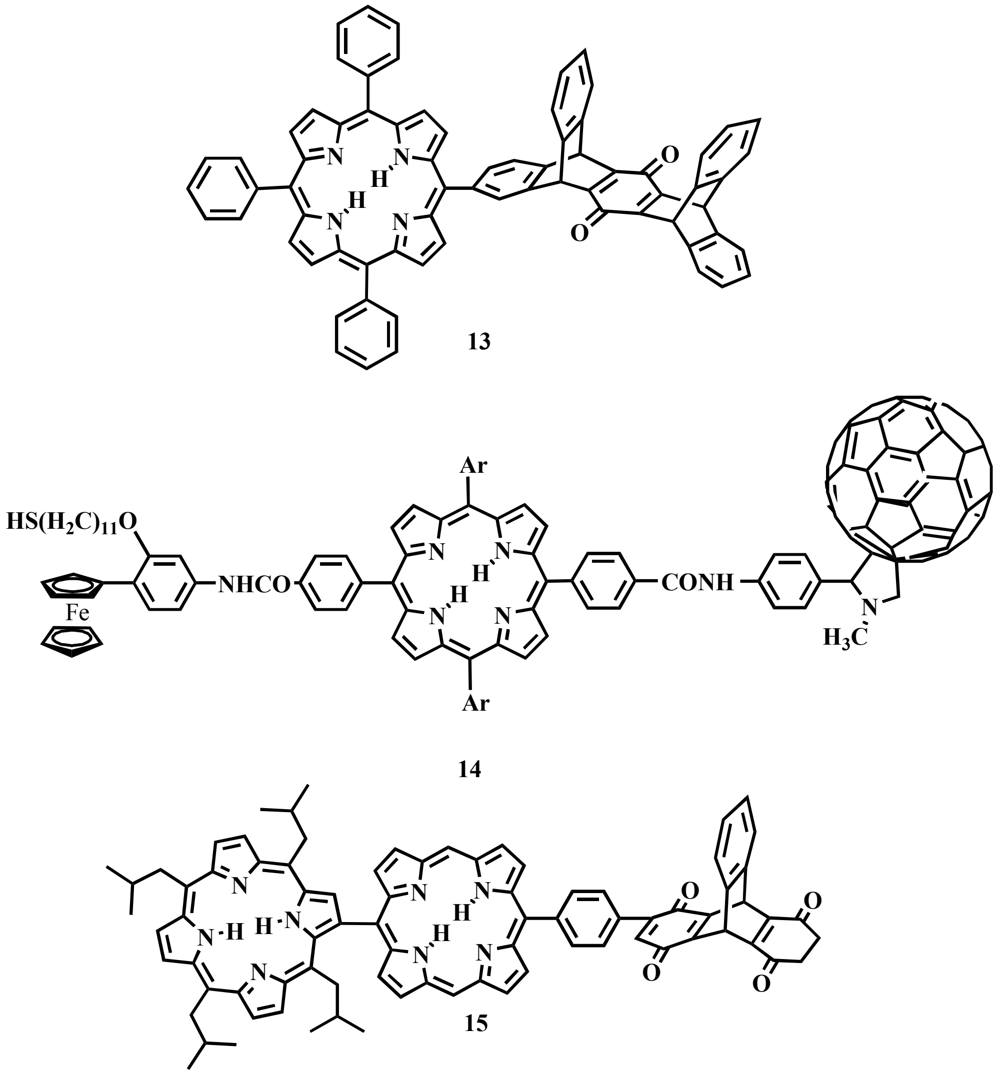

13

14

15

Figure 1-14. Porphyrin Complexes

16 (Fig. 1-15) is used as a photosynthetic light-harvesting system or antenna system for probing the effects of molecular organization on electronic communication.[63,64] These excellent experimental observations provide sound foundations for further study and investigation of porphyrin oligomers and polymers.

16

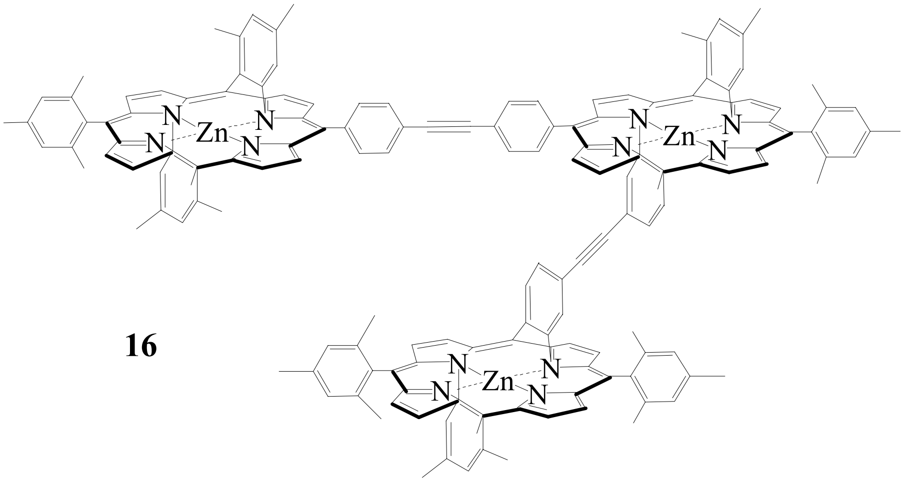

right-angled trimer

Figure 1-15. A Porphyrin Light-harvesting System

1.2.2 Porphyrin oligomers and polymers

As mentioned above, porphyrin arrays are often used as model systems for their corresponding porphyrin polymers. These precise models provide specific information on various properties for polymeric systems. Studies have demonstrated that when monomeric porphyrins are incorporated into oligomeric and polymeric materials, the resulting materials exhibit many properties different or beyond the performance of monomeric porphyrins. For example, preliminary research has indicated promising results that extended π−conjugation in porphyrins can greatly reduce the HOMO-LIUMO energy band gap. As an example shown in Fig. 1-16, ZnDPP (Zn-tetraphenylporphyrin) (**17**) has a band gap Eg = 2.29 eV, but the band gap of the dimer (**18**) of ZnDPP (**17**) is dropped to Eg = 1.81 eV.[50] The reduction of band gap in the conjugated porphyrin system is very efficient. Since porphyrin systems offer many possibilities for manipulating monomers, it is predictable that the band gap of porphyrin polymers will be further reduced through the achievement of a high degree of polymerization or fully extended π−conjugation with the help of designed construction strategies. The absorption and emission spectra of conjugated polymeric or oligomeric porphyrins are red-shifted and the Q-band absorption intensity increases (Fig. 1-17). The red shift of maximum absorption is due to the extended conjugation in the polymer or oligomer chain, reflecting a decreased energy band gap. The absorption intensity increase is due to the structure changes such as symmetry changes, resulting in switches between allowed and forbidden

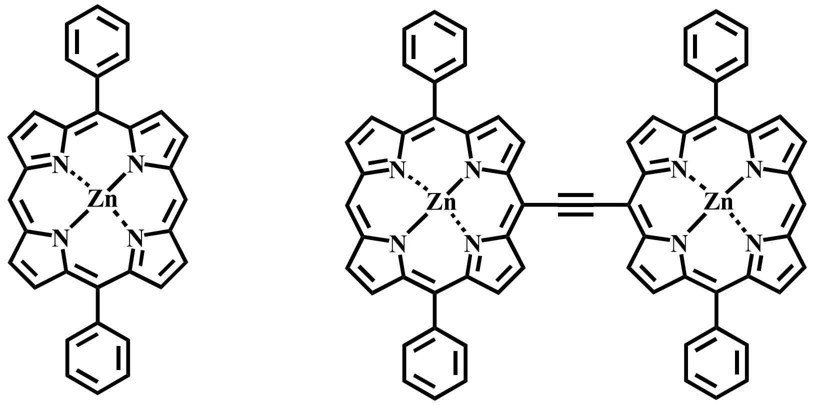

17 **18**

Figure 1-16. Structures of ZnTTP and its Dimer

excitations. The increased absorption maximum wavelength and intensity are greatly desirable for applications in light-emitting devices (LEDs) or photodynamic therapy

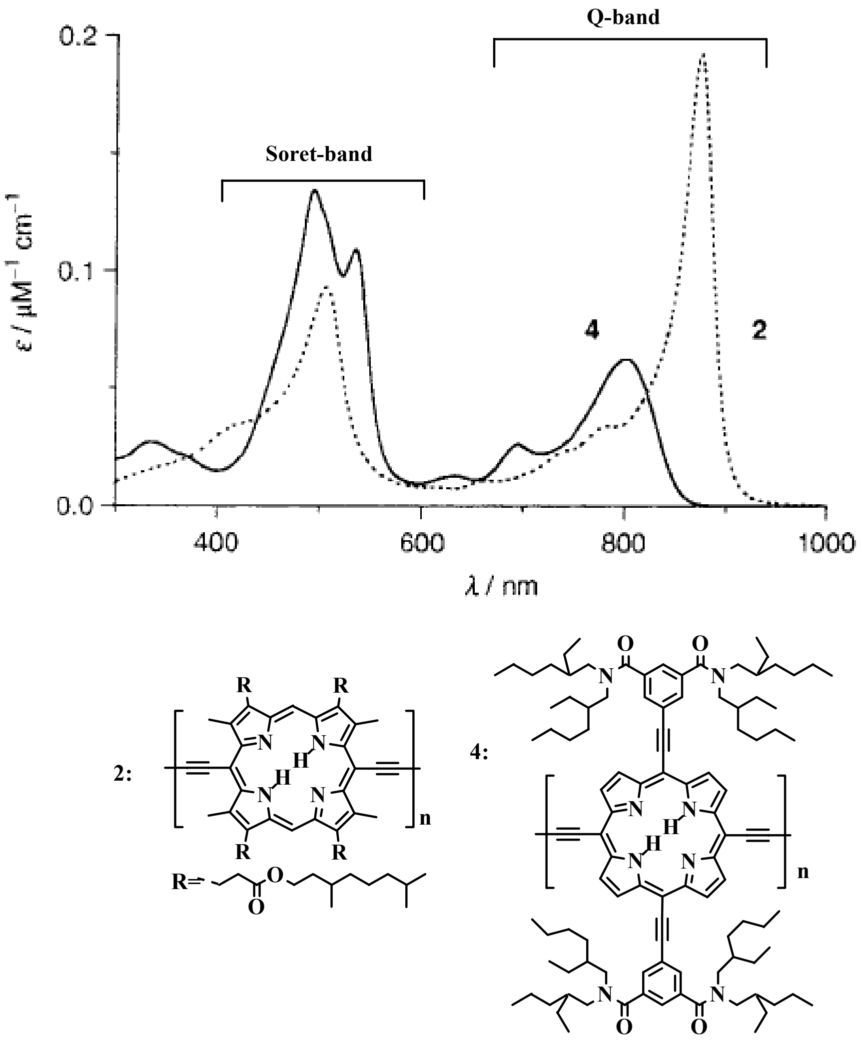

Figure 1-17. Absorption Spectra of Two Porphyrin Polymers[47]

(PDT). In LEDs, the emitting light color can be tuned from near-infrared to blue by adjusting different degrees of polymerization or conjugation length. In PDT applications, longer wavelength (red light) is more desirable for the irradiating light to travel a long way through tissue and helps to produce highly toxic singlet oxygen inside tumors. Low energy (long wavelength) light travels further through tissue than does high-energy light (which gets scattered). Substantial π-electron delocalization along the conjugated porphyrin polymer backbone also leads to large third-order electronic polarizability, which is useful in unique nonlinear optical (NLO) devices.[47,48,50] Metalloporphyrins incorporated into electrochemically polymerized polymer electrodes have also been developed as efficient electrocatalysts for chemical as well as for photochemical applications, or used directly as chemical and biological sensors.[50]

Tremendous efforts have been dedicated to obtain a wide variety of porphyrin-based polymeric materials for their interesting properties and potential applications. The porphyrin materials systems that have been prepared and studied intensively include porphyrin oligomers,[47,50,51,65-67] porphyrin dendrimers,[68] porphyrin copolymers,[8,12,15,24-28,30,69-75] porphyrin polymers[46-48,50,52-56,76-83] and other porphyrin-containing materials.

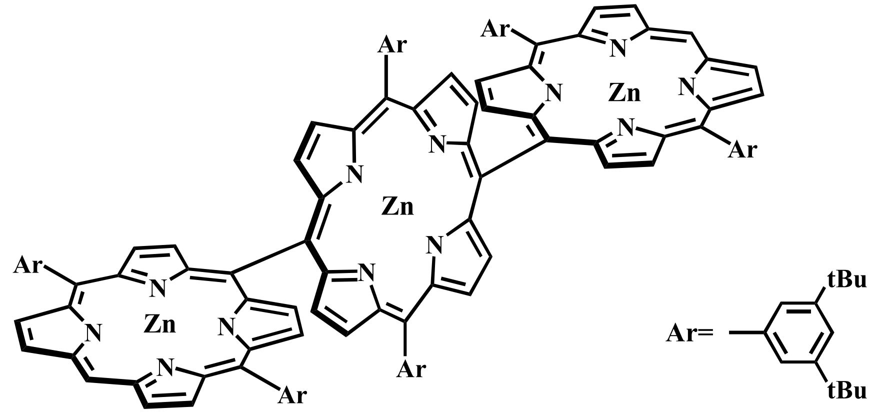

Figure 1-18. Steric Hindrance Prevents Coplanar Conjugation of Porphyrins[84]

Since steric hindrance between directly bonded porphyrin units often disturbs the formation of an extended π–conjugated system (Fig. 1-18), the common strategy to make a conjugated porphyrin polymer is to incorporate π–structured spacing groups between aromatic porphyrin units. The most commonly used spacing groups are shown in Fig. 1-19.

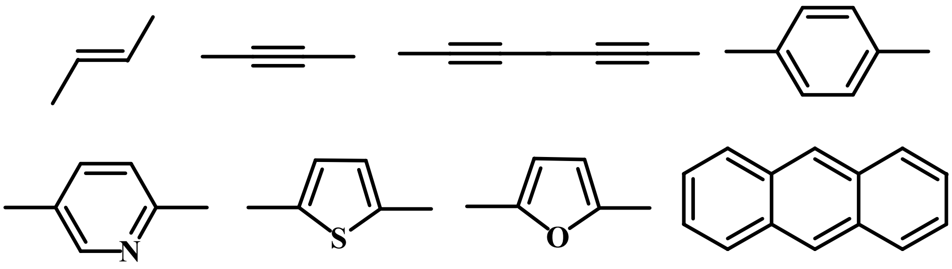

Figure 1-19. Spacing Groups Used in Conjugated Porphyrin Polymers

A variety of conjugated porphyrin oligomers and polymers or copolymers have been synthesized and studied intensively by bridging these spacing groups between porphyrins units. Examples of conjugated porphyrin materials recently developed are shown in Fig. 1-20 to 1-22.[47,55,79,82,85]

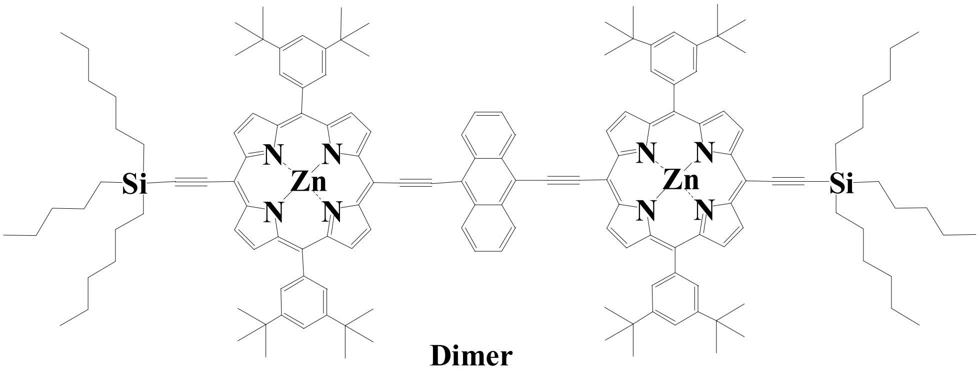

Figure 1-20. A Conjugated Porphyrin Dimer

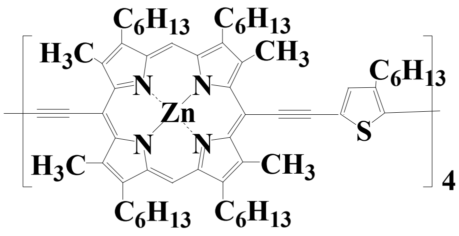

Oligomer 1

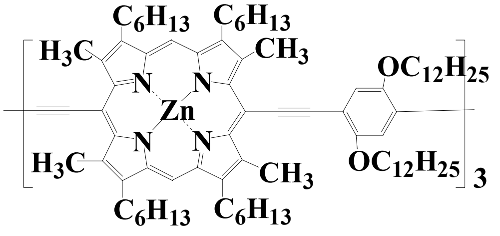

Oligomer 2

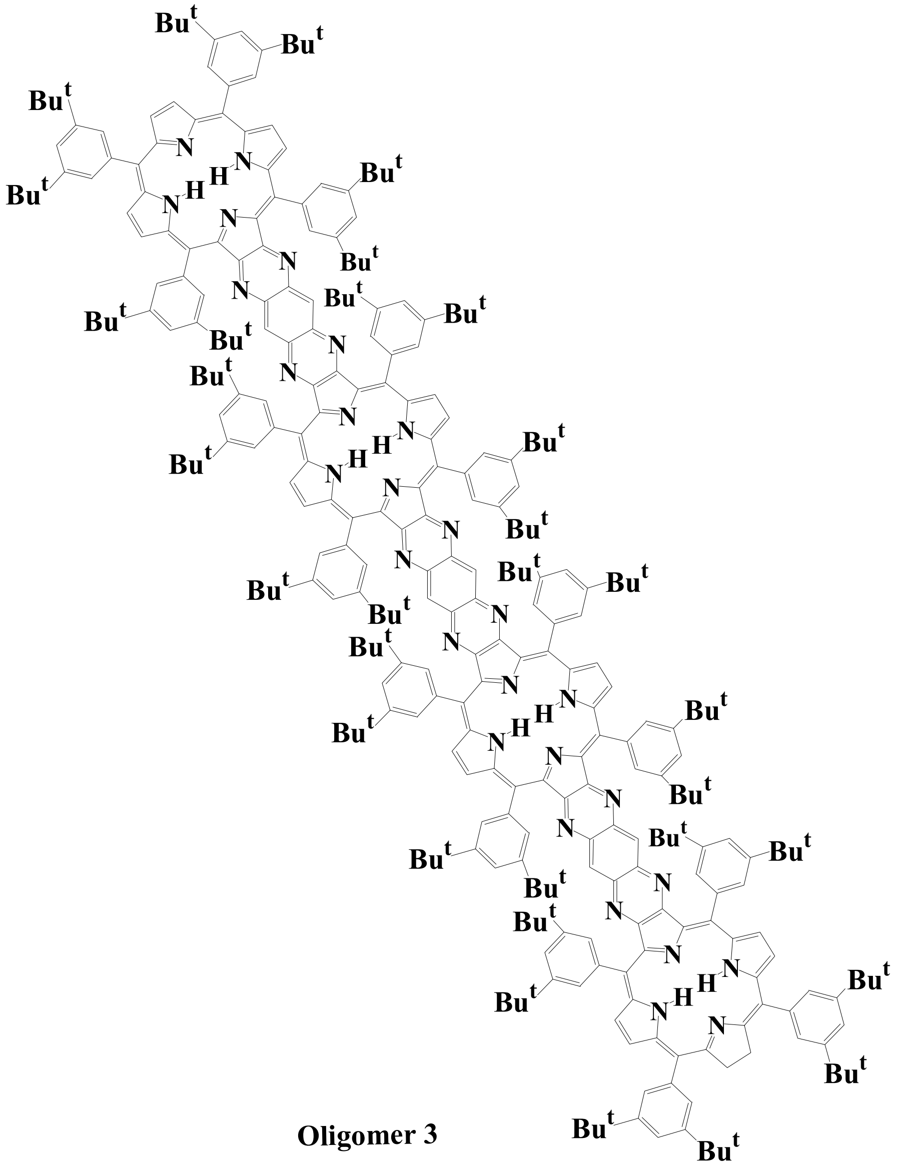

Oligomer 3

Figure 1-21. Conjugated Porphyrin Oligomers

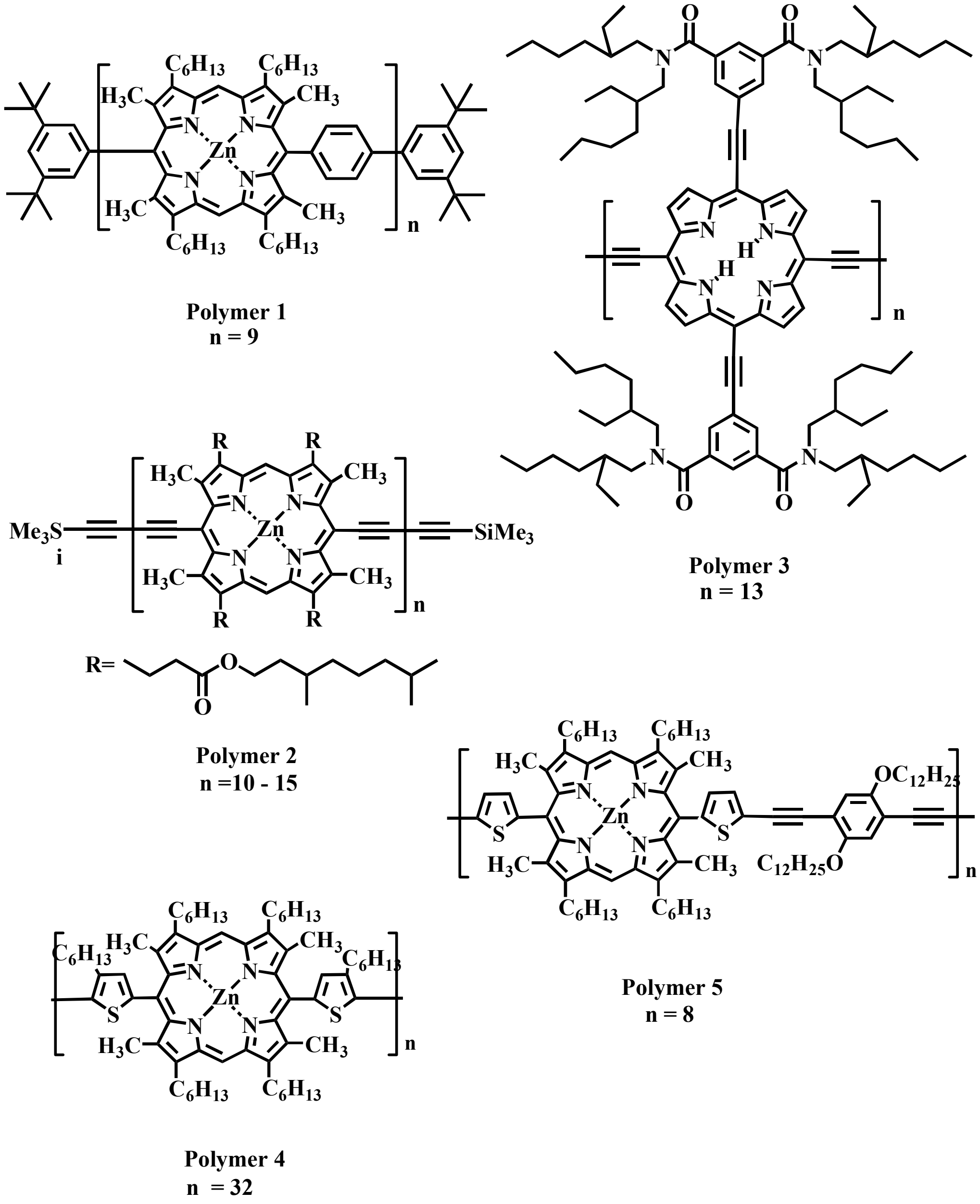

Polymer 1
n = 9

Polymer 2
n =10 - 15

Polymer 3
n = 13

Polymer 4
n = 32

Polymer 5
n = 8

Figure 1-22. Conjugated Porphyrin Polymers

In addition to properties related to their corresponding monomers and those property changes mentioned before, these porphyrin oligomers and polymers have also exhibited many unique properties including photo-activity,[37,86-91] conductivity,[77,78,92,93] luminescence,[78,82] and especially remarkable nonlinear optical (NLO) behavior with high third-order susceptibilities $\chi^{(3)}$.[47,48] These properties are presumably due to large and polarizable π−systems, long conjugation lengths and small HOMO-LUMO energy band gaps. The potential applications of these porphyrin materials are mainly in solar energy conversion,[61,94,95] organic metals,[34] LEDs,[64-66,96-105] ultra-fast switching technology,[49] catalysts,[106-109] liquid crystals[52,78] and so forth.

For example, the porphyrin oligomer **3**[50] (Fig. 1-21) can be an approach to porphyrin-based molecular wire, because such porphyrin systems can meet the criteria for the realization of molecular electronic devices: (1) It is electron conducting. (2) It has a defined length capable of spanning a supporting element such as a monolayer or bilayer lipid membrane. (3) It has porphyrins as termini to allow redox reactions. In this system, the electrical conductivity is achieved through porphyrin rings being bridged by coplanar aromatic systems and that porphyrin can be readily oxidized or reduced to π−cation radicals or π−anion radicals. This example demonstrates that the unique chemical property (redox reversibility) of porphyrins has contributed to the electrical conductivity of the materials. Therefore, it further demonstrates that porphyrin molecules are good building blocks for conducting materials not only due to their unique macro π−system structures but also due to their chemical or electronic properties.

1.2.3 Current limitations of porphyrin materials

Despite the remarkable properties exhibited by porphyrin-based materials, there are several limitations or difficulties in the field that prevent this group of advanced materials from being fully explored and exploited. These limitations include low solubility of porphyrin monomers, oligomers and polymers, and lack of appropriate polycondensation or polymerization methods for constructing high molecular weight and high quality conjugated porphyrin polymers.

1.2.3.1 The solubility of porphyrins

Porphyrins are a class of compounds with intrinsically low solubility in both aqueous solutions and organic solvents, owing to their fundamentally hydrophobic aromatic rings and exceptionally strong π−π interactions among porphyrin molecules. The solubility of alkylporphyrins (with different alkyl chains substituted on either the *meso*−, or the *β*–position of porphyrin) ranges from 0.02 to18.40 mmol/L or from 0.01 to 9.2 g/L.[110] When such a large π−system is further extended through conjugation in porphyrin polymers, the π−π interaction between polymer chains becomes even stronger. As it has been recognized that π−π interaction is a major force to drive aggregation and precipitation of porphyrin molecules, the stronger π−π interaction in porphyrin oligomers and polymers will certainly cause the solubility of these systems to be even lower than porphyrin monomers. Among the porphyrin materials shown in Fig. 1-21 and 1-22, the solubility of "soluble porphyrin polymers" is only around 2 g/L, for other porphyrin polymers referred to as partially soluble or insoluble, the solubility is even lower.[82]

As we see in Fig. 1-21 and 1-22, long-chained or branched side groups are utilized as solubilizing groups in almost every porphyrin oligomer or polymer. Since porphyrin materials are typically synthesized and processed in organic solvents, the application of long-chain or branched solubilizing groups in porphyrin polymers seems to be the best way so far to increase solubility of porphyrin materials. However, the solubility of these porphyrin materials is still unsatisfactory.

The low solubility of porphyrin molecules and materials will not only result in processing problems, but also limit the formation of higher molecular weight porphyrin polymers or conjugation length to obtain a small energy band gap. By structure analysis of porphyrin materials and our understanding of the major driving force in porphyrin systems, we believe that the low molecular weight of porphyrin materials is closely related to their low solubility. The authors, who made some of the porphyrin materials shown in Fig. 1-21 and 1-22, also mentioned that “these polymers prepared did not show high solubility, presumably due to a tendency to form a π−π stacked structure between the zinc porphyrin units.”[82] The comparison between porphyrin polymer **4** and oligomer **1** (Fig. 1-23) can be used to demonstrate the relationships between molecular weight (porphyrin units in polymer chains), extended conjugation (coplanar structures) and solubility. Polymer **4** contains about 32 monomer units while oligomer **1** has only 4 monomer units (both calculated according to GPC) in the chain. They both have the same solubilizing group ($-C_6H_{13}$) and the same spacing group (thiophene). The only difference is in the position of the acetylene spacing group between the porphyrin and thiophene units in the chains of oligomer **1**. This structural difference causes many differences for porphyrin-porphyrin intramolecular and intermolecular interactions, and the π−system. Polymer **4** has the thiophene group directly linked to porphyrins. The repulsion between the 4-proton on thiophene and the methyl group on the *β*−position of the porphyrin forces the thiophene plane away from a coplanar conformation with the porphyrin plane and results in decreased overlap of their π−systems. Oligomer **1** has an acetylene bridge between the thiophene and the porphyrin. The separation of proton-4 on the thiophene from the methyl group on the β–position of the porphyrin eliminates the repulsion, and

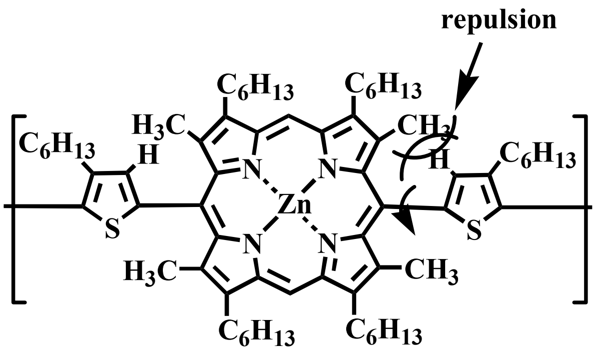

Polymer 4
n = 32 (GPC)

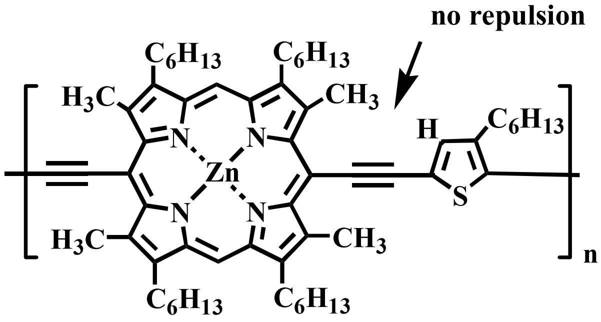

Oligomer 1
n = 4 (GPC)

Figure 1-23. Structural Comparison of Polymer 4 and Oligomer 1

allows these π–systems to remain coplanar over the entire length of the polymer backbone. Oligomer **1** therefore has a larger π–system, which introduces stronger π–π attraction between polymer chains. When the polymer chains grow, attractions between oligomer **1** chains increase and finally reach a point where the chains start aggregating and precipitating, therefore preventing further growth. In contrast, polymer **4,** with less attraction between their growing chains, can maintain soluble in the solution and continue to undergo chain growth. This explains why under the same polymerization conditions, polymer **4** grows to about 32 units in the chain, while oligomer **1** only reaches 4 porphyrin units.[82]

1.2.3.2 Current synthetic methodologies for porphyrin materials

There are versatile synthetic routes for constructing organic polymers, such as stepwise polymerization through functional groups or coordination, or chain reaction polymerization through free radical or ring-opening processes. For the synthesis of conjugated organic polymers, the fundamental challenge is to use typical organic chemistry methodology to construct covalently linked (mostly C-C covalent bonding) polymer structures by formation of conjugated linkers between aromatic building blocks (unsaturated carbon linkers). There are various metal-catalyzed C-C coupling reactions to form covalent bonds between unsaturated carbon atoms. These include

1. Heck reaction: Pd-catalyzed coupling of aryl and alkenyl halides with alkenes.
2. Suzuki reaction: cross coupling of organoboron compounds with organic halides.
3. Other cross coupling with organometals containing Zn, Mg, Al, Zr, Sn, etc. to build unsaturated C-C bond linkers.

In the porphyrin-based materials field, most of the conjugated porphyrin materials are synthesized through these metal-catalyzed C-C coupling reactions, especially Pd (Cu)-catalyzed coupling among dihalogenated or diethynylated porphyrins and spacing groups to form an ethyne-linked porphyrin polymer, or oxidative homocoupling to form a butadiyne-linked porphyrin polymer (Scheme 1-2).[34,55,82]

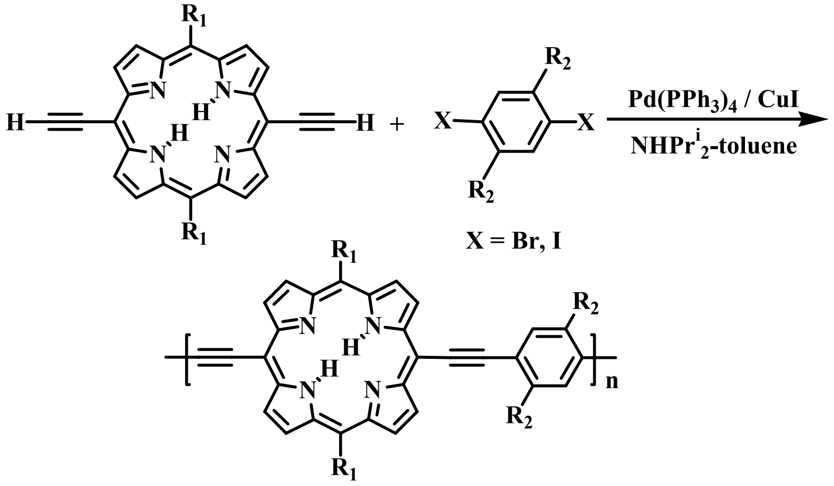

Pd(0) mediated ethyne-linked porphyrin polymer

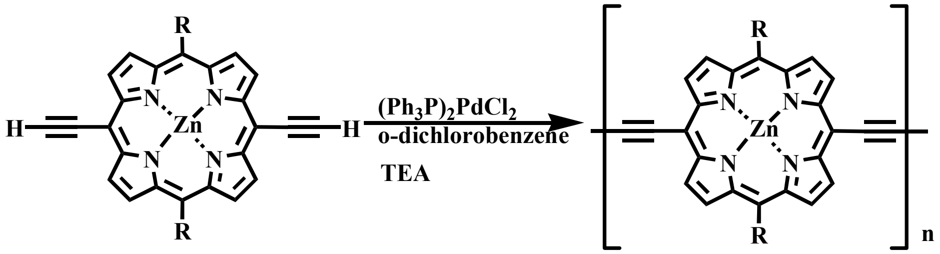

Pd(II) mediated butadiyne-linked porphyrin polymer

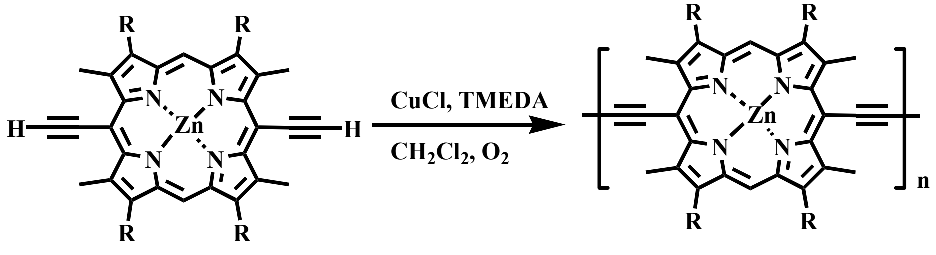

Cu(I) mediated butadiyne-linked porphyrin polymer

Scheme 1-2. Pd and Cu-mediated Coupling for the Preparation of Porphyrin Polymers

According to some reports, there are several distinct shortcomings in the popular Pd and Cu-catalyzed coupling reactions: (1) Pd (or Cu) is one of the metals in the main chain of transition metal-acetylide polymers (Fig. 1-24),[111] which indicates that Pd (or Cu) can be very stably linked with acetylene groups that result not only in defects of the porphyrin polymer chains, but also prevent further chain growth owing to the metal-capping at the end of polymer chains. (2) Some butadiyne defects are produced in the ethyne-linked porphyrin polymers due to the homocoupling of alkyne monomers, which is promoted by Pd(II) in the presence of oxygen and the necessary reduction of the Pd (II) catalyst precursors. (3) The end groups in polymers are sometimes ambiguous due to the Pd-capping, dehalogenation or transfer of triphenylphosphine (PPh_3) group to the end of the chain. (4) The complete removal of palladium and phosphorus-containing catalyst residues is not always facile.[112] Therefore, the search for alternative polymerization methods is necessary to construct high quality conjugated porphyrin polymers.

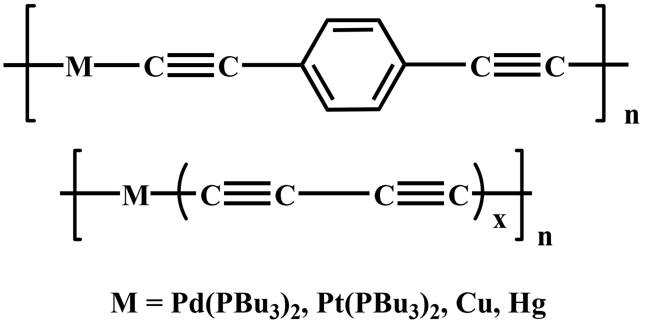

Figure 1-24. Transition Metal-Acetylide Polymers

1.2.3.3 Molecular weights of porphyrin materials

The molecular weights of porphyrin materials are relatively low compared to other conjugated polymers built from different building blocks. By searching the literature about porphyrin materials, the longest porphyrin polymer made in Professor Aratani's group in Kyoto University of Japan is a *meso-meso* coupled porphyrin 128-mer (Z128, $C_{8192}H_{10498}N_{512}O_{512}Zn_{128}$),[103] but it is not a conjugated porphyrin polymer because each porphyrin unit in this polymer chain is perpendicular to its neighboring porphyrin units (Fig. 1-25). Among conjugated porphyrin polymers published up to date, there are no polymers that have more than 32 units (by GPC calculation) in the chain.

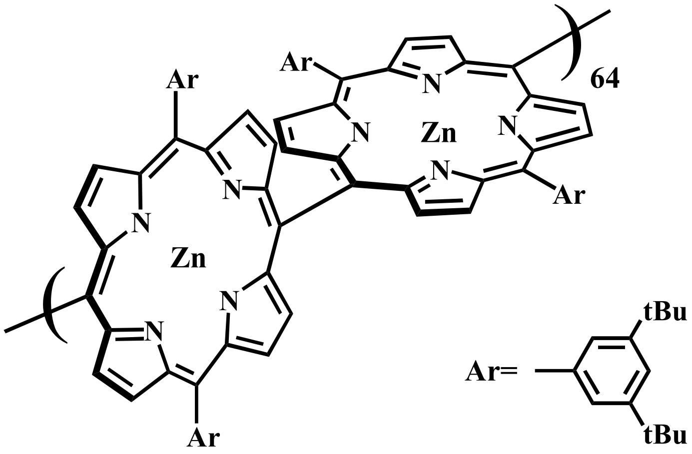

Figure 1-25. The Porphyrin 128-mer

Although some porphyrin materials are claimed to have molecular weights over 10,000 Daltons (by GPC estimation), the number of porphyrin units in the polymer chain is still only around 10 due to the fact that most porphyrin monomers already have high molecular weights (about 1000 or more Daltons). In addition, according to our experimental observations, GPC (Gel Permeation Chromatography) overestimates the molecular weight of rigid polymers by 3-5 times due to the spatial size difference between rigid porphyrin polymers and the polystyrene standard.

The molecular weight limitation of conjugated porphyrin polymers is not only connected to the solubility problems as mentioned above, but also results from the limitation of polymerization methods. Porphyrin polymerization is a stepwise reaction of the random union of monomer molecules to form dimers, trimers, and higher species anywhere in the monomer matrix. According to Carothers' simple equation[113] for relating the degree of polymerization (**DP**, the average number of repeating units in all polymer and oligomer chains) to percent conversion (**p**) of monomers:

$$\mathbf{DP} = \frac{N_0}{N} = \frac{1}{1-\mathbf{p}}$$

$$\mathbf{p} = \frac{N_0-N}{N_0}$$

N_0- molecules initially
N - molecules left (total)

high reaction conversions (**p**) are necessary to generate high **DP** polymers or achieve practical molecular weights as polymeric materials. As shown in Table 1-1, only when the reaction conversion **p** approaches to almost completion, the average **DP** could reach higher values. In Pd (Cu) mediated coupling reactions, most of the yields are between 60-90%.[114] The conversion of polymerization reactions seldom reaches above 0.95, therefore, the DP is correspondingly low. In the synthesis of poly (*p*-phenyleneethynylene)s (PPEs, Fig. 1-26), for example, the obtained degrees of polymerization almost never exceed 50-80 and more often are within the region of 20-40.[112]

Table 1-1. **Relationships between reaction conversion (p) and degree of polymerization (DP)**

$$DP = \frac{1}{1 - p}$$

p	DP
0.90	10
0.95	20
0.99	100

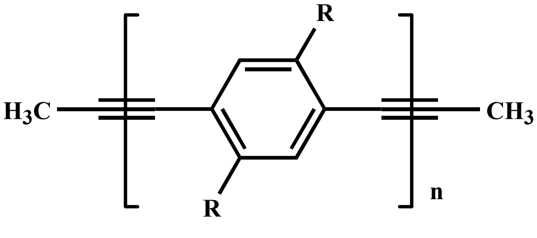

PPEs

Figure 1-26. Poly(*p*-phenyleneethynylene)s

Considering the low solubility of the porphyrins, the coupling efficiency and compatibility of in Pd (Cu)-catalyzed coupling reactions, it is not surprising then that the DP obtained for conjugated porphyrin polymers has not exceeded 32 porphyrin units.[46-48,50,52-56,76-83,92]

1.3 Objectives of this project

1.3.1 Long-term objectives

The long-term objective of this research project is to push the development of porphyrin-based materials up to the next level by using novel and/or modified porphyrin monomers and polymerization methods to construct small band-gap conjugated porphyrin polymers and intrinsically conducting porphyrin polymers, and to explore the novel chemical and physical properties of new organic materials which may be useful in various fields. The research topics and necessary collaborations include:

(1) Design and synthesis of new porphyrin molecules
(2) Study of the relationship between solubility and structure in porphyrins
(3) Explore new polymerization methods to obtain high molecular weight porphyrin polymers
(4) Routine characterization of porphyrin materials including measurements of conductivity and magnetism.

1.3.2 Specific aims of the project

As we have discussed above, the search for new porphyrin materials currently suffers from low solubility with limited synthetic methodologies for the fabrication of polymers. These limitations have prevented porphyrins from being fully explored as potential building blocks in the field of conjugated and conducting polymers. The specific aims of this project are to construct a solid foundation for the development of advanced porphyrin materials by synthesizing novel porphyrin molecules, study and increase porphyrin solubility, and investigate new polymerization methods for conjugated porphyrin materials. To increase porphyrin solubility, it is necessary to better understand structure−solubility relations in porphyrin compounds, analyze major factors affecting porphyrin solubility and develop more efficient strategies to control these factors and obtain soluble porphyrin monomer and polymers. In addition to enhanced solubility, the development of polymerization methods that are compatible with the synthesis of conjugated porphyrin free-base and metalloporphyrin polymers is also very critical to obtain high degrees of polymerization and incorporate more porphyrin units into the conjugated polymer chain.

References:

1. Saunders, K. J. *Organic Polymer Chemistry*; 2nd ed.; Chapman and Hall: New York, 1988.
2. Gurunathan, K.; Murugan, A. V.; Marimuthu, R.; Mulik, U. P.; Amalnerkar, D. P., “Electrochemically Synthesized Conducting Polymeric Materials for Applications Towards Technology in Electronics, Optoelectronics and Energy Storage Devices”, *Mat. Chem. Phys.* **1999**, *61,* 173-191.
3. Shirakawa, H.; Louis, E. J.; MacDiarmid, A. G.; Chiang, C. K.; Heeger, Y. W. A. J. “Polyacetylene-Conductive Polymer”, *J. Chem. Soc. Chem. Commun.* **1977**, 578.
4. Chiang, C. K.; C. R. F.; Jr.; Park, Y. W.; Heeger, Y. W. A. J.; Shirakawa, H; Louis, E. J.; Gau, S. C.; MacDiarmid, A. G., “Electrical Conductivity in Doped Polyacetylene”, *Phys. Rev. Lett.* **1977**, *39,* 1098-1101.
5. D'Amore, F.; Zappettini, A.; Facchini, G.; Pietralunga, S. M.; Martinelli, M.; Dell'Erba, C.; Cuniberti, C.; Comoretto, D.; Dellepiane, G., “Third Order Optical Characterisation of a π–Conjugated Polydiacetylene by Maker Fringes Technique”, *Synthetic Met.* **2002***, 127*, 143-146.
6. Beljonne, D.; Shuai, Z.; Cornil, J.; Calbert, J. P.; Bredas, J. L., “On the Luminescence Efficiency of Polymer Light-Emitting Diodes: A Quantum-Chemical Investigation”, *J. Photochem. Photobio A* **2001**, *144,* 57-62.
7. Gowri, R.; Padmanaban, G.; Ramakrishnan, S., “An Approach for the Control of Conjugation Length in Ppv Derivatives”, *Synthetic Met.* **1999**, *101,* 166-169.
8. Park, S.-J.; Choi, E.-S.; Oh, E.-J.; Lee, K.-W., “Optical Properties of Luminescent PPV Copolymers”, *Synthetic Met.* **2001**, *117,* 95-97.

9. Taylor, R. M.; Burn, P. L.; Bradley, D. D. C., “Substituted PPVs for Blue Light”, *Synthetic Met.* **1999**, *102,* 1120-1121.

10. Ng, S. C.; Chan, H. S. O.; Wong, P. M. L.; Tan, K. L.; Tan, B. T. G., “Novel Heteroarylene Polyazomethines: Their Syntheses and Characterizations”, *Polymer* **1998**, *39,* 4963-4968.

11. Suh, S. C.; Shim, S. C., “Synthesis and Properties of a Novel Polyazomethine, the Polymer with High Photoconductivity and Second-Order Optical Nonlinearity”, *Synthetic Met.* **2000**, *114,* 91-95.

12. Bakhshi, A. K., “Molecular Designing of Copolymers of Donor-Acceptor Polymers Based on Polythiophene”, *J. Mol. Struct-THEOCHEM* **2000**, *499,* 105-110.

13. Langeveld-Voss, B. M. W.; Janssen, R. A. J.; Meijer, E. W., “On the Origin of Optical Activity in Polythiophenes”, *J. Mol. Struct.* **2000**, *521,* 285-301.

14. Osaka, I.; Shibata, S.; Toyoshima, R.; Akagi, K.; Shirakawa, H., “Synthesis and Properties of Liquid Crystalline Polythiophene Derivatives”, *Synthetic Met.* **1999**, *102,* 1437-1438.

15. Pilston, R. L.; McCullough, R. D., “Toward Highly Fluorescent Polythiophenes: Head-to-Tail Coupled Copolymers of 3-(Methoxyethoxyethoxymethyl)Thiophene and 3-(Perfluoroalkyl)Thiophene”, *Synthetic Met.* **2000**, *111-112,* 433-436.

16. Roman, L. S.; Chen, L. C.; Pettersson, L. A. A.; Mammo, W.; Andersson, M. R.; Johansson, M.; Inganas, O., “Multifunctional Polythiophenes in Photodiodes”, *Synthetic Met.* **1999**, *102,* 977-978.

17. Schottland, P.; Bouguettaya, M.; Chevrot, C., “Soluble Polythiophene Derivatives for NO_2 Sensing Applications”, *Synthetic Met.* **1999**, *102,* 1325.

18. Cosnier, S.; Gondran, C.; and Senillou, A., “Functionalized Polypyrroles: A Sophisticated Glue for the Immobilization and Electrical Wiring of Enzymes”, *Synthetic Met.* **1999**, *102,* 1366-1369.

19. Park, J.-W.; Lee, J.-H.; Lee, J.-Y.; Kho, S.-I.; Kim, T.-W., “Characteristics of Organic Electroluminescent Devices Using Polypyrrole Conducting Layer and Undoped Conjugated Polymer Layer”, *Thin Solid Films* **2000**, *363,* 259-262.

20. Shilabin, A. G.; Entezami, A. A., “Electrochemical Behaviour of Conducting Polyfuran Derivatives Containing Pyrrole, Thiophene and Ethylenic Spacers”, *Eur. Polym. J.* **2000**, *36,* 2005-2020.

21. Talu, M.; Kabasakaloglu, M.; Yildirim, F.; Sari, B., “Electrochemical Synthesis and Characterization of Homopolymers of Polyfuran and Polythiophene and Bipolymer Films Polyfuran/Polythiophene and Polythiophene/Polyfuran”, *Appl. Surf. Sci.* **2001**, *181,* 51-60.

22. Nicho, M. E.; Trejo, M.; Garcia-Valenzuela, A.; Saniger, J. M.; Palacios, J.; Hu, H., “Polyaniline Composite Coatings Interrogated by a Nulling Optical-Transmittance Bridge for Sensing Low Concentrations of Ammonia Gas”, *Sensor Actuat B-Chem.* **2001**, *76,* 18-24.

23. Wu, Q.; Wu, L.; Qi, Z.; Wang, F., “The Fractal Structures in Highly Sulfonated Polyaniline”, *Synthetic Met.* **1999**, *105,* 13-16.

24. Leung, L. M.; Liu, C. M.; Wong, C. K.; Kwong, C. F., “Short Poly(Phenylene Vinylene) Chains Grafted Poly(Organophosphazene)”, *Polymer* **2002**, *43,* 233-237.

25. Tanaka, S.; Kumei, M., “Soluble Conjugated Copolymers Constituted of Pyridine and Phenylene Units”, *Synthetic Met.* **1999**, *102,* 1524-1525.

26. Wang, G.; Li, M.; Guo, C.; Wu, F.; Tian, W.; Chen, X.; Shen, J., “Soluble Conjugated Copolymers Based on Poly(1,4-Phenylenevinylene)”, *Polymer* **2000**, *41,* 2309-2312.

27. Xu, H.; Sun, Q.; Pui-Sze Lee, P.; Kwok, H. S.; Tang, B. Z., “Synthesis and Light-Emitting Properties of C60-Containing Poly(1-Phenyl-1-Butyne)s”, *Thin Solid Films* **2000**, *363,* 143-145.

28. Zhan, X.; Liu, Y.; Zhu, D.; Liu, X.; Xu, G.; Ye, P., “Large Third-Order Nonlinear Optical Response of a Conjugated Copolymer Consisting of 2,5-Diethynylthiophene and Carbazole Units”, *Chem. Phys. Lett.* **2001**, *343,* 493-498.

29. Blom, P. W. M.; Vissenberg, M. C. J. M., “Charge Transport in Poly(P-Phenylene Vinylene) Light-Emitting Diodes”, *Mat. Sci. Eng. R* **2000**, *27,* 53-94.

30. Kim, J. L.; Kim, J. K.; Cho, H. N.; Kim, D. Y.; Hong, S. I., "Polyquinoline Copolymers as Electron Transporting Layer in Light-Emitting Diodes", *Synthetic Met.* **2000**, *114,* 97-100.

31. Martin, R. E.; Geneste, F.; Holmes, A. B., "Synthesis of Conjugated Polymers for Application in Light-Emitting Diodes (PLEDs)", *Synthetic Met.* **2000**, *115,* 447-470.

32. Palilis, L. C.; Lidzey, D. G.; Redecker, M.; Bradley, D. D. C.; Inbasekaran, M.; Woo, E. P.; Wu, W. W., "Bright and Efficient Blue and Green Light-Emitting Diodes Based on Conjugated Polymer Blends", *Synthetic Met.* **2000**, *111-112,* 159-163.

33. Palilis, L. C.; Lidzey, D. G.; Redecker, M.; Bradley, D. D. C.; Inbasekaran, M.; Woo, E. P.; Wu, W. W., "High Performance Blue Light-Emitting Diodes Based on Conjugated Polymer Blends", *Synthetic Met.* **2001**, *121,* 1729-1730.

34. Pron, A.; Rannou, P., "Processible Conjugated Polymers: From Organic Semiconductors to Organic Metals and Superconductors", *Prog. Polym. Sci.* **2002**, *27,* 135-190.

35. McGehee, M. D.; Gupta, R.; Miller, E. K.; Heeger, A. J., "Characterization of Semiconducting Polymer Laser Materials and the Prospects for Diode Lasers", *Synthetic Met.* **1999**, *102,* 1030-1033.

36. Neugebauer, H.; Yohannes, T.; Sariciftci, N. S., "Semiconductor/Conjugated Polymer/Electrolyte Interfaces Studied with Infrared Photospectroelectrochemistry", *Synthetic Met.* **2001**, *119,* 379-380.

37. Kim, H.; Young Kim, J.; Lee, K.; Park, Y.; Jin, Y.; Suh, H., "Organic Photovoltaic Cells Based on Conjugated Polymer/Fullerene Composites", *Curr. Appl. Phys.* **2001**, *1,* 139-143.

38. Graeff, C. F. O.; Onmori, R. K.; Guimaraes, F. E. G.; Faria, R. M., "Field Effect Transistor Using Poly(O-Metoxyaniline) Films", *Synthetic Met.* **1999**, *105,* 151-153.

39. Arbizzani, C.; Marinangeli, A. M.; Mastragostino, M.; Meneghello, L.; Hamaide, T.; Guyot, A., "Lithium/Polymer/Polymer Solid-State Rechargeable Batteries", *J. Power Sources* **1993**, *44,* 453-460.

40. Oleda, M. C.; Acosta, J. L., "Polymer Electrodes Based on Carbonaceous Compounds for Solid-State Rechargeable Batteries. 1. Effect of Green Coke on the Microstructure of Polyether Mixtures", *Fuel Energy Abstracts* **1997**, *38,* 237.

41. Kalaji, M.; Murphy, P. J.; Williams, G. O., "The Study of Conducting Polymers for Use as Redox Supercapacitors", *Synthetic Met.* **1999**, *102,* 1360-1361.

42. Mastragostino, M.; Arbizzani, C.; Soavi, F., "Polymer-Based Supercapacitors", *J. Power Sources* **2001**, *97-98,* 812-815.

43. O'Brien, D. F.; Giebeler, C.; Fletcher, R. B.; Cadby, A. J.; Palilis, L. C.; Lidzey, D. G.; Lane, P. A.; Bradley, D. D. C.; Blau, W., "Electrophosphoresence from a Doped Polymer Light Emitting Diode", *Synthetic Met.* **2001**, *116,* 379-383.

44. Plocharski, J.; Wycislik, H., "Mixed Conductivity in Poly(*p*-Phenylene) Doped with Iron Chloride", *Solid State Ionics* **2000**, *127,* 337-344.

45. van Mullekom, H. A. M.; Vekemans, J. A. J. M.; Havinga, E. E.; Meijer, E. W., "Developments in the Chemistry and Band Gap Engineering of Donor-Acceptor Substituted Conjugated Polymers", *Mat. Sci. Eng. R* **2001**, *32,* 1-40.

46. O'Keefe, G. E.; Halls, J. J. M.; Walsh, C. A.; Denton, G. J.; Friend, R. H.; Anderson, H. L., "Ultrafast Field-Induced Dissociation of Excitons in a Conjugated Porphyrin Polymer", *Chem. Phys. Lett.* **1997**, *276,* 78-83.

47. Screen, T. E. O.; Lawton, K. B.; Wilson, G. S.; Dolney, N.; Ispasoiu, R.; Goodson, T.; Martin, S. J.; Bradley, D. D. C.; Anderson, H. L., "Synthesis and Third Order Nonlinear Optics of a New Soluble Conjugated Porphyrin Polymer", *J. Mat. Chem.* **2001**, *11,* 312-320.

48. Kuebler, S. M.; Denning, R. G.; Anderson, H. L., "Large Third-Order Electronic Polarizability of a Conjugated Porphyrin Polymer", *J. Am. Chem. Soc.* **2000**, *122,* 339-347.

49. Thorne, J. R. G.; Kuebler, S. M.; Denning, R. G.; Blake, I. M.; Taylor, P. N.; Anderson, H. L., "Degenerate Four-Wave Mixing Studies of Butadiyne-Linked Conjugated Porphyrin Oligomers", *Chem. Phys.* **1999**, *248,* 181-193.

50. Anderson, H. L., "Building Molecular Wires from the Colors of Life: Conjugated Porphyrin Oligomers", *Chem. Comm.* **1999**, 2323-2330.

51. Taylor, P. N.; Huuskonen, J.; Rumbles, G.; Aplin, R. T.; Williams, E.; Anderson, H. L., "Conjugated Porphyrin Oligomers from Monomer to Hexamer", *Chem. Comm.* **1998**, 909-910.
52. Martin, S. J.; Bradley, D. D. C.; Anderson, H. L., "Quadratic Electrooptic Response of a Conjugated Porphyrin Polymer", *Mol Cryst. Liq. Crys. A* **1994**, *256,* 649-655.
53. Anderson, H. L., "Supramolecular Orientation of Conjugated Porphyrin Oligomers in Stretched Polymers", *Adv. Mat.* **1994**, *6,* 834-836.
54. Anderson, H. L.; Martin, S. J.; Bradley, D. D. C., "Synthesis and 3rd-Order Nonlinear-Optical Properties of a Conjugated Porphyrin Polymer", *Angew. Chem. Int. Ed. Eng.* **1994**, *33,* 655-657.
55. Jiang, B. W.; Yang, S. W.; Barbini, D. C.; Jones, W. E., "Synthesis of Soluble Conjugated Metalloporphyrin Polymers with Tunable Electronic Properties", *Chem. Comm.* **1998**, 213-214.
56. Jiang, B. W.; Yang, S. W.; Jones, W. E., "Conjugated Porphyrin Polymers: Control of Chromophore Separation by Oligophenylenevinylene Bridges", *Chem. Mat.* **1997**, *9,* 2031-2036.
57. Milgrom, L. R. *The Colors of Life*: *An Introduction to the Chemistry of Porphyrins and Related Compounds*; Oxford University Press: London, 1997.
58. Smith, K. M.; Ed.; *Porphyrins and Metalloporphyrins*; Elsevier Scientific Publishing Company: Amsterdam, the Netherland, 1975.
59. Roncali, J., "Synthetic Principles for Bandgap Control in Linear π–Conjugated Systems", *Chem. Rev.* **1997**, *97,* 173-205.
60. Udal'tsov, A. V., "Characteristics of Donor-Acceptor Complexes Formed in Porphyrin-Polymer Systems and Their Photoactivation in Electron Transfer Photoreaction", *J. Photochem. Photobio. B* **1997**, *37,* 31-39.
61. Cao, Y.; Zhang, B. W.; Qian, W. Y.; Wang, X. D.; Bai, J. W.; Xiao, X. R.; Jia, J. G.; Xu, J. W., "An Artificial Photosynthesis Porphyrin Tetrad Molecule for Photoelectric Conversion", *Sol. Energ. Mat. Sol. C.* **1995**, *38,* 139-155.
62. Wiehe, A.; Senge, M. O.; Schafer, A.; Speck, M.; Tannert, S.; Kurreck, H.; Roder, B., "Electron Donor-Acceptor Compounds: Exploiting the Triptycene

Geometry for the Synthesis of Porphyrin Quinone Diads, Triads, and a Tetrad", *Tetrahedron* **2001**, *57,* 10089-10110.

63. Seth, J.; Palaniappan, V.; Wagner, R. W.; Johnson, T. E.; Lindsey, J. S.; Bocian, D. F., "Soluble Synthetic Multiporphyrin Arrays .3. Static Spectroscopic and Electrochemical Probes of Electronic Communication", *J. Am. Chem. Soc.* **1996**, *118,* 11194-11207.
64. Strachan, J. P.; Gentemann, S.; Seth, J.; Kalsbeck, W. A.; Lindsey, J. S.; Holten, D.; Bocian, D. F., "Effects of Orbital Ordering on Electronic Communication in Multiporphyrin Arrays", *J. Am. Chem. Soc.* **1997**, *119,* 11191-11201.
65. Taylor, P. N.; Anderson, H. L., "Cooperative Self-Assembly of Double-Strand Conjugated Porphyrin Ladders", *J. Am. Chem. Soc.* **1999**, *121,* 11538-11545.
66. Piet, J. J.; Taylor, P. N.; Anderson, H. L.; Osuka, A.; Warman, J. M., "Excitonic Interactions in the Singlet and Triplet Excited States of Covalently Linked Zinc Porphyrin Dimers", *J. Am. Chem. Soc.* **2000**, *122,* 1749-1757.
67. Osuka, A.; Okada, T.; Taniguchi, S.; Nozaki, K.; Ohno, T.; Mataga, N., "Synthesis of Partially Metalated, Conformationally Restricted Oligomeric Porphyrins for Studying Photosynthetic Charge Separation", *Tetrahedron Lett.* **1995**, *36,* 5781-5784.
68. Behnke, B. J.; Kindig, C. A.; Musch, T. I.; Koga, S.; Poole, D. C., "Dynamics of Microvascular Oxygen Pressure across the Rest- Exercise Transition in Rat Skeletal Muscle", *Resp. Physiol.* **2001**, *126,* 53-63.
69. Xiao, Y.; Yu, W.-L.; Chen, Z.-K.; Lee, N. H. S.; Lai, Y.-H.; and Huang, W., "Synthesis and Characterization of a Novel Light-Emitting Copolymer with Improved Charge-Balancing Property", *Thin Solid Films* **2000**, *363,* 102-105.
70. Udal'tsov, A. V.; Paschenko, V. Z.; Churin, A. A.; Tusov, V. B.; Pshezhetskii, V. S., "Donor-Acceptor Interactions in Porphyrin Associates Immobilized in Biphilic Copolymer", *J. Photochem. Photobio. B* 1993, *21,* 87-94.
71. Tenenbaum, S.; Laks, B., "Study of Conformational Stability of Polycarbonitrile-Polyazine Copolymers", *Synthetic Met.* **1999**, *102,* 1222-1223.

72. Martin, R. E.; Geneste, F.; Chuah, B. S.; Fischmeister, C.; Ma, Y.; Holmes, A. B.; Riehn, R.; Cacialli, F.; Friend, R. H., "Versatile Synthesis of Various Conjugated Aromatic Homo- and Copolymers", *Synthetic Met.* **2001**, *122,* 1-5.
73. Leung, L. M.; Tan, K.-H.; Lam, T. S.; WeiDong, H., "Electrical and Optical Properties of Polyacetylene Copolymers", *React. Funct. Polym.* **2002**, *50,* 173-179.
74. Lee, J.-I.; Klaerner, G.; Davey, M. H.; Miller, R. D., "Color Tuning in Polyfluorenes by Copolymerization with Low Band Gap Comonomers", *Synthetic Met.* **1999**, *102,* 1087-1088.
75. Bai, F.; Zheng, M.; Lin, T.; Yang, J.; He, Q.; Li, Y.; Zhu, D., "The New Approaches to Light Emitting Conjugated Polymers-Alternating Copolymers with Hole Transport Chromophores and Hyperbranched Polymers", *Synthetic Met.* **2001**, *119,* 179-180.
76. Jiang, B.; Niver, R.; Yang, S.-W.; Jones, W. E. J., "Metalloporphyrin Polymers Bridged with Conjugated Cyano-Substituted Stilbene Units", *Synthetic Met.* **1998**, *94,* 205-210.
77. Jiang, B. W.; Yang, S. W.; Niver, R.; Jones, W. E., "Metalloporphyrin Polymers Bridged with Conjugated Cyano-Substituted Stilbene Units", *Synthetic Met.* **1998**, *94,* 205-210.
78. Pichler, K.; Anderson, H. L.; Bradley, D. D. C.; Friend, R. H.; Hamer, P. J.; Harrison, M. G.; Jarrett, C. P.; Martin, S. J.; Stephens, J. A., "Photophysical and Transport-Properties of a Novel Soluble Conjugated Polymer-Based on Zn-Porphyrin Units Edge-Linked by Acetylenic Spacers", *Mol. Cryst. Liq. Crys. A* **1994**, *256,* 415-422.
79. Qureshi, F. M.; Martin, S. J.; Long, X.; Bradley, D. D. C.; Henari, F. Z.; Blau, W. J.; Smith, E. C.; Wang, C. H.; Kar, A. K.; Anderson, H. L., "Optical Limiting Properties of a Zinc Porphyrin Polymer and Its Dimer and Monomer Model Compounds", *Chem. Phys.* **1998**, *231,* 87-94.
80. Shimidzu, T.; Segawa, H.; Wu, F.; Nakayama, N., "Approaches to Conducting Polymer Devices with Nanostructures: Photoelectrochemical Function of One-

Dimensional and Two-Dimensional Porphyrin Polymers with Oligothienyl Molecular Wire", *J. Photochem. Photobio. A* **1995**, *92,* 121-127.

81. Tanaka, K.; Kosai, N.; Maruyama, H.; Kobayashi, H., "Electronic Structure of Two-Dimensional Porphyrin Polymers", *Synthetic Met.* **1998**, *92,* 253-258.

82. Yamamoto, T.; Fukushima, N.; Nakajima, H.; Maruyama, T.; Yamaguchi, I., "Synthesis and Chemical Properties of Pi-Conjugated Zinc Porphyrin Polymers with Arylene and Aryleneethynylene Groups between Zinc Porphyrin Units", *Macromolecules* **2000**, *33,* 5988-5994.

83. Yang, S. W.; Jiang, B. W.; Lam, P. T.; Jones, W. E., "Electronic Communication and Dynamics in Hybrid Porphyrin Polymers", *Abstr. Pap. Am. Chem. Soc.* **1998**, *216,* 585-POLY.

84. Aratani, N.; Osuka, A., "Monodisperse Giant Porphyrin Arrays", *Macromol. Rapid Comm.* **2001**, *22,* 725-740.

85. Taylor, P. N.; Wylie, A. P.; Huuskonen, J.; Anderson, H. L., "Enhanced Electronic Conjugation in Anthracene-Linked Porphyrins", *Angew. Chem. Int. Ed.* **1998**, *37,* 986-989.

86. Anderson, H. L.; Hunter, C. A.; Sanders, J. K. M., "Assembly of a Photoactive Supramolecule Using Porphyrin Coordination Chemistry", *J. Chem. Soc., Chem. Comm.* **1989**, 226-227.

87. Fung, S.; Moratti, S. C.; Graham, S. C.; Friend, R. H.., "Photoinduced Doping in Conjugated Polymers", *Synthetic Met.* **1999**, *102,*167-1168.

88. Gust, D.; Moore, T. A., "A Synthetic System Mimicking the Energy Transfer and Charge Separation of Natural Photosynthesis", *J. Photochem.* **1985**, *29,* 173-184.

89. Ho, P. K. H.; Tessler, N.; Friend, R. H., "Towards Solution-Processible Semiconducting Polymer-Based Photonic Devices", *Synthetic Met.* **1999**, *102,* 1020.

90. Kawai, T.; Yamaue, T.; Onoda, M.; Yoshino, K., "Photoinduced Charge Separation in Multilayered Heterostructures of Conducting Polymers and Their Doping Effects", *Synthetic Met.* **1999**, *102,* 971-972.

91. Knor, G., "Photocatalytic Reactions of Porphyrin-Based Multielectron Transfer Sensitizers", *Coord. Chem. Rev.* **1998**, *171,* 61-70.

92. Okeefe, G. E.; Halls, J. J. M.; Walsh, C. A.; Denton, G. J.; Friend, R. H.; Anderson, H. L., "Ultrafast Field-Induced Dissociation of Excitons in a Conjugated Porphyrin Polymer", *Chem. Phys. Lett.* **1997**, *276,* 78-83.

93. Piet, J. J.; Warman, J. M.; Anderson, H. L., "Photo-Induced Charge Separation on Conjugated Porphyrin Chains", *Chem. Phys. Lett.* **1997**, *266,* 70-74.

94. Takahashi, K.; Nakatani, S.; Yamaguchi, T.; Komura, T.; Ito, S.; Murata, K., "Enhanced Quantum Yield in Porphyrin/Electron-Donor Double-Layer Solar Cells", *Sol. Energ. Mat. Sol. C.* **1997**, *45,* 127-139.

95. Kurreck, H.; Aguirre, S.; Dieks, H.; Gersdorff, J. v.; Kay, C. W. M.; Mossler, H.; Newman, H.; Niethammer, D.; Schlupmann, J.; Sobek, J., "Mimicking Primary Processes in Photosynthesis Photochemistry of Covalently Linked Porphyrin Quinones Studied by EPR Spectroscopy", *Sol. Energ. Mat. Sol. C.* **1995**, *38,* 91-110.

96. Li, J. Z.; Ambroise, A.; Yang, S. I.; Diers, J. R.; Seth, J.; Wack, C. R.; Bocian, D. F.; Holten, D.; Lindsey, J. S., "Template-Directed Synthesis, Excited-State Photodynamics, and Electronic Communication in a Hexameric Wheel of Porphyrins", *J. Am. Chem. Soc.* **1999**, *121,* 8927-8940.

97. Seth, J.; Palaniappan, V.; Johnson, T. E.; Prathapan, S.; Lindsey, J. S.; Bocian, D. F., "Investigation of Electronic Communication in Multi-Porphyrin Light-Harvesting Arrays", *J. Am. Chem. Soc.* **1994**, *116,* 10578-10592.

98. Seth, J.; Bocian, D. F., "Electron-Paramagnetic-Resonance Studies of Metalloporphyrin Anion-Radicals - Effects of Solvent, Counterion, Temperature, and Isotopic-Substitution on the Jahn-Teller Active(2)E(G) Ground-State", *J. Am. Chem. Soc.* **1994**, *116,* 143-153.

99. Nakano, A.; Aratani, N.; Furuta, H.; Osuka, A., "Directly Linked Dehydropurpurin-Porphyrin Dyads from Ag(I)- Promoted Oxidation of Meso-Phenylethynyl Substituted Zinc(II) Porphyrins", *Chem. Comm.* **2001**, 1920-1921.

100. Aratani, N.; Osuka, A., "A New Strategy for Construction of Covalently Linked Giant Porphyrin Arrays with One, Two, and Three Dimensionally Arranged Architectures", *B. Chem. Soc. Jpn*. **2001**, *74,* 1361-1379.

101. Min, C. K.; Joo, T.; Yoon, M. C.; Kim, C. M.; Hwang, Y. N.; Kim, D.; Aratani, N.; Yoshida, N.; Osuka, A., "Transient Absorption Anisotropy Study of Ultrafast Energy Transfer in Porphyrin Monomer, Its Direct Meso-Meso Coupled Dimer and Trimer", *J. Chem. Phys.* **2001**, *114,* 6750-6758.

102. McEwan, K. J.; Bourhill, G.; Robertson, J. M.; Anderson, H. L., "The Nonlinear Optical Characterization of Meso-Substituted Porphyrin Dyes", *J. Nonlinear Opt. Phys.* **2000**, *9,* 451-468.

103. Aratani, N.; Osuka, A.; Kim, Y. H.; Jeong, D. H.; Kim, D., "Extremely Long, Discrete Meso-Meso-Coupled Porphyrin Arrays", *Angew. Chem. Int. Ed.* **2000**, *39,* 1458-1463.

104. Jiang, B. W.; Yang, S. W.; Bailey, S. L.; Hermans, L. G.; Niver, R. A.; Bolcar, M. A.; Jones, W. E., "Toward Transparent Molecular Wires: Electron and Energy Transfer in Transition Metal Derivatized Conducting Polymers", *Coord. Chem. Rev.* **1998**, *171,* 365-386.

105. Jiang, B. W.; Jones, W. E., "Synthesis and Characterization of a Conjugated Copolymer of Poly(Phenylenevinylene) Containing a Metalloporphyrin Incorporated into the Polymer Backbone", *Macromolecules* **1997**, *30,* 5575-5581.

106. Matsufuji, A.; Nakazawa, S.; Yamamoto, K., "Electrocatalysis of the Reduction of Dioxygen by Pi-Conjugated Polymer Complexes with Dinuclear Cobalt Porphyrins", *J. Inorg. Organomet. Polym.* **2001**, *11,* 47-61.

107. Stamp, L. M.; Mang, S. A.; Holmes, A. B.; Knights, K. A.; de Miguel, Y. R.; McConvey, I. F., "Polymer Supported Chromium Porphyrin as Catalyst for Polycarbonate Formation in Supercritical Carbon Dioxide", *Chem. Comm.* **2001**, 2502-2503.

108. Tangestaninejad, S.; Habib, M. H.; Mirkhani, V.; Moghadam, M., "Preparation of an Insoluble Polymer-Supported Mn (III) Porphyrin and Its Use as a New Alkene Epoxidation and Alkane Hydroxylation Catalyst", *J. Chem. Res-S* **2001**, 444-445.

109. Zhutaeva, G. V.; Radyushkina, K. A.; Marinich, M. A.; Bogatyreva, G. P.; Tarasevich, M. R., "Electrocatalysis of the Oxygen Reaction on Electrodes Prepared Using Disperse Synthetic Diamond Promoted with Cobalt Porphyrin and Its Pyropolymer", *Russ. J. Electrochem.* **2001**, *37,* 1059-1064.

110. Galina M. Mamardashvili, N. Z. M. a. B. D. B., “Solubility of Alkylporphyrin”, *Molecules* **2000**, *5,* 762-764.

111. Nguyen, P.; Gomez-Elipe, P.; Manners, I., “Organometallic Polymers with Transition Metals in the Main Chain”, *Chem. Rev.* **1999**, *99,* 1515-1548.

112. Kloppenburg, L.; Jones, D.; Bunz, U. H. F., “High Molecular Weight Poly(P-Phenyleneethynylene)S by Alkyne Metathesis Utilizing "Instant" Catalysts: A Synthetic Study”, *Macromolecule* **1999**, *32,* 4194-4203.

113. Stevens, M. P. *Polymer Chemistry: An Introduction;* Oxford University Press: New York, 1990.

114. Diederich, F.; Stang, P. J.; Ed.; *Metal-Catalyzed Cross-Coupling Reactions;* Wiley-VCH: Weinheim, Germany, 1998.

CHAPTER II

SOLUBILITY-STRUCTURE STUDIES OF PORPHYRINS

2.1 Monomeric porphyrin solubility in organic solvents

As we have discussed in Chapter I, low solubility of building blocks results in low molecular weights of conjugated polymers and short overlapping π–systems. The purpose of this solubility-structure study is to increase porphyrin solubility by structural modification and achieve highly extended π-conjugation in porphyrin polymers. The paucity of data about monomeric porphyrin solubility, especially in organic solvents, is probably due to the low concentration needed in most studies or their applications in aqueous solutions, such as in catalysts or photosynthetic model systems. However, our solubility-structure studies must be conducted in organic solvents, since porphyrin materials are typically synthesized and processed in organic solvents.

2.1.1 Solvation effect on monomeric porphyrin solubility

It is generally believed that solvation effects and changes of crystalline lattice energy are the controlling factors for solubility. Compound solubility in low dielectric organic solvents is usually expected to increase as the attached alkyl chains get longer, due to the increased solvation effect. We have seen many successful examples to increase conjugated polymer solubility and processability by adding long-chain or branched solubilizing groups to the polymer backbone, such as the soluble PPV systems (Fig. 2-1),[1] where the solvation effect can be one of the controlling factors for solubility.

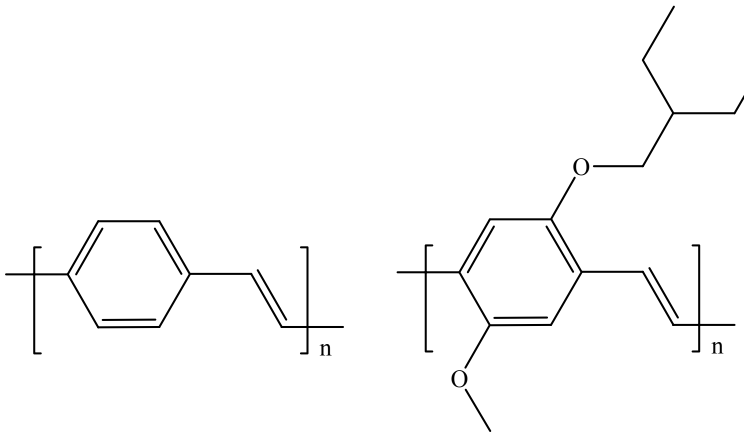

PPV, Insoluble **MEH-PPV, Soluble**

Figure 2-1. Soluble and Insoluble PPV systems

In porphyrin systems, both the increase of solvation effects and decrease of crystalline lattice energy can only be achieved by changes of substituents on the periphery. The core structure of porphyrins already predominates their macrocyclic conformation. As we have seen in Chapter I, most of porphyrin molecules are substituted with long-chained or branched alkyl and alkoxyl groups to help to increase the solubility of porphyrin materials in organic solvents. A comprehensive study of the influence of alkyl substituents on porphyrin solubility has been conducted by Mamardashvili and coworkers.[2,3] This study indicated that the solubility values for the majority of octalkylporphyrins with alkyl substituents on the β–positions (2, 3, 7, 8, 12, 13, 17, 18 positions, Fig. 2-2) are approximately 10^{-3} mol/L in benzene (Fig. 2-2). By changing the alkyl group number, the length of the alkyl chains (from CH_3 to C_4H_9) and the relative positions of alkyl groups on the β– and *meso*– positions, the solubility values are only changed by 2-5 times except for porphyrin **I** and **II**, which have extremely low

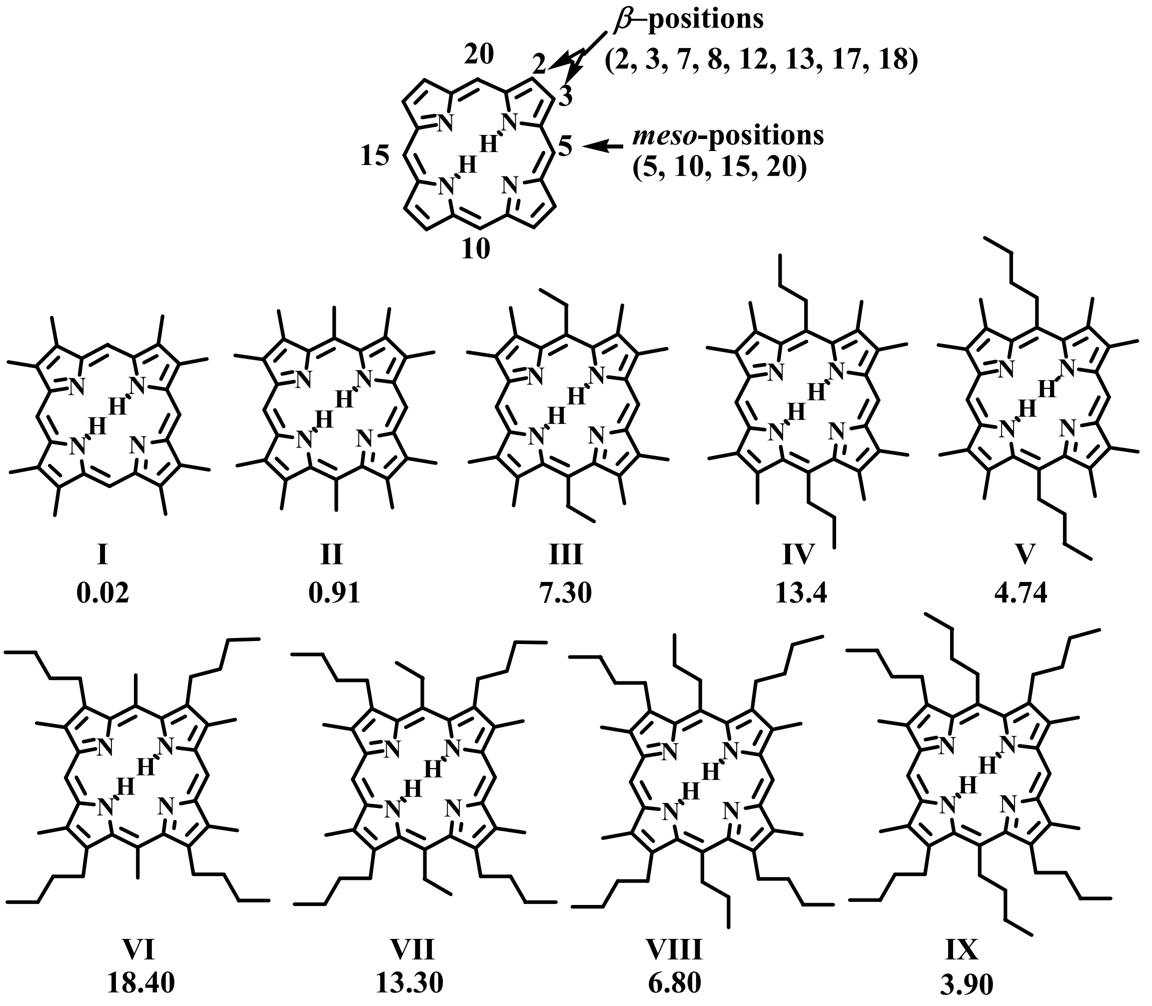

Figure 2-2. Solubility of Alkylporphyrins in Benzene (mmol/L)

solubility.[2] The solubility of these alkylporphyrins is not increased as the attached alkyl chains get longer. For porphyrins **I** to **V** (Fig. 2-2), there are methyl groups on the eight *β*–positions, and substituents on *meso*–positions are gradually increased from H, CH_3, C_2H_5, and C_3H_7 to C_4H_9. The solubility values of porphyrins **I** to **V** increase with the increasing length of the *meso*-alkyl chains from H, CH_3, C_2H_5 to C_3H_7, but decrease again when the *meso*-alkyl groups increase further to C_4H_9. For porphyrins **VI** to **IX**, the solubility again decreases with the increase of the *meso*-alkyl chain length. This study of alkylporphyrin solubility provides us with some insight into the solvation effect of alkyl substituents, as well as an understanding of the factors that control porphyrin solubility. Increasing the alkyl chains only helps to increase porphyrin solubility to a certain extent. It indicates that the solvation effect in porphyrins is not very efficient. According to the trend shown in Fig. 2-2, the solubility of most of alkylporphyrins decrease with increasing alkyl-chain, we believe that the van der Waals attractive interaction among these substituents is probably the controlling force responsible for the change in porphyrin solubility. Since van der Waals' interaction is proportional to the area of the interacting molecules, longer alkyl chains have stronger van der Waals attractive interactions among the chains, leading to more efficient porphyrin aggregation and lower alkylporphyrin solubility.

2.1.2 Crystalline lattice energy of monomeric porphyrin

Crystalline lattice energy in molecular crystals can affect the compound solubility in solutions. Molecular crystals consist of discrete molecules held together by intermolecular forces that are weaker than covalent bonding energies. Generally, the lattice energy, E_{latt}, comprises three major intermolecular interactions: van der Waals (repulsive and attractive) forces (E_{vdW}), electrostatic (Coulombic) forces ($E_{\mathrm{electrostatic}}$), and hydrogen-bonding energy (E_{H}), as expressed in equation (1).[4] Contributions of the three

$$E_{\mathrm{latt}} = E_{\mathrm{vdW}} + E_{\mathrm{electrostatic}} + E_{\mathrm{H}} \tag{1}$$

forces to the whole lattice energy vary in different molecular systems. For example, in the free base ephedrine derivatives (Fig. 2-3), the van der Waals energy is the dominant intermolecular force in bases, where E_{vdW} is between 15.7 – 19.9 kcal/mol, $E_{\mathrm{electrostatic}}$ is 3.6 – 5.4 kcal/mol and E_{H} is 3.5 – 6.4 kcal/mol; In their salt form, however, these energies change substantially with $E_{\text{electrostatic}}$ becoming 14.3 – 43.5 kcal/mol, which is the dominant force in some compounds.[4]

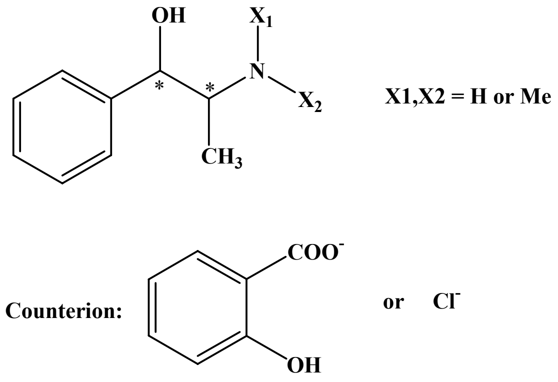

Figure 2-3. Ephedrine Derivatives

Although there is no such detailed data for the force distribution in porphyrin systems, the π–π interaction energy, through both computational and experimental observation, demonstrates that it may well be the dominant intermolecular interaction in porphyrin systems.[5] It has been recognized for over half a century that ubiquitously existing π–π interactions affect or control diverse phenomena, such as complexation in many host-guest systems, the stable helical structure of DNA and the tertiary structure of proteins. Hunter and Sanders point out that porphyrin aggregation is mainly controlled by π–π interaction between porphyrins. With such a large aromatic system in porphyrins, the π–π interaction energy between two unsubstituted porphyrins can reach 11.5 to 5.6 kcal/mol according to both computational and experimental observation.[5] Compared to the π–π interaction energy levels in smaller aromatic systems, such as the 1.4 kcal/mol interaction energy between two benzene units, or between a benzene and a naphthalene unit, or between a benzene and an acridine,[6] the π−π interaction energy in porphyrin systems is higher by a factor of 10 times. The structural comparison of porphyrins with ephedrine derivatives allows us to estimate that hydrogen bonding and van der Waals interaction in porphyrin systems will be much smaller than ephedrine derivatives, due to the rigid ring structure in porphyrins. Therefore the strong π−π interaction plays a very important and predominant role over other intermolecular forces in the crystalline lattice energy porphyrins.

2.2 Strategies to reduce strong interaction between porphyrins

According to our understanding of the controlling interaction forces among porphyrins, the strategy to increase solubility of porphyrin molecules and conjugated porphyrin polymers is to interrupt the strong π−π attractions. Hunter and Sanders have indicated that when two porphyrins adopt a face-to-face offset stacking geometry (Fig. 2-4), the π−π interaction can reach the highest attraction energy level (15.6 kcal/mol). Crystallographic evidence in Cambridge Structural Database (CSD) has also shown the preferred face-to-face offset stacking geometry in many porphyrin systems. Examples of face-to-face offset stacking geometries are shown in Fig. 2-5.

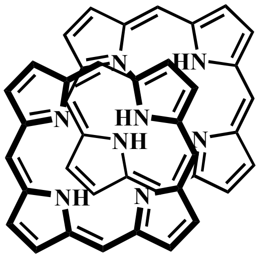

Figure 2-4. Face-to-Face Offset Stacking Modeling for Porphyrin Interaction

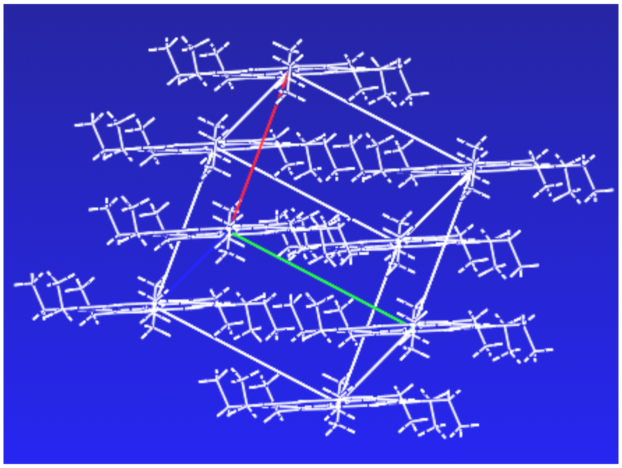

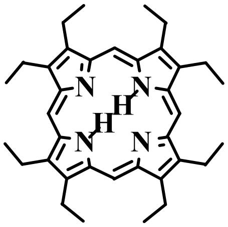

octaethylporphyrin

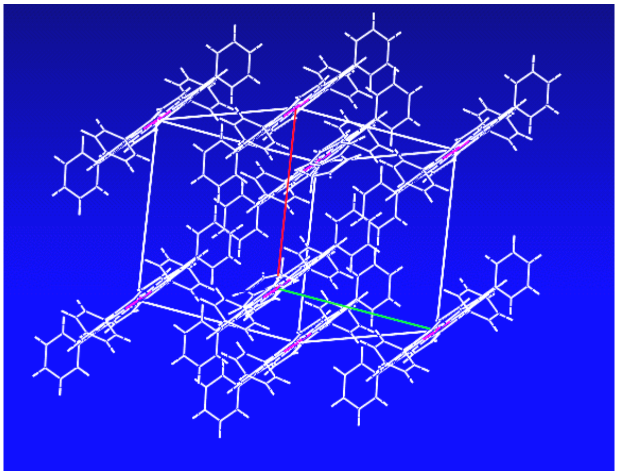

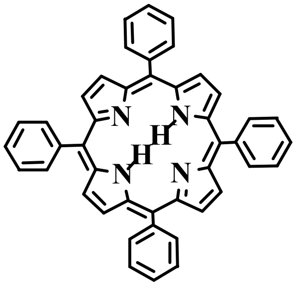

Tetraphenylporphyrin

Figure 2-5. Face-to-Face Offset Stacking Geometries in Porphyrin Crystals[7,8]

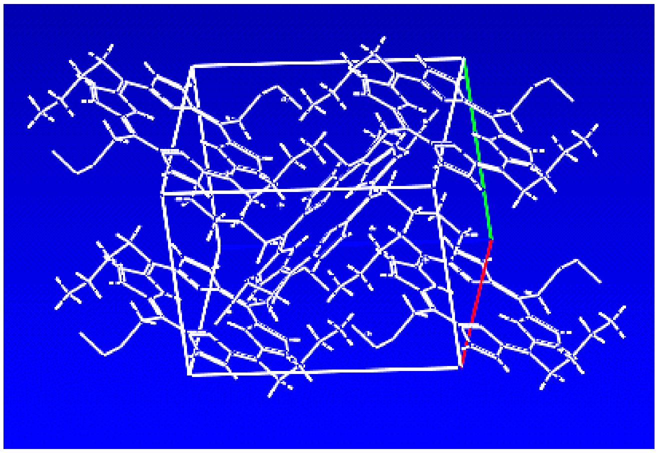

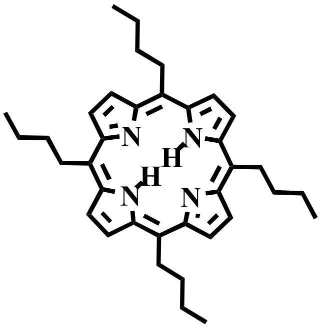

Tetrabutylporphyrin

Figure 2-6. T-shaped Stacking Geometry in the Porphyrin Crystal[9]

There are also many porphyrin crystals that adopt a T-shaped stacking geometry, in which every two neighboring porphyrin molecules are perpendicular to each other as shown in Fig. 2-6. Molecular modeling of porphyrin systems by Hunter and Sanders predict the $\pi-\pi$ interaction as a function of the relative orientation of neighboring porphyrins as shown in Fig. 2-7 and 2-8.[5] With the help of this molecular modeling, it is clearly demonstrated that the preferred face-to-face offset stacking and T-shaped stacking geometries are the consequences of the strong $\pi-\pi$ interaction between

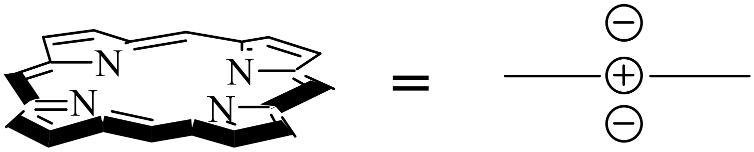

Figure 2-7. A Simple Model of Porphyrins

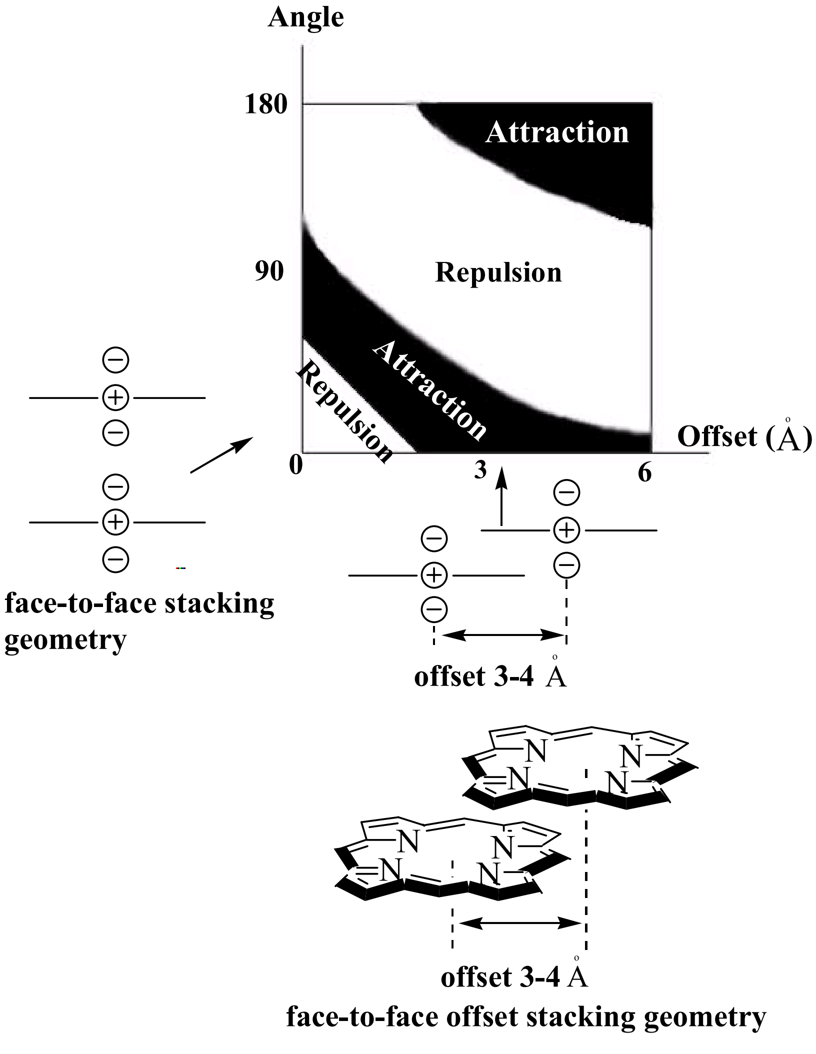

Figure 2-8. π−π Interaction Varies as a Function of Their Relative Orientation

neighboring porphyrins. These face-to-face offset stacking and T-shaped stacking geometries facilitate the strong attraction between porphyrin molecules. The simple model for porphyrins consists of a positively charged σ–framework, and two negatively charged π–electron clouds above and below the σ–frame (Fig. 2-7). Fig. 2-8 shows the repulsion areas and attraction areas for π–π interaction between neighboring porphyrin molecules, where the X-axis is the offset between the centers of two neighboring porphyrins; the Y-axis is the angle between two neighboring porphyrin planes. When two porphyrins are face-to-face stacking without any offset (X=0), their interaction belongs to the repulsion area. It is clearly shown in Fig. 2-8 that the negatively charged π–clouds on two porphyrins repel each other. When two porphyrins are offset with respect to each other by a distance of 2.5 - 6 Å the π–π interaction between them changes from repulsion to attraction, which is a result of an electrostatic attractive interaction between the positively charged σ–frame and the negatively charged π–cloud. Consequently, most of face-to-face stacked porphyrin crystals have their centers offset from 3 - 4 Å[7,8] in the crystal state. And it can be presumed that this attraction holds porphyrins in this geometry and in solution as well.

Similarly, the T-shaped stacking geometry can also facilitate strong π–π attractive interactions between two neighboring porphyrin rings, as illustrated in Fig. 2-9. When one of the two neighboring porphyrin planes turns away from another and the porphyrin rings become perpendicular to each other (Y is about 90 ^{0}C), the π–π interaction gradually changes from the repulsion to the attraction area, which reflects again the electrostatic attractive interaction between the positively charged σ–frame and the

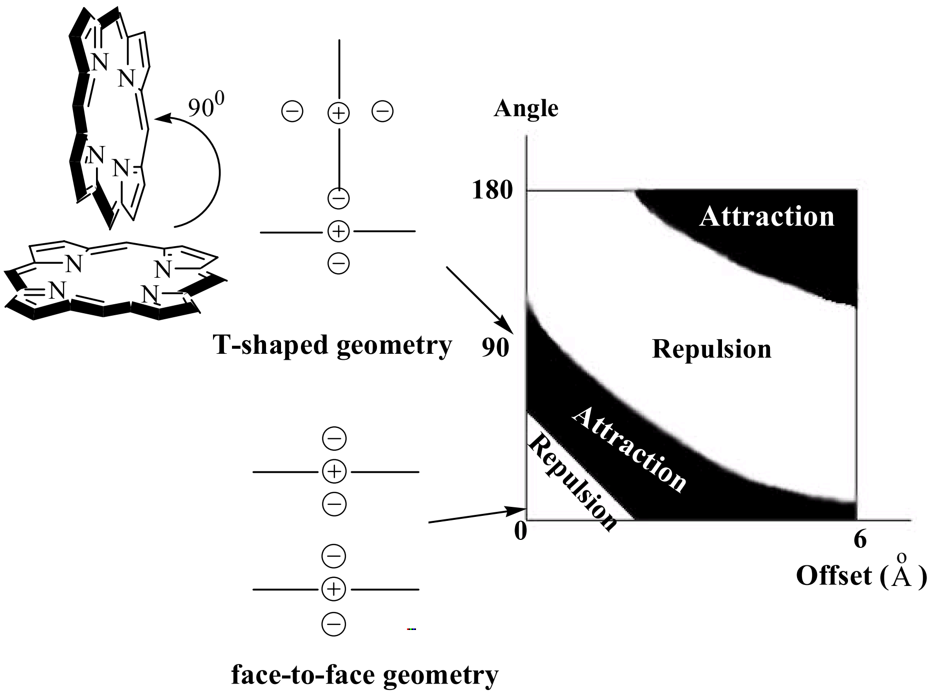

Figure 2-9. T-shaped Geometry Favors π−π Attractive Interaction

negatively charged π−could again. The fact that most porphyrin crystals adopt either face-to-face offset stacking or T-shaped stacking as preferred structures, demonstrates that the π−π interaction is probably the controlling force in most of the porphyrins' intermolecular interactions. It also shows that the π−π attractive interactions in porphyrins come from electrostatic attraction between the positively charged σ−frame and the negatively charged π−electron clouds. Porphyrin crystallization, aggregation and precipitation are actually the results of π−σ attractions that overcome π−π repulsions.[5]

Strategies to reduce this major π−π interaction between porphyrins are now addressed to interrupt the face-to-face offset stacking and T-shaped stacking. Lindsey and co-workers[10] first introduced the concept of facial-encumbrance to explain some substitution effects on porphyrin properties. In this structure-solubility study, we introduce facial- and edge-encumbering substituents on porphyrin peripheries to interrupt porphyrin face-to-face offset and T-shaped stacking. The facial- and edge-encumbrance can be realized by attaching *ortho*-substituted phenyl rings to the *meso*-positions of porphyrins. The repulsion between the β-hydrogen on porphyrins and the *ortho*-substituents on the phenyl rings cause the phenyl plane to turn away from a coplanar conformation with the porphyrin plane. These *ortho*-substituents thus project above and below the porphyrin ring. If the *ortho*-substituents are bulky and rigid enough, they will provide very good facial-encumbrance thus pushing adjacent porphyrin molecules apart from each other and preventing the porphyrins from their preferred face-to-face offset stacking. The *para*-substituents on the phenyl rings can also be used to interrupt edge-on stacking through steric hindrance. Therefore, the molecular design for improving porphyrin solubility through facial- and edge-encumbering groups in the arylporphyrins is defined using the *meso*-positions to attach both *ortho*- and *para*-substituents (Fig. 2-10).

.

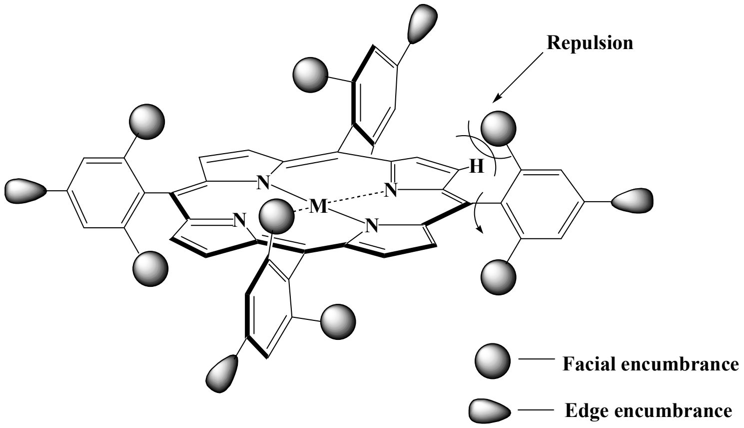

Figure 2-10. Facial and Edge Encumbrance in Porphyrins

2.3 Syntheses of designed porphyrin molecules

According to the molecular design for the synthesis of soluble porphyrin monomers for linear porphyrin polymers, the *trans*-A_2B_2 porphyrins with two aryl groups on two of the *meso*-positions and two linkers (A) on another two *meso*-positions, are our target molecules in this study as shown in Fig. 2-11. Several **R** groups were selected to build differently facial- and edge-encumbered porphyrins for the comparison of encumbrance efficiency.

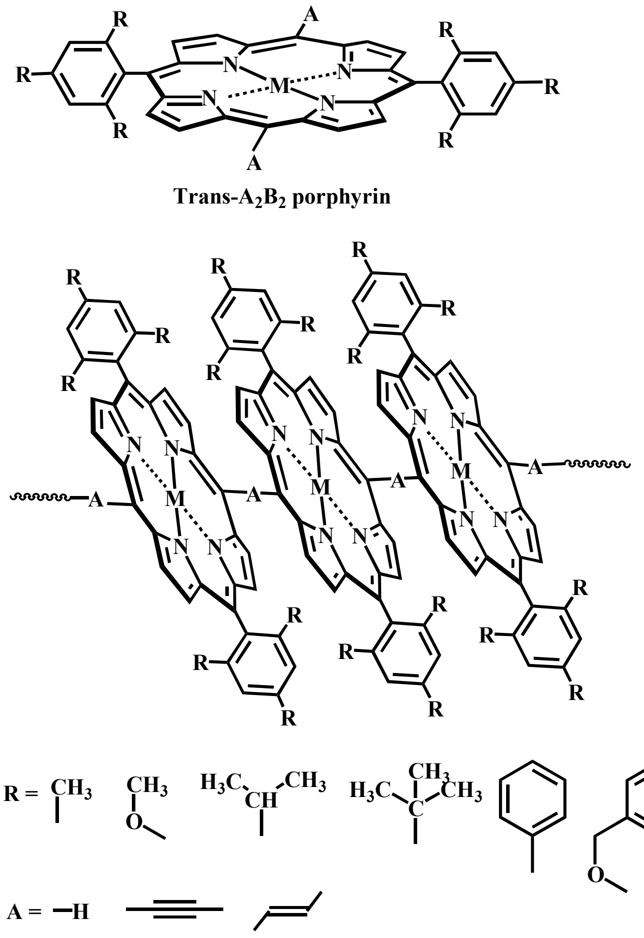

Figure 2-11. ***Trans*-A_2B_2 Porphyrin Design for Soluble Porphyrins**

2.3.1 Synthetic method for *trans*-A_2B_2 porphyrins

Since tetraphenylporphyrin (TPP) was first synthesized by Rothmund in 1936,[11] many synthetic methodologies have been developed and modified to make functionalized porphyrins with improved conditions, yields and quantities. Although Adler-Longo method, which uses milder conditions than Rothmund's method to react benzaldehyde and pyrrole in refluxing propionic acid, can be scaled up to give multi-gram quantities, its drawbacks are the inevitable formation of mixtures of products and low yields. For the synthesis of trans-A_2B_2 porphyrins, for example, the condensation of equivalent amounts of A-aldehyde and B-aldehyde with pyrrole will afford six different porphyrin products in a binomial distribution (Fig. 2-12). This procedure causes purification problems, and also leads to low yields of the major product. According to the probability calculated by the binomial distribution in equation (2), the theoretical yield of the *trans*-A_2B_2 porphyrin is only 12.5% (Fig. 2-13).

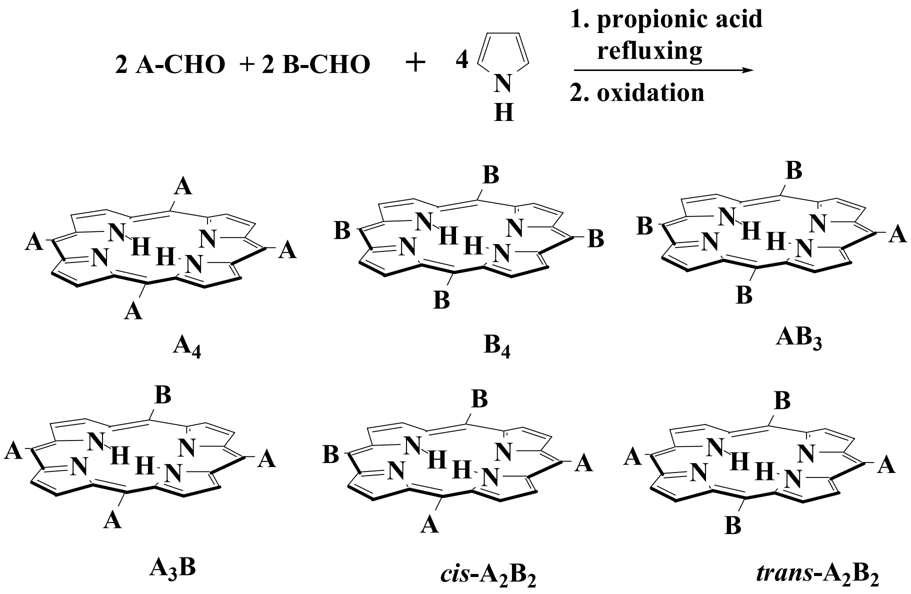

Figure 2-12. The Traditional Procedure for Porphyrin Synthesis

$$P(A_xB_{4-x}) = \left(\frac{4!}{x!(4-x)!}\right)\left(\frac{a}{a+b}\right)^{x}\left(\frac{b}{a+b}\right)^{4-x} \qquad \textbf{(2)}$$

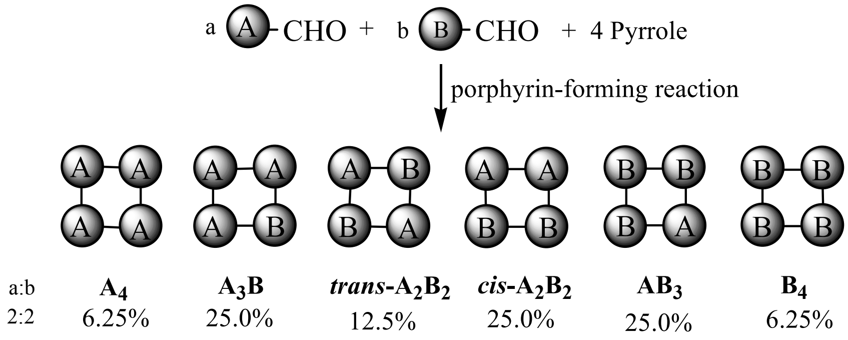

Figure 2-13. The Probabilities of Porphyrins in the Mixture from Traditional Porphyrin-Forming Reaction

Compared to other synthetic methods including porphyrin formation from 2-substituted pyrroles, 2 + 2 porphyrin synthesis, 3 + 1 porphyrin synthesis, and cyclization from linear tetrapyrroles, Lindsey's method is the most suitable procedure for the synthesis of *trans*-A_2B_2 porphyrins (Fig. 2-4). By further modification and optimization,[12-14] Lindsey's procedure affords improved yields, more facile reaction and better purification conditions. Most importantly, it facilitates the formation of *ortho*-substituted tetraarylporphyrins, which are usually difficult to prepare with other methods due to their sterically hindered nature. Lindsey's method requires high-dilution conditions (about 10^{-2} M) because it relies on the chain cyclization to form porphyrinogen and is therefore not amendable to scale up, but it is still a good synthetic methodology for research purpose.

The general procedure for the synthesis of *trans*-A_2B_2 porphyrin includes two steps at room temperature: (1) Aldehyde A is condensed with excess pyrrole (25 to 40 equivalents), which is also used as a solvent, with 0.1 to 0.3 equivalents of TFA or boron trifluoride diethyl etherate to afford *meso*-substituted dipyrromethane, (2) 1 equivalent of aldehydes B is condensed with 1 equivalent of dipyrromethane using 0.1 to 0.3 equivalent of boron trifluoride diethyl etherate to form an intermediate porphyrinogen, which is further oxidized by dichloro-dicyano-benzoquinone (DDQ) into the *trans*-A_2B_2 porphyrin. (Fig. 2-14).

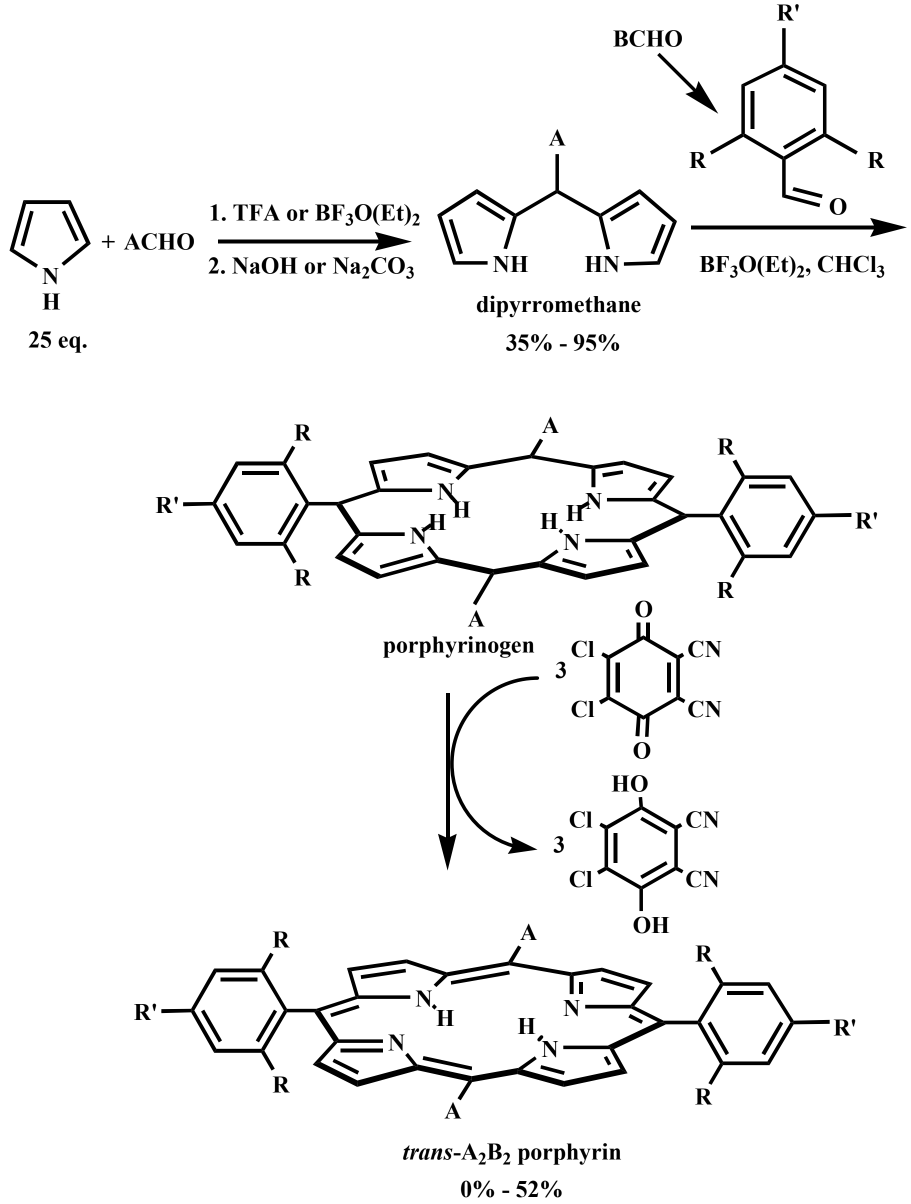

Figure 2-14. The General Procedure for *trans*-A_2B_2 Porphyrins (Lindsey's method)

2.3.2 Syntheses of designed porphyrin molecules

A group of structurally related porphyrins were synthesized in our laboratory for the solubility-structure study (Fig. 2-15). In this group, all of the novel porphyrin molecules are designed to explore the relationships between the solubility and encumbering effects. Two of unencumbered *trans*-A_2B_2 porphyrin molecules were also synthesized for the comparison between encumbered and unencumbered porphyrins (Fig. 2-16).

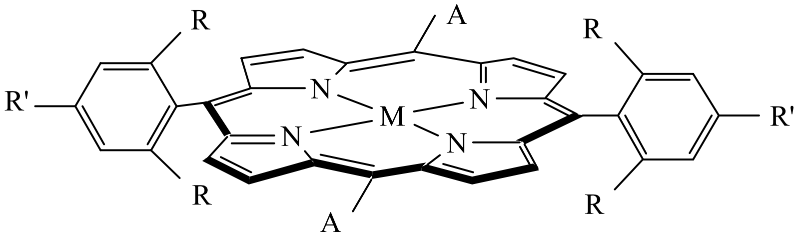

R	R'	A	M	Porphyrin	R	R'	A	M	Porphyrin
H	H	H	2H	**1**	CH_3	H	H	2H	**8**
H	H	H	Zn	**1'**	CH_3	H	H	Zn	**8'**
CH_3	CH_3	H	2H	**2**	H	CH_3	H	2H	**9**
CH_3	CH_3	H	Zn	**2'**	H	$CH(CH_3)_2$	H	2H	**10**
$CH(CH_3)_2$	$CH(CH_3)_2$	H	2H	**3**	H	$CH(CH_3)_2$	H	Zn	**10'**
$CH(CH_3)_2$	$CH(CH_3)_2$	H	Zn	**3'**	H	H	≡–TMS	Zn	**11**
$CH(CH_3)_2$	$CH(CH_3)_2$	H	Ni	**3"**	CH_3	CH_3	≡–TMS	Zn	**12**
$C(CH_3)_3$	$C(CH_3)_3$	H	2H	**4**	$CH(CH_3)_2$	$CH(CH_3)_2$	≡–TMS	Zn	**13**
C_6H_5	C_6H_5	H	2H	**5**	OCH_3	OCH_3	≡–TMS	Zn	**14**
OCH_3	OCH_3	H	2H	**6**	OCH_2Ph	OCH_2Ph	≡–TMS	Zn	**15**
OCH_2Ph	OCH_2Ph	H	2H	**7**	OCH_3	H	≡–TMS	Zn	**16**

Figure 2-15. A Group of Novel Porphyrins Designed for Increasing Solubility

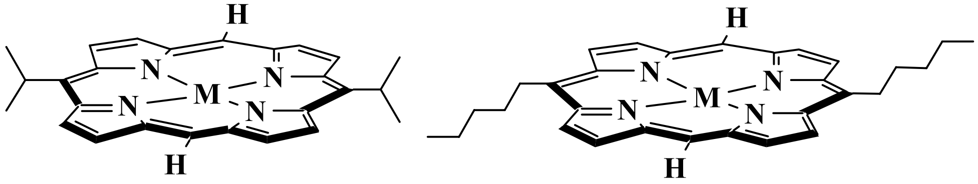

17 (M=2H)

18 (M=2H), 18' (M=Zn)

Figure 2-16. Porphyrins without Facial- and edge-Encumbrance

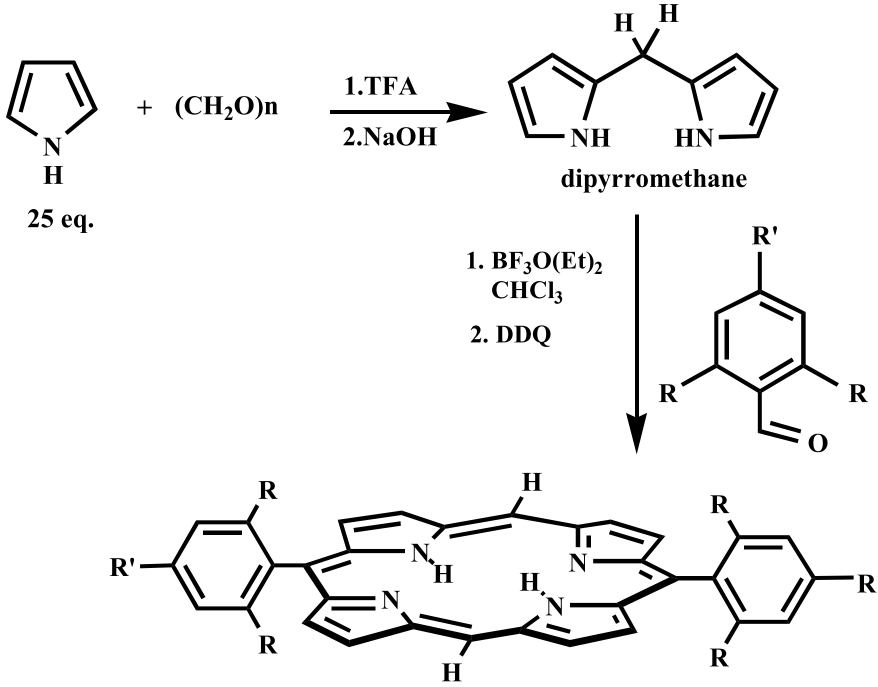

Figure 2-17. Synthesis of Porphyrins 1-10, 17 and 18

Porphyrins **1-10** and **17, 18**, which are unsubstituted at the 10- and 20-*meso*-positions, were prepared by the condensation of **dipyrromethane** (1H, 1'H-2,2'-methanel-bis-pyrrole, Fig. 2-17) with the corresponding benzadehyde following the general procedure in Fig. 2-14. ^{1}H NMR spectra for some of the porphyrins, benzaldehydes and dipyrromethanes are shown in Fig. 2-18 to Fig. 2-23. Detailed procedures for the synthesis of these porphyrin molecules and their precursors, ^{1}H NMR, ^{13}C NMR data and elemental analysis data are described below.

Dipyrromethane. A suspension of paraformaldehyde (1.73 g, 57.7 mmol) in pyrrole (96.7 mL, 1.49 mol) was heated to 70 ^{0}C in an oil bath with stirring. Trifluoroacetic acid (444 μL, 5.76 mmol) was added whereupon the suspension went partially into solution. The heating was maintained for an additional 30 min and the reaction mixture was allowed to cool slightly before addition to 100 mL of ethyl acetate. This solution was washed with two 50 mL portions of 5% aqueous sodium carbonate. The ethyl acetate and excess pyrrole were removed *in vacuo* and the brown oily residue was purified via Keugelrohr distillation (140-150 ^{0}C, 150 mtorr) to provide 4.15 g (49%) of the title compound as a white solid. MP: 75-76 ^{0}C. ^{1}H NMR (400 MHz, CDCl3, 25 ^{0}C, Fig. 2-18) δ = 7.81 (br s, 2H), 6.80 (m, 2H), 6.17 (m, 2H), 6.02 (s, 2H), 3.98 (s, 2H); ^{13}C NMR (100 MHz, $CDCl_3$) δ = 129.06, 117.31, 108.31, 106.42, 26.33.

5,15-diphenyl-10*H*, 20*H*-porphyrin (1). A solution of dipyrromethane (1.47 g, 10.0 mmol) and benzaldehyde (purchased from Aldrich, 1.05 g, 10.0 mmol) in 1 L of $CHCl_3$ was purged with argon for 15 min. $BF_3{\bullet}Et_2O$ (0.127 mL, 0.142 g, 1.0 mmol) was added and the reaction was protected from light with aluminum foil. The reaction was stirred for 30 to 50 minutes followed by the addition of DDQ (1.70 g, 7.5 mmol). The solvent was removed *in vacuo* and the crude product purified by silica gel column chromatography using dichloromethane:hexanes (2:1, v/v) as the eluant to provide 0.42 g wine-red solid of pure porphyrin (**1**) in 18% yield. ^{1}H NMR (400 MHz, $CDCl_3$, Fig. 2-19)

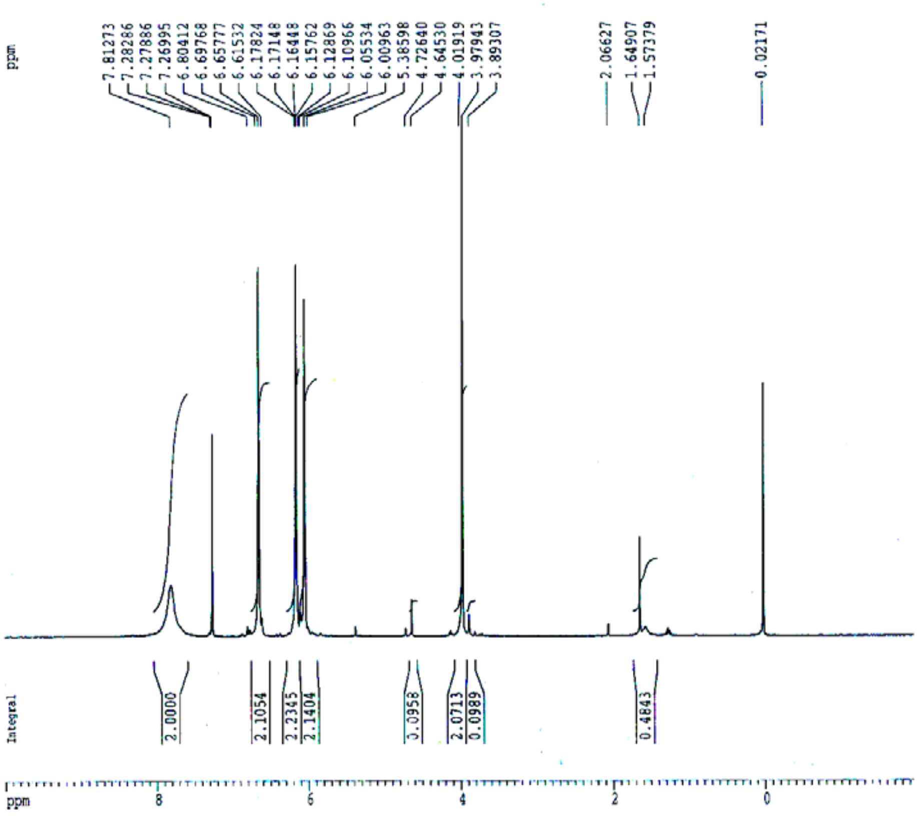

Figure 2-18. ^{1}H NMR Spectrum of dipyrromethane

δ = 10.34 (s, 2H), 9.41 (d, *J* = 4.56 Hz, 4H), 9.11 (d, *J* = 4.56, 4H), 8.30 (m, 4H), 7.83 (m, 6H), -3.10 (s, 2H); ^{13}C NMR (100 MHz, $CDCl_3$) δ =147.42, 145.53, 141.78, 134.88, 131.62, 131.05, 127.71, 126.97, 118.86, 105.50.

5,15-dimesityl-10*H*, 20*H*-porphyrin (**2**). A solution of dipyrromethane (0.63 g, 4.32 mmol) and mesitaldehyde (purchased from Aldrich, 0.64 g, 4.32 mmol) in 430 mL of $CHCl_3$ was purged with argon for 15 min. BF_3•Et_2O (0.016 mL, 0.43 mmol) was added and the reaction was protected from light with aluminum foil. The reaction was stirred for

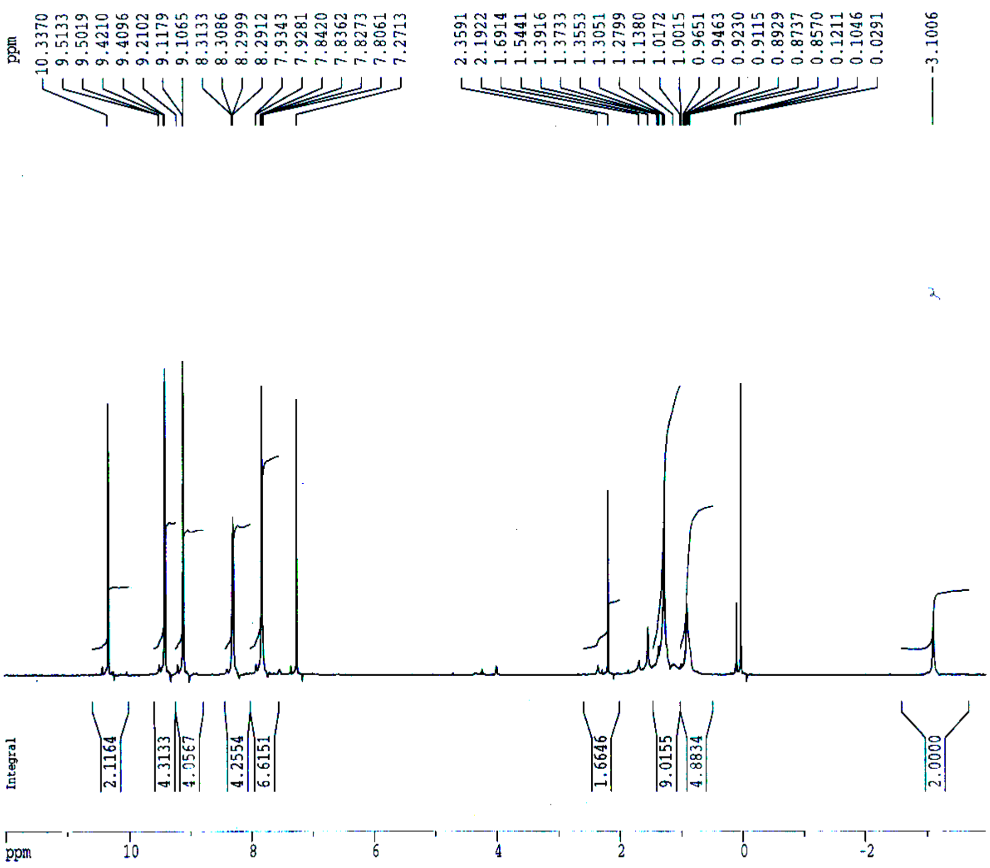

Figure 2-19. ^{1}H NMR Spectrum of 5,15-diphenyl-10*H*, 20*H*-Porphyrin (1)

30 to 50 minutes followed by the addition of DDQ (1.38 g, 6.5 mmol). The solvent was removed *in vacuo* and the crude product purified by silica gel column chromatography using dichloromethane:hexanes (2:1, v/v) as the eluant to afford 0.22 g of 5,15-dimesityl-10*H*, 20*H*-porphyrin (**2**) in 19% yield. ^{1}H NMR (400 MHz, $CDCl_3$, Fig. 2-20) δ = 10.25 (s, 2H), 9.35 (d, *J* = 4.56Hz, 4H), 8.91 (d, *J* = 4.56Hz, 4H), 7.35 (s, 4H), 2.67 (s, 6H), 1.87 (s, 12H), -3.05 (s, 2H). ^{13}C NMR (100 MHz, $CDCl_3$) δ =145.67, 139.46, 138.00, 137.88, 131.79, 129.99, 127.84, 117.50, 111.27, 96.11, 21.71, 21.50.

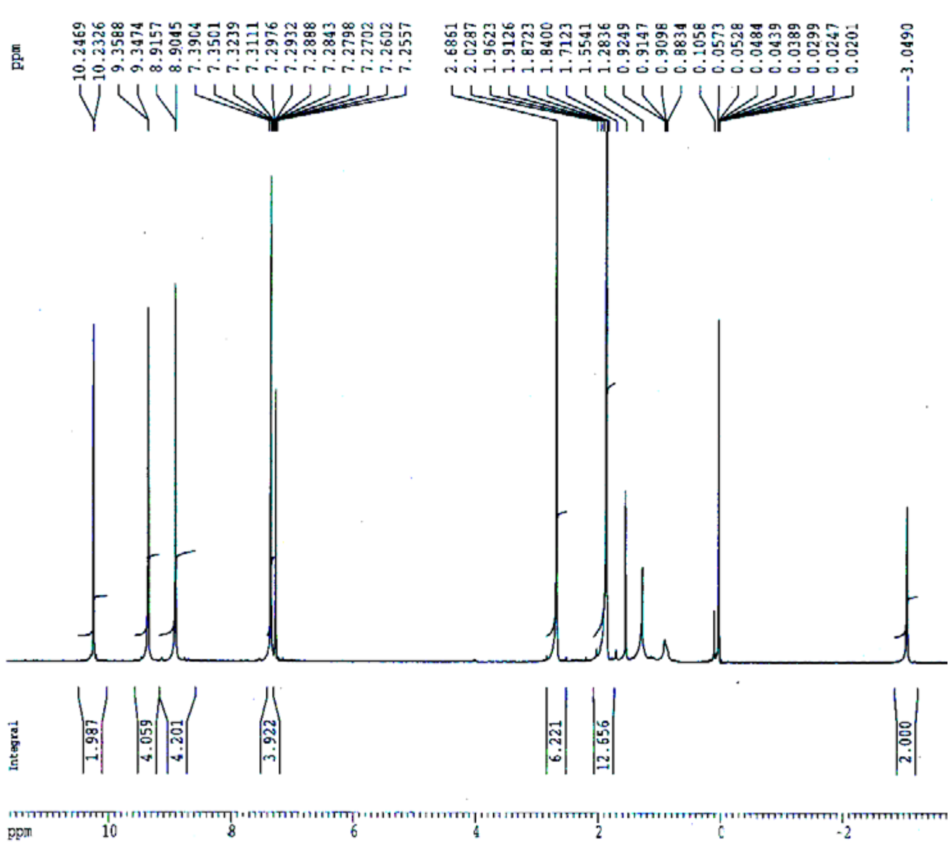

Figure 2-20. ^{1}H NMR Spectrum of 5,15-dimesityl-10*H*, 20*H*-porphyrin (2)

2, 4, 6-triisopropylbenzaldehyde.[15] A 250-mL three-necked flask was equipped with a thermometer, reflux condenser, dropping funnel (protected with a calcium chloride drying-tube) and magnetic stirrer, and a gas absorption trap was attached to the top of the condenser. 12.1 mL (10.22 g, 0.05 mol) of 1, 3, 5-triisopropylbenzene and 50 mL of dried CH_2Cl_2 (distilled under Argon over CaH_2) were added into the flask and cooled to 0 °C in an ice-bath. To the stirred solution, 11 mL (19 g, 0.1mol) of titanium (IV) chloride was added from a dropping funnel, and the solution turned brown. Then 4.5 mL (5.8 g, 0.05 mol) of dichloromethyl methyl ether was slowly added over 30 minutes, the solution became more viscous and HCl was evolved and absorbed in a gas trap. The ice-bath was

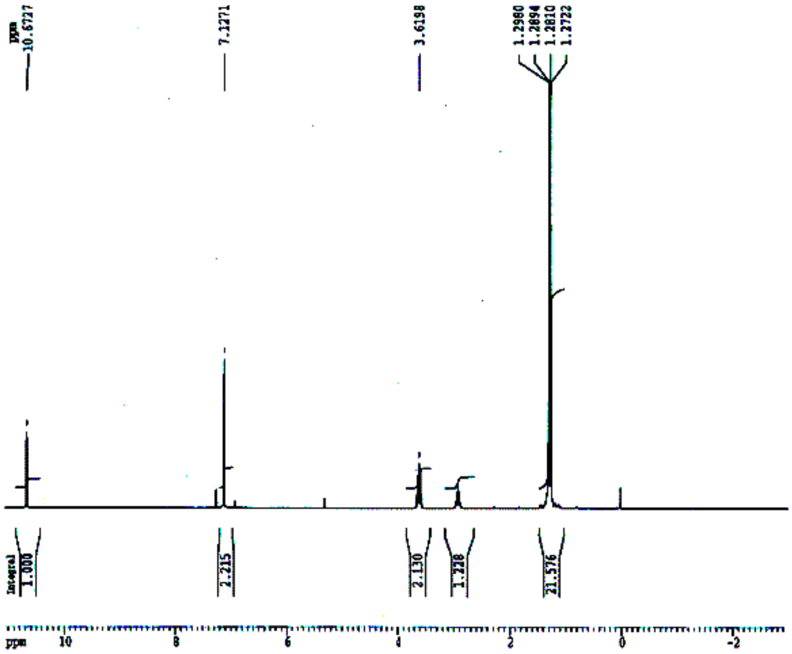

Figure 2-21. ^{1}H NMR Spectrum of 2,4,6-triisopropylbenzaldehyde

removed and the temperature gradually increased to room temperature. Then the reaction was heated to about 35 ^{0}C, and stirred for 1 hour. The solution was poured into ice water and the organic layer was separated from aqueous layer. The organic layer was washed with water and the aqueous layer was washed with CH_2Cl_2. All organic extracts were combined, and dried with $MgSO_4$. The solvent was removed in *vacuo* to afford a light-brown and cloudy liquid. After silica gel chromatographic purification using dichloromethane:hexanes (2:1, v/v) as the eluant to afford 11 g (yield 94%) of 2, 4, 6-triisopropylbenzaldehyde. ^{1}H NMR (400 MHz, $CDCl_3$, 25 ^{0}C, Fig. 2-21) δ =10.67 (s, 1H), 7.13 (s, 2H), 3.62 (p, J = 8Hz, 2H), 2.92 (p, J = 8Hz, 1H), 1.29 (d, J = 8Hz, 12H), 1.28 (d, J = 8Hz, 6H).

5,15-bis(2, 4, 6-triisopropylphenyl)-10*H*, 20*H*-porphyrin (**3**). A solution of dipyrromethane (1.46 g, 10.0 mmol) and 2, 4, 6-triisopropylbenzaldehyde (2.32 g, 10 mmol) in 1000 mL of $CHCl_3$ was purged with argon for 15 min. $BF_3 \bullet Et_2O$ (0.41 mL, 3.3 mmol) was added and the reaction was protected from light with aluminum foil. The reaction was stirred for 30 to 50 minutes followed by the addition of DDQ (3.7 g, 15.0 mmol). The solvent was removed *in vacuo* and the crude product purified by silica gel column chromatography using dichloromethane:hexanes (2:1, v/v) as the eluant to afford 0.79 g (yield 22%) of 5,15-bis(2, 4, 6-triisopropylphenyl)-10*H*, 20*H*-porphyrin (**3**). ^1H NMR (400 MHz, $CDCl_3$, Fig. 2-22) $\delta = 10.27$ (s, 2H), 9.35 (d, $J = 4.56$, 4H), 8.98 (d, $J = 4.56$, 4H), 7.42 (s, 4H), 3.28 (m, 4H), 2.18 (m, 6H), 1.62 (d, 12H), 0.93 (d, 24H), -2.97 (s, 2H). ^{13}C NMR (100 MHz, $CDCl_3$) $\delta = 150.16$, 149.60, 147.84, 145.51, 135.16, 131.38, 131.06, 120.43, 117.36, 34.82, 31.57, 24.65, 24.36. Elemental Analysis: C% 82.40 (83.9 0), H% 8.21 (8.18), N% 7.59 (7.70)

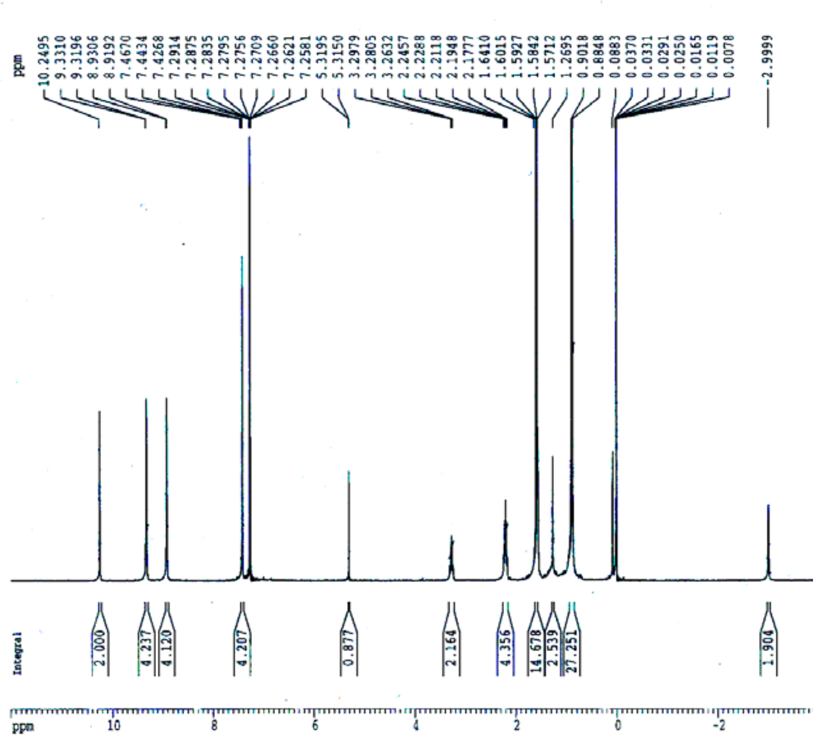

Figure 2-22. ^1H NMR spectrum of 5,15-bis(2, 4, 6-triisopropylphenyl)-10*H*, 20*H*-porphyrin (3)

1, 3, 5-tri-*t*-butylbenzene.[16-18] 10 mL (0.113 mol) of benzene and 74 mL (0.678 mol) of2-chloro-2-methylpropane were placed into a 250-mL three-necked flask attached with a gas absorption trap and cooled to −40 ^{0}C. 5 g of aluminum chloride was then added into the stirred solution in small portions. HCl was evolved and absorbed in gas trap. After all of the $AlCl_3$ was added, the mixture was stirred at −40 °C for 30 minutes. Then the reaction was warmed slowly to room temperature and stirred continually for 2 hours. The solution was poured over ice water, separated, washed and dried to give the crude product. Under vacuum distillation, 7.7 g (0.04 mol, yield 36%) of di-*t*-butylbenzene (mp 76~78 ^{0}C, distilled at 70 ^{0}C/0.5 mmHg) and 10 g (0.04 mol, yield 36%) of 1,3,5-tri-*t*-butylbenzene (mp 69~71 ^{0}C) was obtained.

1-bromo-2, 4, 6-tri-*t*-butylbenzene. 5 g (0.02 mol) of 1, 3, 5-tri-*t*-butylbenzene was dissolved in 172 mL of glacial acetic acid and 43 mL of dioxane, the solution of $AgNO_3$ (5 g, 0.029 mol), HNO_3 (concentrated, 1.43 mL) and H_2O (22.5 mL) was then added. The mixture became cloudy and some white precipitate was formed. 5 g (0.032 mol, 1.6 mL) of Br_2 was added into the solution, which was stirred for 16 hours. 720 mL of H_2O was added to dilute and Na_2SO_3 was added to decolorize the solution. The reaction was extracted with n-pentane, washed with 10% NaOH, and crystallized from ethanol to obtain 1.5 g (yield 23%) of 1-bromo-2, 4, 6-*t*-butylbenzene (mp 169-171^{0}C).

2, 4, 6-tri-*t*-butylbenzaldehyde.[19] 0.55 g of vacuum dried 1-bromo-2, 4, 6-tri-*t*-butylbenzene (1.7 mmol) was added in 6.5 mL of dried THF (distilled in Na and benzophenone until it was blue) and cooled to –78 °C. 0.35 mL of n-butyllithium (10.0 M in hexane, 3.5 mmol) was added over 10 minutes and the reaction was stirred overnight. The solution was then gradually warmed up to room temperature. 0.5 mL (6.2

mmol) of dried ethyl formate was added and the solution was stirred for 10 hours. The reaction was quenched by 10 mL of saturated NH_4Cl solution. The crude product was extracted with diethyl ether, and purified by silica flash chromatographic column (1:1 hexanes:CH_2Cl_2) to give 0.056 g (yield 12%) of 2, 4, 6-tri-*t*-butylbenzaldehyde (mp 196~198 ^{0}C): ^{1}H NMR (400 MHz, $CDCl_3$, 25 ^{0}C, Fig. 2-23) δ =10.13 (s, 1H), 7.38 (s, 2H), 1.38 (s, 18H); ^{13}C NMR (400 MHz, $CDCl_3$, 25 ^{0}C) δ = 196.1, 155.7, 149.9, 142.0, 119.5, 35.2, 32.5, 31.6, 30.8.

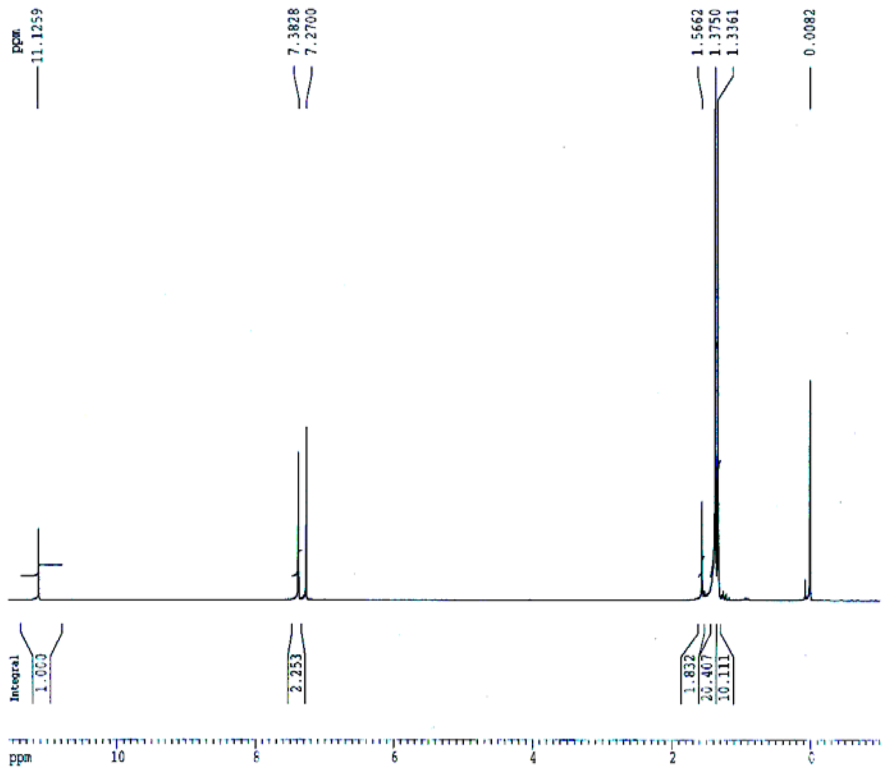

Figure 2-23. ^{1}H NMR spectrum of 2, 4, 6-tri-*t*-butylbenzadehyde

5, 15-bis(2, 4, 6-tri-*t*-butylphenyl)-10*H*, 20*H*-porphyrin (**4**). A solution of dipyrromethane (0.29 g, 0.2 mmol) and 2, 4, 6-tri-*t*-butylbenzaldehyde (0.55 g, 0.2 mmol) in 200 mL of CHCl3 was purged with argon for 15 min. BF3•Et2O (0.8 uL, 0.006 mmol) was added and the reaction was protected from light with aluminum foil. The reaction was stirred for 30 to 50 minutes followed by the addition of DDQ (0.068 g, 0.3 mmol). TLC showed no porphyrin spot in this reaction. So the procedure we used failed to give 5,15-Bis (tri-*t*-butylphenyl)-10*H*, 20*H*-porphyrin (**4**). It is believed that *t*-butyl group is much more bulky than methyl and isopropyl group to hinder the condensation in the porphyrin formation reaction.

1-bromo-2, 4, 6-triphenylbenzene. 12 mL (0.24 mol) of Br_2 was added into a solution of 33 g of 1, 3, 5-triphenylbenzene (0.108 mol) in 250 mL of carbon disulfide. The mixture was stirred over night and left to evaporate to give crude yellow crystal, which was recrystalized in methanol to give 37.5 g (yield 90%) of 1-bromo-2, 4, 6-triphenylbenzene (mp 130-132 ^{0}C).

2, 4, 6-triphenylbenzaldehyde.[20] 3.53 g (9.2 mmol) of 2, 4, 6-triphenylbromobenzene was added in 200 mL of dried diethyl ether in a 250 mL three-necked flask with a dropping funnel. The solution was cooled to –78 ^{0}C. 7 mL of n-butyllithium (1.6 M in hexane, 11 mmol) was added over 40 minutes and the solution became cloudy. After it was gradually warmed to room temperature, the solution became clear and light yellow. It was stirred for 17 hours. 2.7 mL (18.4 mmol) of DMF was added and the reaction was stirred for another 17 hours. By flash silica chromatographic separation using dichloromethane:hexanes (1:1, v/v) and recrystalization in 1:1 ether: hexanes, 1 g (yield 33%) of 2, 4, 6-triphenylbenzaldehyde was obtained (mp 133-134 °C). ^{1}H NMR (400 MHz, $CDCl_3$) δ =10.01 (s, 1H), 7.64 (s, 2H), 7.75 ~ 7.27 (m, 15H), ^{13}C NMR (400 MHz, $CDCl_3$) δ = 195.2,145.2, 139.7, 129.6 ~127.4.

5, 15-bis(2, 4, 6-triphenylphenyl)-10*H*, 20*H*-porpohyrin (**5**). A solution of dipyrromethane (0.29 g, 2 mmol) and 2, 4, 6-triphenylbenzaldehyde (0.67 g, 2 mmol) in 200 mL of $CHCl_3$ was purged with argon for 15 min. $BF_3{\bullet}Et_2O$ (8 uL, 0.2 mmol) was added and the reaction was protected from light with aluminum foil. The reaction was stirred for 30 to 50 minutes followed by the addition of DDQ (0.68 g, 3 mmol). The solvent was removed *in vacuo* and the crude product purified by silica gel column chromatography using dichloromethane:hexanes (2:1, v/v) as the eluant to afford 0.09 g (yield 2%) of 5,15-bis(2, 4, 6-triphenylphenyl)-10*H*, 20*H*-porpohyrin (**5**). ^{1}H NMR (400 MHz, $CDCl_3$) $\delta = 10.31$ (s, 2H), 9.19 (d, 2H), 9.16 (d, 2H), 9.06 (d, 2H), 8.95 (d, 2H), 8.29 (m, 2H), 8.10 (m, 2H), 8.04 (m, 2H), 8.00 (m, 2H), 7.98 (m, 2H), 2H), 7.78 (m, 2H), 7.65 (m, 2H), 7.53 (m, 2H), 7.14 (m, 2H), 6.93 (m, 2H), 6.82 (m, 2H), 6.44 (m, 2H), 6.28 (m, 2H), 6.24 (m, 2H), 6.07 (m, 2H). ^{13}C NMR (100 MHz, $CDCl_3$) $\delta = 140.21$, 129.21, 127.78, 127.41, 126.94, 126.54, 126.37.

5,15-bis(2, 4, 6-trimethoxylphenyl)-10*H*, 20*H*-porphyrin (**6**). A solution of dipyrromethane (0.14 g, 1 mmol) and 2, 4, 6-trimethoxylbenzaldehyde (purchased from Aldrich, 0.21 g, 1 mmol) in 100 mL of $CHCl_3$ was purged with argon for 15 min. $BF_3{\bullet}Et_2O$ (4 uL, 0.1 mmol) was added and the reaction was protected from light with aluminum foil. The reaction was stirred for 30 to 50 minutes followed by the addition of DDQ (0.68 g, 3 mmol). The solvent was removed *in vacuo* and the crude product purified by silica gel column chromatography using dichloromethane:hexanes (2:1, v/v) as the eluant to afford 0.05 g of 5,15-bis(2, 4, 6-trimethoxylphenyl)-10*H*, 20*H*-porphyrin (**6**) in yield 14%. ^{1}H NMR (400 MHz, $CDCl_3$) $\delta = 10.16$ (s, 2H), 9.30 (d, $J = 4.56$, 4H), 9.00 (d, $J = 4.56$, 4H), 6.63 (s, 4H), 4.14 (s, 6H), 3.53 (s, 12H), -3.03 (s, 2H). ^{13}C NMR (100

MHz, $CDCl_3$) δ= 144.61, 130.73, 131.44, 123.45, 91.00, 56.00. Elemental Analysis: C% 70.70 (71.01), H% 5.83 (5.33), N% 8.43 (8.70).

2, 4, 6-tribenzoxybenzaldehyde.[21] 1.54 g (10.00 mmol) of phloroglucinaldehyde (purchased from Lancaster Synthesis Inc.) and 5.64 g (3.90 mL, 33.00 mmol) of benzyl bromide were dissolved in 40 mL of DMF, 12.44 g (9.0 eq.) of potassium carbonate was added as a base and a few crystals of potassium iodide as catalyst. The reaction proceeded for about 3 days. The organic layer was extracted by ethyl acetate. The product was precipitated from ethyl acetate and washed by hot ethanol to give 2.14 g of 2, 4, 6-tribenzoxybenzaldehyde (yield 50%, mp = 129-132^{0}C). ^{1}H NMR (400 MHz, $CDCl_3$) δ = 10.47 (s, 1H), 7.50 m, 15H), 6.64 (s, 2H), 5.31 (s, 6H).

5,15-bis(2, 4, 6-tribenzoxyphenyl)-10*H*, 20*H*-porphyrin (**7**). A solution of dipyrromethane (0.30 g, 2 mmol) and 2, 4, 6-tribenzoxybenzaldehyde (0.85 g, 2 mmol) in 200 mL of $CHCl_3$ was purged with argon for 15 min. BF_3•Et_2O (8 uL, 0.1 mmol) was added and the reaction was protected from light with aluminum foil. The reaction was stirred for 30 to 50 minutes followed by the addition of DDQ (0.68 g, 3 mmol). The solvent was removed *in vacuo* and the crude product purified by silica gel column chromatography using dichloromethane:hexanes (2:1, v/v) as the eluant to afford 55 mg of 5,15-Bis (2, 4, 6-tribenzoxyphenyl)-10*H*, 20*H*-porphyrin (**7**) in 5% yield. ^{1}H NMR (400 MHz, $CDCl_3$) δ = 10.24 (s, 2H), 9.36 (d, J = 4.48, 4H), 9.10 (d, J = 4.48, 4H), 7.61 (m, 4H), 7.52 (m, 4H), 7.46 (m, 2H), 7.38 (s, 4H), 6.88 (m, 4H), 6.78 (m, 8H), 6.73 (s, 4H), 6.60 (m, 8H), 5.25 (s, 4H), 4.88 (s, 8H). ^{13}C NMR (100 MHz, $CDCl_3$) δ = 159.89, 136.75, 128.77, 127.91, 127.05, 126.34, 94.04, 70.20, 29.69. Elemental Analysis: C% 81.02 (80.85), H% 5.64 (5.32), N% 5.32 (5.10).

5,15-bis(2,6-dimethylphenyl)-10*H*, 20*H*-porphyrin (**8**). A solution of dipyrromethane (0.59 g, 4.02 mmol) and 2,,6-dimethylbenzaldehyde (0.54 g, 4 mmol) in 400 mL of $CHCl_3$ was purged with argon for 15 min. BF_3•Et_2O (31 uL, 0.24 mmol) was added and the reaction was protected from light with aluminum foil. The reaction was stirred for 30 to 50 minutes followed by the addition of DDQ (1.36 g, 6 mmol). The solvent was removed *in vacuo* and the crude product purified by silica gel column chromatography using dichloromethane:hexanes (2:1, v/v) as the eluant to afford 0.12 g of 5,15-bis(2,6-dimethylphenyl) -10*H*, 20*H*-porphyrin (8) in 12% yield. ^{1}H NMR (400 MHz, $CDCl_3$) δ =10.24 (s, 2H), 9.35 (d, 4H), 8.87 (d, 4H), 7.64 (m, 2H), 7.51 (m, 4H), 1.89(s, 12H). ^{13}C NMR (100 MHz, $CDCl_3$) δ = 146.60, 145.28, 140.51, 139.67, 136.16, 133.00, 131.94, 131.22, 129. 90, 129.28, 128. 35, 127.07, 117.12, 104.75, 29.36, 22.69.

5,15-bis(*p*-tolyl)-10*H*, 20*H*-porphyrin (**9**). A solution of dipyrromethane (0.58 g, 4.02 mmol) and *p*-tolualdehyde (0.48 g, 4 mmol) in 400 mL of $CHCl_3$ was purged with argon for 15 min. BF_3•Et_2O (31 uL, 0.24 mmol) was added and the reaction was protected from light with aluminum foil. The reaction was stirred for 30 to 50 minutes followed by the addition of DDQ (1.36 g, 6 mmol). The solvent was removed *in vacuo* and the crude product purified by silica gel column chromatography using dichloromethane:hexanes (2:1, v/v) as the eluant to afford 0.21 g of 5,15-bis(*p*-tolyl)-10*H*, 20*H*-porphyrin (**9**) in 20% yield. ^{1}H NMR (400 MHz, $CDCl_3$) δ = 10.32 (s, 2H), 9.40 (d, J = 4.60, 4H), 9.12 (d, J = 4.60, 4H), 8.18 (d, J = 7.84, 4H), 7.63 (d, J = 7.84, 4H), 2.75 (s, 6H). ^{13}C NMR (100 MHz, $CDCl_3$) δ = 134.77, 131.04, 127.71, 21.53. Elemental Analysis: C% 82.44 (83.24), H% 5.24 (5.34), N% 10.62 (11.02).

5, 15-bis(*p*-isopropylphenyl)-10*H*, 20*H*-porphyrin (**10**). A solution of dipyrromethane (0.58 g, 4.02 mmol) and *p*-isopropylbenzaldehyde (purchased from Aldrich, 0.59 g, 4 mmol) in 400 mL of $CHCl_3$ was purged with argon for 15 min. BF_3•Et_2O (31 uL, 0.24 mmol) was added and the reaction was protected from light with aluminum foil. The reaction was stirred for 30 to 50 minutes followed by the addition of DDQ (1.36 g, 6 mmol). The solvent was removed *in vacuo* and the crude product purified by silica gel column chromatography using dichloromethane:hexanes (2:1, v/v) as the eluant to afford 0.17 g of 5, 15-bis(*p*-isopropylphenyl)-10*H*, 20*H*-porphyrin (**10**) in 15% yield. ^{1}H NMR (400 MHz, $CDCl_3$) $\delta = 10.32$ (s, 2H), 9.44 (d, 4H), 9.20 (d, 2H), 8.19 (m, 4H), 7.66 (m, 4H), 3.33 (m, 2H), 1.60 (s, 12H). Elemental Analysis: C% 75.06 (74.81), H% 5.06 (5.29), N% 8.99 (9.12)

5, 15-diisopropyl-10*H*, 20*H*-porphyrin (**17**): A solution of dipyrromethane (0.58 g, 4.02 mmol) and isobutyraldehyde (purchased from Aldrich, 0.29 g, 4 mmol) in 400 mL of $CHCl_3$ was purged with argon for 15 min. BF_3•Et_2O (31 uL, 0.24 mmol) was added and the reaction was protected from light with aluminum foil. The reaction was stirred for 30 to 50 minutes followed by the addition of DDQ (1.36 g, 6 mmol). The solvent was removed *in vacuo* and the crude product purified by silica gel column chromatography using dichloromethane:hexanes (2:1, v/v) as the eluant to give 0.17 g of 5, 15-diisopropyl-10*H*, 20*H*-porphyrin (**17**) in 21% yield. ^{1}H NMR (400 MHz, $CDCl_3$) $\delta = 10.21$(s, 2H), 9.74 (d, 4H), 9.42 (d, 4H), 5.71 (m, 2H), 2.50 (s, 12H). ^{13}C NMR (100 MHz, $CDCl_3$) $\delta = 175.03$, 147.10, 131.93, 124.75, 104.407, 34.44, 28.88. Elemental Analysis: C% 80.45 (79.16), H% 6.36 (6.64), N% 14.40 (14.20).

5, 15-dihexyl-10*H*, 20*H*-porphyrin (**18**): A solution of dipyrromethane (0.58 g, 4.02 mmol) and hexanal (purchased from Aldrich, 0.4 g, 4 mmol) in 400 mL of $CHCl_3$ was purged with argon for 15 min. BF_3•Et_2O (31 uL, 0.24 mmol) was added and the reaction was protected from light with aluminum foil. The reaction was stirred for 30 to 50 minutes followed by the addition of DDQ (1.36 g, 6 mmol). The solvent was removed *in vacuo* and the crude product purified by silica gel column chromatography using dichloromethane:hexanes (2:1, v/v) as the eluant to give 0.12 g of 5, 15-dihexyl-10*H*, 20***H***-porphyrin (**18**) in 15% yield. ^{1}H NMR (400 MHz, $CDCl_3$) $\delta = 10.13$ (s, 2H), 9.54 (d, *J* = 2.56, 4H), 9.38 (d, *J* = 2.56, 4H), 4.97 (m, 4H), 2.56 (m, 4H), 1.81 (m, 4H), 1.58 (m, 4H), 1.33 (m, 4H), 1.02 (m, 6H). ^{13}C NMR (100 MHz, $CDCl_3$) $\delta = 147.37$, 144.10, 131.80, 127.72, 118.74, 38.32, 34.54, 32.73, 22.80, 14.19. Elemental Analysis: C% 79.70 (79.96), H% 7.40 (7.61), N% 12.88 (12.43).

The syntheses of porphyrins **11-16** are outlined in Fig. 2-24. The yields and reaction conditions are very similar. The ^{1}H NMR spectra for some porphyrins, benzaldehydes and dipyrromethane used in the synthesis of porphyrins **11-16** are shown in Fig. 2-25 to Fig. 2-27. Detailed procedures for these syntheses are described below.

Trimethylsilylpropynal.[22] To a magnetically stirred solution of 0.13 mol of EtMgBr, 10.5 g of trimethylsilyacetylene (0.11 mol) was added and dissolved in 75 mL dried THF. The temperature was maintained at 10-15 ^{0}C using an ice-water bath. After stirring for 1 hour, the mixture was transferred into a dropping funnel and added to a mixture of 28.2 mL of DMF and 50 mL of diethyl ether at –25 ^{0}C over a period of 45 minutes. The white suspension was allowed to reach RT, stirred for 1 hour, heated at 30 ^{0}C for 15 minutes and poured into 200 mL of 5% H_2SO_4 at 0 ^{0}C. The organic layer was

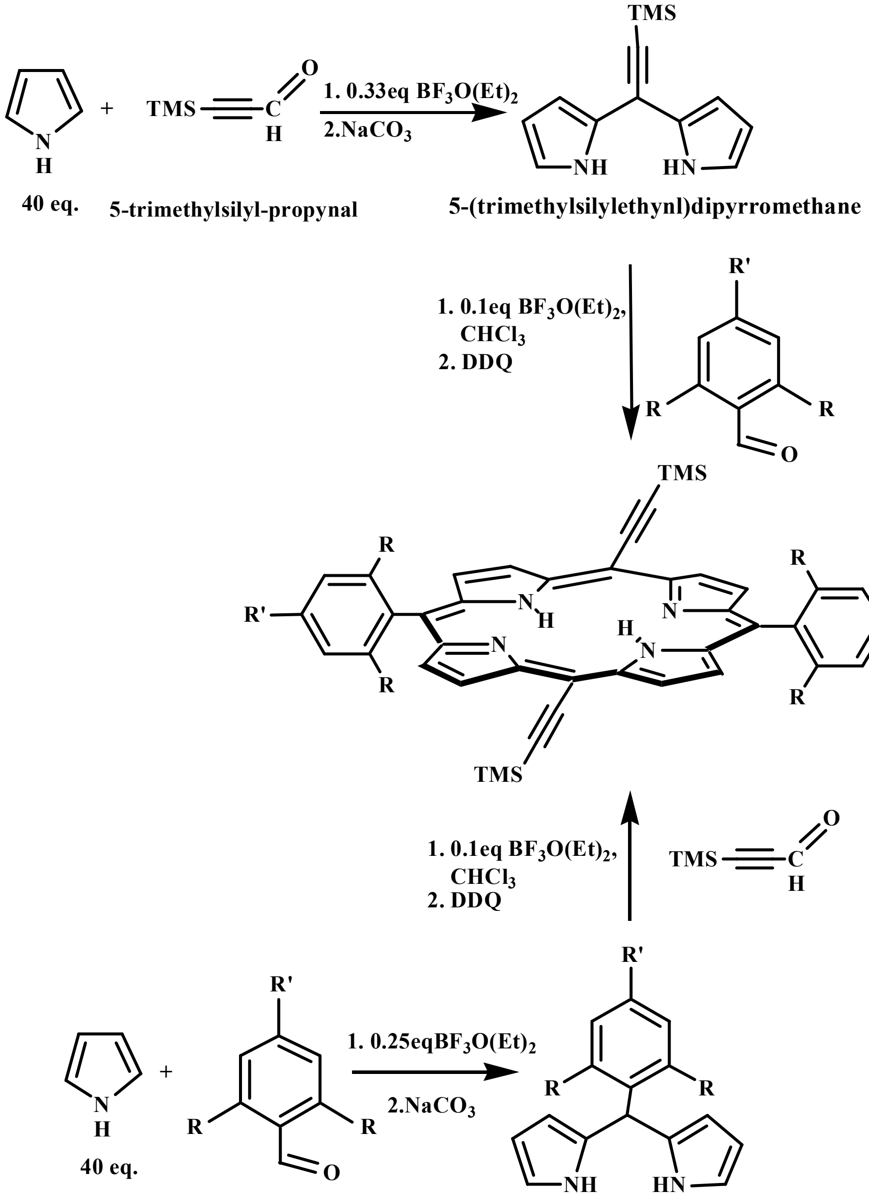

Figure 2-24. Syntheses of Porphyrins 11-16

separated and washed with saturated NH_4Cl solution and dried. Distillation of the organic layer (trace of hydroquinone added) at 44-45 ^0C at 20 mmHg afforded 9.0 g of trimethylsilylpropynal in 65% yield. ^{1}H NMR (250 MHz, $CDCl_3$, 25 ^{0}C) δ = 9.11 (s, 1H), 0.14 (s, 9H). ^{13}C NMR (62.5 MHz, $CDCl_3$, 25 ^{0}C) δ = 177.24, 103.38, 102.76.

5-(trimethylsilylethynl)dipyrromethane. 1.0 g (8.0 mmol) of trimethylsilylpropynal was added into 22.2 mL (320 mmol, 40 eq.) of pyrrole. The solution was purged with argon for 30 minutes. 0.34 mL (2.64 mmol, 0.33 eq.) of $BF_3{\bullet}Et_2O$ was added at RT. After 30 minutes, the solution was extracted with ethyl acetate, washed with 10% $NaCO_3$ solution, dried with $MgSO_4$ and evaporated in *vacuo* to remove solvent. Excess pyrrole was removed by distillation to leave oily mixture, which was purified by silica chromatography using cyclohexane:ethyl acetate:triethylamine (20:1:0.1) to obtain 0.6 g (yield 31%) of 5-(trimethylsilylethynl)dipyrromethane. ^{1}H NMR (400 MHz, $CDCl_3$, 25 ^{0}C) δ = 8.05 (br s, 2H), 6.71 (d, 2H), 6.22 (d, 2H), 6.19 (d, 2H), 5.19 (s, 1H), 0.29 (s, 9H). ^{13}C NMR (100 MHz, $CDCl_3$, 25 ^{0}C) δ = 128.90, 117.90, 117.77, 108.78, 108.65, 108.28, 106.73, 106.55, 103.55, 103.36, 88.01, 31.26, 0.20.

5-phenyldipyrromethane. 0.85 g (8.0 mmol) benzaldehyde was added into 22.2 mL (320 mmol) of pre-distilled pyrrole. The solution was purged with argon for 30 minutes then 0.34 mL (2.64 mmol) of $BF_3{\bullet}Et_2O$ was added. After 40 minutes, the reaction was extracted with ethyl acetate, washed with 10% $NaCO_3$ solution, dried with $MgSO_4$ and evaporated in *vacuo* to remove solvent. Excess pyrrole was removed by distillation to leave a yellow semisolid, which was purified by using chromatography (silica) with cyclohaxane:ethyl acetate:triethylamine (20:1:0.1) to afford 1.18 g of 5-phenyldipyrromethane in 67% yield. ^{1}H NMR (400 MHz, $CDCl_3$, Fig. 2-25) δ = 7.91 (br s, 2H), 7.36-7.23 (m, 5H), 6.69 (d, 2H), 6.19 (d, 2H), 5.94 (d, 2H), 5.49 (s, 1H). ^{13}C NMR (100 MHz, $CDCl_3$) δ = 141.5, 134.7, 128.2, 127.1, 121.9, 107.1, 102.9, 101.0

5-mesityldipyrromethane. 2.94 g (20 mmol) mesitaldehyde was added into 55.8 mL (800 mmol) of pre-distilled pyrrole. The solution was purged with argon for 30 minutes then 1.2 mL (9.5 mmol) of BF_3•Et_2O was added. After 40 minutes, the reaction was extracted with ethyl acetate, washed with 10% $NaCO_3$ solution, dried with $MgSO_4$ and evaporated in *vacuo* to remove solvent. Excess pyrrole was removed by distillation to leave a yellow semisolid, which was purified by using chromatography (silica) with cyclohaxane:ethyl acetate:triethylamine (20:1:0.1) to afford 1.8 g of 5-mesityldipyrromethane in 34% yield. ^{1}H NMR (400 MHz, $CDCl_3$) δ = 7.96 (br s, 2H), 6.89 (s, 2H), 6.68 (d, 2H), 6.20 (d, 2H), 6.03 (d, 2H), 5.94 (s, 1H), 2.30 (s, 6H), 2.08 (s, 3H). ^{13}C NMR (100 MHz, $CDCl_3$) δ = 137.6, 136.6, 134.5, 131.2, 130.3, 116.1, 108.6, 106.5, 38.3, 20.8, 20.6

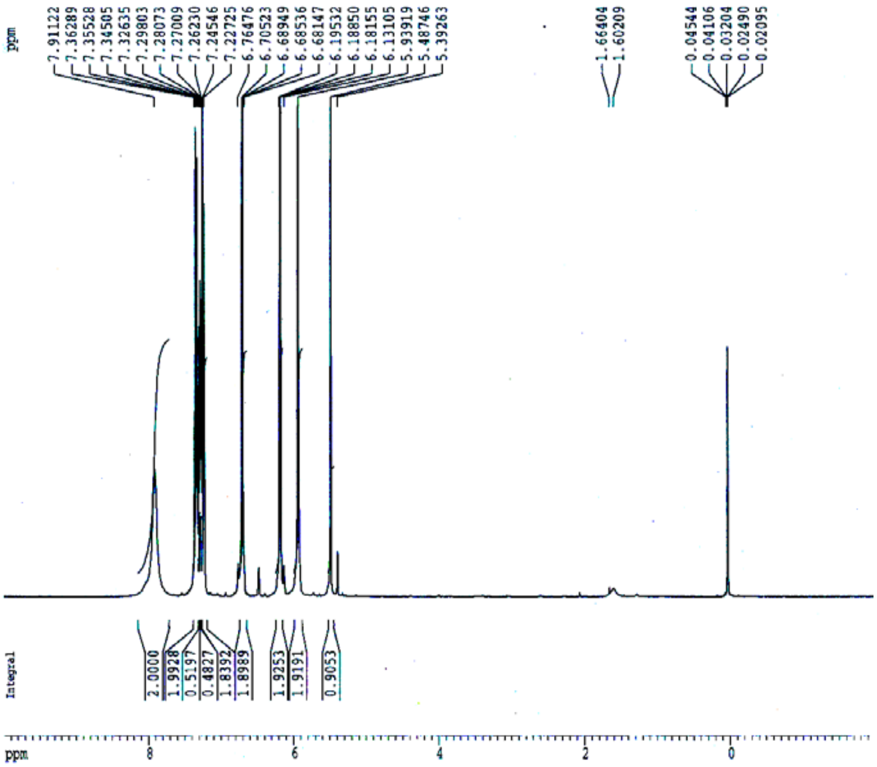

Figure 2-25. ^{1}H NMR spectrum of 5-phenyl-dipyrromethane

5-(2,4,6-triisopropylphenyl)dipyrromethane. 1.86 g (8 mmol) 2,4,6-triisopropylbenzaldehyde was added into 22.2 mL (320 mmol) of pre-distilled pyrrole. The solution was purged with argon for 30 minutes then 0.09 mL (0.66 mmol) of BF_3•Et_2O was added. After 40 minutes, the reaction was extracted with ethyl acetate, washed with 10% $NaCO_3$ solution, dried with $MgSO_4$ and evaporated in *vacuo* to remove solvent. Excess pyrrole was removed by distillation to leave a yellow semisolid, which was purified by using chromatography (silica) with cyclohaxane:ethyl acetate:triethylamine (20:1:0.1) to afford 1.5 g of 5-(2,4,6-triisopropylphenyl)dipyrromethane in 31% yield. ^{1}H NMR (400 MHz, $CDCl_3$) $\delta = 7.96$ (br s, 2H), 7.06 (s, 2H), 6.67(m, 2H), 6.20 (m, 2H), 6.14(m, 2H), 6.08 (s, 1H), 2.92 (m, 3H), 1.28(m, 18H). ^{13}C NMR (100 MHz, $CDCl_3$) $\delta = 136.6$, 135.4, 132.1, 125.8, 124.3, 113.1, 102.6, 101.5, 64.2, 33.9, 20.1, 19.7.

5-(2,4,6-trimethoxyphenyl)dipyrromethane. 2.0 g (10.2 mmol) 2,4,6-trimethoxybenzaldehyde (purchased from Aldrich) was added into 27.5 mL (408 mmol) of pre-distilled pyrrole. The solution was purged with argon for 30 minutes then 0.64 mL (5.1 mmol) of BF_3•Et_2O was added. After 40 minutes, the reaction was extracted with ethyl acetate, washed with 10% $NaCO_3$ solution, dried with $MgSO_4$ and evaporated in *vacuo* to remove solvent. Excess pyrrole was removed by distillation to leave a yellow semisolid, which was purified by using chromatography (silica) with cyclohaxane:ethyl acetate:triethylamine (10:8:1) to afford 0.6 g of 5-(2,4,6-trimethoxyphenyl)dipyrromethane in 19% yield. ^{1}H NMR (400 MHz, $CDCl_3$) $\delta = 7.51$ (br s, 2H), 7.04 (m, 2H), 6.82 (m, 2H), 6.26 (m, 2H), 6.10 (m, 2H), 6.02 (s, 1H), 3.82 (s, 9H). ^{13}C NMR (100 MHz, $CDCl_3$) δ = 143.6, 139.6, 136.5, 134.2, 133.3, 126.1, 118.1, 116.3, 68.3, 50.8, 50.2

5-(2,4,6-tribenzoxyphenyl)dipyrromethane. 1.0 g (2.4 mmol) of 2,4,6-tribenzoxybenzaldehyde was added into 6.5 mL (96 mmol) of pre-distilled pyrrole. The solution was purged with argon for 30 minutes then 0.076 mL (0.6 mmol) of BF_3•Et_2O was added. After 40 minutes, the reaction was extracted with ethyl acetate, washed with 10% $NaCO_3$ solution, dried with $MgSO_4$ and evaporated in *vacuo* to remove solvent. Excess pyrrole was removed by distillation to leave a yellow semisolid, which was purified by using chromatography (silica) with cyclohexane:ethyl acetate:triethylamine (80:20:1) to afford 0.77 g of 5-(2,4,6-tribenzoxyphenyl)dipyrromethane in 71% yield. ^{1}H NMR (400 MHz, $CDCl_3$) δ = 8.40 (br s, 2H), 7.40 (m, 15H), 6.84 (s, 2H), 6.42 (s, 1H), 6.32 (s, 2H), 6.15 (s, 2H), 5.96 (s, 2H), 5.15 (s, 4H), 5.07 (s, 2H); ^{13}C NMR (100 MHz, $CDCl_3$) δ = 159.2, 157.8, 136.7, 133.2, 128.7, 128.6, 128.2, 127.6, 117.7, 116.1, 112.9, 108.1, 107.8, 106.0, 94.4, 71.0, 70.3, 32.6, 26.9

5, 15-diphenyl-10, 20-bis(trimethylsilylethynl)porphyrin (11). 0.32 g (1.44 mmol) of 5-phenyldipyrromethane and 0.178 g (1.4 mmol) of trimethylsilyl-propynal was added to 144 mL of $CHCl_3$ and degassed by bubbling argon for 15 minutes. 55 uL (0.06 g, 0.042 mmol, 0.3 eq.) of BF_3•Et_2O was added and the reaction vessel was wrapped in aluminum foil. The reaction was quenched after 30 minutes with addition of 0.49 g (2.16 mmol) of DDQ and left to stir for one hour, whereupon the reaction mixture was washed with 50 mL of H_2O, dried with Na_2SO_4 and filtered. The resultant crude product was subjected to silica column chromatography (CH2Cl2: hexanes, 2:1, v/v) to yield 0.05 g (10%) of porphyrin (**11**). ^{1}H NMR (400 MHz, $CDCl_3$, Fig. 2-26) δ = 9.69 (d, 4H), 8.88

(d, 4H), 8.22 (m, 4H), 7.80 (m, 6H), 0.69 (s, 18H), -2.16 (s, 2H). ^{13}C NMR (100 MHz, $CDCl_3$) δ = 141.5, 134.7, 128.2, 127.1, 121.9, 107.1, 102.9, 101.0

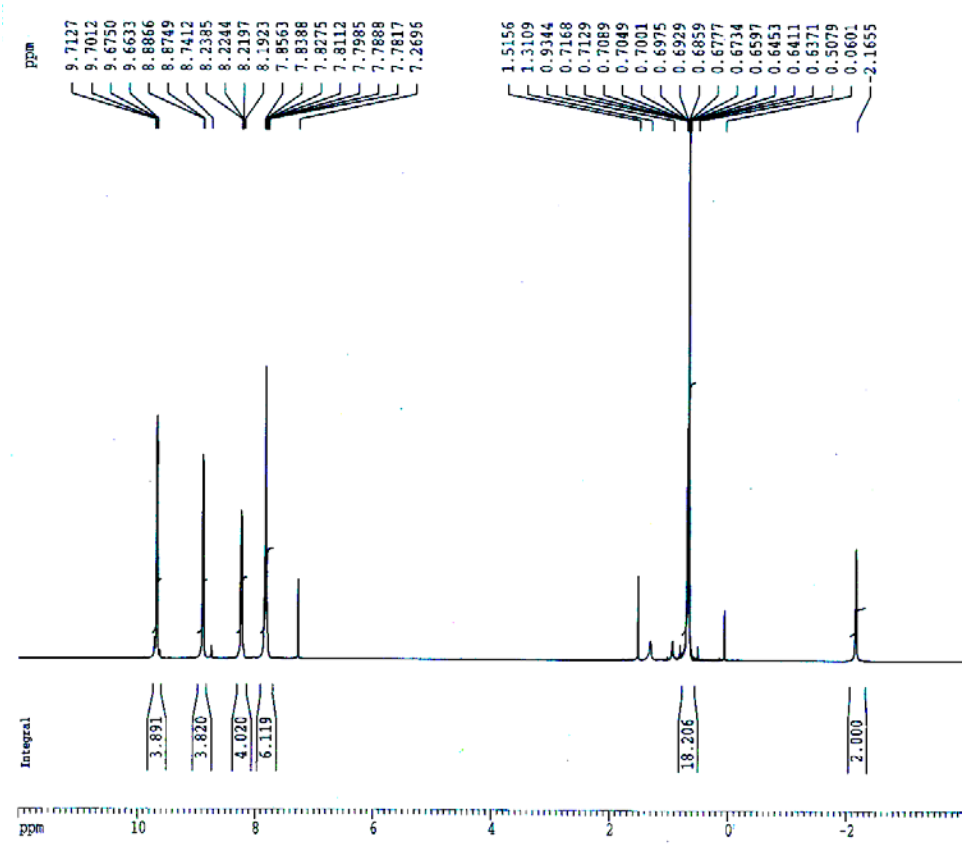

Figure 2-26. ^{1}H NMR Spectrum of 5,15-diphenyl-10, 20-bis (trimethylsilylethynl)porphyrin (11)

5,15-dimesityl-10, 20-bis(trimethylsilylethynl)porphyrin (**12**): 0.5 g (1.89 mmol) of 5-mesityl-dipyrromethane along with 0.240 g (1.89 mmol) of trimethylsilylpropynal were added to 189 mL of $CHCl_3$ and degassed by bubbling with argon for 15 minutes. 53.4 mg (47.6 μL, 0.376 mmol) of BF_3•Et_2O was added and the reaction vessel was wrapped in aluminum foil. The reaction was quenched after 30 minutes with addition of 0.74 g (0.282 mmol) of DDQ and left to stir for one hour, whereupon the reaction mixture was washed with 50 ml of H_2O, dried with Na_2SO_4 and filtered. The resultant crude product was subjected to silica column chromatography using dichloromethane:hexanes (1:2, v/v) to yield 262 mg (23.3%) of 5,15-dimesityl-10, 20-bis(trimethylsilylethynl)porphyrin. ^{1}H NMR (250 MHz, $CDCl_3$) δ = 9.54 (d, 4H), 8.65 (d, 4H), 7.29 (s, 4H), 2.65 (s, 6H), 1.94 (s, 12H), 0.57 (s, 18H), -2.06 (s, 2H). ^{13}C NMR (100 MHz, $CDCl_3$) δ =139.2, 138.0, 137.5, 129.8, 98.9, 85.1, 84.4, 29.7, 23.8, 21.5, 21.4, 19.5, 13.5.

5,15-bis(2,4,6-triisopropylphenyl)-10,20-bis(trimethylsilylethynl)porphyrin (13). 0.5 g (1.44 mmol) of 5-(2,4,6-triisopropylphenyl)-dipyrromethane along with 0.178 g (1.44 mmol) of trimethylsilylpropynal were added to 144 mL of $CHCl_3$ and degassed by bubbling with argon for 15 minutes. 60 mg (55 μL, 0.432 mmol) of $BF_3{\bullet}Et_2O$ was added and the reaction vessel was wrapped in aluminum foil. The reaction was quenched after 30 minutes with addition of 0.49 g (2.16 mmol) of DDQ and left to stir for one hour, whereupon the reaction mixture was washed with 50 ml of dH_2O, dried with Na_2SO_4 and filtered. The resultant crude product was subjected to silica column chromatography (CH_2Cl_2:hexanes 1:2) to yield 243 mg (19%) of 5,15-bis(2,4,6-triisopropylphenyl)-10,20-bis(trimethylsilylethynl)porphyrin. ^{1}H NMR (400 MHz, $CDCl_3$, Fig. 2-27) δ = 9.54 (d, 4H), 8.72 (d, 4H), 7.39 (s, 4H), 3.26 (m, 2H), 2.20 (m, 4H), 1.58 (m, 12H), 0.90 (m, 24H), 0.61 (s, 18H), -2.02 (s, 2H). ^{13}C NMR (100 MHz, $CDCl_3$) δ =151.0, 149.8, 141.8, 136.1, 132.8, 123.3, 121.1, 119.2, 34.6, 31.5, 24.4, 17.5.

5, 15-bis(2,4,6-tribenzoxylphenyl)-10, 20-bis(trimethylsilylethynl)porphyrin (15): 1.018 g (1.88 mmol) of 5-(2,4,6-tribenzoxylphenyl)-dipyrromethane and 0.238 g (1.88 mmol) of trimethylsilylpropynal were added to 188 mL of $CHCl_3$ and degassed by

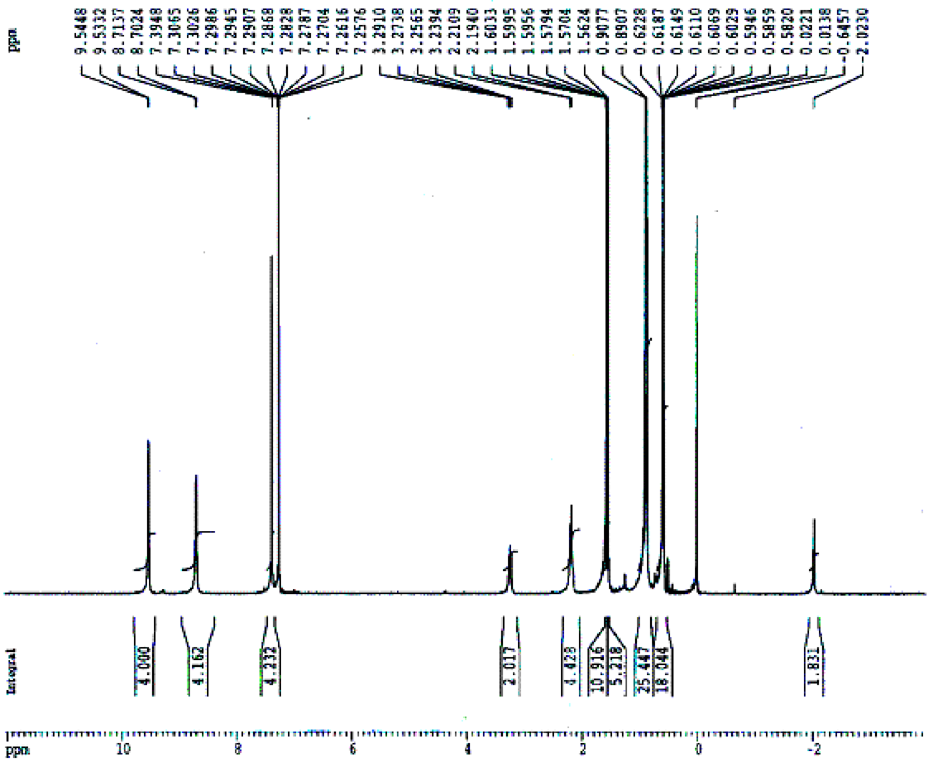

Figure 2-27. ^{1}H NMR Spectrum of 5,15-bis(2,4,6-triisopropylphenyl)-10, 20-bis(trimethylsilylethynl)porphyrin (13)

bubbling with argon for 15 minutes. 53.4 mg (47.6 μL, 0.376 mmol) of BF_3•Et_2O was added and the reaction vessel was wrapped in aluminum foil. The reaction was quenched after 1 hour with the addition of 0.74 g (0.282 mmol) of DDQ and left to stir for one hour whereupon the reaction mixture was washed with 50 ml of dH_2O, dried with Na_2SO_4 and filtered. The resultant crude product was subjected to silica column chromatography (ethyl acetate:hexanes 1:2) to afford 146 mg of porphyrins (**5**) in 12% isolated yield. ^{1}H NMR (250 MHz, $CDCl_3$) $\delta = 9.55$ (d, 4H), 8.85 (d, 4H), 7.57-7.48 (m, 10H), 6.92-6.81 (m, 12H), 6.65 (m, 8H), 6.62 (s, 4H), 5.21 (s, 4H), 4.87 (s, 8H), 0.62 (s, 18H), -2.08 (s, 2H). ^{13}C NMR (100 MHz, $CDCl_3$) δ = 160.6, 159.9, 151.9, 136.8, 136.7, 131.9, 130.8, 128.8, 128.2, 128.0, 127.9, 127.1, 126.5, 114.8, 113.9, 98.0, 93.8, 87.3, 82.3, 77.5, 70.4.

Metalation of porphyrins 1-18 (Fig. 2-28). Porphyrins **1-18** were metalated with Zn^{2+} in the following procedure. The free base porphyrin was dissolved into a minimal amount of dichloromethane:methanol (9:1, v/v) solution. The solution was degassed for 10 minutes, then 1.2 equivalents of $Zn(AcO)_2$ was added, and stirred overnight at RT. NMR spectroscopy (Fig. 2-29, proton changes on nitrogen atoms) and UV-Vis spectroscopy (Fig. 2-30, shifted absorption maximum wavelength) were used to monitor the completion of the metalation reaction. The reaction mixture was washed with 50 mL of $NaHCO_3$ and 50 mL of H_2O three times, then dried over $MgSO_4$. The solvent was removed to obtain Zn-metalloporphyrins in 95~98% yield. For the insertion of Ni^{2+} into porphyrins, this metalation procedure was changed by increasing reaction temperature to 140 ^{0}C and refluxing the reaction in DMF.

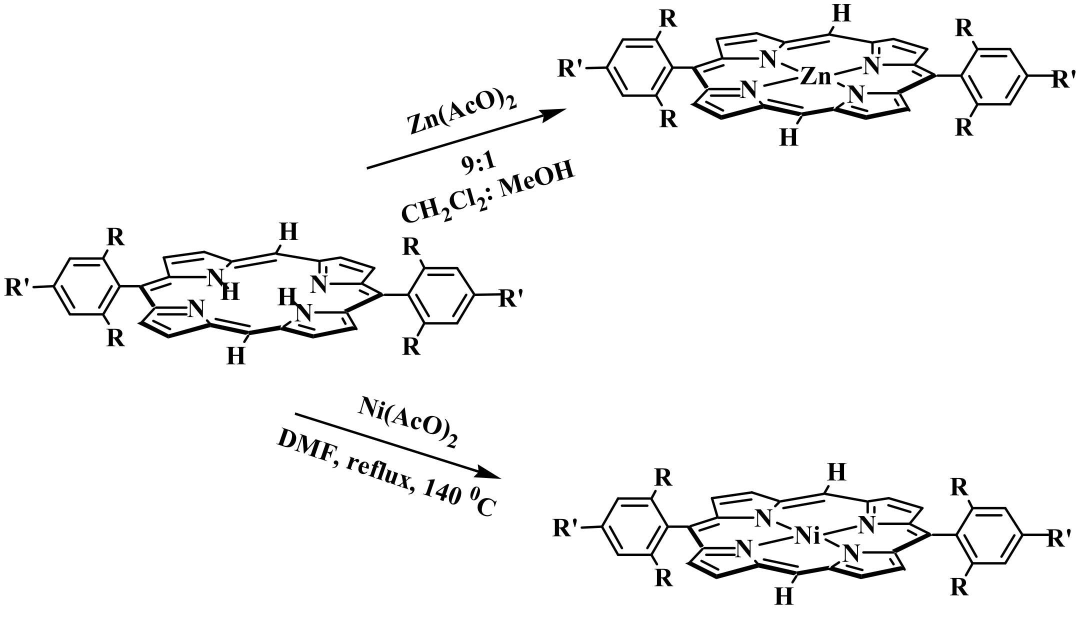

Figure 2-28. Insertion of Zn(II) and Ni(II) into Porphyrins 1-18

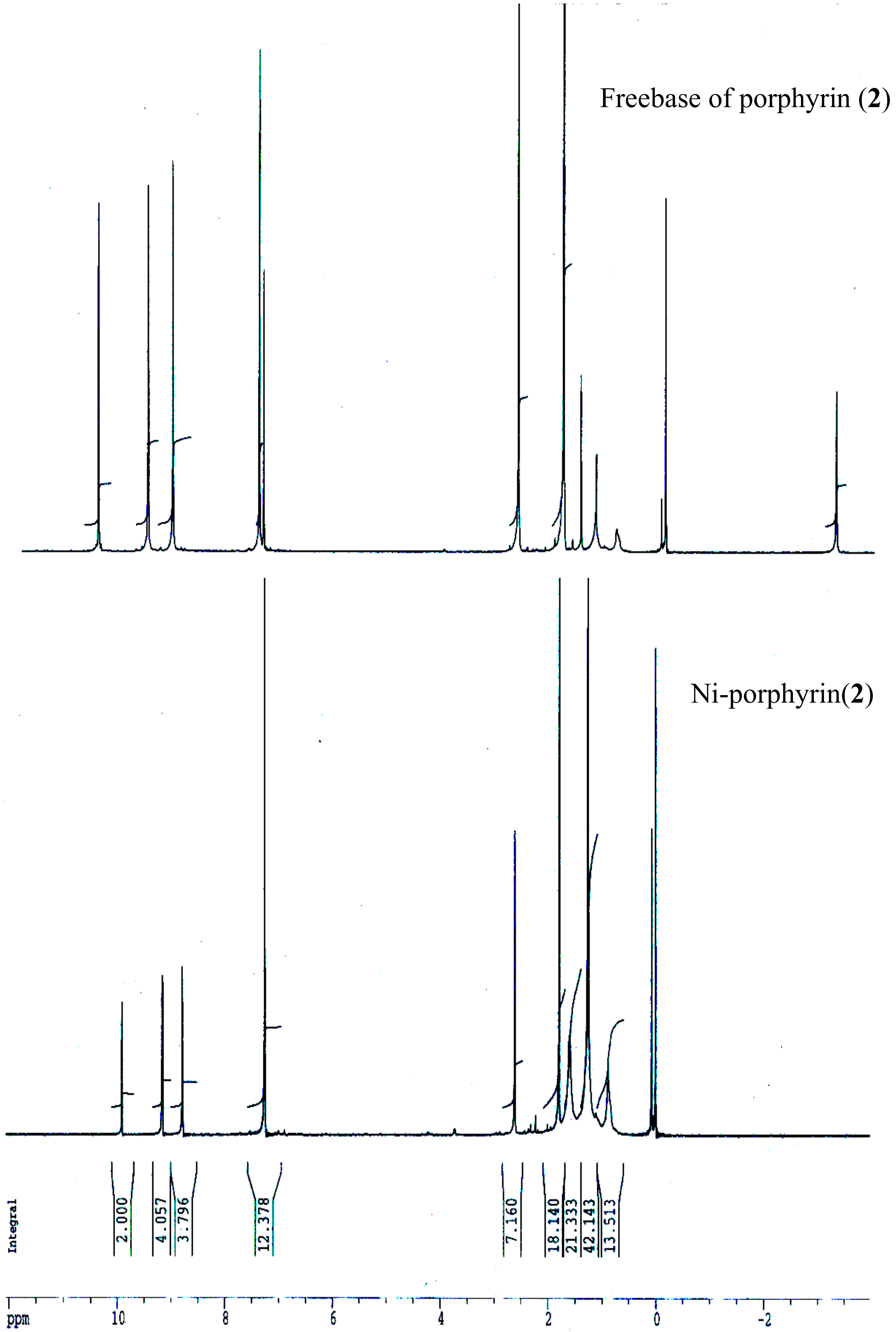

Figure 2-29. ^{1}H NMR Spectra of Freebase and Ni-Porphyrin (2)

As shown in Fig. 2-30, the difference in the UV-Visible spectra of free base porphyrin and metalloporphyrin is mainly in the Q-band region, where the peaks at 502 nm, 536 nm, 574 nm, and 650 nm in the free base porphyrins were replaced by peaks at 557 nm and 595 nm in the metalloporphyrin. The difference is even more obvious by the NMR spectra shown in Fig. 2-29. The free base porphyrin has two protons inside of the porphyrin ring, which are shifted greatly to negative chemical shift (around -2.0 ppm) owing to the ring current of large aromatic system in porphyrins. This peak disappeared after metal insertion.

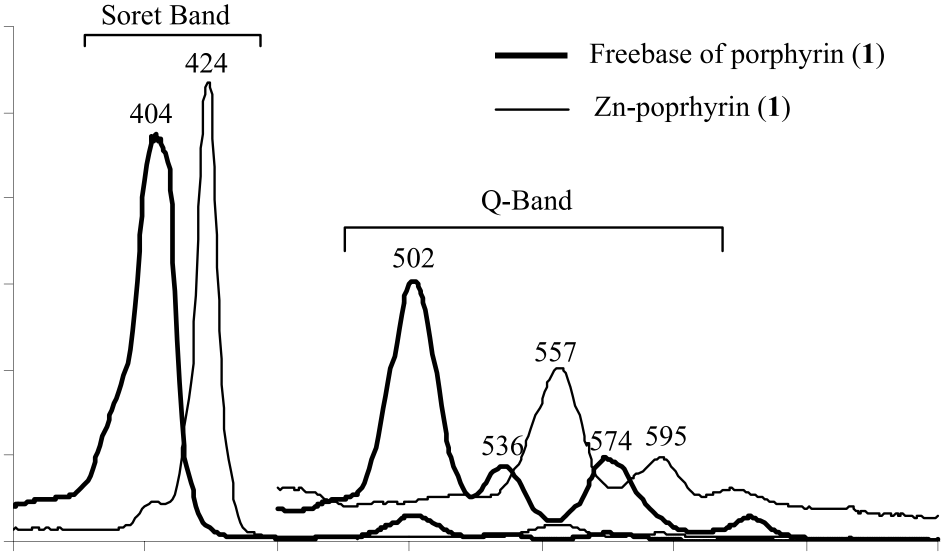

Figure 2-30. UV-Vis Spectra of Freebase and Metalloporphyrin (1)

2.4 Solubility-structure relationships in designed porphyrins

2.4.1. Solubility measurements

The measurement of porphyrin solubility is based on Lambert-Beer’s Law in equation (2) for the light absorption.

$$\mathbf{A = lg\,\frac{\mathit{I_0}}{\mathit{I}} = \varepsilon \cdot c \cdot \mathit{l}} \qquad (2)$$

where
A = UV-Vis absorbance
ε = molar extinction coefficient
c = concentration
***l* = cell thickness**

In most situations, the molar extinction coefficients of porphyrins are close to 5 x 10^5. Therefore, we used this value as ε for some porphyrins' solubility calculations. For important porphyrin compounds, the actually measured molar extinction coefficients are used for the solubility calculations (see Table 1). The steps shown in Fig. 2-31 were taken to measure porphyrin solubility by meeting following requirements.

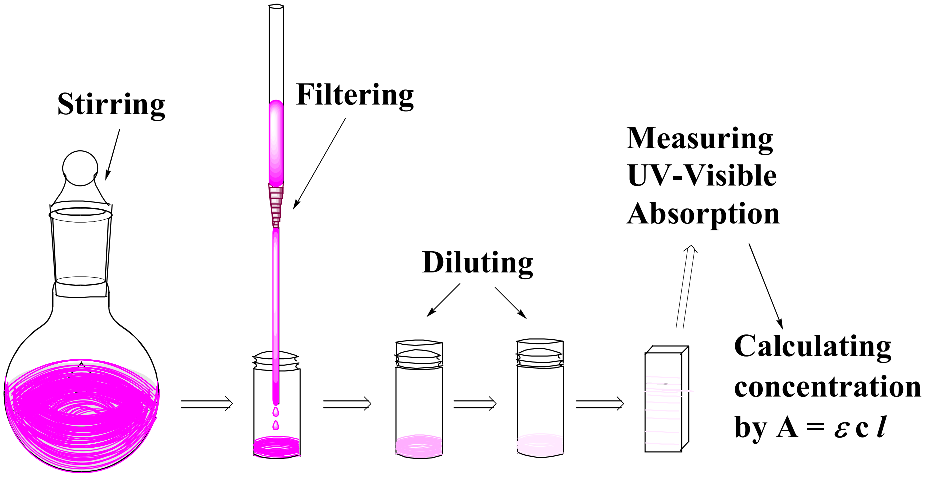

Figure 2-31. Five Steps for the Solubility Measurement

1. The porphyrins in solution are in equilibrium with the porphyrins in the solid state. This is achieved by stirring a saturated solution for 24 hours before taking samples for solubility measurements.

2. Only porphyrins dissolved in the solution are used to determine their solubility, so filtration is necessary.
3. The saturated porphyrin solution is diluted until its concentration is within the range where Lambert-Beer's law is applicable, i.e. the linear region.

To compare the solvent effect, porphyrin solubility was measured in several organic solvents, including chloroform ($CHCl_3$), dichloromethane (CH_2CL_2), tetrahydrofuran (THF), *ortho*-dichlorobenzene (*o*-DCB), methanol, hexane and benzene (Bz). $CHCl_3$, CH_2Cl_2 and THF were used because they are the most common solvents. *o*-DCB was the solvent used for many coupling reactions in the construction of porphyrin polymers. Methanol and hexane are two solvents in which porphyrin compounds are usually insoluble. For comparison with literature data obtained in benzene,[2,3] we also measured one sample (porphyrin **3**) in benzene.

The solubility data for our designed porphyrin molecules in different solvents are shown in Table 1 (Item **1-16, 20-25)**. We have also measured non-encumbered porphyrins' solubility including *trans*-A_2B_2-porphyrins (**17-19**), tetraphenylporphyrins (**26-29**) and an alkylporphyrin (**30,** Aldrich Chemicals) for comparison.

Table 2-1. Porphyrin Solubility (mmol/L) in Different Solvents

Porphyrins	$CHCl_3$	CH_2Cl_2	THF	*o*-DCB	MeOH	Hexa-ne	Bz
5,15-diphenyl-10*H*, 20*H*-porphyrin (1) **($\varepsilon = 3.88 \times 10^5$)**	25.0^*	14.6^*	20.0	18.0	0.1		
Zn (II)-5,15-diphenyl-10*H*, 20*H*-porphyrin (1') **($\varepsilon = 4.45 \times 10^5$)**	10.1^*	6.9^*					

5,15-dimesityl-10*H*, 20*H*-porphyrin (2) (ε = 4.75 x 10^5)	59.9*	14.4*	3.0	23.0	0.1		
Zn (II)-5,15-dimesityl-10*H*, 20*H*-porphyrin (2’) (ε = 5.84 x 10^5)	105.7*	30.2*					
5,15-bis(2,4,6-triisopropylphenyl)-10*H*, 20*H*-porphyrin (3) (ε = 5.02 x 10^5)	192.9*	81.6*	110.	113.2	1.0	2.3	
Zn (II)-5,15-bis(2,4,6-triisopropylphenyl)-10*H*, 20*H*-porphyrin (3’)(ε = 6.00 x 10^5)	294.2*	200.0*	89.0		3.6	13.5	206.0*
Ni (II)-5,15-bis(2,4,6-triisopropylphenyl)-10*H*, 20*H*- porphyrin (3”)	184.0	108.0					
5,15-bis(2,4,6-triphenylphenyl)-10*H*, 20*H*-porpohyrin (5)	13.8						
Zn (II)-5,15-bis(2,4,6-triphenylphenyl)-10*H*, 20*H*-porpohyrin (5’)	5.8						
5,15-bis(2,4,6-trimethoxylphenyl)-10*H*, 20*H*-porphyrin (6)	2.0		0.8				
5,15-bis(2,4,6-tribenzoxylphenyl)-10*H*, 20*H*-porphyrin (7)	5.0		2.0	3.2	0.1		
5,15-bis(2,6-dimethylphenyl) -10*H*, 20*H*-porphyrin (8)	2.5						
Zn (II)-5,15-bis(2,6-dimethylphenyl)-10*H*, 20*H*-porphyrin (8’)	3.6						
5,15-bis(p-tolyl)-10*H*, 20*H*-porphyrin (9)	6.0	17.0					
5,15-bis(p-isopropylphenyl) -10*H*, 20*H*-porphyrin (10)	47.0	22.8					
Zn (II)-5,15-bis(p-isopropylphenyl)-10*H*, 20*H*- porphyrin (10’)	62.0						

5,15-dihexyl-10*H*, 20*H*-porphyrin (18)	41.0	35.7					
Zn (II)-5,15-dihexyl-10*H*, 20*H*-porphyrin (18')	2.0	4.6					
5,15-diisopropyl-10*H*, 20*H*-porphyrin (17)	22.5						
Zn (II)-5, 15-dimesityl-10, 20-diethynylporphyrin (12')	19.4						
Zn (II)-5, 15-bis(2,4,6-triisopropylphenyl)-10, 20-diethynylporphyrin (13')	28.4						
Zn (II)-5, 15-bis(2,4,6-triisopropylphenyl)-10, 20-bis(trimethylsilylethynyl)porphyrin (13)	86.7						
Zn (II)-5, 15-bis(2,4,6-tribenzoxylphenyl)-10, 20-diethynylporphyrin (15')	6.0						
Zn (II)-5, 15-bis(2,4-didecoxylphenyl)-10, 20-diethynylporphyrin	13.0						
Zn (II)-5, 15-bis(2,4-didecoylphenyl)-10, 20-bis(trimethylsilylethynyl)porphyrin	47.0						
5,10,15,20-tetraphenylporphyrin	37.5	10.0					
Zn (II)-5,10,15,20-tetraphenylporphyrin	23.5	19.3					
5,10,15,20-tetramesitylporphyrin	7.7	19.2					
Zn (II)-5,10,15,20-tetramesitylporphyrin	1.5	5.5					
2,3,7,8,12,13,17,18-octaethyl-21*H*, 23*H*-porphyrin	3.5						

* Adjusted according to their measured extinction coefficient, others are obtained according to the extinction coefficient as 5.0 x 10^5 for most porphyrins.

2.4.2 Solubility-structure studies

The solubility values in chloroform ($CHCl_3$) for all the porphyrin molecules in table 1 are shown in Fig. 2-32, which gives an entire picture for the solubility differences among this group of porphyrins. One can see that the bars corresponding to solubility of porphyrins **2**, **3** and **13** in Fig. 2-32 are significantly higher than their neighbors. Porphyrin **3**, which is designed with isopropyl groups in the *ortho*-, and *para*-positions of the phenyl ring to act as facial- and edge-encumbrance, has the highest solubility in each organic solvent (Fig. 2-32 to 2-37). Its solubility shows an increase of 3 to 15,000 times compared to all of the other porphyrins in this study.

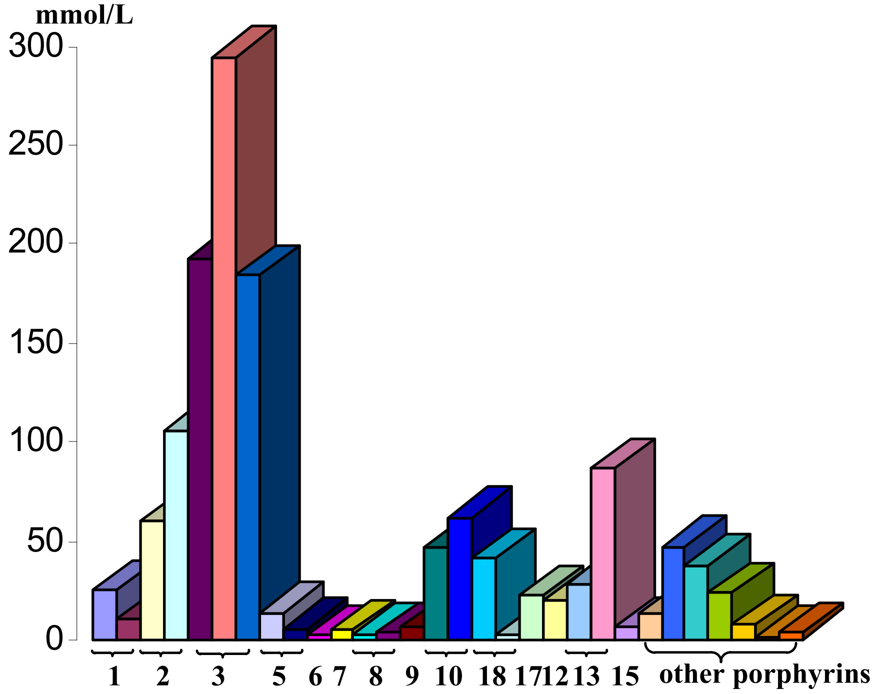

Figure 2-32. Porphyrin Solubility in $CHCl_3$

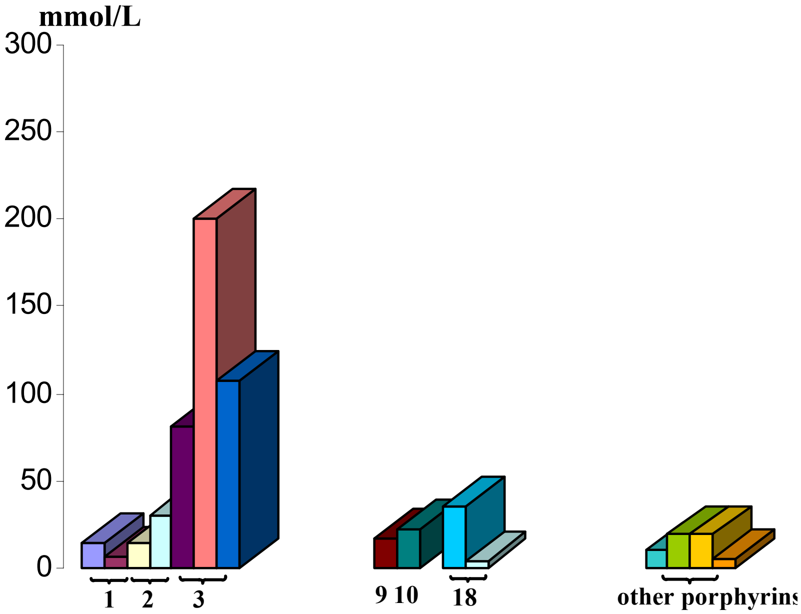

Figure 2-33. Porphyrin Solubility in CH_2Cl_2

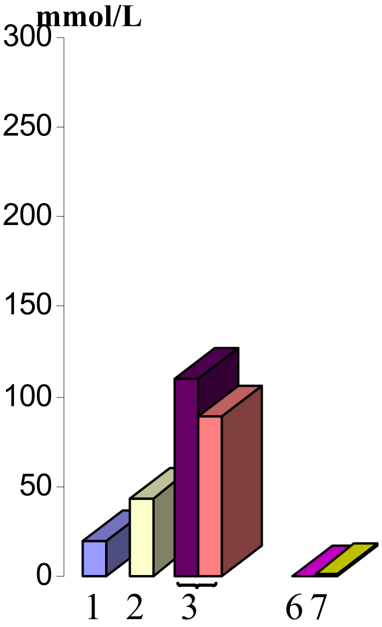

Figure 2-34. Porphyrin Solubility in THF

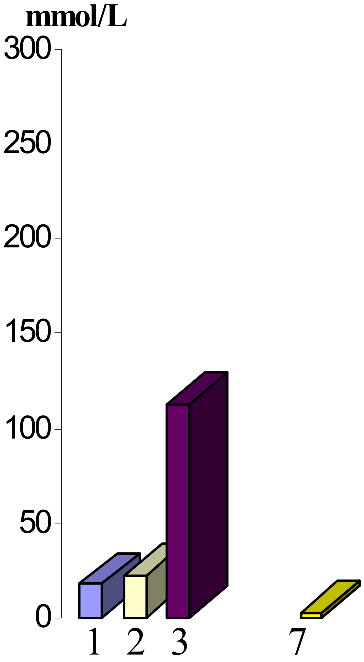

Figure 2-35. Porphyrin Solubility in *o*-DCB

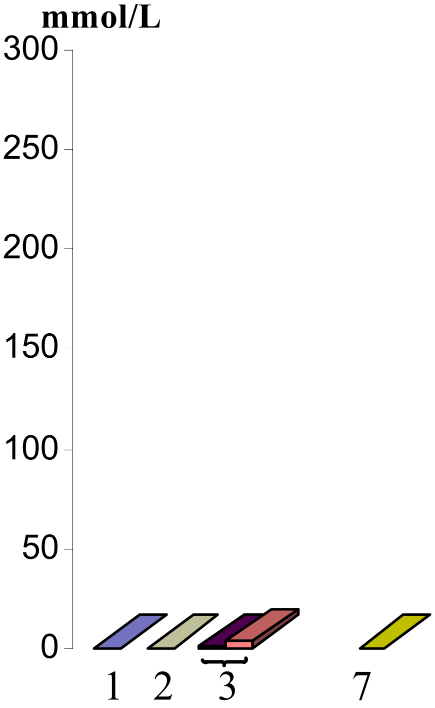

Figure 2-36. Porphyrin Solubility in methanol

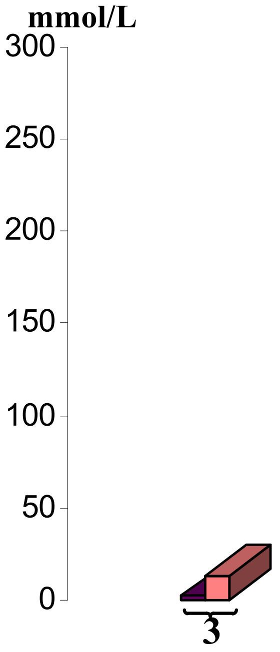

Figure 2-37. Porphyrin Solubility in hexanes

To further analyze and understand structure-solubility relations of these porphyrins, we divided them into several groups for discussion according to their structural features as follows.

1. Facial- and edge-encumbered porphyrins vs. non-encumbered porphyrins (Fig. 2-38).

The solubility and structure comparison in this group indicates that (1) facial- and edge-encumbered porphyrins (**2** and **3**) have higher solubility than non-encumbered porphyrins (**17**, **18** and octaethylporphyrin). Fig. 2-39 also shows the big solubility difference between facial- and edge-encumbered porphyrin **3** and non-encumbered alkylporphyrins; (2) when comparing porphyrin **3** with solubility being 192.9 mmol/L to porphyrin **17** with solubility being 22.5 mmol/L, while both having the same isopropyl groups as substituents, the isopropyl groups in facial- and edge-encumbered structure (porphyrin **3**) can increase the porphyrin solubility by 10 times from non-encumbered porphyrin **7**. Therefore, it indicates that the substitution position can affect porphyrin solubility significantly; (3) since porphyrins **17** and **18** (*meso*-substituted A_2B_2-porphyrin) are more soluble than octaethylporphyrin (β-substituted porphyrin), even though they have less alkyl groups on the periphery of porphyrins, it demonstrates that *meso*-substituted A_2B_2-porphyrins can achieve higher solubility than β-substituted porphyrins.

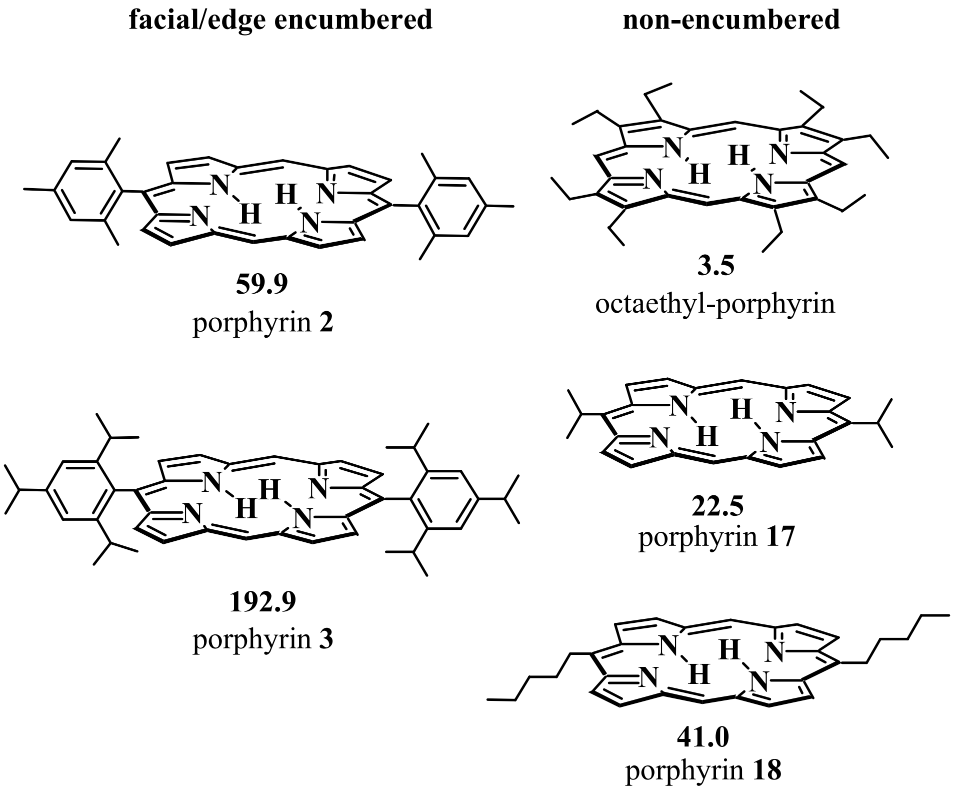

Figure 2-38. Solubility Comparison of Facial and edge-encumbered and non-encumbered Porphyrins in $CHCl_3$ (mmol/L)

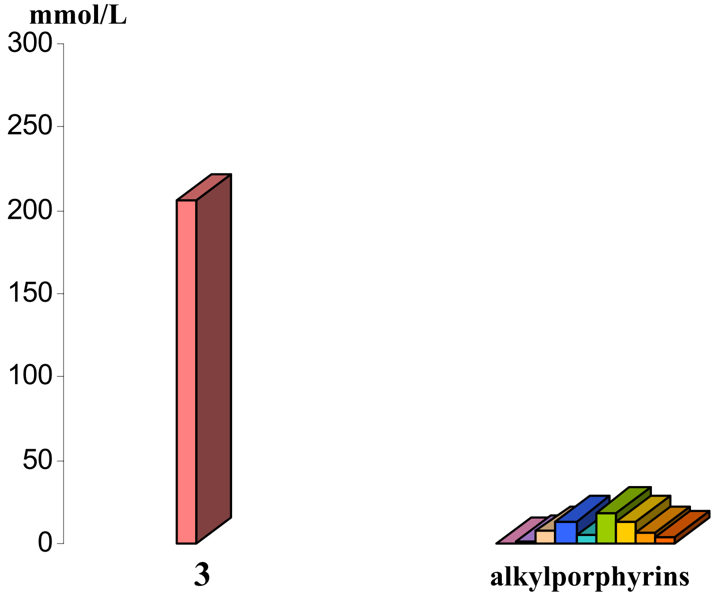

Figure 2-39. Solubility of Zn-porphyrin 3 and alkylporphyrins in Benzene

2. Alkoxyl group vs. alkyl group as facial- and edge-encumbrance (Fig. 2-40).

Alkoxyl groups in the *ortho*- and *para*- positions of a phenyl ring were presumably to have the same facial- and edge-encumbering effect as alkyl groups. They seemed even more bulky than alkyl encumbrance, but the measured solubility is surprisingly disappointing and much lower (30 to 40 times less!) than alkyl-encumbered porphyrins.

From the crystal structure analysis of tetra(2,4,6-trimethoxyphenyl)porphyrin with a similar structure as A_2B_2-bis(2,4,6-trimethoxyphenyl)porphyrin (porphyrin **6**) in Fig. 2-41, we can find an explanation for such low solubility of alkoxy-encumbered porphyrins. The structural difference between tetra(2,4,6-trimethoxyphenyl)porphyrin and A_2B_2 bis(2,4,6-trimethoxyphenyl)porphyrin (porphyrin **6**) is that there are four trimethoxyphenyl groups on all *meso*-positions of tetra(trimethoxyphenyl)porphyrin but two trimethoxyphenyl groups in porphyrin **6**. Although this difference may probably

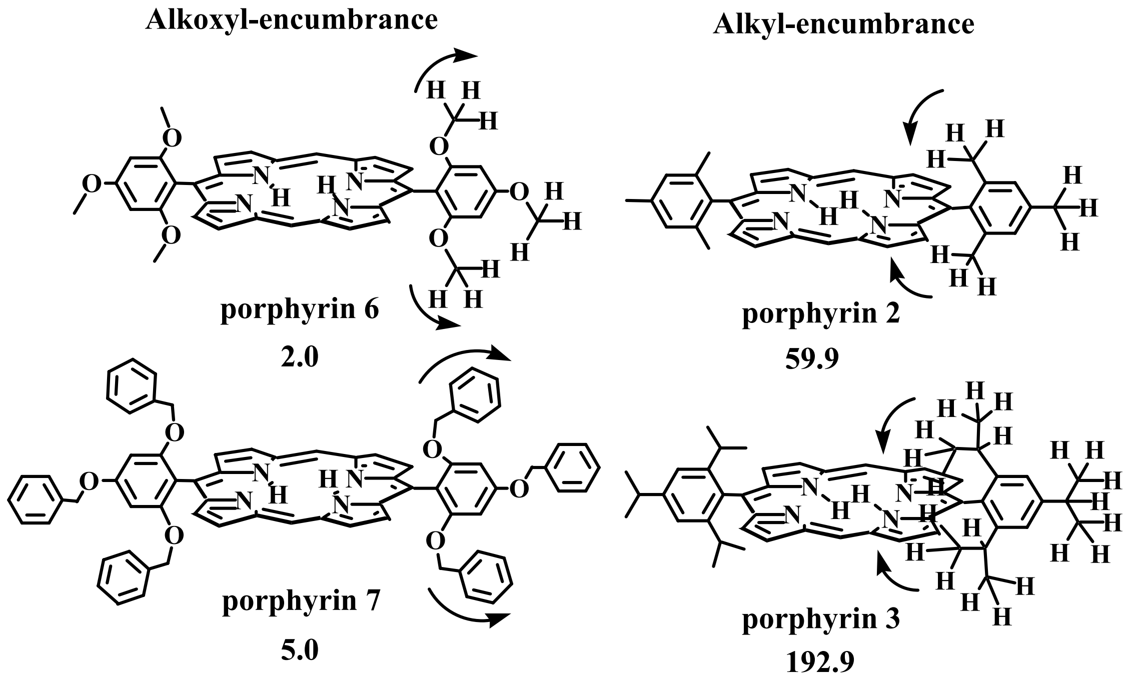

Figure 2-40. Comparison of Porphyrins Solubility ($CHCl_3$, mmol/L) with Alkoxyl and Alkyl Groups as Facial- and edge-encumbrance

affect crystal packing, the single molecule structure and orientation should be similar. The special structural feature in this crystal is that those *ortho*- and *para*-substituted alkoxy groups are flipped away from the porphyrin core structure at the position of the oxygen-linker. The presence of oxygen in this porphyrin gives the following two possible reasons why alkoxy-encumbrance failed to increase porphyrin solubility by preventing π–π interactions (Fig. 2-41). (a) The realization of facial- and edge-encumbrance is based on the *ortho-,* and *para*-substituents of the phenyl rings pointing out above and below the porphyrin plane. When these substituents cannot stay steadfast in proper positions, they will not be able to efficiently prevent porphyrins from attracting each other through strong π–π attractive interaction. As demonstrated in Fig. 2-40, those alkoxy or benzyloxy groups in porphyrins **6** and **7** are turned away from the porphyrin plane, while the methyl and isopropyl groups in porphyrin **2** and **3** are steadily sticking toward the porphyrin plane. Therefore, the flexible structure of alkoxy groups cannot provide rigid encumbrance to push the porphyrin molecules away from each other. The face-to-face offset stacking is only tilted a certain degree (approximately 20 to 30 degree) by these substituents, so the π−π interaction is still in the attractive area (Fig. 2-8). (b) The strong polarity of the C-O bonds has also increased the electrostatic attraction between the alkoxy-substituted porphyrins. With so many polar C-O bonds around the porphyrin periphery, the total electrostatic interaction, as well as the dipole-dipole interaction, is not negligible. This strong attractive interaction between porphyrin molecules will certainly have significant consequence for porphyrin's solubility.

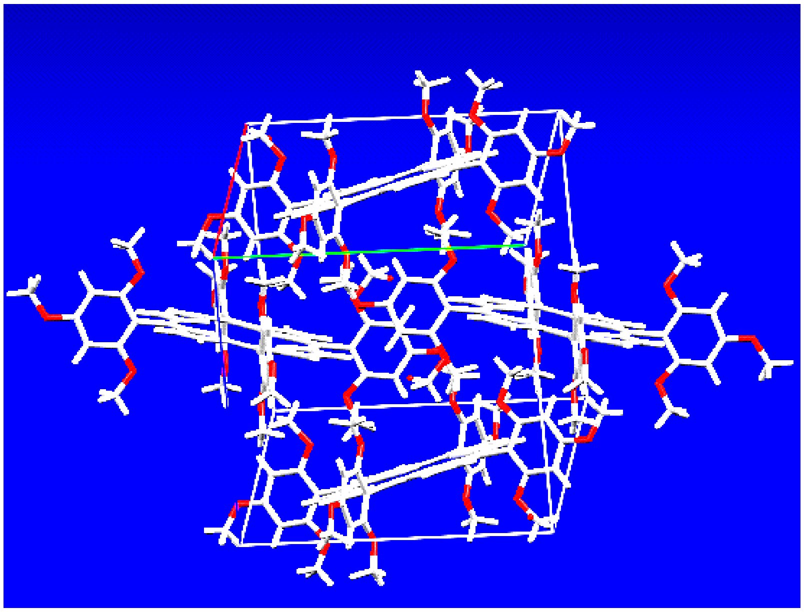

Figure 2-41. Crystal Structure of Tetra (trimethoxyphenyl)porphyrin[23]

3. Aromatic groups vs. alkyl groups as facial- and edge-encumbrance (Fig. 2-42).

As we have shown from the alkoxy-encumbering porphyrins, the o*rtho*- and *para*-substituents need be very bulky and rigid to perform effective facial- and edge-encumbering. When we designed and synthesized porphyrin **5**, in which the rigid phenyl groups are in the *ortho*- and *para*-positions of phenyl rings attached to the porphyrin, it was believed that these facial- and edge-encumbrances should be very rigid and bulky owing to the rigid phenyl ring, and therefore porphyrin **5** should be very soluble. However, the solubility of this porphyrin is again very disappointing compared to alkyl-encumbering porphyrins, although porphyrin **5** has a little higher solubility than alkoxy-encumbering porphyrins. Strouse and co-workers pointed out by the analysis of molecular packing in over 200 tetraarylporphyrin-based clathrates, that there are interactions between these phenyl groups on adjacent porphyrin molecules. "The interaction is similar to that seen in solid benzene."[24] The crystal structure of tetraphenylporphyrin (TTP)'s (Fig. 2-43) also shows us that these phenyl groups are in face-to-face offset stacking geometry. According to the function of $\pi-\pi$ interactions

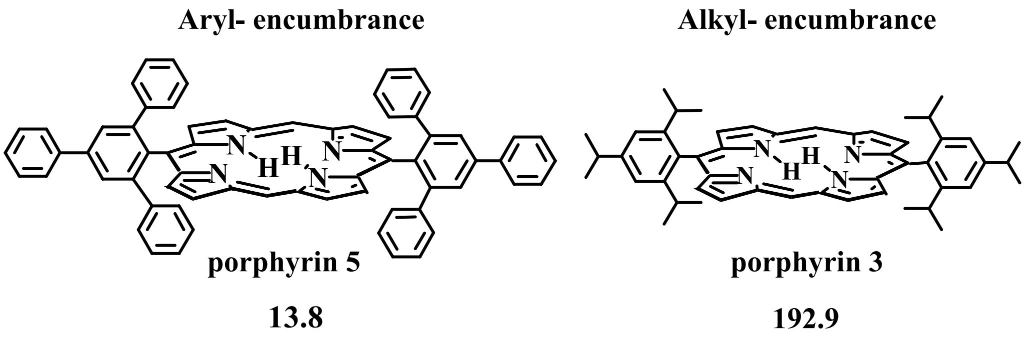

Figure 2-42. Solubility Comparison of aryl-encumbered and alkyl-encumbered Porphyrins in $CHCl_3$ (mmol/L)

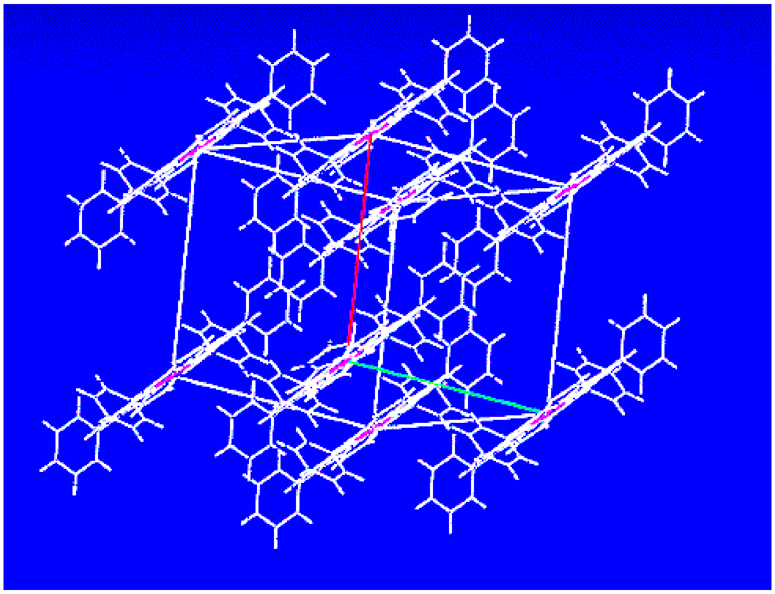

Figure 2-43. Molecular Packing of Tetraphenylporphyrin(TPP)'s Crystal[24]

vs. their relative orientations, these face-to-face offset geometries will lead to attractive interactions between these aromatic side groups. Considering that there are so many aromatic side groups in porphyrin **5**, the π–π interaction between these aromatic systems will also play an important role in porphyrin's interactions. As illustrated in Fig. 2-44, in addition to the major interactions between porphyrin π–systems, those side aromatic systems also have interactions with each other and even with porphyrin molecules as well. Therefore, the total π–π interaction in porphyrin **5** includes porphyrin-to-porphyrin interactions 1, porphyrin to aromatic side group interactions 2, and aromatic side group to aromatic side group interactions 3. The increased total π–π attractive interaction between porphyrin molecules can be the cause for the low solubility of porphyrin **5**. The comparisons of alkoxyphenyl-porphyrin and arylphenyl-porphyrin with alkylphenylporphyrin have shown us that the substituents not only need to be bulky and rigid, but also need to be those groups which do not introduce strong attractive molecular interactions including π–π interaction, electrostatic interaction and dipole-dipole interaction, etc.

Total π–π interaction = 1 + 2 + 3

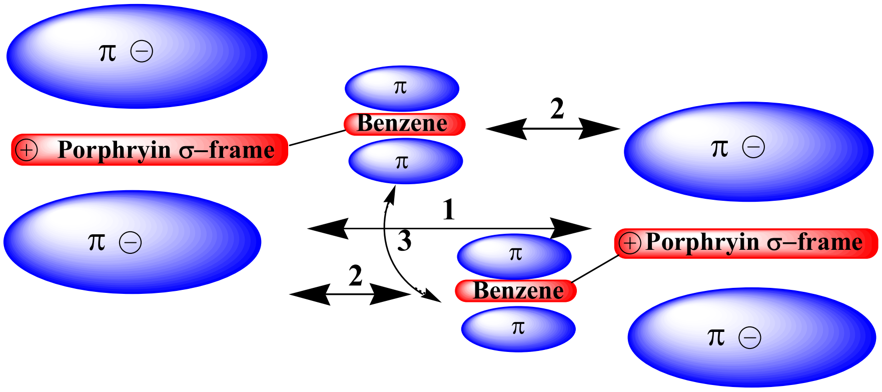

Figure 2-44. Total π–π Interaction in Porphyrins with Aromatic Side Groups.

4. Comparison of porphyrin solubility in different solvents (Fig. 2-45).

The comparison of porphyrin solubility in different solvents can be used to understand solvent-solute and solute-solute interactions in porphyrin solutions, and therefore aid in our understanding of the dominating factor(s) that affect porphyrin solubility.

From the data shown in Fig. 2-45, we can see that alkyl-encumbered porphyrins (porphyrins **1-3**) have higher solubility than alkoxy- and aryl-encumbered porphyrins in all solvents. The weakened π–π interaction by facial- and edge-encumbrance in these porphyrin systems has resulted in weakened solute-solute (porphyrin–porphyrin) interactions, therefore, solute-solvent interaction becomes relatively strong to lead

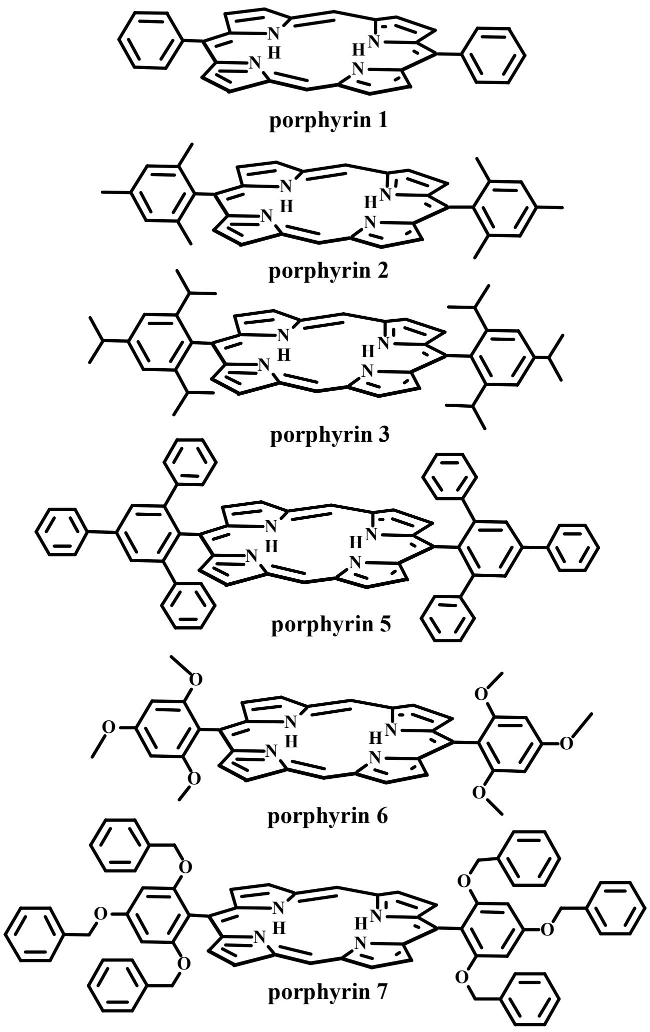

	$CHCl_3$	THF	o-DCB	MeOH
porphyrin 1	25.0	20.0	18.0	0.1
porphyrin 2	59.9	43.0	23.0	0.1
porphyrin 3	192.9	110.0	113.2	1.0
porphyrin 5	13.8			
porphyrin 6	2.0		0.8	
porphyrin 7	5.0	2.0	3.2	0.1

Figure 2-45. Porphyrin Solubility in Different Solvents (mmol/L)

to solute dissociations. For porphyrins **6** and **7** with alkoxy- and aromatic-encumbrance, the solubility values are very low in chloroform, THF, o-DCB or methanol, which indicates that the solute-solute interaction or the attraction between porphyrins is very strong, while the solvent–solute interaction is not strong enough to interrupt the aggregation of porphyrins.

By comparison among porphyrins **1** to **3**, the fact that solubility increases with the alkyl group size, clearly demonstrates the facial- and edge-encumbering effect for interrupting facial- and edge-on stacking. The bulkier the *ortho-* and *para*-substituents are, the more efficient their encumbering ability. Porphyrin **3** is the most soluble porphyrin in all solvents. Even in methanol, a solvent that normally does not solvate porphyrins, the solubility of porphyrin **3** still reaches 1.0 mmol/L, ten times higher than other porphyrins. This data further supports the idea that we have found a better method to interrupt solute-solute interactions and increase porphyrin solubility.

5. Comparison of solubility for freebase porphyrin and metalloporphyrin

According to experimental observations, porphyrin solubility is generally decreased after the insertion of a metal to form a metalloporphyrin.[5] This solubility decrease can be easily explained by the π−π interaction shown in Fig. 2-8 and Fig. 2-9. Since metalation places a large positive charge (+0.4 in the case of zinc)[5] in the central cavity of the porphyrin π−system, when two neighboring porphyrins are in either face-to-face offset or T-shaped stacking, the attraction between the negatively charged π−electron cloud and the positively charged σ−frame becomes greater because the increased positive charges on the σ−frame. However, this situation only applies to porphyrins that do not have efficient facial- and edge-encumbrance (Fig. 2-46).

According to the discussions above, we have shown that porphyrins without facial- and edge-encumbrance mostly adopt face-to-face offset or edge-on geometry. In metalloporphyrin molecules, face-to-face offset geometry will not only help to increase the electrostatic attraction between π−electrons and σ−frames due to the increased positive charge in the central cavity of the porphyrin π−systems, but also help the coordination interactions between metals and nitrogen atoms as shown in Fig. 2-47.

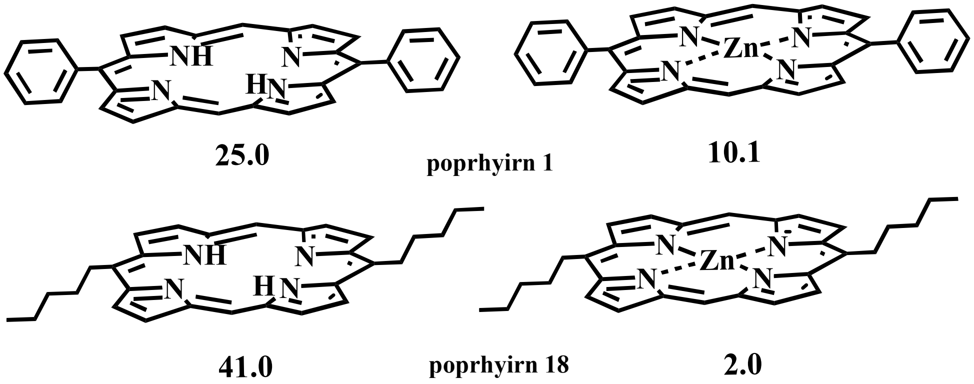

Figure 2-46. Solubility of Metalloporphyrins without Facial- and edge-encumbrance in $CHCl_3$ (mmol/L)

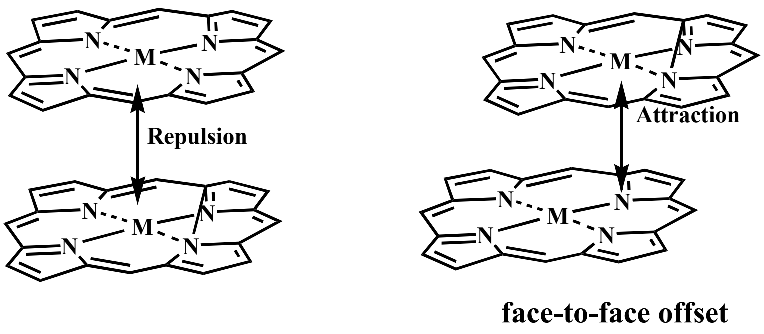

Figure 2-47. Coordinative Interaction in Metalloporphyrins

This phenomenon is totally different in facial- and edge-encumbered porphyrins. The solubility of metalloporphyrin was increased (instead of decrease) significantly compared to its free base (Fig. 2-48). Because those porphyrins with facial- and edge-encumbrance no longer adopt face-to-face offset stacking, or T-shaped stacking, the electrostatic interactions between the π−electron cloud and the σ−frame has been disturbed. Even though the net charge was increased with the metal insertion, the electrostatic attractive interaction was not reinforced in metalloporphyrins. When the metalloporphyrin does not adopt face-to-face offset stacking or T-shaped stacking, the porphyrin-porphyrin (or solute-solute) interaction is much weaker, while the solute-solvent interaction became stronger. Metal insertion can increase polarity of porphyrin molecules or deform porphyrin planar structures. Increased polarity in porphyrins can increase interactions between solute molecules (porphyrins) and solvent molecules through dipole-dipole interactions in polar organic solvent such as $CHCl_3$. Changed symmetry or conformation resulted from metalation can also increase the difficulty for porphyrin molecules to line-up and stack together. Therefore, the solubility of metalloporphyrins with facial- and edge-encumbrance is increased, and a metalloporphyrin becomes more soluble than its freebase.

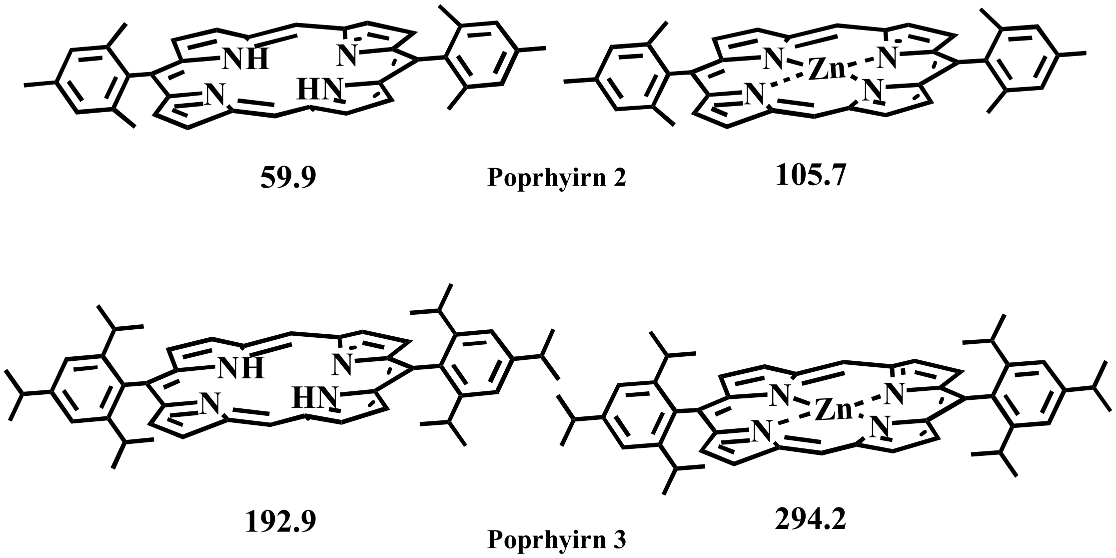

Figure 2-48. Metalloporphyrin Solubility with Facial- and edge-encumbrances in $CHCl_3$ (mmol/L)

2.4.3 Crystal structure of the highly soluble porphyrin 3

The crystal structure of porphyrin **3**, the most soluble porphyrin obtained in these studies, shows unique structural properties including the successful interruption of both face-to-face stacking and edged-on stacking (Fig. 2-49 and 2-50, other structure data are listed in Table 2-2). It is confirmed through the crystal structure of the porphyrin (**Fig**. 2-49), that the porphyrin ring and the phenyl rings are not co-planar but perpendicular to each other. This structure conformation results in isopropyl groups pointing above and below the porphyrin plane owing to the repulsion between *β*–protons on porphyrin and isopropyl groups on phenyl rings, as we have predicted for the design of facial and edge-encumbrance. The unit cell (Fig. 2-50) further shows the unique packing geometry of the porphyrin molecules in that there is no face-to-face offset stacking or edge-on stacking between two neighboring porphyrin molecules in the unit cell. As we discussed above, when porphyrins do not adopt geometries that facilitate the strong π–π interactions, the attraction between porphyrins molecules is reduced dramatically and therefore the solubility of the porphyrin increases greatly.

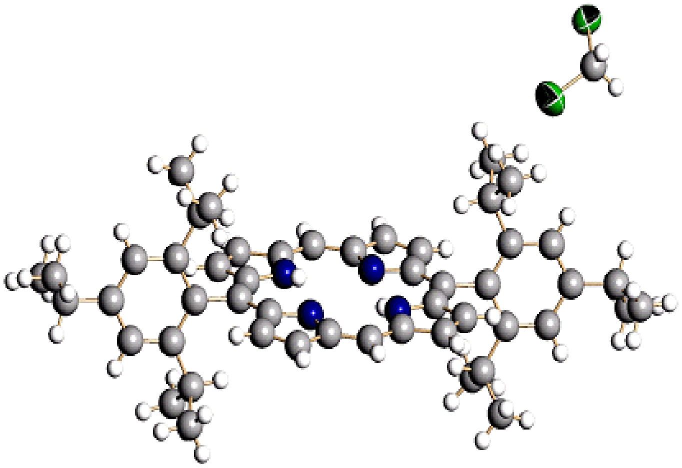

Figure 2-49. Crystal Structure of 5,15-bis(2,4,6-triisopropylphenyl)-10*H*, 20*H*-porphyrin (3)

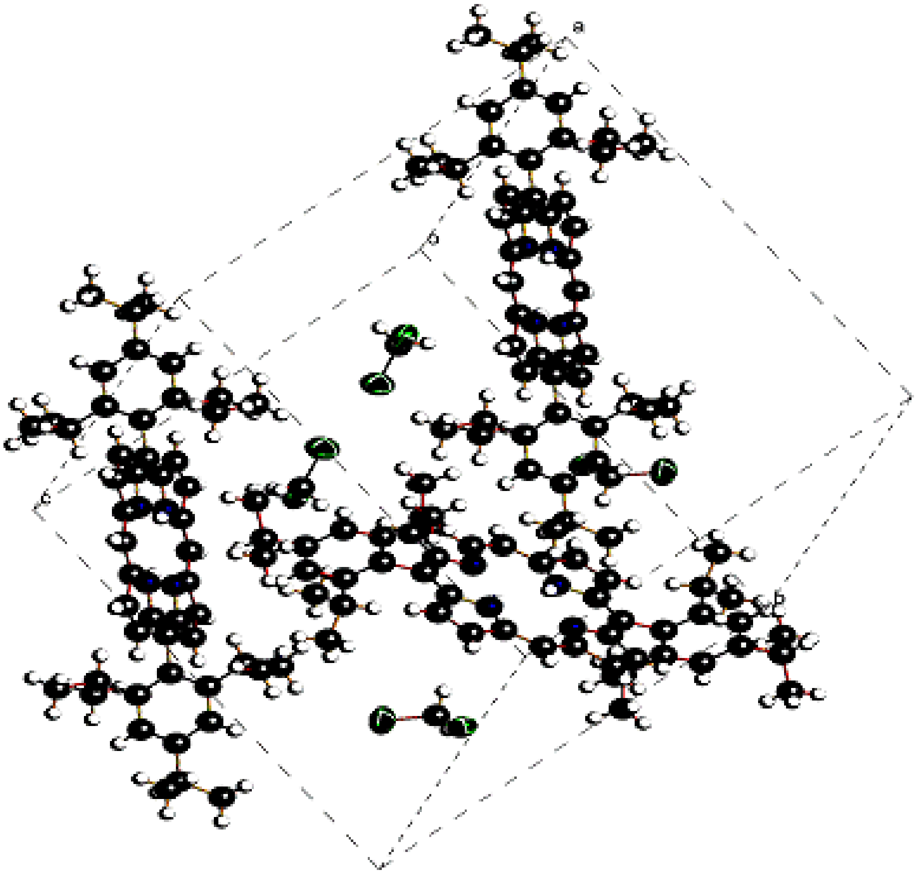

Figure 2-50. Molecular Packing of 5,15-bis(2,4,6-triisopropylphenyl) -10*H*, 20*H*-porphyrin (3)

Table 2-2. Crystal Data* and Structure Refinement for Porphyrin (3)

* See other data in Appendices 2-1 to 2-6

Identification code	5,15-bis(2,4,6-triisopropylphenyl) -10*H*, 20*H*-porphyrin (**3**)
Empirical formula	C52 H62 Cl4 N4
Formula weight	884.86
Temperature	100(2) K
Wavelength	1.54178 Å

Crystal system	Monoclinic	
Space group	C2/c	
Unit cell dimensions	a = 21.1820(4) Å	α= 90°.
	b = 18.1384(4) Å	β= 128.7640(10)°.
	c = 16.2986(3) Å	γ = 90°.
Volume	4882.71(17) Å^3	
Z	4	
Density (calculated)	1.204 mg/m^3	
Absorption coefficient	2.488 mm^{-1}	
F(000)	1880	
Crystal size	0.20 x 0.09 x 0.08 mm^3	
Theta range for data collection	3.62 to 30.98°.	
Index ranges	-14<=h<=14, -12<=k<=12, -10<=l<=10	
Reflections collected	3186	
Independent reflections	768 [R(int) = 0.0398]	
Completeness to theta = 30.98°	100.0 %	
Absorption correction	SADABS	
Max. and min. transmission	1.000 and 0.837163	
Refinement method	Full-matrix least-squares on F^2	
Data / restraints / parameters	768 / 0 / 137	
Goodness-of-fit on F^2	1.077	
Final R indices [I>2sigma(I)]	R1 = 0.0734, wR2 = 0.1986	
R indices (all data)	R1 = 0.0762, wR2 = 0.2009	

Largest diff. peak and hole	0.445 and -0.304 e.Å^{-3}

2.5 Conclusions

By comparisons among all of the porphyrins synthesized in our laboratory and some of commercially available porphyrin molecules, it is clearly demonstrated that $\pi-\pi$ attractive interactions are the major driving force for the porphyrin's low solubility. Facial and edge-encumbrance can efficiently interrupt face-to-face stacking and T-shaped stacking to reduce $\pi-\pi$ interactions in both freebase and metalated porphyrins. The strategy of adding facial- and edge-encumbrances to the *meso*-positions of *trans*-A_2B_2 porphyrins is highly efficient in its ability to increase porphyrin solubility. This structure-property study indicates that branched alkyl groups that are rigid and bulky provide the best facial- and edge-encumbrance. The substituents including aromatic rings, long chain alkyl groups, and electronegative atoms, such as oxygen, are not effective for facial- and edge-encumbrance. In fact, they may even strengthen the interactions between porphyrins by additional $\pi-\pi$ interactions (aromatic side-groups), van der Waals interactions (long-chain alkyl groups) and electrostatic interactions (electronegative atoms to form polar bonding).

In conclusion, we have successfully designed and synthesized highly soluble porphyrins. Porphyrin **3** has achieved the highest solubility in $CHCl_3$ among all of the porphyrins in this study. Compared to other porphyrins (solubility from 0.02 to 60 mmol/L), the solubility of porphyrin **3** has been increased by 3 to 15000 times in mmol/L or 25 ~ 23 000 times in g/L.

References:

1. Pron, A.; Rannou, P., "Processible Conjugated Polymers: From Organic Semiconductors to Organic Metals and Superconductors", *Prog. Polym. Sci.* **2002**, *27*, 135-190.
2. Mamardashvili, G. M.; Mamardashvili, N. Z.; Golubchicov, O. A.; Berezin, B. D., "The Influence of Alkyl Bridge Substitution on the Porphyrin Solubility", *J. Mol. Liq.* **2001**, *91*, 189-191.
3. Mamardashvili, G. M.; Mamardashvili, N. Z.; Berezin, B. D., "Solubility of Alkylporphyrins", *Molecules* **2000**, *5*, 762-766.
4. Jane Li, Z.; Ojala, W. H.; Grant, D. J., "Molecular Modeling Study of Chiral Drug Crystals: Lattice Energy Calculations", *J. Pharm. Sci.* **2001**, *90*, 1523-1539.
5. Hunter, C. A.; Sanders, J. K. M., "The Nature of π-π Interaction", *J. Am. Chem. Soc.* **1990**, *112*, 5525.
6. Poh, B.-L.; Yian, Y. N., "Complexation of Aromatic Hydrocarbons with a Macrocycle Containing Four Tropolone Units in Water", *Tetrahedron* **1997**, *53*, 11913-11918.
7. Lauher, J. W.; Ibers, J. A., "1,2,3,4,5,6,7,8-Octaethylporphyrin", *J. Am .Chem. Soc.* **1973**, *95*, 5148.
8. Byrn, M. P.; Curtis, C. J.; Yu, Hsiou; Khan, S. I.; Sawin, P.A.; Tendick, S. K.; Terzis, A.; Strouse, C. E., "TPP, $C_{44}H_{28}N_4Zn1,2(C_9H_8)$", *J. Am. Chem. Soc.* **1993**, *115*, 9480.
9. Senge, M. O.; I. B.; Nelson, N. Y.; Smith, K. M., "5,10,15,20-Tetra-n-Butylporphyrin", *J. Porphyr. Phthalocya.* **1999**, *3*, 99.
10. Lindsey, J. S.; Wagner, R. W.; Li, F., "Modular Synthesis of Multiporphyrin Arrays for Studies in Photosynthesis and Molecular Photonics", *Book of Abstracts, 212th ACS National Meeting, Orlando, FL, August 25-29* **1996**, INOR-168.
11. Shanmugathasan, S.; Edwards, C.; Boyle, R. W., "Advances in Modern Synthetic Porphyrin Chemistry", *Tetrahedron* **2000**, *56*, 1025-1046.

12. Lee, C.-H.; Lindsey, J. S., "One-Flask Synthesis of meso-Substituted Dipyrromethanes and Their Application in the Synthesis of Trans-Substituted Porphyrin Building Blocks", *Tetrahedron* **1994**, *50*, 11427-11440.
13. Littler, B. J.; Ciringh, Y.; Lindsey, J. S., "Investigation of Conditions Giving Minimal Scrambling in the Synthesis of Trans-Porphyrins from Dipyrromethanes and Aldehydes", *J. Org. Chem.* **1999**, *64*, 2864-2872.
14. Littler, B. J.; Miller, M. A.; Hung, C. H.; Wagner, R. W.; O'Shea, D. F.; Boyle, P. D.; Lindsey, J. S., "Refined Synthesis of 5-Substituted Dipyrromethanes", *J. Org. Chem.* **1999**, *64*, 1391-1396.
15. Furniss, B. S.; Hannaford, A. J.; Smith, P. W. G.; Tatchell, A. R. *Vogel's Textbook of Practical Organic Chemistry;* 5th ed.; John Wiley & Sons, Inc.: New York, 1989.
16. Barclay, L. R. C.; Hudson, J. C.; Sonawane, H. R., "Sterically Hindered Aromatic-Compounds .4. Solvolysis of t-Butyl-Benzyl, Phenyl-Benzyl, and Trialkyl-Benzyl Chlorides in Ethanol-Water - Evidence for Steric Acceleration in 2,4,6-Tri Tert Butylbenzyl Chloride", *Can. J. Chemistry* **1972**, *50*, 2318-2322.
17. Barclay, L. R. C.; Sonawane, H. R.; Macdonal, Mc., "Sterically Hindered Aromatic-Compounds .3. Acid-Catalyzed Reactions of 2,4,6-Tri -t-Butylbenzyl and 2-Methyl-4,6-Di-t-Butylbenzyl Alcohols and Chlorides", *Can. J. Chemistry* **1972**, *50*, 281-286.
18. Barclay, L. R. C.; McMaster, I. T., "Photolysis of 2,4,6-Tri-t-Butylnitrobenzene", *Can. J. Chemistry* **1971**, *49*, 676-679.
19. Ishii, A.; Ishida, T.; Kumon, N.; Fukuda, N.; Oyama, H.; Inamoto, N.; Iwasaki, F.; Okazaki, R., "Synthesis, Structure, and Some Reactions of (2,4,6-Tri-t-Butyl)Thiobenzaldehyde, the First Stable Aromatic Thioaldehyde", *B. Chem. Soc. Jpn.* **1996**, *69*, 709-717.
20. Suslick, K. S.; Fox, M. M., "A Bis-Pocket Porphyrin", *J. Am. Chem. Soc.* **1983**, *105*, 3507-3510.
21. Wagner, R. W.; Lindsey, J. S.; Turowska-Tyrk, I.; Scheidt, W. R., "Synthesis of Porphyrins Tailored with Eight Facially-Encumbering Groups. An Approach to Solid-State Light-Harvesting Complexes", *Tetrahedron* **1994**, *50*, 11097-11112.

22. Kruithof, K. J. H.; R. F. S.; Klumpp, G. W., "Lithiated 2-Alkylnyl-1,3-Dioxanes as Fully Oxygenated Acyl-Anion Equivalents: Synthesis of 1-Alkynyl Ketones", *Tetrahedron* **1983**, *39*, 3073-3081.

23. Gold, K. W.; D. J. H.; Gold, A.; Savrin, J. E.; Toney, G. E., "Crystal Structure of Tetramethoxyporphyrin", *Chem. Commun. (Cambridge)* **1985**, 563.

24. Byrn, M. P.; Curtis, C. J.; Hsiou, Y.; Khan, S. I.; Sawin, P. A.; Tendick, S. K.; Terzis, A.; Strouse, C. E., "Porphyrin Sponges - Conservation of Host Structure in over 200 Porphyrin-Based Lattice Clathrates", *J. Am. Chem. Soc.* **1993**, *115*, 9480-9497.

CHAPTER III

INVESTIGATION ON PORPHYRIN POLYMERIZATION METHODS

3.1 Palladium-mediated polymerization

With highly soluble porphyrin molecules having been synthesized, the focus of this project shifted toward the search for polymerization methods for the synthesis of porphyrin polymers. Porphyrin polymerization is a step-wise reaction involving porphyrin molecules that have at least two reactive functional groups substituted on the periphery. It occurs via a sequence of reactions to incorporate porphyrin units into the main chain. Carbon-carbon bond-forming reactions are necessary for this step-wise polymerization. As discussed in previous Chapters, $\pi-$structured linkers or spacing groups are required in the polymer chain to maintain the $\pi-$conjugation. Furthermore, small band-gap conjugated porphyrin polymers or intrinsically conductive polymers require linkers without steric hindrance between neighboring units in the chain to avoid the interruption of $\pi-$conjugation. Therefore, the search for polymerization methods was focused on those reactions that can produce acetylene, ethylene or butadiyne linkers between porphyrin units.

Over the past 30 years, a wide variety of cross coupling methods have been developed for carbon-carbon bond-formation between unsaturated species such as vinyl, aryl and alkynyl moieties. These methods have emerged among the most powerful synthetic tools that are useful in the synthesis of complex compounds, supramolecular chemistry and materials science.[1] Among many of the metal-mediated cross coupling reactions, palladium (Pd) or copper (Cu)-mediated reactions are most widely used. They follow a generally acknowledged mechanistic scheme involving an oxidative addition-transmetalation-reductive elimination sequence.[2-5] In the Heck-Cassar-Sonogashira reaction (Scheme 3-1), an aryl halide **2** (bromide or iodide) is coupled with a terminal alkyne **1** in the presence of a homogeneous palladium catalyst, a copper(I) species, and an amine as solvent or co-solvent. Scheme 3-1 shows both the general reaction of forming an alkyne linkage and the presumed mechanism. Through an oxidative addition, the aryl halide forms intermediate **4**, which after transmetalation with a molecule of **3** forms the organometallic species **5**. This species is reductively eliminated from the palladium to form product **7** and regenerate the active palladium catalyst **6.**

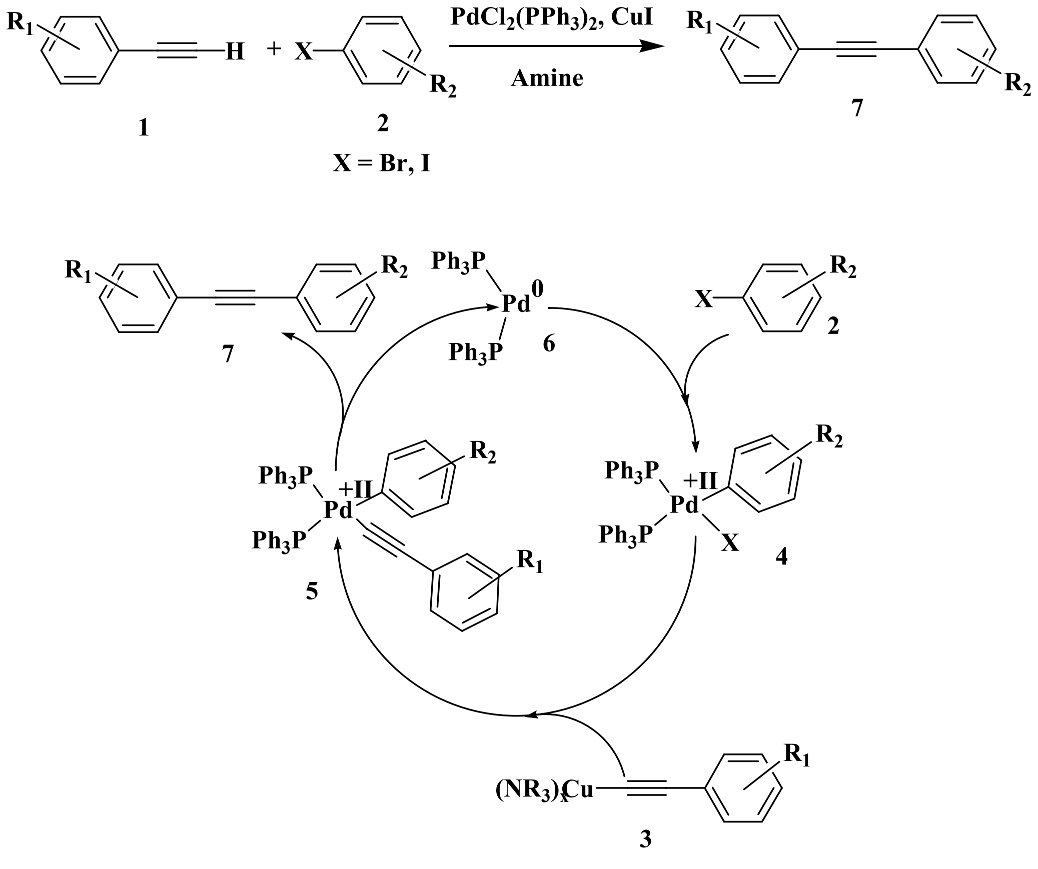

Scheme 3-1. Heck-Cassar-Sonogashira Reaction and Mechanism

The active catalyst-Pd(0) species **6** is produced in situ through self-coupling of terminal alkynes as shown in Scheme 3-2. The source of homogeneous palladium catalyst is usually the commercially available bis-triphenylphosphine palladium(II) chloride [$Pd(PPh_3)_2Cl_2$], which is initially less active until it reacts with cuprated alkyne **4** to form palladium catalyst precursor **5** through transmetalation, This bis-alkyne palladium species **5** is unstable and reductively eliminates to form a symmetrical butadiyne **8** and the active catalyst **6.**

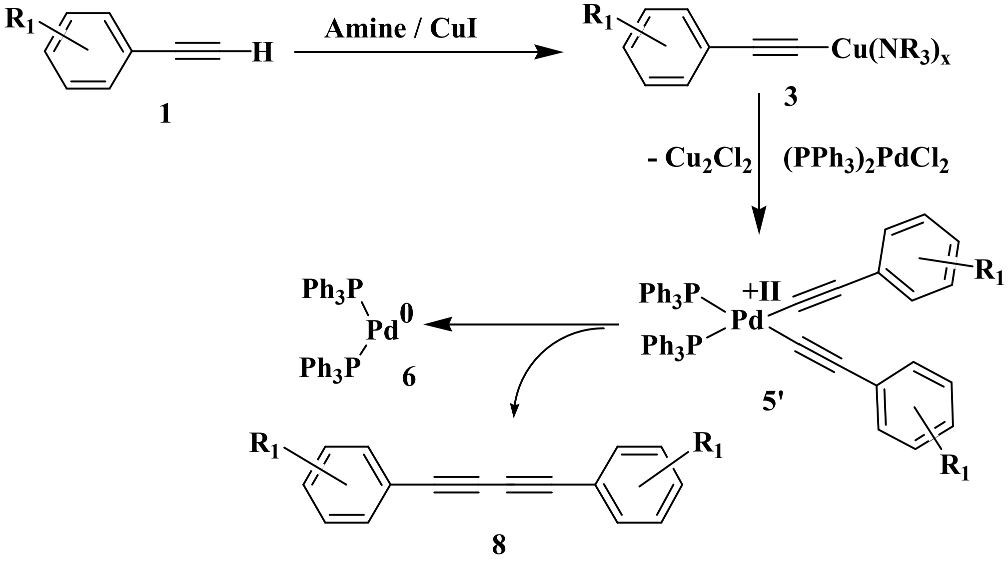

Scheme 3-2. Generation of Active Catalyst 6 (L_2Pd^0)

From the mechanism of the cross coupling reaction between an aryl halide and a terminal alkyne as shown in Scheme 3-1 and 3-2, one disadvantage of this method can be seen. The inclusion of several percent butadiyne linked compound (**8**), which is formed during the activation step of the palladium catalyst, along with the expected product (**7**) indicates that there will inevitably be some butadiyne defects in the resulting ethyne-linked polymer.

Pd-mediated coupling reactions are the most widely used methods in the synthesis of porphyrin materials. Despite the disadvantages of the Pd-mediated reaction for polymer synthesis, we initially presumed that the low DPs in porphyrin polymers produced by this method were due to the low solubility of the reactants. We decided to re-investigate the Pd(II) catalyzed coupling method to synthesize conjugated porphyrin polymers with high molecular weights by using highly soluble porphyrin monomers. A Pd(II)-mediated self-coupling reaction between terminal alkynyl porphyrins was employed in the presence of oxygen to build butadiyne linkages in the porphyrin polymer chains (Scheme 3-3 and 3-4).

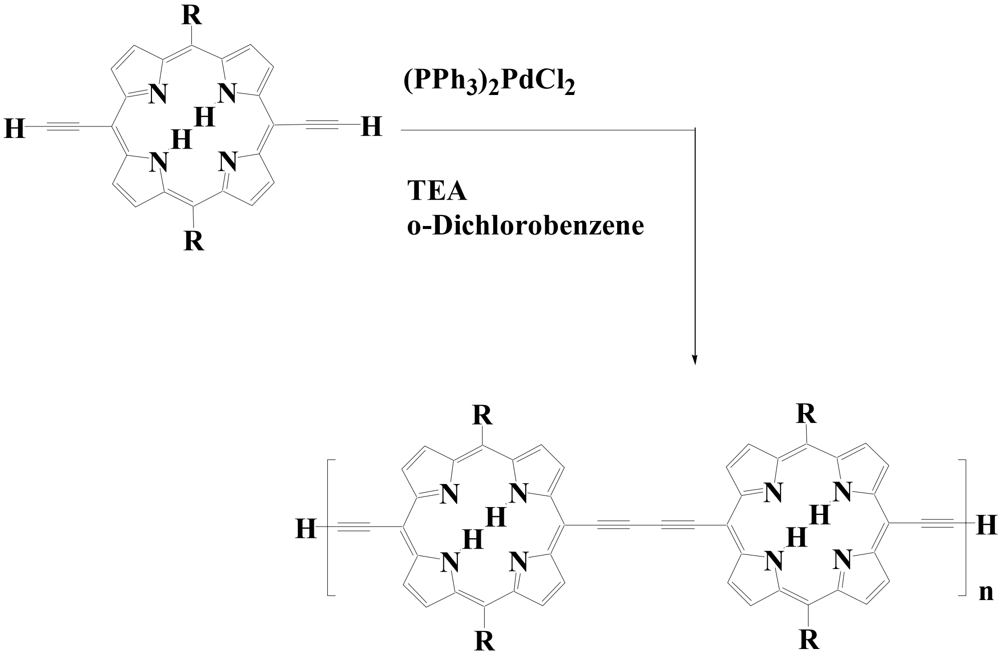

Scheme 3-3. Pd(II)-Catalyzed Self-coupling of Terminal Alkynyl Porphyrins

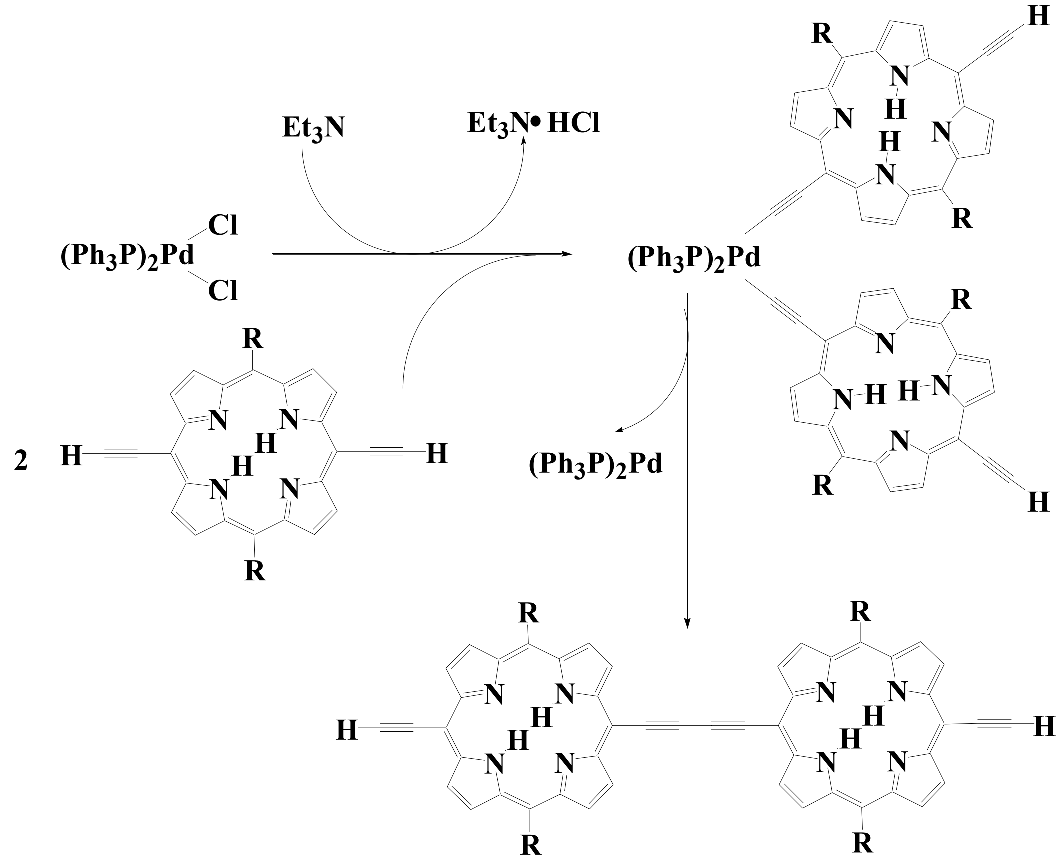

Scheme 3-4. Production of Butadiyne Linkages for Porphyrin Materials

3.1.1 Synthesis of monomer I

The synthesis of monomer **I** (5, 15-diethynyl-porphyrin) for this Pd-mediated polymerization method was described in Chapter II (See 2.3.2 Synthesis of designed porphyrin molecules) and it is again summarized in Scheme 3-5. NMR spectra for 5, 15-diethynyl-10,20-bis(2,4,6-triisopropylphenyl)porphyrin in its protected freebase (porphyrin **13**), metalated and deprotected forms (porphyrin **13'**, monomer **I**) are shown in Fig. 3-1 to Fig. 3-3.

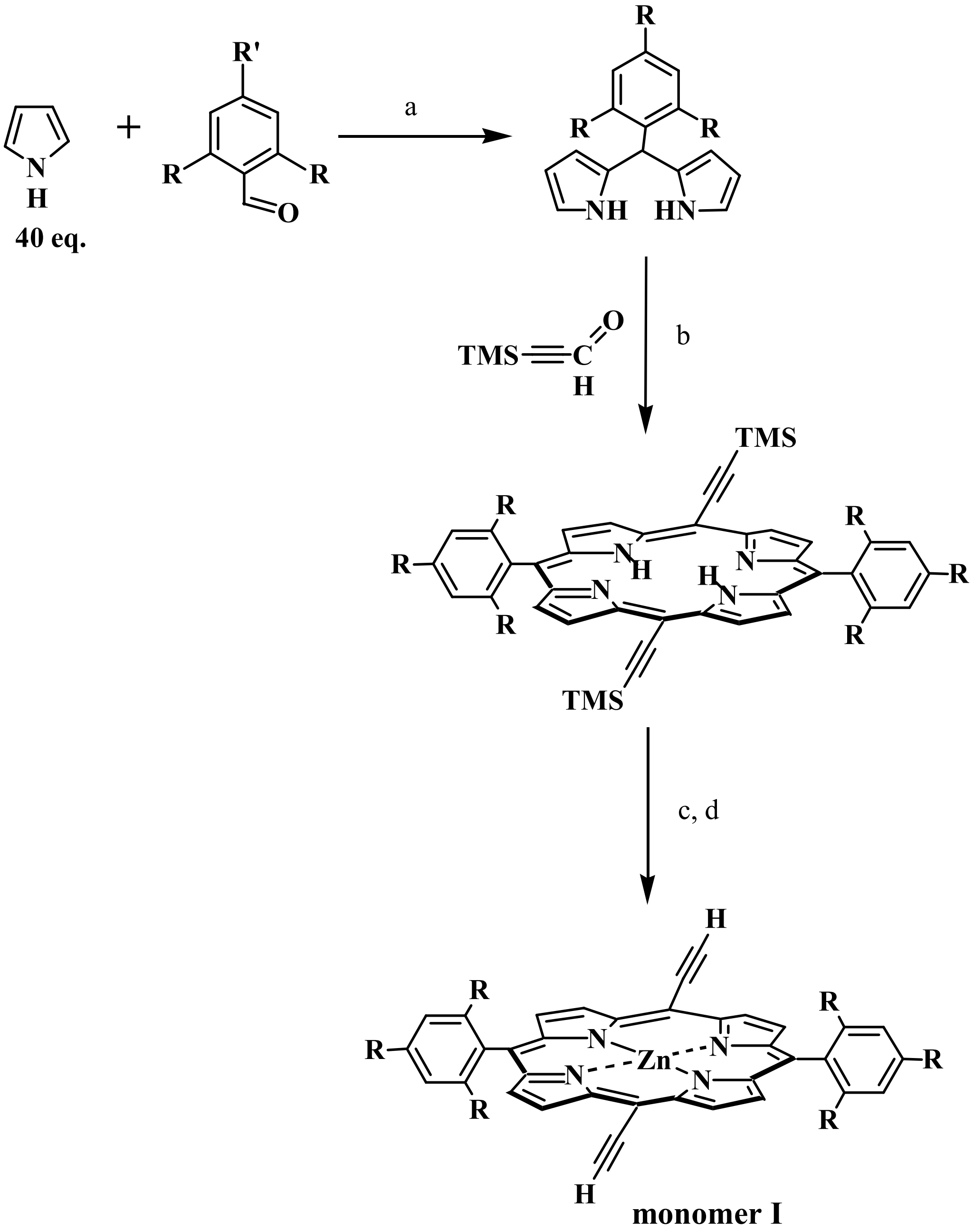

(a) 0.25 eq $BF_3O(Et)_2$, Na_2CO_3; (b) 0.1 eq $BF_3O(Et)_2$, $CHCl_3$, DDQ; (c) 2 eq $Zn(OAc)_2$, 9:1 CH_2Cl_2: MeOH; (d) 2.1 eq TBAF, 1: 1 THF: $CHCl_3$

Scheme 3-5. Synthesis of 5, 15-diethynyl-10, 20-bis(2,4,6-trialkylphenyl)porphyrin (monomer I)

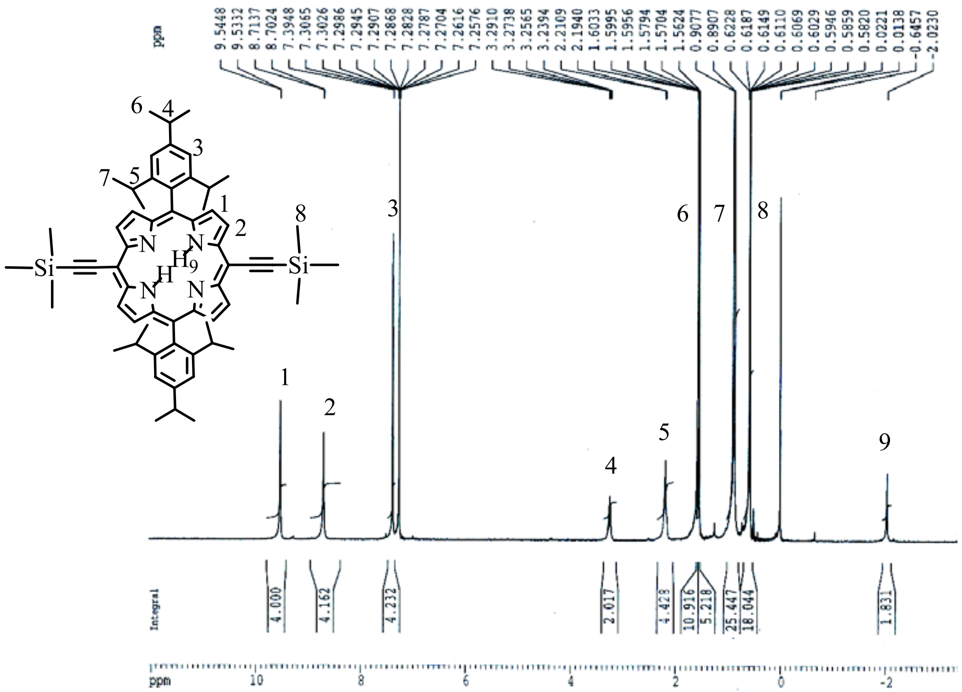

Figure 3-1. ^{1}**H NMR spectrum for 5, 15-bis(trimethylsilylethynyl)-10, 20-bis (2,4,6-triisopropylphenyl)porphyrin Freebase**

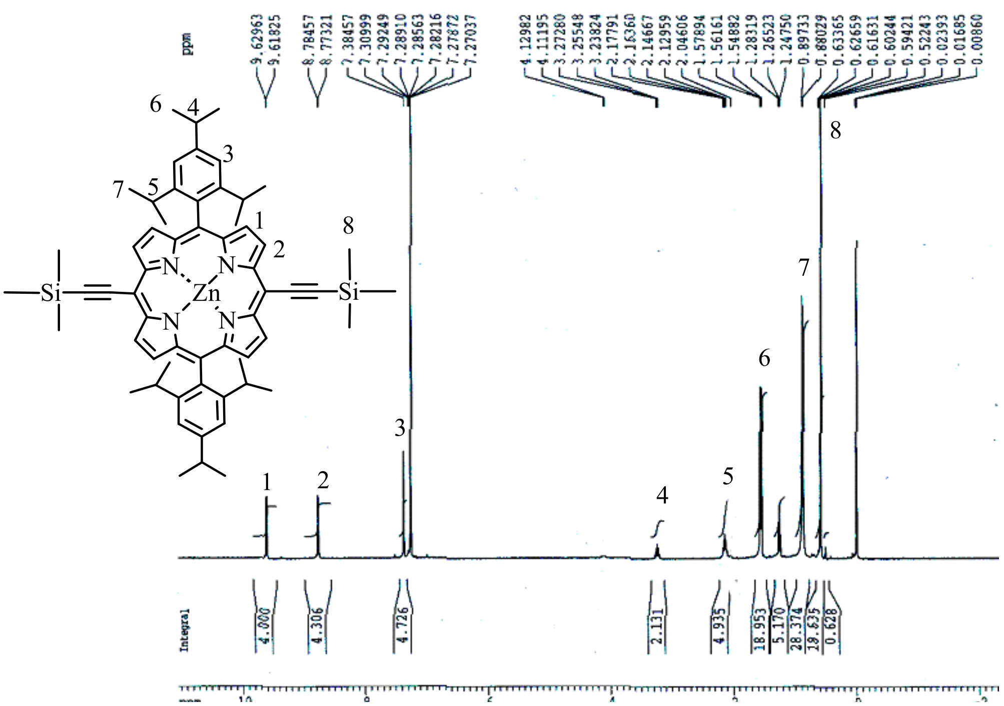

Figure 3-2. ^{1}**H NMR Spectrum of Zn-5, 15-bis(trimethylsilylethynyl)-10, 20-bis (2,4,6-triisopropylphenyl)porphyrin**

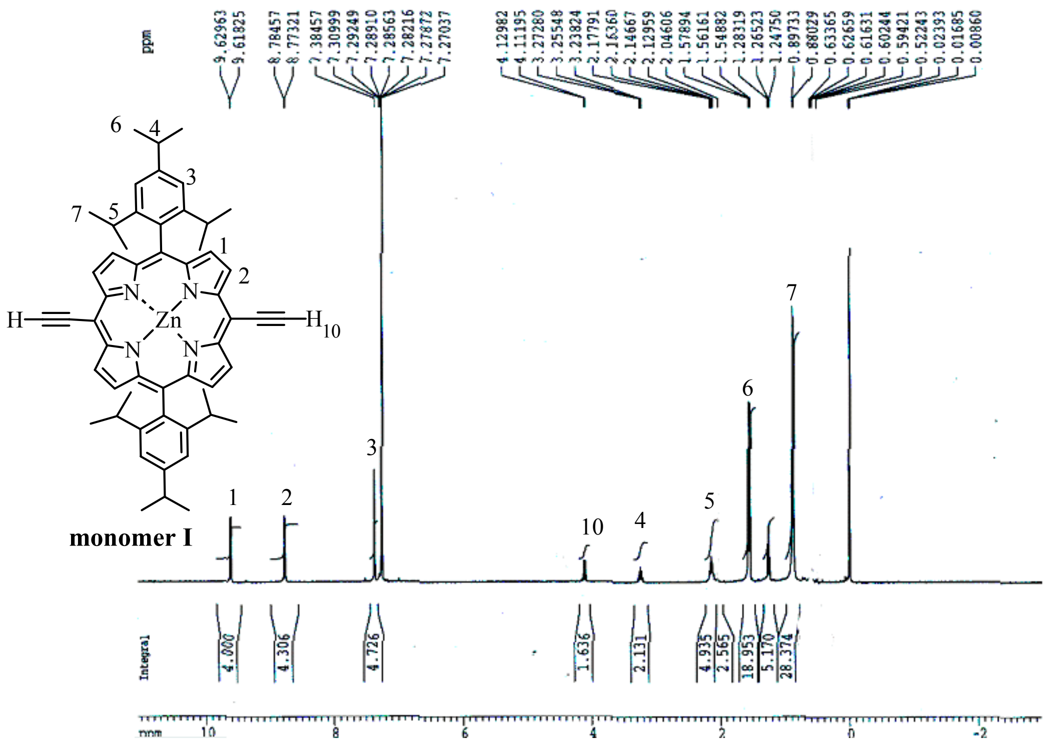

Figure 3-3. ^{1}H NMR Spectrum of Zn-5, 15-diethynyl-10, 20-bis(2,4,6-triisopropylphenyl)porphyrin (monomer I, porphyrin 13')

The structural difference of monomer **I** between its freebase and metalated forms can be easily characterized by NMR spectroscopy. As shown in Fig. 3-1 to Fig. 3-3, the *β*–pyrrole protons (signal 1 and 2), *meta*-proton on phenyl rings (signal 3), methine protons in the isopropyl groups (signal 4 and 5), and methyl protons of the isopropyl groups (signal 6 and 7) in either freebase, metalated or deprotected 5, 15-bis(2,4,6-triisopropylphenyl)-10, 20-bis(trimethylsilylethynyl)porphyrin are practically unchanged. The major difference of metalated porphyrin **13** and its freebase form is the disappearance of signal 9 (protons on nitrogen atoms inside of the porphyrin ring) when Zn was inserted into porphyrin **13**. The difference after the terminal alkyne is deprotected is the disappearance of signal 8 (protons in the trimethylsilyl group) and appearance of signal 10, the protons on the terminal alkyne groups. This deprotected Zn-5, 15-diethynyl-porphyrin is the desired monomer **I** for further Pd-mediated polymerization.

3.1.2 Pd-mediated Polymerization

General procedure for Pd-mediated polymerization. Porphyrin monomer **I** was dissolved in *o*-dichlorobenzene (*o*-DCB) to afford a 5 mM solution. A small amount of triethylamine (TEA) (1:9 v/v TEA:o-DCB) was added as base, as well as co-solvent to help increase solubility. One equivalent of $(PPh_3)_2PdCl_2$ was added as catalyst. The reaction proceeded at room temperature for several days, and GPC (Gel Permeation Chromatography) was used to monitor the progress of the reaction (Fig. 3-4 to Fig. 3-7).

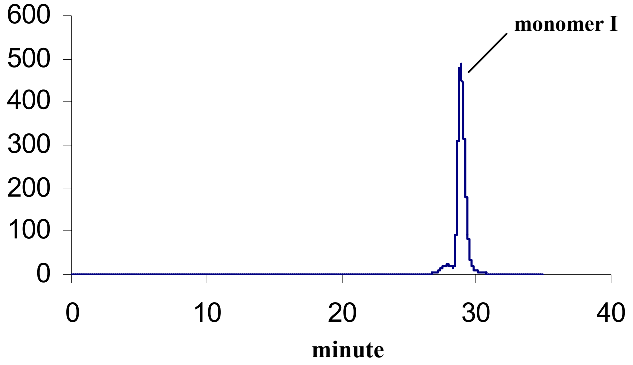

Figure 3-4. GPC of Porphyrin Monomer I

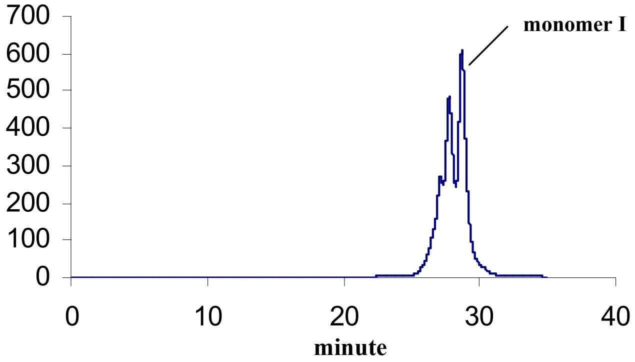

Figure 3-5. GPC of Pd-mediated Polymerization of 5, 15-diethynyl-10, 20-bis(2,4,6-triisopropylphenyl)porphyrin after 2 hours

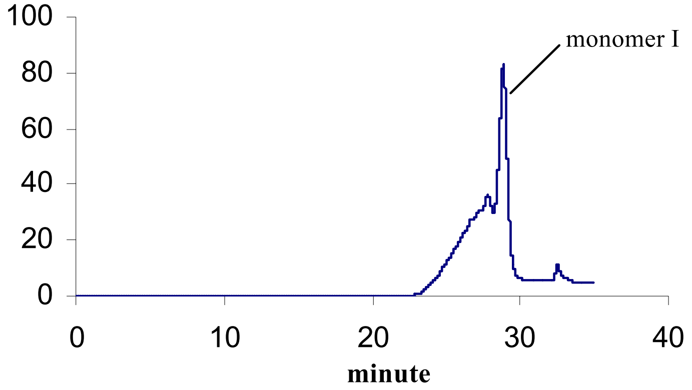

Figure 3-6. GPC of Pd-mediated Polymerization of 5, 15-diethynyl-10, 20-bis(2,4,6-triisopropylphenyl)porphyrin after 12 hours

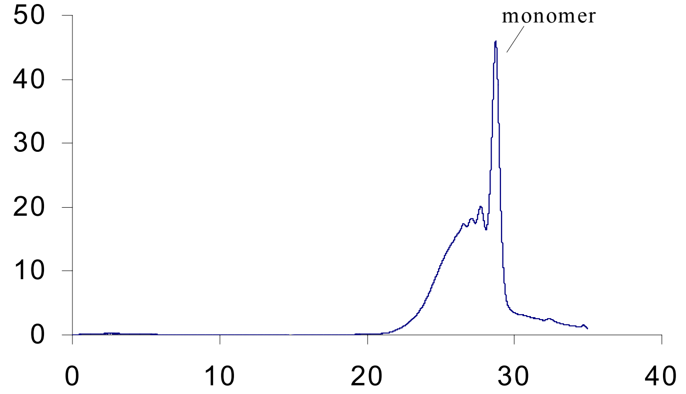

Figure 3 -7. GPC of Pd-mediated Polymerization of 5, 15-diethynyl-10, 20-bis(2,4,6-triisopropylphenyl)porphyrin after 12 days

Although the resolution of GPC (HP Series 1100, Phenogel 5 u 500 A → Phenogel 5 10^4A → Phenogel 5 10^3A) is not sufficient to provide baseline separation of the porphyrin oligomers, the profile of the chromatogram still shows us that the Pd-mediated polymerization produces conjugated porphyrin dimer, trimer, tetramer and other higher oligomers. By comparison with polystyrene standards using in the same

GPC conditions (Fig. 3-8), the molecular weights of peaks at retention time 28.80, 27.60, and 25.50 minutes (counted as monomer, dimer and pentamer by peak positions, Fig. 3-7) can be estimated to be 2,700, 3,700, and 13,700 Daltons, respectively. Since the molecular weight of the monomer is 826.5 Daltons, the molecular weights corresponding to those peaks with retention times at 28.80, 27.60, and 25.50 can be estimated by this GPC spectrum as 3, 4 and 16 repeating units (DP) in the porphyrin chains. However, the molecular weight estimated by GPC is higher than the actual value if we consider the monomer as an internal standard. At 826.5 Da., the molecular weight of the monomer is overestimated by more than three times of the known value. Other research groups have also noted that molecular weight comparisons using polystyrene standards is overestimated by a factor of 3 to 5, especially for the rigid-rod type polymer classes.[6] MALDI mass spectral analysis for the Pd-mediated porphyrin polymerization reaction indicates that there are about 8 porphyrins units in the polymer (Fig. 3-9).

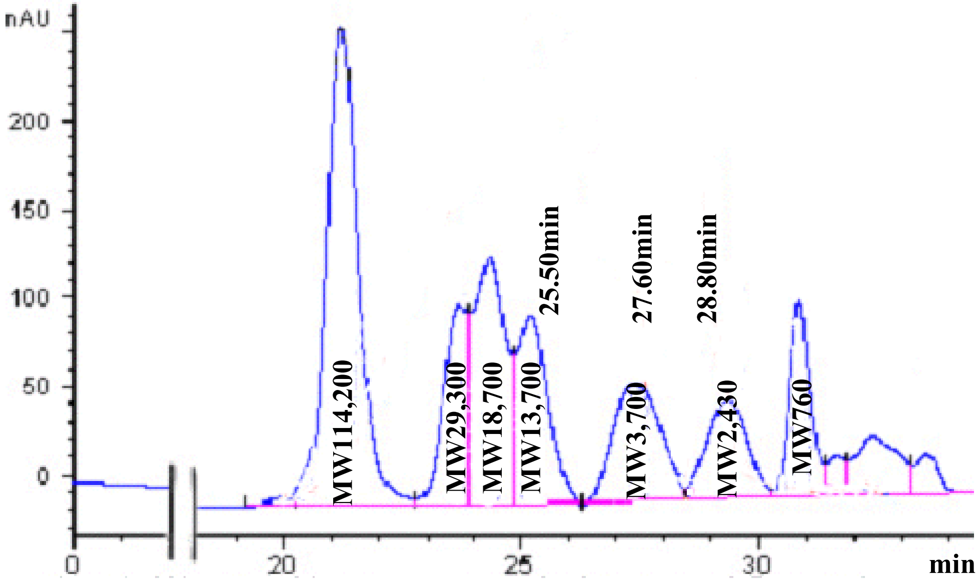

Figure 3 -8. GPC of Polystyrene Standard Series

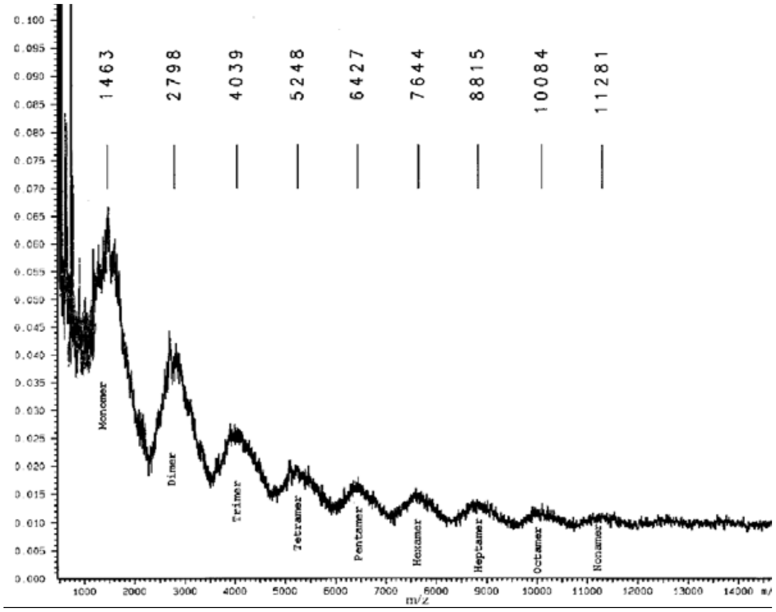

Figure 3-9. MALDI Mass Spectral Analysis of Pd-mediated Polymerization of 5,15-diethynl-bis(2,4,6-tribenzoxyphenyl)porphyrin

3.1.3 Discussion

One significant phenomenon in the Pd-mediated porphyrin polymerization (Fig. 3-4 to Fig. 3-8) is that the monomer remains the most abundant species in the reaction mixture. This indicates that a large number of monomers do not participate in the polymerization. The mass difference between the measured value and the actual value of the monomer, dimer or other oligomers (measured monomer mass is 1463 and formula mass is 1211) suggests that there is something attached to the terminal alkyne. We considered some possible species as shown in Fig. 3-10 where Pd or $P(Ph)_3$ groups are the likely groups that have been transferred to the porphyrin monomer. Both Pd(II) and Pd(0) species can attach to the terminal end of the porphyrin with different ligands.

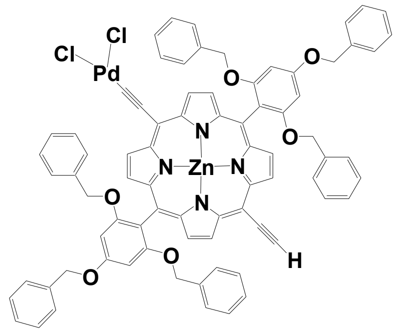

Exact Mass: 1383.18
Mol. Wt.: 1387.01
a

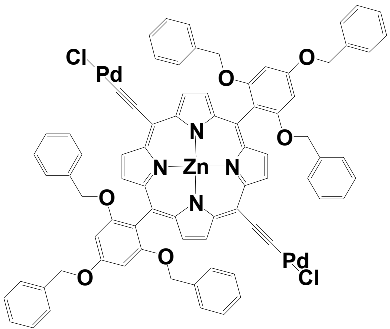

Exact Mass: 1488.08
Mol. Wt.: 1492.42
b

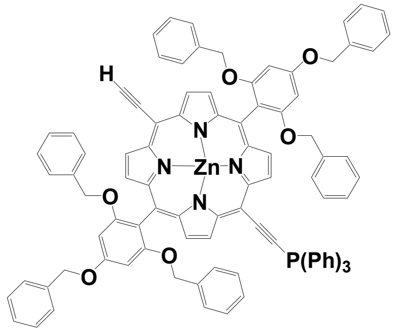

Exact Mass: 1469.43
Mol. Wt.: 1471.97
c

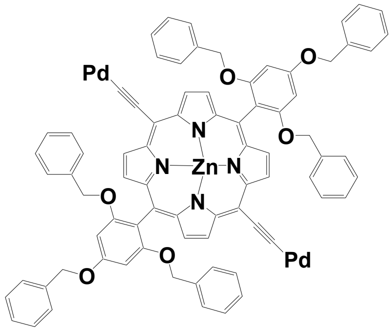

Exact Mass: 1418.14
Mol. Wt.: 1421.52
d

Figure 3-11. End-capped Porphyrin Monomer I in Pd-mediated Polymerization

Of these suggested examples, some intermediates may still undergo condensation reactions to form oligomers but with metal defects in the chain, others may remain as monomer-like species in the solution without further reaction. GPC shows the monomer-like species are left in the reaction in a large percentage. This end capping may have inhibited monomer activity and terminated chain growth. This problem can also occur at the dimer, trimer or any higher oligomer stages. Therefore, Pd-mediated polymerizations may not only introduce structural defects and end group ambiguities, but also stop chain growth and result in low molecular weight materials.

3.2 Acyclic diyne metathesis (ADIMET) polymerization

To search for different polymerization methods with more efficient and less interfering catalyst systems, we sought to study and apply the acyclic diyne metathesis (ADIMET) polymerization method to conjugated porphyrin systems. As Bunz and co-workers pointed out, “the chemistry of the C-C triple bond has been dominated almost exclusively by the admittedly extremely effective Pd-catalyzed couplings of the Stille or Heck-Cassar-Sonogashira-Hagihara type.”[7] It is the same situation in the synthesis of porphyrin polymers that almost all the polymerization methods employed for the construction of triple bond linkage are the Stille or Heck-Cassar-Sonogashira-Hagihara type coupling reactions.

Alkyne metathesis has never received as much attention as its cousin, alkene metathesis. Bunz and co-workers are among a relatively few number of research groups that have successfully prepared high molecular weight poly(*p*-phenyleneeethynylene)s by alkyne metathesis utilizing “instant” catalysts (Scheme 3-6). The acyclic diyne metathesis (ADIMET) polymerization of 1,4-dipropynyl benzenes has produced defect free polyphenyleneethynylenes (PPEs) polymers of very high DP.[7-16]

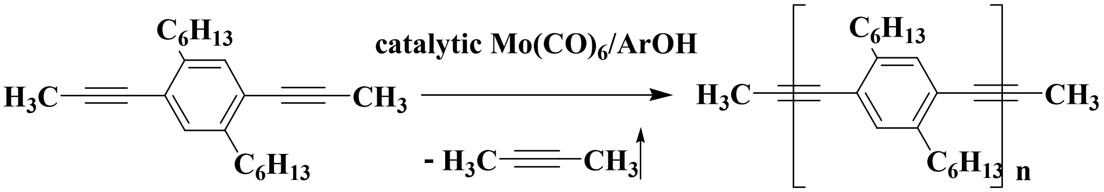

Scheme 3-6. Alkyne Metathesis for (*p*-phenyleneethynylene)s (Bunz’ reaction)

Inspired by Bunz’s reaction for the construction of defect-free PPEs with acyclic diyne metathesis, we sought to synthesize a *trans*-bispropynylporphyrin (monomer **II**) in order to explore the applicability of analogous ADIMET type chemistry towards the production of high DP ethyne-linked porphyrin polymers (Scheme 3-7).

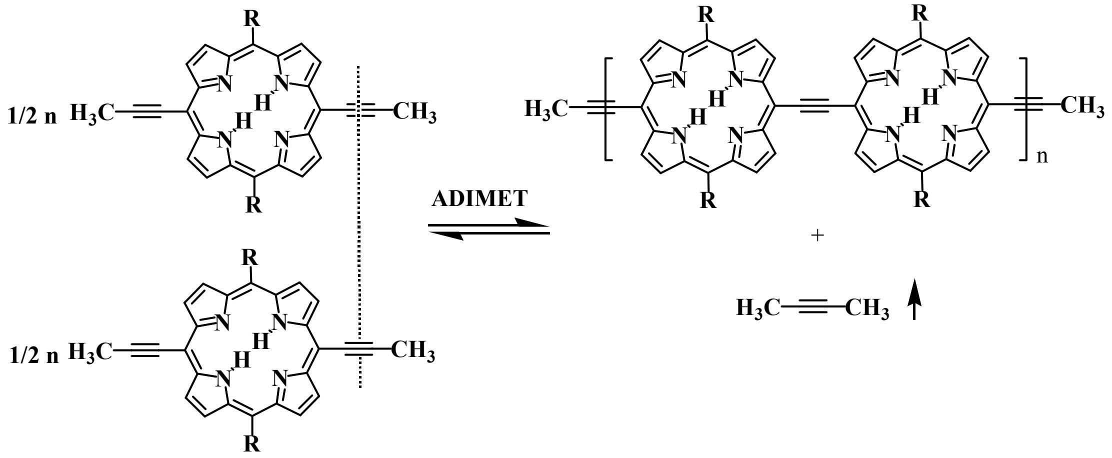

Scheme 3-7. Alkyne Metathesis for Ethyne-linked Porphyrin Polymers

3.2.1 Synthesis of porphyrin monomer II for acyclic diyne metathesis (ADIMET)

We first attempted to prepare monomer **II** via a Stille coupling of dibromo-porphyrin with tributyl(1-propynyl)tin. This reaction did not afford satisfactory yields for the desired 5,15-dipropynyl-porphyrin. Based on similar reactions reported by Therien and co-workers,[17] the reaction of propyne with 5,15-dibromo-porphyrin was expected to afford the *trans*-bispropynylporphyrin designed for use in the ADIMET reaction. Scheme 3-8 shows the total synthesis of monomer **II**.

Synthesis of porphyrin monomer II. Two different porphyrin molecules were synthesized as the monomer **II** (Scheme 3-8). One is the dipropynyl-dimesitylporphyrin derived from porphyrin **2** and the other is the dipropynyl-bis(2,4,6-triisopropylphenyl)porphyrin derived from porphyrin **3**. The procedures for the synthesis of dipropynyl-bis(2,4,6-triisopropylphenyl)porphyrin is described as following.

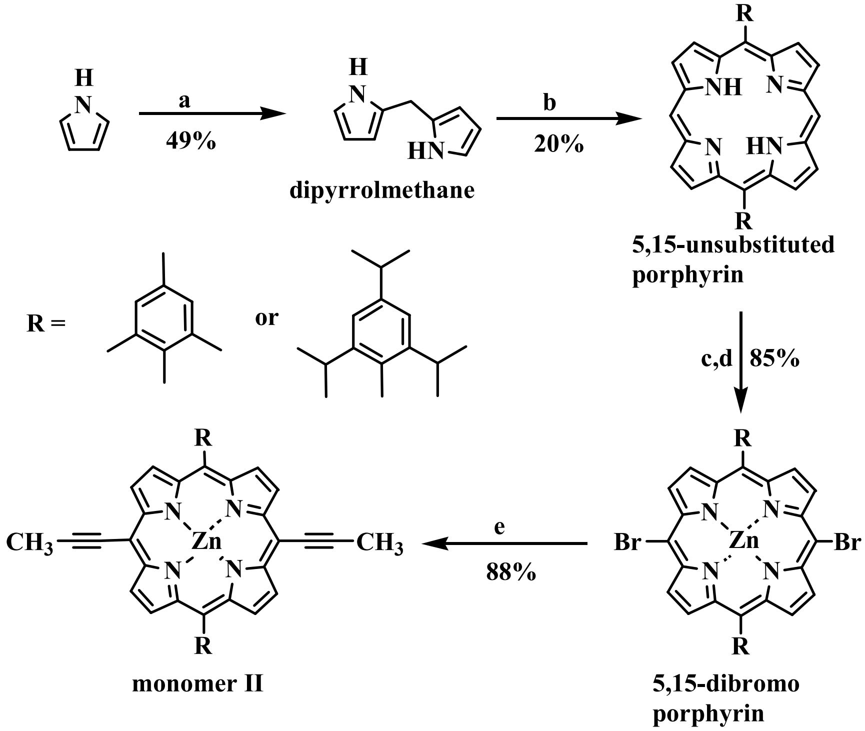

(a) $(CH_2O)_n$, TFA, 70°C, 30 min; (b) 2, 4, 6-trimethylbenzaldehyde or 2, 4, 6-triisopropylbenzaldehyde, BF_3•Et_2O, DDQ, $CHCl_3$, 30 min; (c) N-bromosuccinimide, pyridine (trace), rt, 3 hrs; (d) $Zn(OAc)_2$, methanol : $CHCl_3$ (5:1 v/v), 3hrs; (e) $(Ph_3P)_2PdCl_2$, propyne (1.0 M in THF), CuI, TEA, 70 °C, 2 hrs.

Scheme 3-8. **Total Synthesis of Porphyrin Monomer II**

The synthesis of porphyrin monomer **II** began with the preparation of 5,15-bis(2,4,6-triisopropyl)-10*H*,20*H*-porphyrin (see synthesis of porphyrin **3** in Chapter II). 0.67 g (0.844 mmol) of 5,15-bis(2,4,6-triisopropyl)-10*H*,20*H*-porphyrin was dissolved in 186 mL of $CHCl_3$ and chilled to 0 ^{0}C. 2.2 eq. of NBS (0.33 g, 1.86 mmol) and 0.5 mL of pyridine were added and the mixture was stirred for 1 hour. TLC analysis showed only one product spot and spots corresponding to the starting materials and mono-brominated porphyrin had almost completely disappeared. Acetone was added to quench the reaction and the solvent was removed *in vacuo*. The crude product was crystallized from methanol to provide 0.70 g (0.74 mmol) 5,15-dibromo-porphyrin in 88% yield. The 5,15-dibromo-porphyrin was metalated using Zn(OAc)$_2$ in order to prevent Cu or other metal insertion. 95.2 mg (0.1 mmol) of Zn-dibromoporphyrin, 1.16 mL (10 eq., 1 mmol, 1.2 M in THF) of propyne solution, 17.5 mg (0.25 eq.) of (Ph$_3$P)$_2$PdCl$_2$ and 5 mg of CuI were combined in 15 mL of deoxygenated TEA and left to stir for 48 hours. Whereupon TLC showed the reaction had proceeded to completion, the reaction mixture was poured into 0.1 N HCl (50 mL) and extracted into CH$_2$Cl$_2$. The extract was dried over anhydrous Na$_2$SO$_4$, filtered and concentrated to dryness. The residue was purified using a flash silica gel chromatography (dichrolomethane:hexanes, 2:1, v/v) to produce 68 mg of 5, 15-dipropynyl porphyrin (monomer **II**) in 88% yield. ^{1}H NMR (400 MHz, CDCl$_3$, 25 ^{0}C) and ^{13}C NMR (100 MHz, CDCl$_3$, 25 ^{0}C) spectra for both monomers are shown in Fig. 3-9, 3-10 and 3-11.

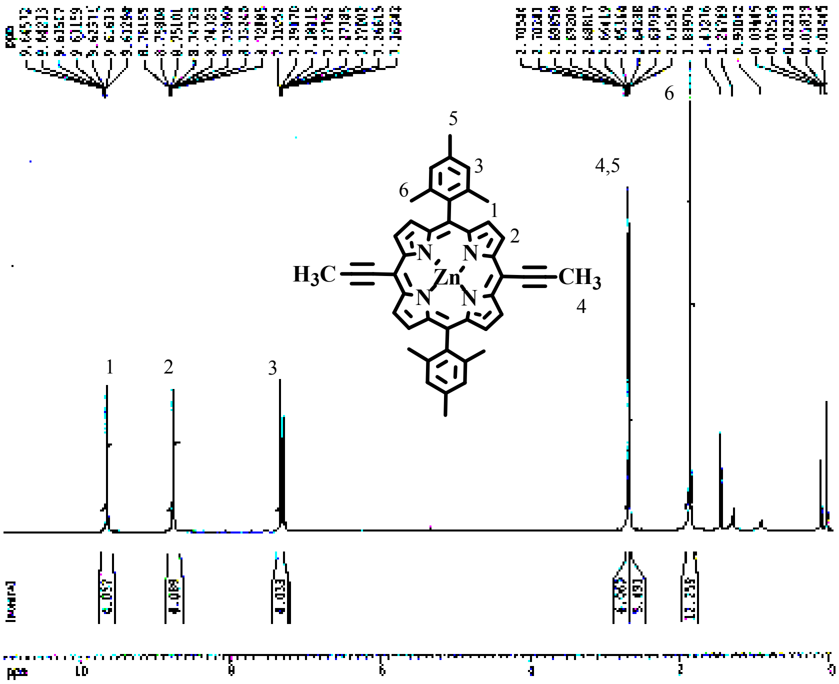

Figure 3-9. ^{1}H NMR Spectrum of dipropynyl-dimesitylporphyrin

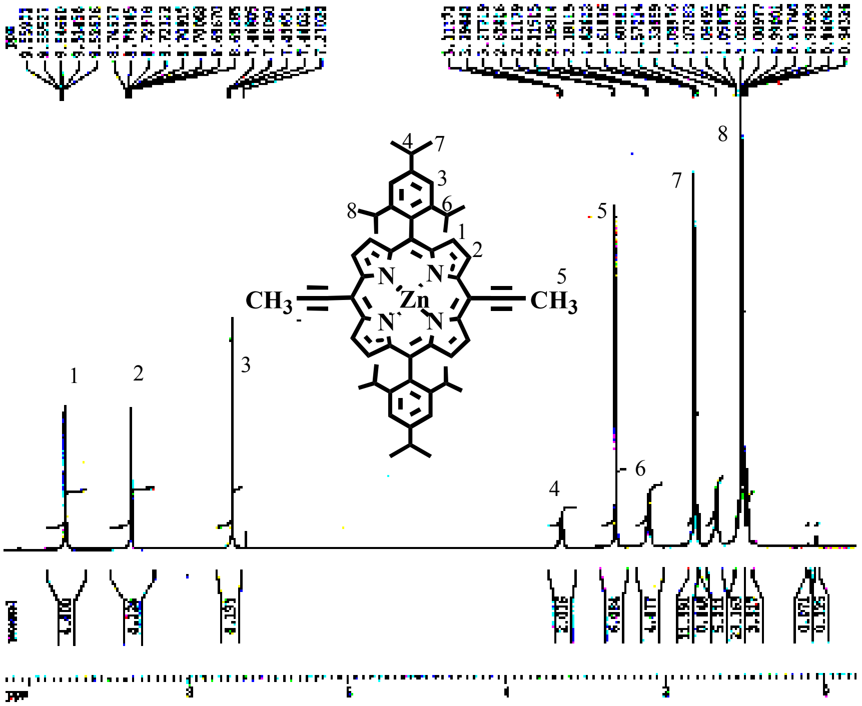

Figure 3-10. ^{1}H NMR Spectrum of dipropynyl-bis(2,4,6-triisopropylphenyl)porphyrin

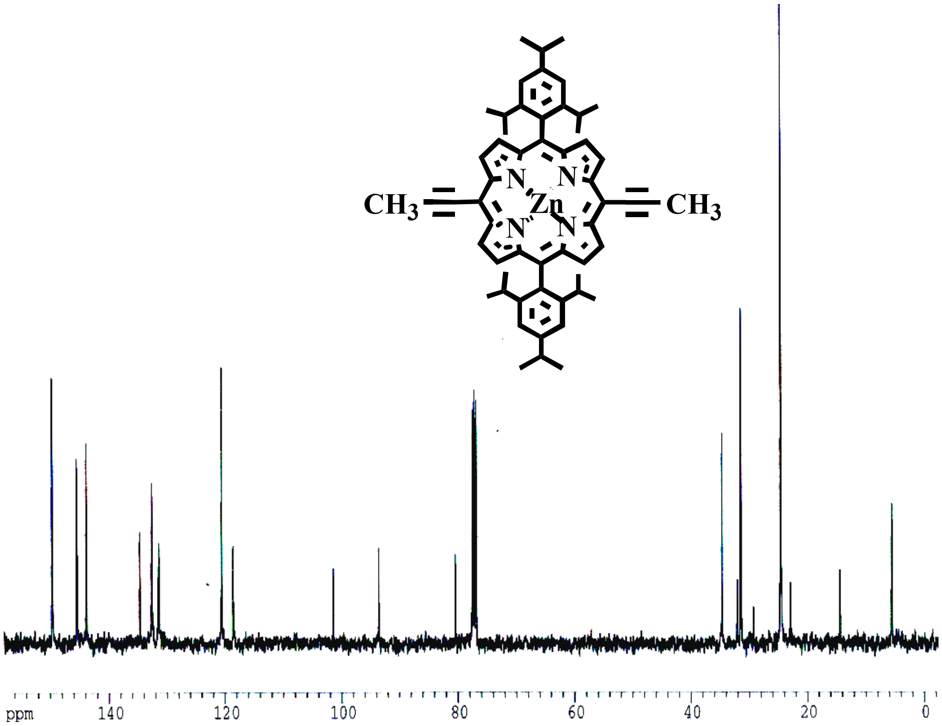

Figure 3-11. ^{13}C NMR Spectrum of dipropynyl-bis(2,4,6-triisopropylphenyl)porphyrin

3.2.2. ADIMET reactions for porphyrin polymerization

We performed both homo- and co-polymerization experiments to investigate applicability of the alkyne metathesis (ADIMET) reaction to the synthesis of conjugated porphyrin polymers.

3.2.2.1. Porphyrin Homopolymerization

In this polymerization method, the metathesis reaction occurs between *trans*-dipropynyl porphyrins (Scheme 3-11).

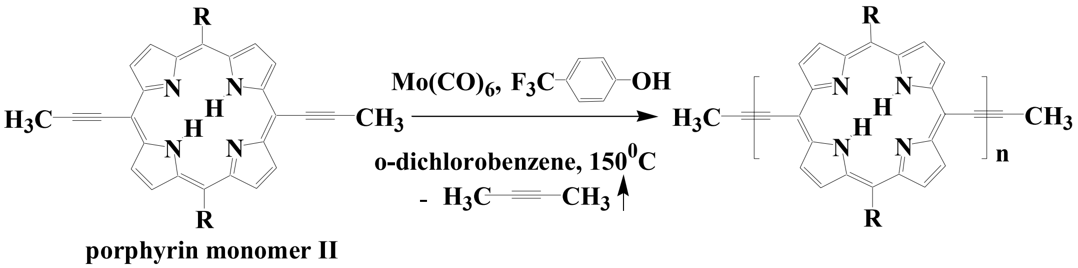

Scheme 3-11: ADIMET Reaction for Porphyrin Homopolymerization

Procedures for porphyrin homopolymerization. 0.1 g (0.117 mmol) of porphyrin monomer **II** – the dipropynyl-bis(2,4,6-triisopropylphenyl)porphyrin was dissolved in 5 mL of *o*-dichlorobenzene at 150 ^{0}C, degassed and stirred for 15 minutes. Then 10 mol% (3.2 mg, 0.012 mmol) $Mo(CO)_6$ and 100 mol% (19.5 mg, 0.12 mmol) 4-(trifluoromethyl)phenol were added. A slow stream of argon gas was passed through the reaction solution to help in the removal of one of the products, the butyne, and further push the reaction to the right side. Aliquots were taken periodically and analyzed by GPC to measure the progress of the polymerization. GPC chromatograms at different reaction times for this porphyrin homopolymerization are shown in Fig. 3-12.

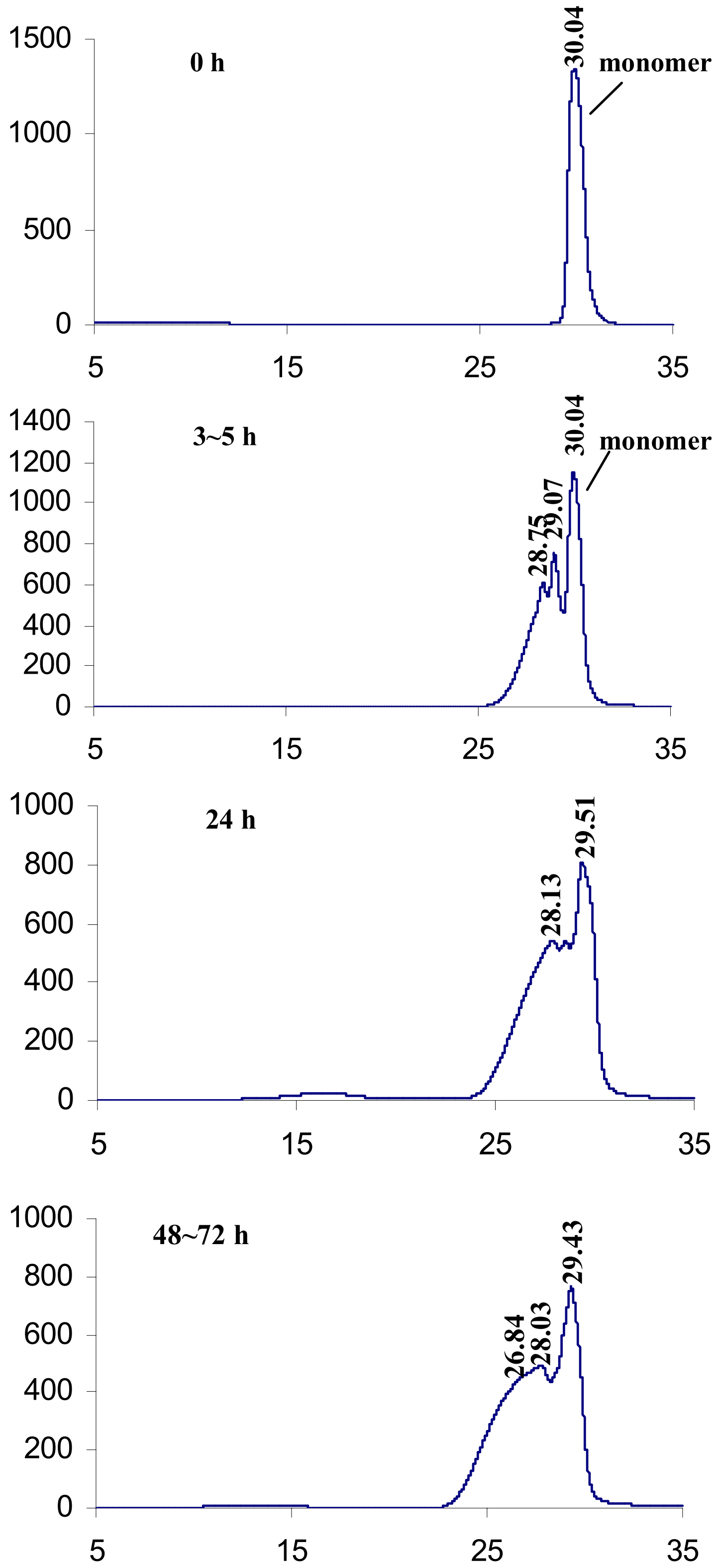

Figure 3-12. GPC of Homopolymerization of dipropynyl-bis(2,4,6-triisopropylphenyl)porphyrin

3.2.2.2 Porphyrin Copolymerization

In this polymerization process the metathesis reaction occurs between *trans*-dipropynylporphyrins (A) and di(ethylhexyl)-dipropynylbenzene(B) to form an AB copolymer (Scheme 3-12). For the metathesis reaction among *trans*-dipropynylporphyrins and di(ethylhexyl)-dipropynylbenzene (Bunz's monomer) as shown in Scheme 3-12, we first synthesized di(ethylhexyl)-dipropynylbenzene according to Bunz's procedure.[7]

Synthesis of di(ethylhexyl)-dipropynylbenzene.

a. 20 g (136 mmol) of 1,4-dichlorobenzene was coupled with 2.1 equivalents of ethylhexylmagnisium bromide (50 g, 286 mmol) using 0.05 mol% 1,3-bis(diphenylphosphino)propane-nickel(II) Chloride (dpppNiCl$_2$) as catalyst to produce 24 g of di(ethylhexyl) benzene in 60% yield.

b. 10 g (34 mmol) of di(ethylhexyl) benzene was iodinated in a mixture of 3.85 g (17 mmol) of KIO$_4$, 26 mL of acetic acid, 8.5 mL of sulfuric acid, 22 mL of CHCl$_3$, 8.5 mL of H$_2$O and 8.6 g of I$_2$ at 90 ^{0}C to obtain diiodo-di(ethylhexyl)benzene in almost quantitative yield.

c. Propyne was first bubbled into dried THF to form 1.2 M of solution. 16 g (29 mmol) of diiodo-di(ethylhexyl)benzene was dissolved in 250 mL of THF, then 61 mL of 1.2 M of propyne THF solution, 0.05 eq. of Pd(Ph$_3$P)$_2$Cl$_2$, 0.1 eq. of CuI and 1 mL of TEA were added. The reaction solution became grey to brown. After stirred overnight, 1:1 (v/v) hexane:H$_2$O was added. The organic layer was extracted with hexanes three times and concentrated *in vacuo* to yield a brown oil, which was crystallized from ethanol twice to afford 9.3 g of pure white crystals of di(ethylhexyl)-dipropynylbenzene in 85% yield. ^{1}H NMR (400 MHz, $CDCl_3$, 25^0C) is shown in Fig. 3-13.

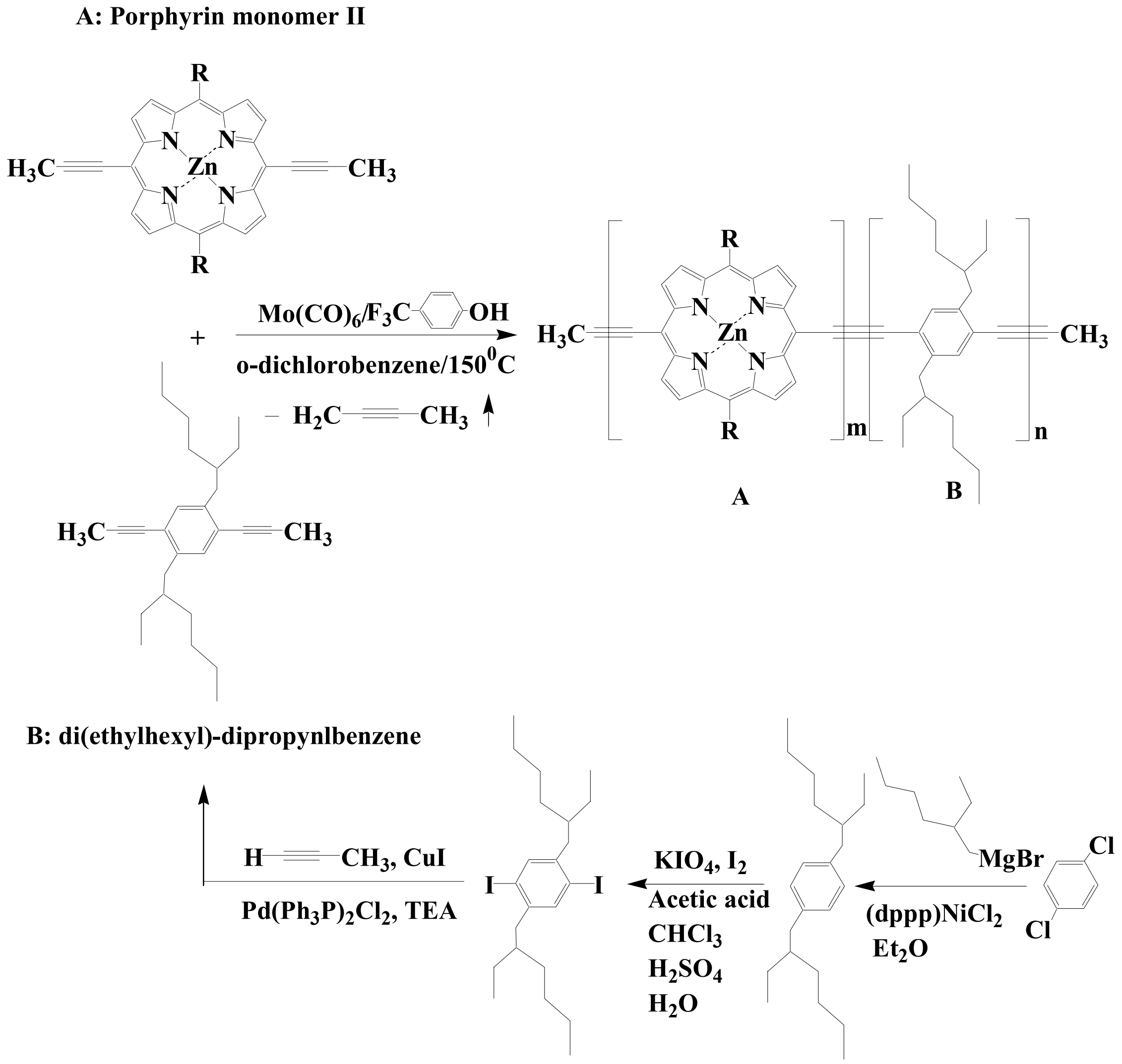

Scheme 3-12. ADIMET Reaction between Porphyrin Monomer II and di(ethylhexyl)-dipropynylbenzene (Porphyrin Copolymerization)

To verify the feasibility of the catalyst and reaction conditions for the metathesis of the dipropynylaromatic system, we first duplicated Bunz's reaction for the AIMET polymerization of di(ethylhexyl)-dipropynylbenzenes. The GPC chromatogram (Fig. 3-14) shows us that a good degree of polymerization has been achieved in this reaction.

From the NMR spectrum of poly[*p*-di(ethylhexyl)phenyleneethynylene] (Fig. 3-15), however, we believe the DP of this reaction is not as high as it was reported in the literature.[7] According to Fig. 3-14, the average retention time for

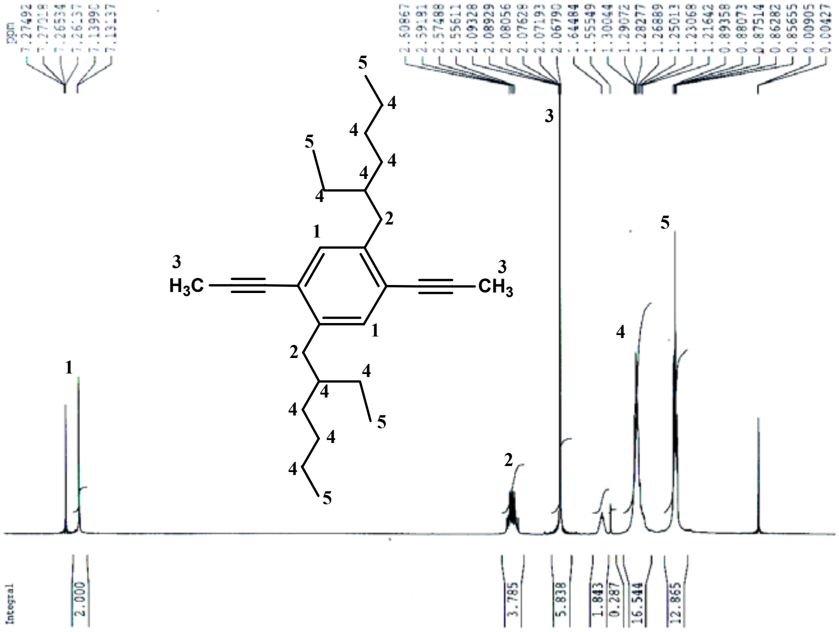

Figure 3-13. ^{1}H NMR Spectrum of di(ethylhexyl)-dipropynylbenzene

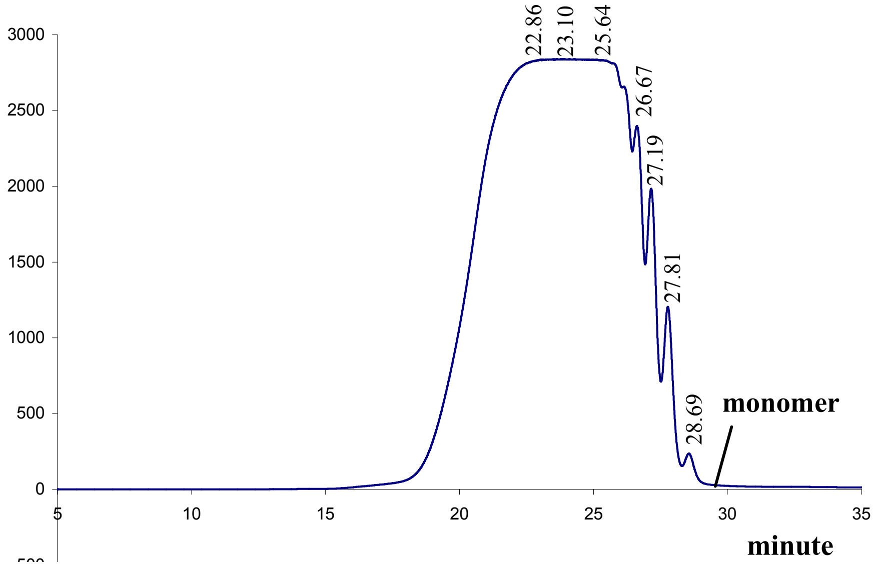

Figure 3-14. GPC of di(ethylhexyl)-dipropynylbenzene Polymerization

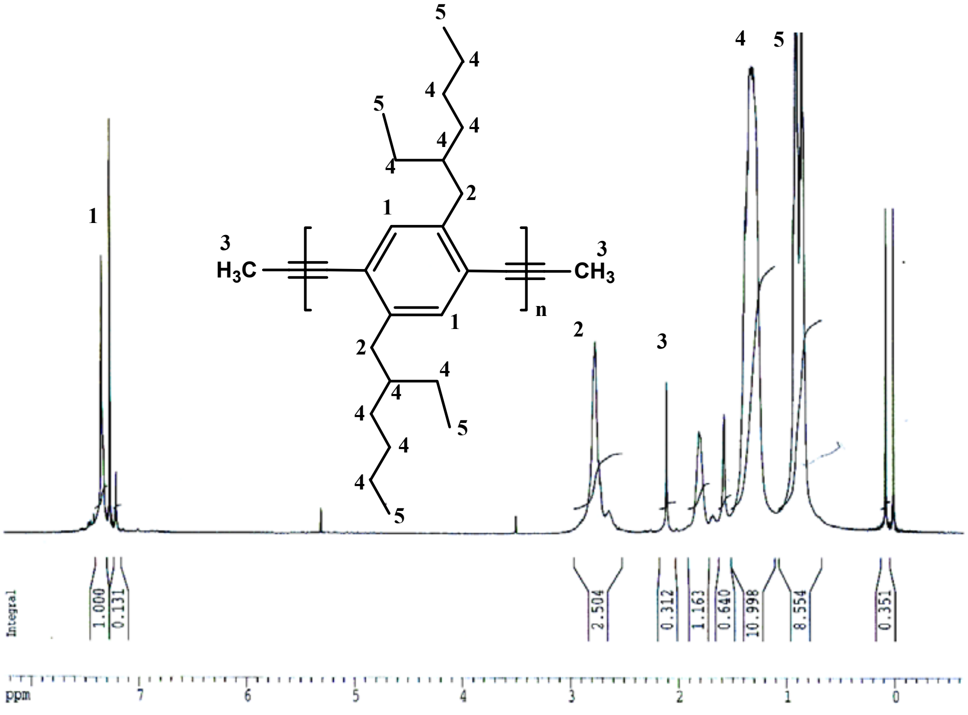

Figure 3-15. ^{1}H NMR Spectrum of di(ethylhexyl)-dipropynylbenzene Polymerization

poly(*p*- phenyleneethynylene) is around 23 minutes, which corresponds to polystyrene standard molecular weight of 28,000 Daltons. While the molecular weight of monomer di(ethylhexyl)-dipropynylbenzene is 378.6 Daltons, GPC gave an estimated average DP (degree of polymerization or units number in polymer chains) of 74 (DP = 28,000/378.63 = 74) for this poly(*p*-phenyleneethynylene). The integrated ratio of the 4 protons at the two methylene group directly attached to benzene (chemical shift around 2.8) to the 6 protons at two methyl groups at the end of chains (chemical shift is 2.1) in the NMR spectrum (Fig. 3-15), gave an estimated DP of 12 (DP = 2.504/0.312 x 6/4 = 12). We have already suggested that GPC estimation for the molecular weight determination of a rigid polymer (especially a rod-like long chained polymer) is overdone by 2 to 5 times. The big difference of molecular weights estimated by GPC and NMR spectroscopy further demonstrates the molecular weight overestimation by the GPC method for porphyrin materials systems.

Copolymerization of *trans*-dipropynyl porphyrins (A) and di(ethylhexyl)-dipropynylbenzene (B, Bunz's monomer). After the success of di(ethylhexyl)-dipropynylbenzene polymerization under Bunz's metathesis conditions, we tried the ADIMET copolymerization for 10%, 25% and 50% porphyrin monomer **II** with 90%, 75% and 50% di(ethylhexyl)-dipropynylbenzene, or in AB ratios 1:9, 1:3 and 1:1, respectively.

General procedure for porphyrin copolymerization. The desired amount and AB ratio of porphyrin monomer **II** (dipropynylporphyrin) and di(ethylhexyl)-dipropynylbenzene were added into *o*-dichlorobenzene at 150 ^{0}C, and the solution was degassed and stirred. 10 mol% $Mo(CO)_6$ and 100 mol% 4-(trifluoromethyl)phenol were added and a slow stream of argon gas was passed through the solution to help with the removal of butyne. Aliquots of the reaction mixture were taken periodically and analyzed by GPC to measure the progress of the polymerization. GPC chromatograms for the porphyrin copolymerizations after 24 hours with different monomer ratios are shown in Fig. 3-16 to 3-19.

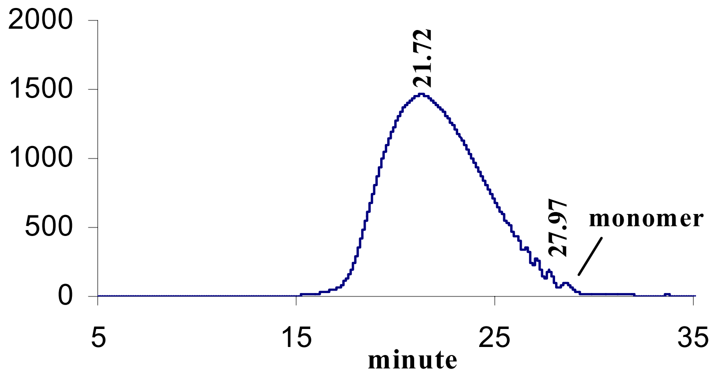

Figure 3-16. GPC of ADIMET Copolymerization of 10% of 5,15-dipropynl-10,20-dimesitylporphyrin with 90% of di(ethylhexyl)-dipropynylbenzene

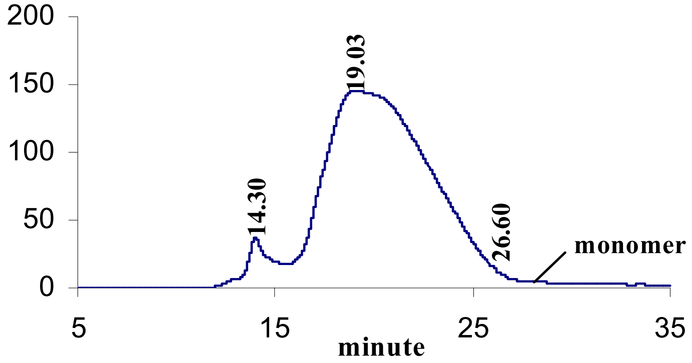

Figure 3-17. GPC of ADIMET Copolymerization of 10% of 5,15-dipropynl-10,20-bis(2,4,6-triisopropylphenyl)porphyrin with 90% of di(ethylhexyl)-dipropynylbenzene

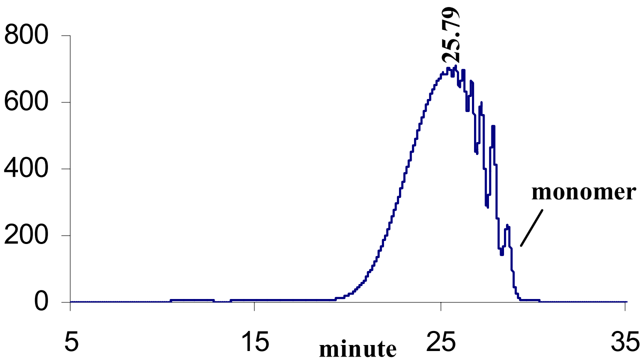

Figure 3-18. GPC of ADIMET Copolymerization of 25% of 5,15-dipropynl-10,20-bis(2,4,6-triisopropylphenyl)porphyrin with 75% of di(ethylhexyl)-dipropynylbenzene

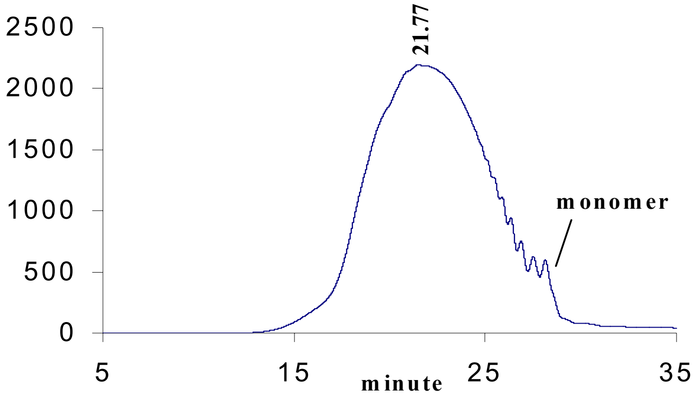

Figure 3-19. GPC of ADIMET Porphyrin Copolymerization of 50% of 5,15-dipropynl-10,20-dimesitylporphyrin with 50% of di(ethylhexyl)-dipropynylbenzene

3.2.3 Discussion

The GPC chromatograms for both the ADIMET porphyrin homopolymerization and copolymerization (Fig. 3-12, 3-16 to 3-19) clearly shows us that the ADIMET reaction does work for porphyrin systems where metathesis occurs between porphyrin monomers, and mixed systems where metathesis occurs between porphyrins and di(ethylhexyl)-dipropynylbenzene. Based on the GPC estimation for molecular weight, the degrees of polymerization for 10%, 25% and 50% dipropynylporphyrin and di(ethylhexyl)-dipropynylbenzene copolymerization are all very high (over 75).

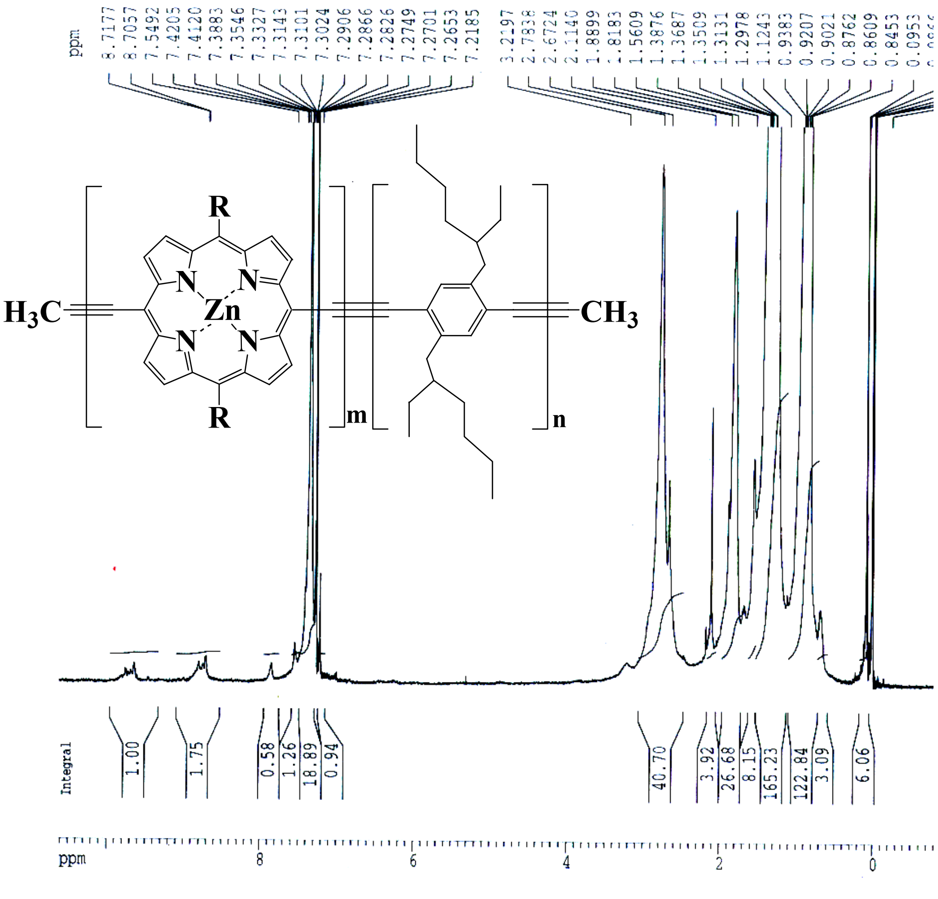

Figure 3-20. ^{1}H NMR Spectrum for 10% of 5,15-dipropynyl-10,20-dimesitylporphyrin and 90% of di(ethylhexyl)-dipropynylbenzene Copolymer

The NMR spectrum for 10% of dipropynylporphyrin and 90% of di(ethylhexyl)-dipropynylbenzene copolymer was also obtained after workup and precipitation in methanol (Fig. 3-20). The calculated DP for 10% porphyrin copolymerization by NMR spectrum is about 16 units. It appears that the metathesis reaction between porphyrins (Fig. 3-12) is slower and less efficient than that between di(ethylhexyl)-dipropynylbenzene (Fig. 3-14). The degree of polymerization in porphyrin homopolymerization reaction is lower than copolymerization between porphyrins and di(ethylhexyl)-dipropynylbenzenes (Fig. 3-16 to 3-19). The difference in ADIMET reactivity for different alkyne systems is determined by the monomers' electrical properties, spatial conformations, or interactions between monomers, etc. What is more important in this preliminary investigation is that the ADIMET polymerization method can be used to produce more porphyrin oligomers than in the Pd-mediated method. According to the generally accepted mechanism for the metathesis reaction, this method avoids structural defects and end group ambiguities in polymer or oligomer chains. From the lower monomer peaks in the GPC chromatograms for porphyrin homopolymerization compared to polymerization method with Pd-mediated cross coupling reactions, especially the almost complete disappearance of the porphyrin monomer peaks in the porphyrin copolymerizations, it indicates that there is almost no end capping on porphyrin monomers in this reaction. If enough active species (reactive carbynes) are produced in the reaction, all of the porphyrin monomers can gradually undergo metathesis to form oligomer and polymer chains. Although metathesis polymerization between porphyrins seems slow and is not as efficient as the metathesis polymerization between di(ethylhexyl)-dipropynylbenzenes, it is believed that by improving and optimizing reaction conditions or other strategies to keep abundant active species for porphyrins, we will be able to accelerate the porphyrin metathesis reaction and push the metathesis polymerization to completion.

Some special experiments were performed to understand the alkyne metathesis process in an effort to optimize the reaction of porphyrin systems. For example, since the metathesis between di(ethylhexyl)-dipropynylbenzenes is faster and more efficient, the active species- metal carbyne(s) in such a system should be produced more quickly and abundantly, which will presumably help to speed up porphyrin metathesis reactions when porphyrin is added in the same reaction system. This metathesis reaction was started by adding only di(ethylhexyl)-dipropynylbenzenes and catalysts first, after the active catalytic carbynes were produced in large amount (the reaction has been developed fully), porphyrin was added to fulfill the copolymerization with di(ethylhexyl)-dipropynylbenzenes. GPC and NMR spectrum for this metathesis reaction by adding A, B monomers in sequence are shown in Fig. 3-21 and 3-22. The similarity of the G P C

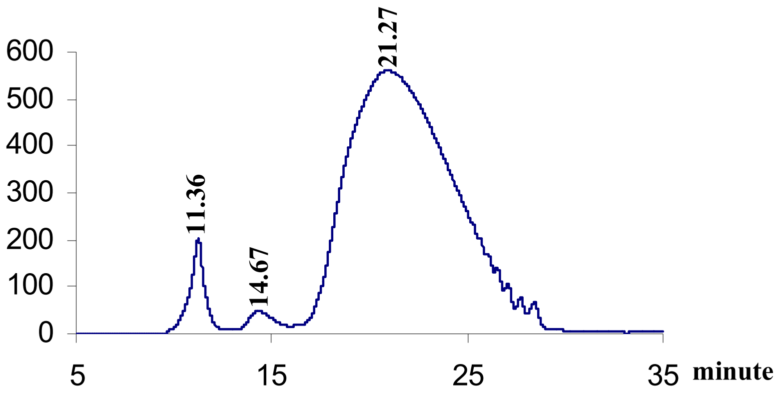

Figure 3-21. GPC of ADIMET Copolymerization by adding dipropynylbenzenes and 10% of dipropynylporphyrin in Sequence

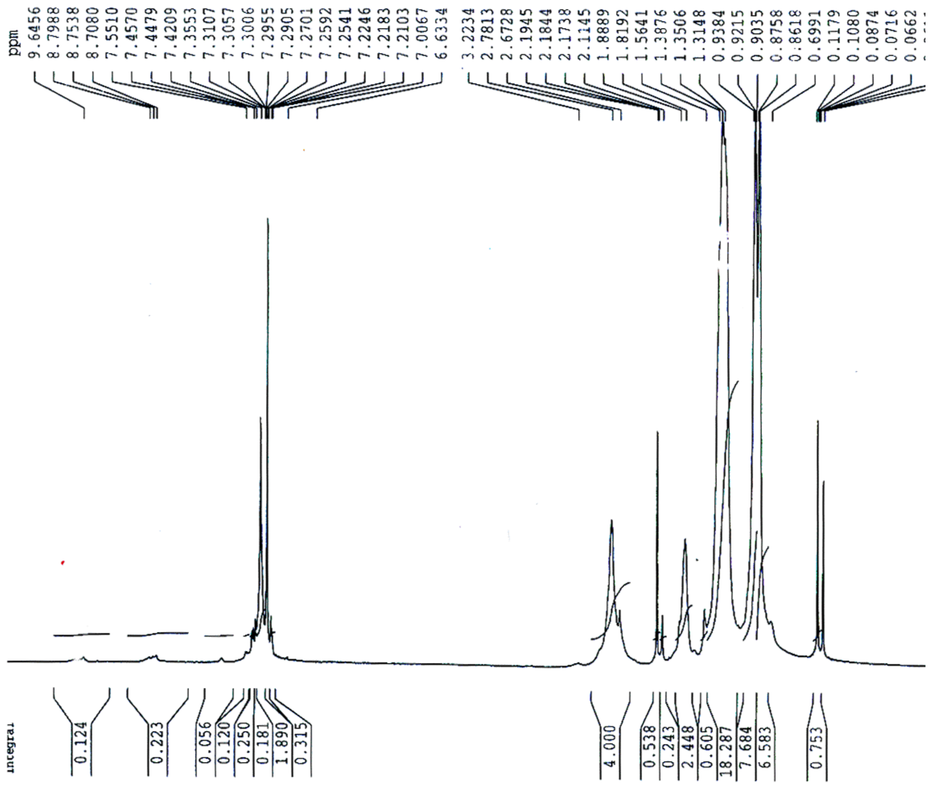

Figure 3-22. ^{1}H NMR spectrum for 10% ADIMET Copolymerization by adding dipropynylbenzenes and Dipropynylporphyrin in Sequence

chromatogram in Fig. 3-21 and NMR spectrum in Fig. 3-22 to those in Fig. 3-17 and 3-20 for 10% ADIMET porphyrin copolymerization indicates that the metal carbynes produced in dipropynylbenzene ADIMET reaction are possibly better active catalyst species than the initial catalysts (Mo(CO)$_6$ and phenol) to catalyze porphyrin metathesis reaction. After the dipropynylbenzene ADIMET reaction has fully developed, most dipropynylbenzene monomers have been involved in ADIMET reaction. When the porphyrin monomer is added at this stage, the porphyrin monomer concentration is relatively high. If there are no carbyne species produced in dipropynylbenzene ADIMET reactions but only the initial catalysts, porphyrin metathesis is slow and incomplete as we see in the ADIMET porphyrin homopolymerization. The complete involvement of porphyrin monomers in this type of copolymerization shows that the porphyrin metathesis is fast and efficient. So it indicates that the carbyne species produced in dipropynylbenzene ADIMET reactions can accelerate porphyrin metathesis reaction. This presumption and the critical controlling factors involving the concentration of "catalyst-assistant" (carbynes produced from other monomer's metathesis), the reaction time or sequences for adding porphyrin monomer need to be further investigated.

3.3 Acyclic diene metathesis (ADMET) polymerization method

Compared to alkyne metathesis, alkenes or olefin metathesis reactions have been more comprehensively studied over the last decades. Many sophisticated catalyst systems have been discovered.[7,10,18-32] Considering that the ADIMET reaction utilizes a catalyst system that performs metathesis at internal alkynes, it is possible that this catalyst continues to cleave the already formed internal alkyne-linked oligomers as well as the monomer, therefore resulting in tempered chain growth. We thus started to investigate an acyclic diene metathesis (ADMET) polymerization method with a bulky catalyst, which has been shown to perform the metathesis only at the external alkene of the monomer and oligomer chains (Scheme 3-13), thus avoiding the chain cleavage.

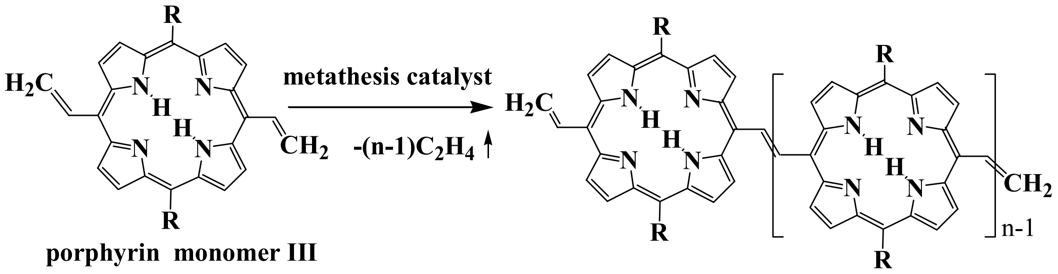

Scheme 3-13. Porphyrin Acyclic Diene Metathesis (ADMET) Polymerization

3.3.1 Experiments in the synthesis of porphyrin monomer III for ADMET

The synthesis of 5,15-divinylporphyrin (monomer **III)** is similar to the synthesis of 5,15-dipropynylporphyrin (monomer **II**). 5,15-*meso*-unsubstituted porphyrin and 5,15-dibromoporphyrin are the necessary precursors. The difference between monomer **II** and **III** is that the attachment of vinyl groups in monomer **III** can be achieved by Stille reaction, while Stille reaction did not work for the attachment of propynyl groups to the *meso*-positions of porphyrins in monomer **II**. The multi-step synthesis of porphyrin monomer **III** is shown in Scheme 3-14.

Synthesis of *tri*-n-butylvinyltin. 61 g (0.57 mol) of vinyl bromide (bp 16 ^{0}C) was added into 500 mL of freshly dried and distilled THF in a three-neck round bottom flask with dry-ice condenser. 15g (0.62mol) of magnesium turnings were added next. To accelerate the Grignard reaction, less than 1 mL of MeI was added. At this time, the reaction became very dramatic and the solution turned brown. The reaction proceeded for 6 hours to ensure that the conversion of vinyl bromide to vinylmagnesium bromide was complete. 100 g (0.31 mol) of *tri*-n-butyltin chloride in 120 mL dried THF was added into the vinylmagnesium bromide solution, which became green-brown with formation of some precipitates. The reaction was allowed to proceed for 15 hours, and then the solution was washed with 100 mL of saturated NH_4Cl. The top layer was separated, the slurry was washed with DEE. The combined organic layers were concentrated in *vacuo* to remove solvent and distilled at 110-115 ^{0}C at 5 mmHg to obtain 86 g (88% yield) of *tri*-n-butylvinyltin. ^{1}H NMR (400 MHz, $CDCl_3$, 25 ^{0}C, Fig. 3-23) $\delta = 6.47$ (dd, 1H), 6.18 (d, 1H), 5.69 (d, 1H), 1.52 (m, 6H), 1.32 (m, 6H), 0.90 (m, 15H).

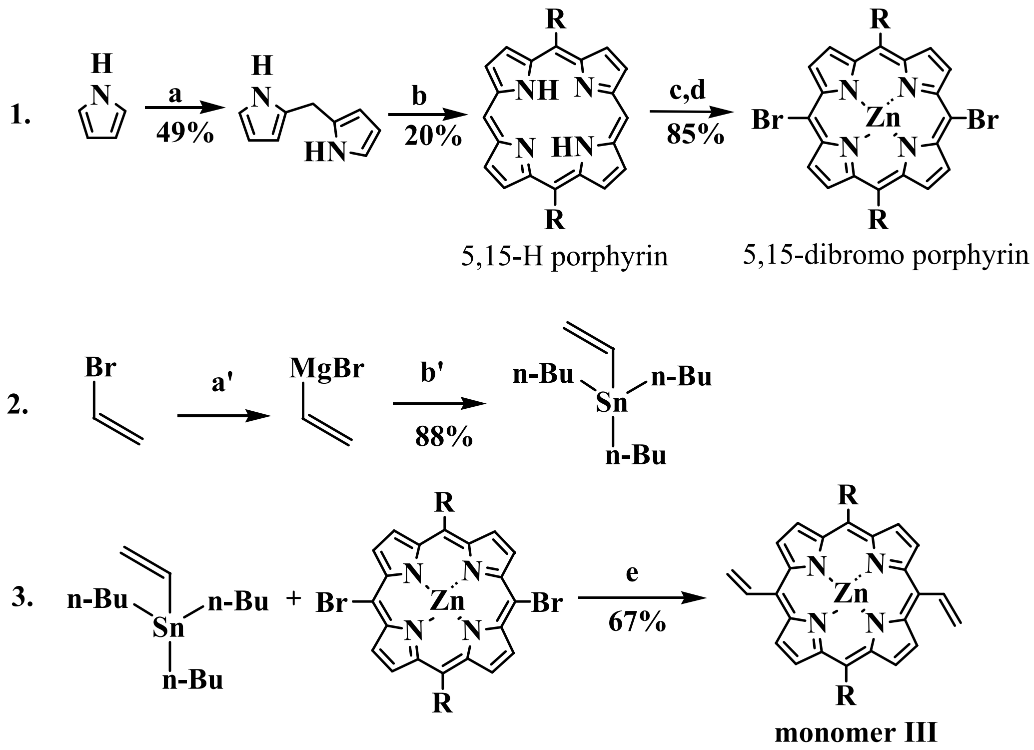

(a) $(CH_2O)_n$, TFA; (b) mesitaldehyde or 2,4,6-triisopropylbenzaldehyde, $BF_3 \bullet Et_2O$, DDQ, $CHCl_3$; (c) N-bromosuccinimide, pyridine (trace); (d) $Zn(OAc)_2$, methanol:$CHCl_3$ (5:1); (a') Mg, THF; (b') $(nBu)_3SnCl$, MeI, THF; (e) $Pd_2(dba)_3$, $As(Ph)_3$,THF

Scheme 3-14. Synthesis of Porphyrin Monomer III for ADMET Polymerization

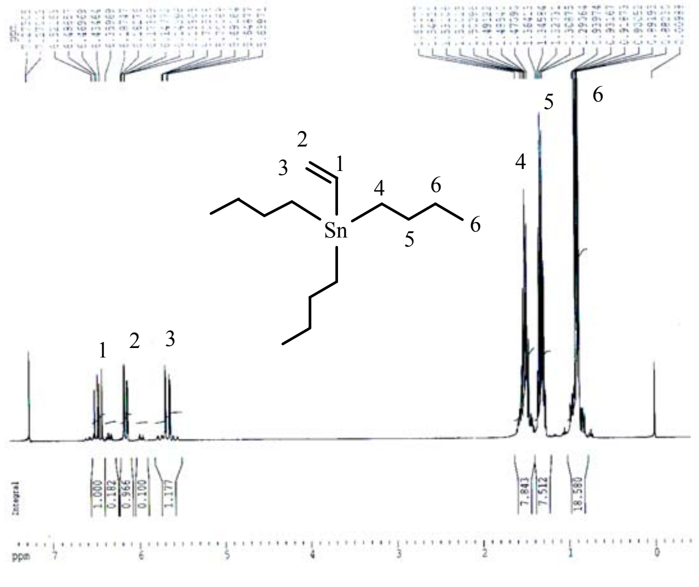

Figure 3-23. ^{1}H NMR Spectrum of *tri*-n-butylvinyltin

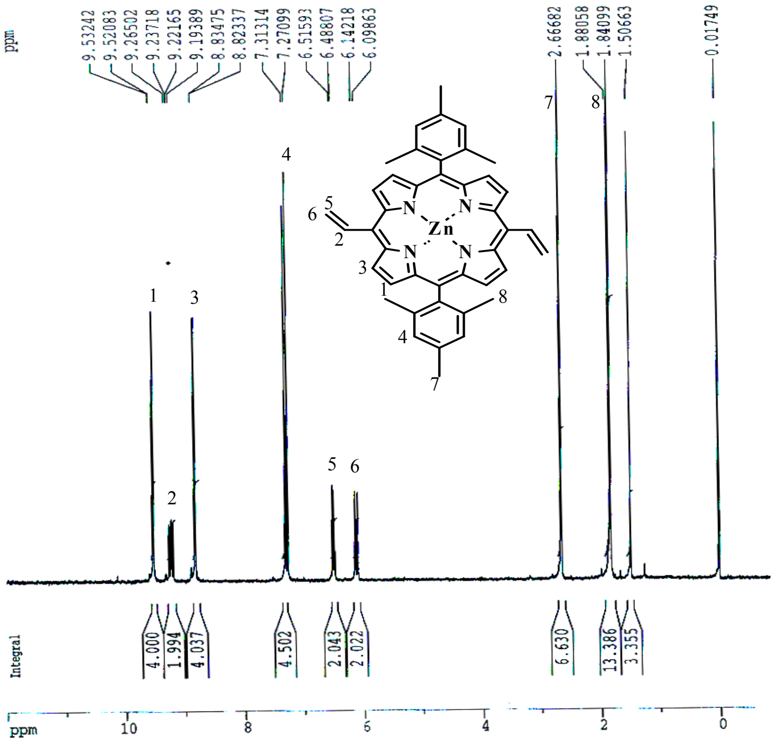

Figure 3-24. ^1H NMR Spectrum of 5, 15-divinyl-10,20-dimesitylporphyrin (monomer III)

Synthesis of porphyrin monomer III. 0.61 g (0.8 mmol) of 5,15-dibromo-Zn-dimesitylporphyrin and 2.5 equivalents of *tri*-n-butylvinyltin (2.0 mmol) were added in 200 mL of dry and deoxygenated THF. 0.05 Equivalents of $Pd_2(dba)_3$ (0.04 mmol) and 0.2 equivalents of $As(Ph)_3$ (0.16mmol) were then added. TLC analysis was used to monitor the reaction progress until the starting material and mono-bromo porphyrin spots had disappeared. Only one spot remained after 48 hours. Recrystallization from CH_2CL_2 and ethanol solution and SEC (size exclusion chromatography using 200-400 mesh S-X3 bio-beads from BioBrad®) using toluene as the eluent produced 0.36 g (0.54 mmol) of 5, 15-divinyl dimesitylporphyrin (monomer **III**) in 67% yield. ^1H NMR (400 MHz, $CDCl_3$, 25 ^0C) (Fig. 3-24) δ = 9.53 (s, 4H), 9.23 (dd, 2H), 8.83 (s, 4H), 7.29 (s, 4H), 6.49 (d, 2H), 6.12 (d, 2H), 2.67 (s, 6H), 1.86 (s, 12H). Elemental analysis: C% 75.96 (76.18), H% 5.34 (5.48), N% 8.39 (8.46).

3.3.2 ADMET reaction for porphyrin polymerization

Fig. 3-26 shows the recently used active carbene catalysts employed for intermolecular olefin metathesis polymerization. Since there have been ADMET reactions applied to porphyrin polymerizations, the selection of the catalysts and reaction conditions for this specific system follows some similar reactions. We believe that among many different types of acyclic diene metathesis for polymerizations,[33-56] ADMET for divinylbenzenes most closely models the characteristic properties of a porphyrin ADMET reaction.

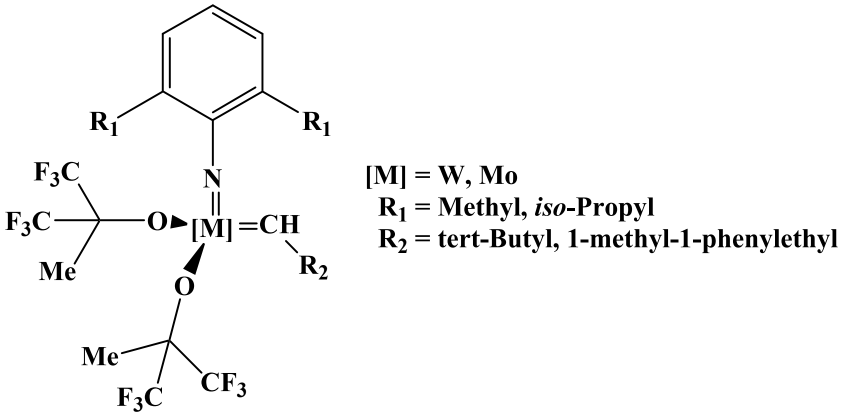

Figure 3-26. Typical Active Carbene Catalysts in Olefin Metathesis for polymerization

Two types of Schrock carbene initiator – Mo catalysts [Mo(=NAr)(=C(H)CMe$_3$)(OCMe(CF$_3$)$_2$)$_2$] (Ar = 2,6-dimethyl-phenyl, **Mo-1** or Ar = 2,6-diisopropyl-phenyl, **Mo-2**) (see structures in Fig. 3-27), are highly active and most widely used in polymerization of divinylbenzenes. **Mo-1** or **Mo-2** have been reported as one of the fastest catalysts among the series of molybdenum catalysts for ADMET polymerization of divinylbenzenes.[55,57-60] For example, in the ADMET reaction shown in Scheme 3-15, the fluorinated Schrock catalyst can be used to produce high molecular weight (DP = 20-50 by GPC) polymers or copolymers.[41,61] For the reaction shown in Scheme 3-16, the units in the polymer chain reach as high as 52 (by GPC).[55]

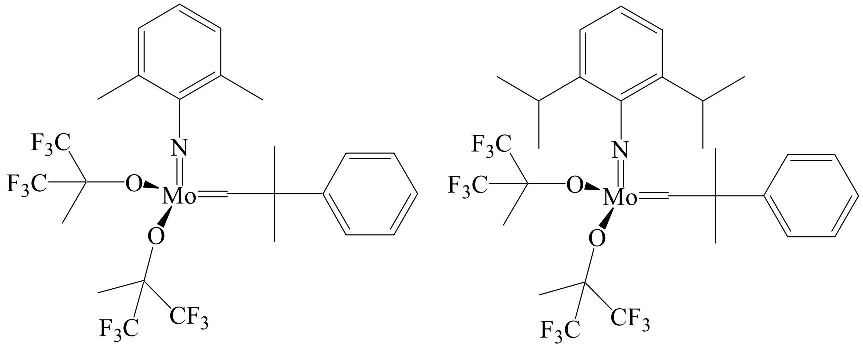

Mo-1 **Mo-2**

Figure 3-27. Schrock-type Mo-catalyst: Mo-1 and Mo-2

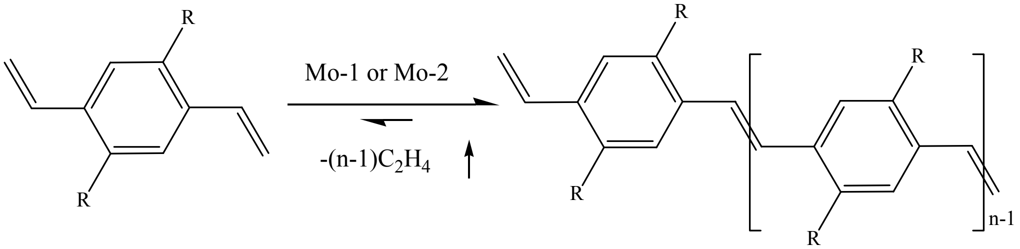

Scheme 3-15. Poly(*p*-phenylenevinylene) (PPV)s Synthesized via ADMET

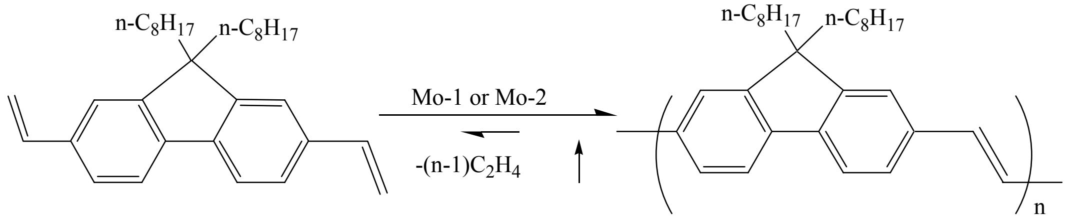

Scheme 3-16. Poly(9,9-di-*n*-octyl-fluorene-2,7-vinylene) Synthesized via ADMET

Schrock's report[62] indicates that since Mo(CHR')(NAr)(OR)$_2$ complexes are electron-deficient 14 electron species, they react bimolecularly with themselves in many ways, such as ligand redistribution reactions, therefore, bulky NAr and OR ligands are imperative to sterically protect the initiator. Consequently, we selected **Mo-2**, which is also commercially available, as the porphyrin ADMET reaction catalyst. Although some papers reported that **Mo-1** can afford higher molecule weight materials,[55] we believe the reaction activity will depend on the substrate and the higher reactivity may also cause an increase in the number of by-products.[62]

General procedure for porphyrin ADMET. Porphyrin monomer **III** was thoroughly dried for 6 days. Toluene was predried over lithium aluminum hydride, distilled over sodium and deoxygenated four times using a freeze-pump-thaw process. The reaction was performed in a glove box. When 0.119 g of porphyrin monomer **III** was dissolved in a minimal amount of toluene, the freeze-pump-thaw cycle was applied again to remove oxygen. 2.4 mg of **Mo-2** (monomer/Mo molar ratio = 20) was added, and the solution was vacuum pumped intermittently to allow the escape of ethylene. GPC analysis shows that porphyrin oligomers were produced after one week at 80 ^{0}C (Fig. 3-28).

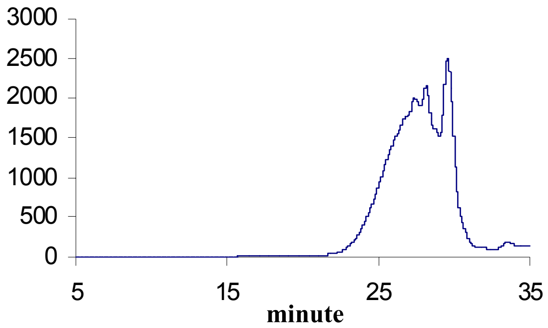

Figure 3-28. GPC of ADMET Porphyrin Polymerization of 5,15-divinyl-10,20-dimesitylporphyrin

3.3.3 Discussion

At the beginning of the ADMET reaction, we kept the reaction at room temperature for several days since some papers mentioned that catalyst would decompose when the temperature is higher than 50 ^{0}C. GPC showed us that almost no reaction occurred at room temperature (Fig. 3-29). Even when we added double, triple and four-fold of the amount of the required catalyst, the room temperature reaction still did not occur. Only when the reaction was heated to 80 ^{0}C, did the reaction finally initiate. After 7 days, GPC chromatogram showed that porphyrin dimer, trimer and other higher oligomers were produced. This result indicates that the ADMET reaction for porphyrin systems has higher activation energy requirement than divinylbenzenes or other olefin systems, which normally undergo ADMET reaction using the same catalyst at lower temperatures.

The sequence to add functional groups on porphyrin precursors during the multi-step synthesis of 5, 15-divinylporphyrin (monomer **III**) is very important for reducing purification steps probably owing to the specific chemical reactivity of dibromoporphyrin and divinylporphyrin. The brominating reaction of unsubstituted porphyrin works better when the porphyrin is in its freebase state, which gives less byproduct. But the dibromoporphyrin must be metalated prior to the Stille reaction to afford a higher yield and cleaner product. The product cannot be purified via silica gel chromatography, in which the impurities are very close to the major product band. And also the active silica gel may catalyze some side reactions between vinylporphyrins, so the major product band became broader and resulted in poor separation. Instead, we recrystallized the product from the reaction to first remove most of impurities. Then we used size exclusion chromatography (in a bio-beads column) to separate the rest of the impurities from the desired product.

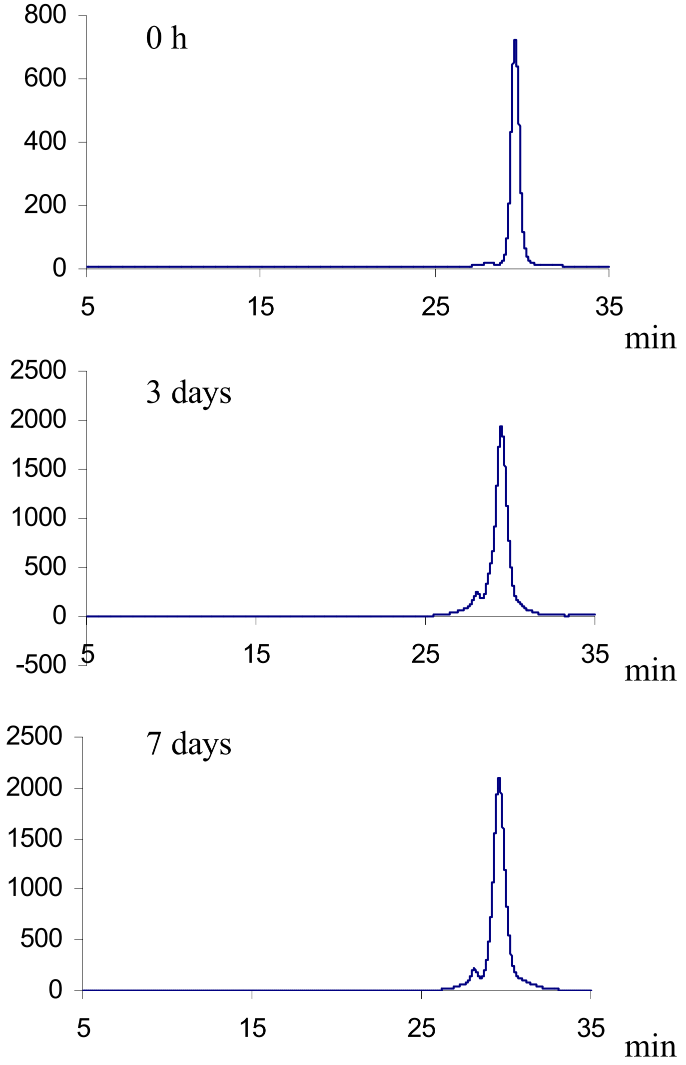

Figure 3-33. GPC of ADMET Reaction for 5,15-divinyl-10,20-dimesityl Polymerization at RT

3.4 Conclusions to the polymerization methods investigation

Three different polymerization methods have been investigated for the synthesis of conjugated porphyrin materials. From highly soluble porphyrin molecules obtained in this project, we have successfully made each monomer (porphyrin monomer **I, II** and **III**) corresponding to the Pd-mediated cross coupling reaction, acyclic diyne metathesis (ADIMET) and acyclic diene metathesis (ADMET) reactions. We are the first group that synthesized these porphyrin monomers for ADIMET and ADMET reactions, and perform these reactions to construct conjugated porphyrin materials. Based on our experimental observation, we have following conclusions for these different methodologies used for porphyrin polymerization:

1. The Pd-mediated cross coupling reaction is almost exclusively applied for porphyrin polymerizations, but the degree of polymerization is limited. The highest DP from published results is around 10-15. Since this method has been utilized by many different groups for a wide variety of porphyrin substrates, we believe that most of conditions have been possibly optimized. Therefore, there is little room for this method to be improved to achieve better results for porphyrin materials. More importantly, this method may possibly cause structure defects and ambiguous end groups according to the reaction mechanism and our experimental results. Structure defects and end group ambiguities are sometimes serious problems for certain specific applications of porphyrin materials, such as conducting materials or anti-electrostatic materials in integrated circuits or computers for precise control.
2. Acyclic diyne metathesis (ADIMET) is a recently re-discovered method used for polymerization. The most outstanding advantage of this method is that its catalyst system is very simple. The initial catalyst system - $Mo(CO)_6$ and *p*-trifloromethylphenol, are common chemicals and commercially available. They

are much less sensitive to oxygen and moisture because the active catalytic species is produced *in situ*. Therefore, this method can be scaled up easily and applied in an industrial setting. According to its mechanism verified by many experimental observations, this method avoids structure defects. It has been successfully applied in synthesis of PPEs with high molecular weight. We have also demonstrated that this method can be used for porphyrins in either homopolymerization or copolymerization reactions. Since this is a brand new method for porphyrin systems, there are many parameters in the reaction yet to be optimized, such as the choice of different catalysts to verify if the internal alkyne is cleaved again after it is formed from monomers' metathesis reaction.

3. Acyclic diene metathesis (ADMET) is a relatively old method in the production of materials, but it has only recently been applied to porphyrin systems. We have demonstrated that this method can be used to produce porphyrin oligomers, the units in porphyrin oligomers (4 to 5, estimated by GPC) have almost reached the same level for other polymer systems, such as poly(dialkoxy-divinylbenzene) with 5 units in the polymer chain.[18] The conditions for the application of this reaction to porphyrin polymerizations must be further optimized. Shrock's catalyst **Mo-2** works for porphyrin ADMET reaction but the initial monomer concentration, catalyst types, temperatures, and reaction times are all variables that can be further investigated and optimized. The problem of the Schrock-type catalyst for ADMET is the availability (special order) and its high sensitivity to air, moisture and impurities.

References:

1. Diederich, F.; Stang, P. J.; Ed.; *Metal-Catalyzed Cross-Coupling Reaction*; Wiley-VCH: Weinheim, 1998.
2. Cassar, L., "Synthesis of Aryl-Substituted and Vinyl-Substituted Acetylene Derivatives by Use of Nickel and Palladium Complexes", *J. Organomet. Chem.* **1975**, *93*, 253-257.
3. Cassar, L.; Foa, M.; Gardano, A., "Use of Phase-Transfer Catalysis in Palladium-Catalyzed Carbonylation of Organic Halides", *J. Organomet. Chem.* **1976**, *121*, C55-C56.
4. Dieck, H. A.; Heck, F. R., "Palladium Catalyzed Synthesis of Aryl, Heterocyclic and Vinylic Acetylene Derivatives", *J. Organomet. Chem.* **1975**, *93*, 259-263.
5. Kruithof, K. J. H.; Schmitz, R. F.; Klumpp, G. W., "Lithiated 2-alkynyl-1,3-dioxanes as Fully Oxygenated acyl anion Equivalents - Synthesis of 1-alkynyl Ketones", *Tetrahedron* **1983**, *39*, 3073-3081.
6. Schumm, J. S.; Pearson, D. L.; Tour, J. M., "Iterative Divergent/Convergent Approach to Linear Conjugated Oligomers by Successive Doubling of the Molecular Length - a Rapid Route to a 128-Angstrom-Long Potential Molecular Wire", *Angew. Chem. Int. Ed. Eng.* **1994**, *33*, 1360-1363.
7. Kloppenburg, L.; Jones, D.; Bunz, U. H. F., "High Molecular Weight Poly(*p*-phenyleneethynylene)s by Alkyne Metathesis Utilizing "Instant" Catalysts: A Synthetic Study", *Macromolecules* **1999**, *32*, 4194-4203.
8. Kloppenburg, L.; Jones, D.; Claridge, J. B.; zur Loye, H. C.; Bunz, U. H. F., "Poly(*p*-phenyleneethynylene)s are Thermotropic Liquid Crystalline", *Macromolecules* **1999**, *32*, 4460-4463.
9. Steffen, W.; Bunz, U. H. F., "Synthesis and Characterization of Nonfluorescent Poly(*p*-aryleneethynylene)s by Alkyne Metathesis", *Macromolecules* **2000**, *33*, 9518-9521.
10. Pschirer, N. G.; Bunz, U. H. F., "Poly(fluorenyleneethynylene)s by Alkyne Metathesis: Optical Properties and Aggregation Behavior", *Macromolecules* **2000**, *33*, 3961-3963.

11. Miteva, T.; Palmer, L.; Kloppenburg, L.; Neher, D.; Bunz, U. H. F., “Interplay of Thermochromicity and Liquid Crystalline Behavior in Poly(*p*-phenyleneethynylene)s: π−π Interactions or Planarization of the Conjugated Backbone?" *Macromolecules* **2000**, *33*, 652-654.
12. Pschirer, N. G.; Byrd, K.; Bunz, U. H. F., “Fluorenone-Containing Poly(*p*-phenyleneethynylene)s (PPE) and Poly(Fluorenyleneethynylene)s (PFE): Tuning the Solid-State Emission of Alkyne-Bridged Polymers by Interchain Energy Transfer", *Macromolecules* **2001**, *34*, 8590-8592.
13. Bangcuyo, C. G.; Evans, U.; Myrick, M. L.; Bunz, U. H. F., “Synthesis and Characterization of a 2,1,3-benzothiadiazole-B- alkyne-B-1,4 bis(2-ethylhexyloxy)benzene Terpolymer, a Stable Low-Band-Gap Poly(Heteroaryleneethynylene)", *Macromolecules* **2001**, *34*, 7592-7594.
14. Marshall, A. R.; Bunz, U. H. F., “Alkyne-Bridged Polymers as Platform for Novel Macromolecular Materials: Catalytic Hydrogenation of Poly[(*p*-dialkylphenylene)ethynylene]s", *Macromolecules* **2001**, *34*, 4688-4690.
15. Perahia, D.; Traiphol, R.; Bunz, U. H. F., “From Molecules to Supramolecular Structure: Self Assembling of Wirelike Poly(*p*-phenyleneethynylene)s", *Macromolecules* **2001**, *34*, 151-155.
16. Bangcuyo, C. G.; Rampey-Vaughn, M. E.; Quan, L. T.; Angel, S. M.; Smith, M. D.; Bunz, U. H. F., “Quinoline-Containing, Conjugated Poly(aryleneethynylene)s: Novel Metal and H^+-Responsive Materials", *Macromolecules* **2002**, *35*, 1563-1568.
17. Lin, V. S. Y.; Dimagno, S. G.; Therien, M. J., “Highly Conjugated, Acetylenyl Bridged Porphyrins - New Models for Light-Harvesting Antenna Systems", *Science* **1994**, *264*, 1105-1111.
18. Thorn-Csanyi, E.; Kraxner, P.; Strachota, A., “Synthesis of Soluble All-Trans Oligomers of 2,5-diheptyloxy-*p*-phenylenevinylene via Olefin Metathesis", *Macromol. Rap. Commun.* **1998**, *19*, 223-228.
19. Shirakawa, E.; Hiyama, T., “The Palladium-Iminophosphine Catalyst for the Reactions of Organostannanes", *J. Organomet. Chem.* **1999**, *576*, 169-178.

20. Thorn-Csanyi, E.; Kraxner, P.;. "All-Trans Oligomers of 2,5-dialkyl-1,4-phenylenevinylenes. Metathesis Preparation and Characterization", *Macromol. Chem. Phys.* **1997**, *198*, 3827-3843.

21. Thorn-Csanyi, E.; Dehmel, J.; Luginsland, H.-D.; Zilles, J. U., “Kinetic Investigations Concerning Selectivity of Different Schrock-Type Carbene Complexes", *J. Mol. Catal. A: Chem.* **1997**, *115*, 29-35.

22. Thorn-Csanyi, E., “Quantitative Metathetic Degradation of Rubbers and Sulfur Crosslinked Rubbers-Including Tires", *Rubber Chem. Technol.* **1994**, *67*, 786-796.

23. Thorn-Csanyi, E.; Dehmel, Joerg, Halle, Olaf, Sciborski, Winfried. "UV/Vis Spectroscopic Proof of Selective Complex Formation between $WOCl_4$ and trimethylaluminum. A Way to Characterize Methylaluminoxanes", *Macromol. Chem. Phys.* **1994**, *195*, 3017-3024.

24. Thorn-Csanyi, E.; Pflug, K. P., “Metathetic Incorporation of Preformed Defined *p*-Phenylenevinylene Sequences into Commercially Available Neodymium Butadiene Rubber", *J. Mol. Catal.* **1994**, *90*, 29-38.

25. Thorn-Csanyi, E.; Pflug, K. P., “Copolymers of 1,5-cyclooctadiene and [2.2]paracyclophane-1,9-diene: Metathetic Preparation and Structure Analysis", *Makromol. Chem.* **1993**, *194*, 2287-2294.

26. Thorn-Csanyi, E., “Mechanism of Olefin Metathesis", *Nachr. Chem. Tech. Lab.* **1981**, *29*, 700-701, 704-705.

27. Thorn-Csanyi, E., “Studies of Reactions in the Metathetic-Catalyst-System of Tungsten(VI)Chloride/tetramethyl(or tetraethyl)-Tin", *Angew. Makromol. Chem.* **1981**, *94*, 181-188.

28. Thorn-Csanyi, E.; Abendroth, H.; Perner, H., “Metathetic Cleavage of Butadiene-Styrene Copolymers; Degradation Products", *Makromol. Chem.* **1980**, *181*, 2081-2089.

29. Thorn-Csanyi, E.; Perner, H., “Sequence Length Distribution of 1,2-Units in Polybutadienes by Means of the Olefin-Polymer/Metathesis Reaction; a Route for Synthesis of mono- and disubstituted cyclopentene- and cyclohexene Compounds", *Makromol. Chem.* **1979**, *180*, 919-928.

30. Ivin, K. J. *Olefin Metathesis*; Academic Press Inc. (London) Ltd.: London, 1983.

31. Kawai, T.; Shiga, K.; Iyoda, T., “Synthesis of [Sigma]-[Pi] Conjugated Oligo(silylene-vinylene)s by Metathesis of divinylsilanes over Re_2O_7-Al_2O_3 Catalyst", *J. Mol. Catal. A: Chem.* **2000**, *160*, 173-179.

32. Kawai, T.; Shiga, K.; Suzuki, T.; Iyoda, T.; . "Acyclic Diene Metathesis (ADMET) of vinylsilanes over Re_2O_7-Al_2O_3 Catalyst", *J. Mol. Catal. A: Chem.* **1999**, *140*, 287-292.

33. Ogara, J. E.; Wagener, K. B., “Acyclic Diene Metathesis (ADMET) Polymerization - Synthesis of Perfectly Linear Polyethylene", *Makromol. Chem.-Rap. Commun.* **1993**, *14*, 657-662.

34. Gomez, F. J.; Wagener, K. B., “Acyclic Diene Metathesis (ADMET) Polymerization Using Aryloxy Tungsten-Based Classical Catalytic Systems", *Macromol. Chem. Phys.* **1998**, *199*, 1581-1587.

35. Konzelman, J.; Wagener, K. B., “Acyclic Diene Metathesis (ADMET) Polymerization. Synthesis of Perfectly Alternating Copolymers from a Single Monomer", *Macromolecules* **1996**, *29*, 7657-7660.

36. Wolfe, P. S.; Wagener, K. B., “Acyclic Diene Metathesis (ADMET) Polymerization: The Investigation of dienes Containing the Boronate Functionality", *Abstr. Paper. Am. Chem. Soc.* **1996**, *211*, 43-POLY.

37. Portmess, J. D.; Wagener, K. B., “Acyclic Diene Metathesis (ADMET) Polymerization: The Synthesis of Unsaturated Polyamines", *J. Polym. Sci. A* **1996**, *34*, 1353-1357.

38. Tsuie, B.; Wagener, K. B.; Reynolds, J. R., “Alkyl-Substituted Poly(thienylene vinylene) by Acyclic Diene Metathesis Polymerization Chemistry", *Abstr. Paper. Am. Chem. Soc.* **1999**, *218*, 182-POLY.

39. Tao, D.; Wagener, K. B., “Conjugated Monomers in Acyclic Diene Metathesis (ADMET) Polymerization", *Macromolecules* **1994**, *27*, 1281-1283.

40. Valenti, D. J.; Wagener, K. B., “Direct Synthesis of Well-Defined Alcohol-Functionalized Polymers Via Acyclic Diene Metathesis (ADMET) Polymerization", *Macromolecules* **1998**, *31*, 2764-2773.

41. Schlick, H.; Stelzer, F.; Tasch, S.; Leising, G., “Highly Luminescent Poly (*m*-phenylenevinylene)-Co-(*p*-phenylenevinylene) Derivatives Synthesized Via Metathesis Condensation (ADMET)", *J. Mol. Catal. A: Chem.* **2000**, *160*, 71-84.
42. Buchmeiser, M. R., “Homogeneous Metathesis Polymerization by Well-Defined Group VI and Group VIII Transition-Metal Alkylidenes: Fundamentals and Applications in the Preparation of Advanced Materials", *Chem. Rev.* **2000**, *100*, 1565-1604.
43. Gomez, F. J.; Abboud, K. A.; Wagener, K. B., “Investigations on Fluorinated Aryloxy Tungsten-Based Catalytic Systems for Acyclic Diene Metathesis Polymerization", *J. Mol. Catal. A: Chem.* **1998**, *133*, 159-166.
44. Walba, D. M.; Keller, P.; Shao, R. F.; Clark, N. A.; Hillmyer, M.; Grubbs, R. H., “Main-Chain Ferroelectric Liquid Crystal Oligomers by Acyclic Diene Metathesis Polymerization", *J. Am. Chem. Soc.* **1996**, *118*, 2740-2741.
45. Miao, Y. J.; Bazan, G. C., “Photophysics of Main-Chain Polychromophores Prepared by Acyclic Diene Metathesis Polymerization", *Macromolecules* **1997**, *30*, 7414-7418.
46. Steiger, D.; Tervoort, T.; Weder, C.; Smith, P., “Poly(*p*-phenylene alkylene)s - a Forgotten Class of Polymers", *Macromol. Rap. Commun.* **2000**, *21*, 405-422.
47. Steiger, D.; Weder, C.; Smith, P., “Poly(*p*-phenylene butylene): A New, Processable, High-Melting Hydrophobic Polymer", *Macromolecules* **1999**, *32*, 5391-5398.
48. Blosch, L. L.; Gamble, A. S.; Boncella, J. M., “Progress toward New Catalysts for Acyclic Diene Metathesis (ADMET) Polymerization Reactions", *J. Mol. Catal.* **1992**, *76*, 229-237.
49. van Aert, H. A. M.; Sijbesma, R. P.; Fischer, H.; de Waal, B. F. M.; Gilberts, J.; Maas, J. H.; Broer, D.; Meijer, E. W., “Selective Photo-Crosslinking of Microphase-Separated Multiblock Copolymers of Poly(dimethylsiloxane) and phenylene diacrylate Polyesters", *Acta Polym.* **1998**, *49*, 18-26.
50. Mullner, R.; inkler, B.; Stelzer, F.; Tasch, S.; Hochfilzer, C.; Leising, G., “Synthesis and Optical Properties of Highly Fluorescent meta- para Oligo-phenylenevinylenes", *Synthetic Met.* **1999**, *105*, 129-133.

51. Chauvin, Y.; Saussine, L., “Synthesis and Properties of a New Polymer with a Cubane- Containing Backbone. Synthesis and Metathesis Polymerization and Copolymerization of 1,4-bis(homoallyl)cubane", *Macromolecules* **1996**, *29*, 1163-1166.

52. Steiger, D.; Ehrenstein, M.; Weder, C.; Smith, P., “Synthesis and Properties of Poly(*p*-phenylene octylene)", *Macromolecules* **1998**, *31*, 1254-1260.

53. Brzezinska, K. R.; Deming, T. J., “Synthesis of ABA triblock Copolymers Via Acyclic Diene Metathesis Polymerization and Living Polymerization of Alpha-Amino Acid-N-Carboxyanhydrides", *Macromolecules* **2001**, *34*, 4348-4354.

54. Tamura, H.; Maeda, N.; Matsumoto, R.; Nakayama, A.; Hayashi, H.; Ikushima, K.; Kuraya, M., “Synthesis of Ester Terminated Telechelic Polymer Via Admet Polymerization", *J. Macromol. Sci. Pure* **1999**, *36*, 1153-1170.

55. Nomura, K.; Morimoto, H.; Imanishi, Y.; Ramhani, Z.; Geerts, Y., “Synthesis of High Molecular Weight trans-Poly(9,9-di-n-octylfluorene-2,7-vinylene) by the Acyclic Diene Metathesis Polymerization Using Molybdenum Catalysts", *J. Polym. Sci. A* **2001**, *39*, 2463-2470.

56. Joo, S. H.; Yun, Y. K.; Jin, J. I.; Kim, D. C.; Zin, W. C., “Synthesis of Liquid Crystalline Polyesters of Various Types by Acyclic Diene Metathesis Polymerization", *Macromolecules* **2000**, *33*, 6704-6712.

57. Thorn-Csanyi, E.; Kraxner, P.; Strachota, A., *Macromol. Rap. Commun.* **1995**, *16*, 147-153.

58. Thorn-Csanyi, E; Kraxner, P., “Investigations of stable molybdenum carbene complexes for the metathesis synthesis of dialkylsubstituted poly(*p*-phenylenevinylene)s (PPVs)”, *J. Mol. Catal.* **1997**, *115*, 21-28.

59. Thorn-Csanyi, E; Kraxner, P., “Synthesis of Soluble *all-trans* oligomers of 2,5-diheptyloxy-*p*-phenylenevinylene via Olefin Metathesis**”** *Macromol. Rap. Commun.* **1998**, *19*, 223-232.

60. Schlick, H. S.; F.; Tasch, S.; Leising, G., “Highly Luminescent poly[(*m*-phenylenevinylene)-*co*-(*p*-phenylenevinylene)] derivatives Synthesized via Metathesis condensation (ADMET)**”**, *J. Mol. Catal.* **2000**, *160*, 71-84.

61. Thorn-Csanyi, E.; Kraxner, P., “Synthesis of Copolymers with a Controllable Sequence Length of *p*-phenylenevinylene Units", *Macromol. Rap. Commun.* **1993**, *14*, 619-624.

62. Schrock, R. R., “Olefin Metathesis by Molybdenum Imido Alkylidene Catalysts", *Tetrahedron* **1999**, *55*, 8141-8153.

CHAPTER IV

CONCLUSIONS

4.1 Achievements in this project

The objectives in this project as mentioned in Chapter I include

Short-term goals:

(1) Design and synthesis of novel porphyrin molecules to achieve high solubility
(2) Study of solubility-structure relationships in porphyrin molecules
(3) Investigation for suitable and efficient polymerization methods for the construction of conjugated porphyrin materials.

Long-term goals:

(1) Design and synthesis of new porphyrin molecules
(2) Study of the relations of solubility-structure in porphyrin
(3) Exploration of new polymerization methodology to obtain high molecular weight porphyrin polymers
(4) Physical characterization of porphyrin materials including measurements of conductivity and magnetism.

This dissertation presents the experimental data and study results to indicate that the short-term objectives for this project have been completed. The goals to obtain highly soluble porphyrin monomers and explore better polymerization methods, then to construct a solid foundation for the development of advanced porphyrin materials are fulfilled.

Through structure-property studies, we have acquired a deeper insight into porphyrin intermolecular interactions, and employed an efficient strategy to increase porphyrin solubility – by adding facial and edge encumbrance to interrupt the strong $\pi-\pi$ interaction between porphyrins. Facial and edge-encumbrance can effectively increase porphyrin solubility in organic solvents by tens, hundreds and even thousands of times compared to peripherally substituted porphyrins. The highest solubility achieved in this research is 294 mmol/L or 229 g/L, while the solubility for other porphyrins range from 0.02 –18.4 mmol/L or 0.01 – 9.2 g/L.

We have also investigated Pd-mediated coupling reactions for porphyrin polymerizations, which are the most popular methods used in this field. Its limitations include structure defects, end group ambiguities and monomer inactivation due to the end capping. We have also pioneered two novel polymerization methods – alkene metathesis (ADMET) and alkyne metathesis (ADIMET) to synthesize porphyrins materials. We are the first group to apply ADMET and ADIMET polymerization methods to porphyrin systems. These methods show us very promising results for the construction of conjugated porphyrin polymers with higher quality and higher molecular weights than porphyrin materials obtained in Pd-mediated coupling reactions.

4.2 Directions of this project in the future

It has been demonstrated that ADMET and ADIMET can be viable alternatives of polymerization methods in porphyrin materials field. However, these metathesis reactions must be thoroughly investigated and further optimized. The behaviors of the porphyrin under these metathesis conditions need to be studied and understood. The results from these studies can be used to direct the selection of reaction conditions and catalyst systems. The analysis of porphyrin materials such as the molecular weight estimation needs to be further improved. Other physical characterization of new porphyrin materials including measurements of conductivity and magnetism also need to be performed in collaboration with other research groups.

APPENDICES FOR CHAPTER II

Appendix 2-1. Crystal Structure Analysis

A suitable crystal of **porphyrin 3** was coated with Paratone N oil, suspended in a small fiber loop and placed in a cooled nitrogen gas stream at 100 K on a Bruker D8 SMART 1000 CCD sealed tube diffractometer with graphite monochromated CuK_{α} (1.54178 Å) radiation. Data were measured using a series of combinations of phi and omega scans with 10 second frame exposures and 0.3° frame widths. Data collection, indexing and initial cell refinements were all carried out using SMART[1] software. Frame integration and final cell refinements were done using SAINT[2] software. The final cell parameters were determined from least-squares refinement on 5577 reflections. The SADABS[3] program was used to carry out absorption corrections.

The structure was solved using Direct methods and difference Fourier techniques (SHELXTL, V5.10).[4] Hydrogen atoms were placed their expected chemical positions using the HFIX command and were included in the final cycles of least squares with isotropic U_{ij} 's related to the atom's ridden upon. The C-H distances were fixed at 0.93 Å(aromatic and amide), 0.98 Å (methine), 0.97 Å (methylene), or 0.96 Å (methyl). All non-hydrogen atoms were refined anisotropically. Scattering factors and anomalous dispersion corrections are taken from the *International Tables for X-ray Crystallography*[5]. Structure solution, refinement, graphics and generation of publication materials were performed by using SHELXTL, V5.10 software. Additional details of data collection and structure refinement are given in Table 2.

Details: The lattice contained two molecules of dichloromethane per molecule of porphyrin.

Reference:

1. SMART Version 5.55, **2000**, Bruker AXS, Inc., Analytical X-ray Systems, 5465 East Cheryl Parkway, Madison WI 53711-5373.
2. SAINT Version 6.02, **1999**, Bruker AXS, Inc., Analytical X-ray Systems, 5465 East Cheryl Parkway, Madison WI 53711-5373.
3. SADABS, **1996**, George Sheldrick, University of Göttingen,
4. SHELXTL V5.10, **1997**, Bruker AXS, Inc., Analytical X-ray Systems, 5465 East Cheryl Parkway, Madison WI 53711-5373.
5. A. J. C. Wilson (ed), *International Tables for X-ray Crystallography, Volume C.* Kynoch, Academic Publishers, Dordrecht, **1992**, Tables 6.1.1.4 (pp. 500-502) and 4.2.6.8 (pp. 219-222).

Appendix 2-2 Atomic coordinates (x 10^4) and equivalent isotropic displacement parameters (Å^{2}x 10^3) for Porphyrin (3).

U(eq) is defined as one third of the trace of the orthogonalized U^{ij} tensor.

	x	y	z	U(eq)
Cl(1S)	480(2)	1374(2)	1829(3)	89(1)
Cl(2S)	1789(2)	2130(2)	3691(3)	117(2)
C(1S)	1514(6)	1649(6)	2612(8)	47(4)
N(1)	1909(4)	1523(4)	9371(5)	7(2)
N(2)	3304(4)	2146(4)	9754(5)	6(2)
C(4)	3255(5)	1496(5)	9268(6)	2(3)
C(8)	974(5)	587(5)	8783(6)	13(3)
C(21)	3376(5)	-2311(5)	7724(7)	22(3)
C(2)	4292(5)	2183(5)	9599(6)	15(3)
C(3)	3888(5)	1542(5)	9191(6)	12(3)
C(7)	1492(5)	363(5)	8640(6)	12(3)
C(24)	938(5)	406(5)	5916(7)	29(3)

C(9)	1240(5)	1314(5)	9256(6)	4(3)
C(22)	4089(5)	-1418(5)	7384(7)	27(3)
C(20)	3325(5)	-1567(5)	7248(7)	14(3)
C(6)	2079(5)	943(5)	8989(6)	6(3)
C(12)	2406(5)	197(5)	7415(7)	15(3)
C(15)	3550(5)	-868(5)	8768(7)	16(3)
C(23)	1766(5)	759(5)	6628(6)	16(3)
C(11)	2836(5)	258(5)	8497(6)	4(3)
C(17)	3864(5)	-216(6)	10360(7)	22(3)
C(5)	2709(5)	928(5)	8932(6)	4(3)
C(13)	2574(4)	-405(5)	7037(7)	5(3)
C(16)	3416(5)	-288(5)	9200(7)	15(3)
C(14)	3143(5)	-937(5)	7693(7)	11(3)
C(19)	4745(5)	-321(6)	10999(7)	47(4)
C(25)	1984(5)	1124(5)	6000(7)	32(3)
C(1)	3928(5)	2583(5)	9970(6)	9(3)
C(18)	3534(7)	-741(7)	10700(10)	96(5)
C(10)	872(5)	1729(5)	9554(6)	7(3)

Appendix 2-3. **Bond lengths [Å] and angles [°] for porphyrin (3).**

l(1S)-C(1S)	1.781(10)
Cl(2S)-C(1S)	1.705(11)
C(1S)-H(1S1)	0.9900
C(1S)-H(1S2)	0.9900
N(1)-C(9)	1.363(10)
N(1)-C(6)	1.380(10)
N(2)-C(1)	1.383(10)
N(2)-C(4)	1.387(10)
N(2)-H(1)	1.0292
C(4)-C(5)	1.381(11)
C(4)-C(3)	1.426(12)
C(8)-C(7)	1.321(11)

C(8)-C(9)	1.453(11)
C(8)-H(8)	0.9500
C(21)-C(20)	1.527(11)
C(21)-H(21A)	0.9800
C(21)-H(21B)	0.9800
C(21)-H(21C)	0.9800
C(2)-C(3)	1.348(11)
C(2)-C(1)	1.438(12)
C(2)-H(2)	0.9500
C(3)-H(3)	0.9500
C(7)-C(6)	1.446(11)
C(7)-H(7)	0.9500
C(24)-C(23)	1.511(11)
C(24)-H(24A)	0.9800
C(24)-H(24B)	0.9800
C(24)-H(24C)	0.9800
C(9)-C(10)	1.371(11)
C(22)-C(20)	1.514(12)
C(22)-H(22A)	0.9800
C(22)-H(22B)	0.9800
C(22)-H(22C)	0.9800
C(20)-C(14)	1.525(12)
C(20)-H(20)	1.0000
C(6)-C(5)	1.395(11)
C(12)-C(11)	1.393(11)
C(12)-C(13)	1.405(11)
C(12)-C(23)	1.531(11)
C(15)-C(16)	1.390(12)
C(15)-C(14)	1.392(11)
C(15)-H(15)	0.9500
C(23)-C(25)	1.514(12)
C(23)-H(23)	1.0000
C(11)-C(16)	1.429(11)
C(11)-C(5)	1.514(12)
C(17)-C(19)	1.474(11)
C(17)-C(18)	1.479(15)

C(17)-C(16)	1.499(12)
C(17)-H(17)	1.0000
C(13)-C(14)	1.384(10)
C(13)-H(13)	0.9500
C(19)-H(19A)	0.9800
C(19)-H(19B)	0.9800
C(19)-H(19C)	0.9800
C(25)-H(25A)	0.9800
C(25)-H(25B)	0.9800
C(25)-H(25C)	0.9800
C(1)-C(10)#1	1.389(11)
C(18)-H(18A)	0.9800
C(18)-H(18B)	0.9800
C(18)-H(18C)	0.9800
C(10)-C(1)#1	1.389(11)
C(10)-H(10)	0.9500

Cl(2S)-C(1S)-Cl(1S)	110.9(6)
Cl(2S)-C(1S)-H(1S1)	109.5
Cl(1S)-C(1S)-H(1S1)	109.5
Cl(2S)-C(1S)-H(1S2)	109.5
Cl(1S)-C(1S)-H(1S2)	109.5
H(1S1)-C(1S)-H(1S2)	108.1
C(9)-N(1)-C(6)	105.5(8)
C(1)-N(2)-C(4)	110.6(8)
C(1)-N(2)-H(1)	126.0
C(4)-N(2)-H(1)	122.4
C(5)-C(4)-N(2)	127.3(9)
C(5)-C(4)-C(3)	127.5(9)
N(2)-C(4)-C(3)	105.2(8)
C(7)-C(8)-C(9)	106.5(9)
C(7)-C(8)-H(8)	126.8
C(9)-C(8)-H(8)	126.8
C(20)-C(21)-H(21A)	109.5
C(20)-C(21)-H(21B)	109.5
H(21A)-C(21)-H(21B)	109.5

C(20)-C(21)-H(21C)	109.5
H(21A)-C(21)-H(21C)	109.5
H(21B)-C(21)-H(21C)	109.5
C(3)-C(2)-C(1)	107.5(9)
C(3)-C(2)-H(2)	126.2
C(1)-C(2)-H(2)	126.2
C(2)-C(3)-C(4)	110.3(9)
C(2)-C(3)-H(3)	124.8
C(4)-C(3)-H(3)	124.8
C(8)-C(7)-C(6)	108.2(9)
C(8)-C(7)-H(7)	125.9
C(6)-C(7)-H(7)	125.9
C(23)-C(24)-H(24A)	109.5
C(23)-C(24)-H(24B)	109.5
H(24A)-C(24)-H(24B)	109.5
C(23)-C(24)-H(24C)	109.5
H(24A)-C(24)-H(24C)	109.5
H(24B)-C(24)-H(24C)	109.5
N(1)-C(9)-C(10)	124.9(9)
N(1)-C(9)-C(8)	110.5(9)
C(10)-C(9)-C(8)	124.6(9)
C(20)-C(22)-H(22A)	109.5
C(20)-C(22)-H(22B)	109.5
H(22A)-C(22)-H(22B)	109.5
C(20)-C(22)-H(22C)	109.5
H(22A)-C(22)-H(22C)	109.5
H(22B)-C(22)-H(22C)	109.5
C(22)-C(20)-C(14)	111.2(7)
C(22)-C(20)-C(21)	110.8(7)
C(14)-C(20)-C(21)	112.3(8)
C(22)-C(20)-H(20)	107.4
C(14)-C(20)-H(20)	107.4
C(21)-C(20)-H(20)	107.4
N(1)-C(6)-C(5)	125.1(8)
N(1)-C(6)-C(7)	109.3(9)
C(5)-C(6)-C(7)	125.6(9)

C(11)-C(12)-C(13)	118.2(8)
C(11)-C(12)-C(23)	122.8(9)
C(13)-C(12)-C(23)	119.0(8)
C(16)-C(15)-C(14)	122.9(9)
C(16)-C(15)-H(15)	118.5
C(14)-C(15)-H(15)	118.5
C(24)-C(23)-C(25)	111.4(7)
C(24)-C(23)-C(12)	110.7(7)
C(25)-C(23)-C(12)	111.9(8)
C(24)-C(23)-H(23)	107.5
C(25)-C(23)-H(23)	107.5
C(12)-C(23)-H(23)	107.5
C(12)-C(11)-C(16)	120.8(9)
C(12)-C(11)-C(5)	119.3(8)
C(16)-C(11)-C(5)	119.8(8)
C(19)-C(17)-C(18)	109.9(9)
C(19)-C(17)-C(16)	113.6(9)
C(18)-C(17)-C(16)	110.0(8)
C(19)-C(17)-H(17)	107.7
C(18)-C(17)-H(17)	107.7
C(16)-C(17)-H(17)	107.7
C(4)-C(5)-C(6)	123.9(9)
C(4)-C(5)-C(11)	115.8(9)
C(6)-C(5)-C(11)	120.3(8)
C(14)-C(13)-C(12)	122.8(9)
C(14)-C(13)-H(13)	118.6
C(12)-C(13)-H(13)	118.6
C(15)-C(16)-C(11)	117.7(8)
C(15)-C(16)-C(17)	122.4(8)
C(11)-C(16)-C(17)	119.9(9)
C(13)-C(14)-C(15)	117.6(9)
C(13)-C(14)-C(20)	120.8(8)
C(15)-C(14)-C(20)	121.6(8)
C(17)-C(19)-H(19A)	109.5
C(17)-C(19)-H(19B)	109.5
H(19A)-C(19)-H(19B)	109.5

C(17)-C(19)-H(19C)	109.5
H(19A)-C(19)-H(19C)	109.5
H(19B)-C(19)-H(19C)	109.5
C(23)-C(25)-H(25A)	109.5
C(23)-C(25)-H(25B)	109.5
H(25A)-C(25)-H(25B)	109.5
C(23)-C(25)-H(25C)	109.5
H(25A)-C(25)-H(25C)	109.5
H(25B)-C(25)-H(25C)	109.5
N(2)-C(1)-C(10)#1	124.5(9)
N(2)-C(1)-C(2)	106.4(8)
C(10)#1-C(1)-C(2)	129.1(9)
C(17)-C(18)-H(18A)	109.5
C(17)-C(18)-H(18B)	109.5
H(18A)-C(18)-H(18B)	109.5
C(17)-C(18)-H(18C)	109.5
H(18A)-C(18)-H(18C)	109.5
H(18B)-C(18)-H(18C)	109.5
C(9)-C(10)-C(1)#1	130.4(9)
C(9)-C(10)-H(10)	114.8
C(1)#1-C(10)-H(10)	114.

Symmetry transformations used to generate equivalent atoms:
#1 -x+1/2,-y+1/2,-z+2

Appendix 2-4. **Anisotropic displacement parameters (Å^2 x 10^3) for porphyrin (3).** The anisotropic displacement factor exponent takes the form: $-2\pi^2[h^2 a^{*2}U^{11} + ... + 2 h k a^* b^* U^{12}]$

	U^{11}	U^{22}	U^{33}	U^{23}	U^{13}	U^{12}
Cl(1S)	79(2)	85(3)	99(3)	6(2)	53(2)	-6(2)
Cl(2S)	126(3)	109(4)	98(3)	-26(3)	61(2)	-12(3)

Appendix 2-5. **Hydrogen coordinates (x 10^4) and isotropic displacement parameters (Å^{2}x 10 ^{3}) for porphyrin (3).**

	x	y	z	U(eq)
H(1S1)	1861	1207	2840	56
H(1S2)	1595	1960	2186	56
H(8)	517	324	8611	15
H(21A)	3823	-2304	8483	34
H(21B)	3471	-2701	7395	34
H(21C)	2866	-2408	7599	34
H(2)	4736	2343	9636	18
H(3)	4008	1172	8893	15
H(7)	1481	-99	8357	15
H(24A)	945	3	5521	43
H(24B)	537	775	5424	43
H(24C)	795	211	6341	43
H(22A)	4035	-947	7049	40
H(22B)	4173	-1815	7054	40
H(22C)	4552	-1394	8135	40
H(20)	2866	-1594	6476	17
H(15)	3936	-1234	9228	19
H(23)	1745	1153	7040	19
H(17)	3769	294	10497	26
H(13)	2286	-448	6300	6
H(19A)	4857	-826	10908	71
H(19B)	5004	-236	11742	71
H(19C)	4961	28	10770	71
H(25A)	2524	1345	6483	47
H(25B)	1587	1509	5551	47
H(25C)	1983	754	5561	47
H(18A)	2943	-695	10238	144
H(18B)	3760	-631	11426	144

H(18C)	3680	-1245	10661	144
H(10)	405	1510	9411	9
H(1)	2861	2308	9798	9

Appendix 2-6. **Torsion angles [°] for porphyrin (3).**

C(1)-N(2)-C(4)-C(5)	-179.7(8)
C(1)-N(2)-C(4)-C(3)	0.2(8)
C(1)-C(2)-C(3)-C(4)	0.3(9)
C(5)-C(4)-C(3)-C(2)	179.6(8)
N(2)-C(4)-C(3)-C(2)	-0.4(9)
C(9)-C(8)-C(7)-C(6)	-1.4(9)
C(6)-N(1)-C(9)-C(10)	179.0(8)
C(6)-N(1)-C(9)-C(8)	-0.5(9)
C(7)-C(8)-C(9)-N(1)	1.2(9)
C(7)-C(8)-C(9)-C(10)	-178.2(8)
C(9)-N(1)-C(6)-C(5)	178.4(8)
C(9)-N(1)-C(6)-C(7)	-0.4(8)
C(8)-C(7)-C(6)-N(1)	1.2(9)
C(8)-C(7)-C(6)-C(5)	-177.6(8)
C(11)-C(12)-C(23)-C(24)	-115.6(10)
C(13)-C(12)-C(23)-C(24)	65.0(11)
C(11)-C(12)-C(23)-C(25)	119.5(10)
C(13)-C(12)-C(23)-C(25)	-59.9(10)
C(13)-C(12)-C(11)-C(16)	-1.8(13)
C(23)-C(12)-C(11)-C(16)	178.8(8)
C(13)-C(12)-C(11)-C(5)	175.8(8)
C(23)-C(12)-C(11)-C(5)	-3.7(13)
N(2)-C(4)-C(5)-C(6)	3.4(13)
C(3)-C(4)-C(5)-C(6)	-176.6(8)
N(2)-C(4)-C(5)-C(11)	-175.7(7)
C(3)-C(4)-C(5)-C(11)	4.3(12)
N(1)-C(6)-C(5)-C(4)	0.9(13)

C(7)-C(6)-C(5)-C(4)	179.5(8)
N(1)-C(6)-C(5)-C(11)	180.0(7)
C(7)-C(6)-C(5)-C(11)	-1.4(12)
C(12)-C(11)-C(5)-C(4)	-95.2(10)
C(16)-C(11)-C(5)-C(4)	82.4(11)
C(12)-C(11)-C(5)-C(6)	85.7(11)
C(16)-C(11)-C(5)-C(6)	-96.7(10)
C(11)-C(12)-C(13)-C(14)	0.5(13)
C(23)-C(12)-C(13)-C(14)	179.9(8)
C(14)-C(15)-C(16)-C(11)	-0.3(14)
C(14)-C(15)-C(16)-C(17)	-179.4(9)
C(12)-C(11)-C(16)-C(15)	1.7(13)
C(5)-C(11)-C(16)-C(15)	-175.8(8)
C(12)-C(11)-C(16)-C(17)	-179.2(8)
C(5)-C(11)-C(16)-C(17)	3.3(13)
C(19)-C(17)-C(16)-C(15)	47.2(13)
C(18)-C(17)-C(16)-C(15)	-76.4(11)
C(19)-C(17)-C(16)-C(11)	-131.8(10)
C(18)-C(17)-C(16)-C(11)	104.6(11)
C(12)-C(13)-C(14)-C(15)	0.9(13)
C(12)-C(13)-C(14)-C(20)	-178.0(8)
C(16)-C(15)-C(14)-C(13)	-0.9(14)
C(16)-C(15)-C(14)-C(20)	177.9(8)
C(22)-C(20)-C(14)-C(13)	99.8(9)
C(21)-C(20)-C(14)-C(13)	-135.4(8)
C(22)-C(20)-C(14)-C(15)	-79.0(11)
C(21)-C(20)-C(14)-C(15)	45.8(11)
C(4)-N(2)-C(1)-C(10)#1	179.5(8)
C(4)-N(2)-C(1)-C(2)	0.0(9)
C(3)-C(2)-C(1)-N(2)	-0.2(9)
C(3)-C(2)-C(1)-C(10)#1	-179.7(8)
N(1)-C(9)-C(10)-C(1)#1	-0.9(15)
C(8)-C(9)-C(10)-C(1)#1	178.4(8)

Symmetry transformations used to generate equivalent atoms:
#1 -x+1/2,-y+1/2,-z+2